

UC Santa Cruz

UC Santa Cruz Electronic Theses and Dissertations

Title

Role of transcriptional regulatory networks in influencing Yersinia pseudotuberculosis pathogenesis

Permalink

<https://escholarship.org/uc/item/5sj1d40g>

Author

Balderas, David Antonio

Publication Date

2021

Peer reviewed|Thesis/dissertation

UNIVERSITY OF CALIFORNIA
SANTA CRUZ

**Role of transcriptional regulatory networks in
influencing *Yersinia pseudotuberculosis* pathogenesis**

A dissertation submitted in partial satisfaction
of the requirements for the degree of

DOCTOR OF PHILOSOPHY

In

MICROBIOLOGY AND ENVIRONMENTAL TOXICOLOGY

By

David Antonio Balderas

June 2021

The Dissertation of David A. Balderas is approved:

Victoria Auerbuch Stone, chair

Karen Ottemann, Ph.D.

Patricia J Kiley, Ph.D.

Quentin Williams
Acting Vice Provost and Dean of Graduate Studies

Table of Contents

Abstract.....	xi
Dedication and Acknowledgments.....	xiv
Chapter 1.....	1
<u>Host factors such as iron and oxygen influence transcriptional regulatory networks in pathogenic bacteria</u>	
By David Balderas and Victoria Auerbuch	
Introduction.....	2
Iron availability.....	3
Oxygen availability.....	6
Iron-Sulfur Clusters.....	7
IscR	8
FNR.....	20
OxyR.....	21
T3SS regulation in <i>Yersinia</i>	23
ChIP-Seq method.....	27
References.....	37
Chapter 2.....	54
<u>Genome scale analysis reveals IscR directly and indirectly regulates virulence factor genes in pathogenic <i>Yersinia</i></u>	

By David Balderas, Erin Mettert, Hanh N. Lam, Rajdeep Banerjee, Tomas Gverzdys, Pablo Alvarez, Geetha Saarunya, Natasha Tanner, Adam Zoubedi, Yahan Wei, Patricia J. Kiley, Victoria Auerbuch

Abstract.....	55
Importance.....	56
Introduction.....	56
Results.....	61
Discussion.....	74
Materials and Methods.....	83
References.....	100
Chapter 3.....	154

IscR promotes *Yersinia* type III secretion system activity by antagonizing the repressive H-NS-YmoA complex at the *IcrF* promoter

By David Balderas, Pablo Alvarez, Mane Ohanyan, Erin Mettert, Natasha Tanner, Patricia J. Kiley, Victoria Auerbuch

Abstract.....	155
Significance Statement.....	157
Introduction.....	158
Materials and Methods.....	162
Results.....	172
Discussion.....	181
References.....	186

Chapter 4.....237

The CpxRA two-component regulatory system modulates the *Yersinia* T3SS through regulation of the YmoA repressor

By David Balderas, Natasha Tanner, Pablo Alvarez, Erin Mettert, Patricia J. Kiley, Victoria Auerbuch

Abstract.....238
Introduction.....239
Results.....242
Discussion.....245
Materials and Methods.....250
References.....256

Chapter 5.....278

Defects in the Ysc type III secretion system modulate activity of the two-component regulatory system CpxRA

By David Balderas, Pablo Alvarez, Victoria Auerbuch

Abstract.....279
Importance.....280
Introduction.....281
Results.....283
Discussion.....288
Materials and Methods.....291
References.....295

List of Figures and Tables

Chapter 1

<u>Figure 1</u> : Iron trafficking in the mammalian host.....	29
<u>Figure 2</u> : Oxygen gradient in the mammalian small intestine.....	31
<u>Figure 3</u> : IscR regulates itself via a negative feedback loop and its activity is influenced by environmental conditions.....	33
<u>Figure 4</u> : LcrF is regulated at both the transcriptional and post-transcriptional level.....	35

Chapter 2

<u>Table 1</u> : Strains used in this study.....	117
<u>Table 2</u> : <i>Y. pseudotuberculosis</i> primers used in this study.....	118
<u>Figure 1</u> : IscR mRNA and protein levels decrease upon iron supplementation.....	122
<u>Figure 2</u> : Iron supplementation modulates the expression of 1373 genes in <i>Yersinia</i>	124
<u>Figure 3</u> : Deletion of <i>iscR</i> leads to expression changes in genes involved in virulence, ion transport, cell envelope, and other processes following prolonged iron starvation.....	126
<u>Figure 4</u> : Several <i>Yersinia</i> genes follow expression patterns consistent with activation or repression by apo-IscR.....	128

<u>Figure 5</u> : ChIP-Seq reveals IscR to be a global regulator in <i>Yersinia</i>	130
<u>Figure 6</u> : IscR binds to the promoters of <i>dusB-fis</i> , <i>ail</i> , <i>sodB</i> , and <i>katA</i> <i>in vivo</i> and <i>in vitro</i>	132
<u>Figure 7</u> : IscR binding site sequences are highly conserved in human pathogenic <i>Yersinia</i>	134
<u>Figure 8</u> : IscR directly regulates the Suf Fe-S cluster biogenesis pathway, which is important for type III secretion activity specifically under aerobic conditions.....	136
<u>Figure 9</u> : Model of how iron modulates IscR levels and leads to differential expression of IscR dependent virulence factors.....	138
<u>Figure S1</u> : 3xFLAG-tagged IscR rescues an <i>iscR</i> deletion.....	140
<u>Figure S2</u> : Global IscR ChIP-seq analysis fails to identify predicted IscR Type I sites.....	142
<u>Figure S3</u> : Conservation of IscR binding sites in <i>Y. pseudotuberculosis</i> (IP2666, IP32953), <i>Y. pestis</i> (CO92), and <i>Y. enterocolitica</i> (8081).....	144
<u>Figure S4</u> : Deletion of DN756_21815 and DN756_21820, identified gene targets of IscR, results in a small but significant decrease in type III secretion.....	146
<u>Figure S5</u> : COG analysis of the IscR regulon, functional regulon, and indirect regulon.....	148
<u>Figure S6</u> : Expression of the <i>suf</i> operon is modulated by iron and requires IscR.....	150

Figure S7: The Suf pathway does not affect motility or growth.....152

Chapter 3

Table 1: Strains used in this study.....200

Table 2: *Y. pseudotuberculosis* primers used in this study.....202

Table 3: Plasmids used in this study.....207

Figure 1: IscR does not directly promote transcription of *yscW-lcrF* *in vitro*.209

Figure 2: Deletion of *iscR* is dispensable for type III secretion in the *ymoA* mutant background.....211

Figure 3: YmoA is epistatic to IscR with respect to *lcrF* transcriptional regulation.....213

Figure 4: IscR does not regulate YmoA or H-NS expression.....215

Figure 5: IscR binding to the *yscW-lcrF* promoter is dispensable in the absence of YmoA.....217

Figure 6: Knockdown of H-NS leads to derepression of LcrF.....219

Figure 7: Analysis of IscR and H-NS-YmoA regulated segments of *yscW-lcrF*.....221

Figure 8: H-NS and IscR bind to the *yscW-lcrF* promoter at different temperatures.....223

Figure 9: Oxygen does not influence *lcrF* levels in *ymoA* mutants.....225

Figure 10: Proposed model for activation of *yscW-lcrF* via IscR.....227

Figure S1: YmoA affects type III secretion activity dependent on LcrF.....229

<u>Figure S2</u> : YmoA mutations do not affect mRNA levels of known transcriptional regulators of LcrF.....	231
<u>Figure S3</u> : 3xFLAG tag allows for detection of H-NS using FLAG antibody.....	233
<u>Figure S4</u> : IscR enrichment at the <i>suf</i> promoter is not influence by temperature.....	235

Chapter 4

<u>Table 1</u> : Strains used in this study.....	264
<u>Table 2</u> : <i>Y. pseudotuberculosis</i> primers used in this study.....	265
<u>Table 3</u> : Plasmids used in this study.....	267
<u>Figure 1</u> : CpxR does not bind to the <i>yscW-lcrF</i> promoter.....	268
<u>Figure 2</u> : CpxR is predicted to bind upstream of the <i>ymoBA</i> promoter.....	270
<u>Figure 3</u> : CpxR promotes expression of YmoA.....	272
<u>Figure 4</u> : YmoA is crucial for CpxRA repression of LcrF and type III secretion activity.....	274
<u>Figure 5</u> : Putative model for how the CpxRA two-component regulatory system indirectly regulates the <i>Yersinia</i> T3SS.....	276

Chapter 5

<u>Table 1</u> : Strains used in this study.....	303
<u>Table 2</u> : <i>Y. pseudotuberculosis</i> primers used in this study.....	305

<u>Figure 1</u> : Deletion of <i>iscR</i> under type III secretion system inducing conditions leads to upregulation of CpxR activated genes.....	306
<u>Figure 2</u> : Deletion of type III secretion system genes leads to upregulation of <i>cpxP</i>	308
<u>Figure 3</u> : Impediment of early and middle substrates leads to activation of CpxRA.....	310
<u>Figure 4</u> : Impediment of middle substrates leads to activation of CpxRA....	312
<u>Figure 5</u> : Overexpression of SycD leads to inhibition of CpxRA activity.....	314
<u>Figure 6</u> : Deletion of <i>sycD</i> does not affect CpxRA activity.....	316
<u>Figure S1</u> : Deletion of <i>iscR</i> does not affect <i>cpxR</i> or <i>cpxA</i> mRNA levels.....	318
<u>Figure S2</u> : Deletion of <i>yadA</i> does not increase <i>cpxP</i> levels.....	320

Abstract

David Balderas

Role of transcriptional regulatory networks in influencing *Yersinia pseudotuberculosis* pathogenesis

The aim of this dissertation is to better understand how facultative pathogens sense their environment, and coordinate the expression of genes important for establishing disease. This dissertation focuses on a facultative enteropathogen, *Yersinia pseudotuberculosis*, which is a Gram-negative bacteria that can be found in the environment or can cause disease in the mammalian host. In order for *Y. pseudotuberculosis* to be successful in causing disease, *Y. pseudotuberculosis* must modulate its transcriptome to reflect its environment. For example, in the mammalian host *Y.pseudotuberculosis* upregulates the type III secretion system (T3SS) an important virulence factor which is crucial for surviving and causing disease in the host.

The first part of this dissertation focused on determining the regulon of the transcription factor, IscR, in *Y. pseudotuberculosis*. This transcription factor was previously shown to positively regulate the T3SS and a heme acquisition pathway in *Yersinia*, but not much else was known regarding the other genes IscR regulates. I employed ChIP-Seq and RNA-Seq to determine

the IscR regulon and showed that IscR modulates many cellular processes including predicted virulence factors.

The second part of my dissertation reports on the molecular mechanism of how IscR positively regulates the T3SS in *Yersinia*. Genes that encode the *Yersinia* T3SS are activated by the transcriptional activator LcrF. Previous data in our lab showed that IscR promotes LcrF transcription, thus activating expression of T3SS genes. Interestingly, IscR does not directly activate RNA-polymerase at the LcrF promoter, but instead antagonizes a repressor of LcrF. In this chapter I demonstrate that the nucleoid proteins H-NS and YmoA repress *lcrF*, and that IscR antagonizes H-NS-YmoA mediated repression of LcrF by binding to the *lcrF* promoter.

The third part of my dissertation introduces the two-component regulatory system CpxRA. Previous data has shown the CpxRA system represses the T3SS in many pathogens including the T3SS in *Yersinia*. The previous model suggested that CpxR directly represses LcrF, however in this chapter I demonstrate that CpxR does not bind to the *lcrF* promoter and evokes indirect regulation of LcrF. I later show that CpxR activates expression of the known repressor of LcrF, YmoA and suggests that CpxR represses the T3SS through an indirect mechanism.

A great deal of my work focuses on how transcriptional regulatory networks govern expression of virulence factors, however not much is known how the expression of virulence factors affects regulatory networks. The last

part of my dissertation provides data to suggest that the disruption to assembly of the *Yersinia* T3SS induces CpxRA activity. Interestingly, specific T3SS mutants induce the CpxRA pathway suggesting that expression of the T3SS can modulate the CpxRA regulon. Together these findings enhance our understanding of how facultative pathogens sense environmental signals and how environmental signals modulate gene regulatory networks.

Dedication and acknowledgements

To my partner Sam, you have been so supportive during my graduate career and you were always there during difficult times. I am grateful for you always providing an empathetic lens to my struggles and challenges, and allowing me to overcome any obstacles I was experiencing throughout my graduate career.

To my family, for all their support and motivation. Thank you for giving me the chance to go back to school and to take this journey. You were always there for me when I needed someone to talk to and you bring such joy to my life.

To Vicki Auerbuch Stone, thank you for helping me grow as an independent scientist and challenging me throughout graduate school. I appreciate you for devoting so much of your time to help develop and progress my research and career.

To Pablo and Natasha, thank you for all your hard work and dedication to the lab. Both of you were instrumental in the progress we made in our research. You both are destined for great things and it was a pleasure to see you develop as young researchers.

To the Auerbuch Stone lab, thank you for all your input and help with my projects. Thank you for making this a great working environment.

To the Kiley lab, thank you Tricia and Erin for being such great collaborators, and being available for any questions or issues I ran into.

Chapter 2,3, and 4 are multi-author publications. I am responsible for all the figures in Chapter 2 except Figure 6B and Figure 8B. For Chapter 3, I am responsible for all the figures except Figure 1. For Chapter 4, I am responsible for all the figures except Figure 1BC.

Chapter 1

Host factors such as iron and oxygen influence transcriptional regulatory networks in pathogenic bacteria

By David Balderas & Victoria Auerbuch

Introduction

Bacteria are able to thrive in many different environmental niches that can range from hot thermal springs to the gastrointestinal tract of a human being. In order for bacteria to colonize these diverse environments bacteria need to respond to environmental signals and modulate their physiology to grow in such dynamic environments. For bacterial pathogens to cause disease they must be able to express key virulence factors when needed in the host (Wu et al., 2008). Many pathogens have evolved sensing mechanisms that tightly regulate the expression of these key virulence factors. Two crucial environmental signals that pathogens sense are iron and oxygen. In this review I will go over iron bioavailability and iron trafficking in the mammalian host and then I will introduce oxygen availability in the mammalian gastrointestinal tract. The next part of the review will highlight on a transcription factor that senses iron and oxygen which is IscR (Iron sulfur cluster regulator). This section will focus on what is known about IscR in non-pathogenic *Escherichia coli* and then expand on how IscR promotes virulence in pathogenic bacteria. Then I will introduce other transcription factors that sense oxygen tension in both pathogenic and non-pathogenic bacteria. Next, I will introduce the type III secretion system, a key virulence factor that has been reported to respond to iron and oxygen bioavailability. Lasty this review will focus on chromatin immunoprecipitation with massively parallel DNA sequencing, a powerful next generation sequencing tool that allows one to

understand what regulatory DNA elements a DNA binding protein binds *in vivo*.

Iron availability

Iron is an essential mineral for almost all studied bacteria with some notable exceptions such as *Lactobacillus plantarum* and *Borrelia burgdorferi* (Archibald, 1983; Posey and Gherardini, 2000). Iron is a vital mineral due to its ability to act as a cofactor for many crucial biological processes including energy generation, DNA replication, and oxygen transport. Accumulation of iron could be detrimental to the cell, because iron has the potential to react with reactive oxygen species (ROS) to catalyze the production of radical ions and cause damage to the cell (Imlay, 2003). These reactive oxygen species can be a by-product of bacterial respiration or can also be produced by professional phagocytes such as macrophages and neutrophils (Filip-Ciubotaru et al., 2016). Thus, iron transport and iron storage must be tightly regulated in order to avoid cellular damage.

Many bacterial pathogens encounter higher levels of obtainable iron in their natural environment (e.g., soil, water, and food) compared to free iron found in the mammalian host. The mammalian immune system efficiently regulates iron throughout the blood/tissues and at the cellular level (Cherayil et al.,

2011). Cellular signaling, inflammation, and the host microbiota contribute to iron homeostasis in the human host.

The healthy human body contains 3 to 4 g of total iron. Iron loss can occur by epithelial cell shedding and minor bleeding, which leads to a total loss of less than 2 mg per day (Von Drygalski and Adamson, 2013). Up to 95% of the deficit is replaced via recycling of red blood cells by macrophages, with the rest of the iron absorbed from food in the duodenum and colon (Kortman et al., 2014; Nairz et al., 2014). Dietary non-heme iron is in the ferric state (Fe^{3+}) and must be converted to ferrous iron (Fe^{2+}) to be transported across the duodenum membrane (Figure 1) (McKie et al., 2001; Choi et al., 2012). After dietary iron is converted to the ferrous state, iron can be transported to enterocytes via DMT1, a divalent metal transporter (Gunshin et al., 1997). Cellular iron can either be stored as ferritin or released into plasma by ferroportin (Vulpe et al., 1999). Iron released into plasma can be coupled to transferrin and lactoferrin, which sequester iron from bacterial pathogens in the blood. Most iron bound to transferrin is destined to be taken up by bone marrow, where the iron is used for synthesis of hemoglobin (DONOHUE et al., 1958). The hemoglobin will then become associated with red blood cells, which will eventually become senescent and be recycled by macrophages completing the cycle.

Hepatocytes are central to iron homeostasis in mammals, serving as the principal site for the production of hepcidin, a master regulator of plasma iron concentration (Park et al., 2001). Production of hepcidin is induced in response to iron and inflammation (Mazur et al., 2003). Hepcidin is able to bind and promote degradation of ferroportin, thus reducing transport of iron in the plasma (Nemeth et al., 2004). Additionally, when levels of hepcidin are high, iron released into plasma circulation is decreased. This explains why hepcidin acts as an antimicrobial against extracellular pathogens, *Vibrio vulnificus* and *Yersinia spp.* (Raida and Buchmann, 2009; Arezes et al., 2015). by limiting iron bioavailability. However, hepcidin has been shown to improve growth of intracellular pathogens such as *Salmonella* and *Mycobacteria* (Paradkar et al., 2008; Fang and Weiss, 2014). This is due to less ferroportin availability and iron transport, which will lead to an increase in cellular iron content.

The lumen of the gastrointestinal tract was originally believed to have high levels of iron because food that enters the digestive tract may contain high levels of iron. Contrary to this, there is evidence supporting that this iron is not available to invading microbes as it may already be bound to iron-binding proteins by members of the microbiota. Indeed some members of the host microbiota found in the intestinal lumen produces siderophores, and these siderophores are only produced when cells are starved for iron (Kortman et

al., 2014). Due to the discrepancy between iron levels found in the natural environment and iron levels found in the human host, iron can be used as an environmental signal to regulate virulence for bacterial pathogens.

Oxygen availability

Not only is there a difference in iron availability between the mammalian host and the natural environment of the bacterial pathogen, but there are also differences in oxygen availability. Oxygen levels in the human body can be characterized as normoxic (10%-20% oxygen), hypoxic (<10% oxygen), and physioxic (>20% oxygen) (Figure 2) (Carreau et al., 2011). Tissues within the human body are supplied with varying concentrations of oxygen, depending on their energy need; tissues with oxygen concentrations lower than atmospheric oxygen concentration are not necessarily encountering hypoxic stress (Guzy and Schumacker, 2006). The oxygen concentration in intestinal tissue has been studied most extensively due to its importance in bacterial pathogenesis. The gastrointestinal tract is characterized as having a steep oxygen gradient across the epithelial layer, with the basolateral side being close in proximity to blood vessels while the apical side being extremely oxygen deficient (Taylor and Colgan, 2007). Non-invasive measurement of tissue oxygen concentration reported oxygen levels of 8% in the small intestinal wall to approximately 3% in the villus and less than 2% in the intestinal lumen (Fisher et al., 2013). Furthermore, oxygen availability can

become further limited during infection. Neutrophils will be recruited to sites of infection and produce ROS which consume a great deal of oxygen. The availability of oxygen can also be observed by mapping where specific microbes in the microbiota reside according to the intestinal tract. The proximal small intestine mainly contains aerotolerant bacteria such as *Helicobacteraceae* and *Lactobacillaceae*, while the colon harbors mostly strictly anaerobic bacteria, such as *Lachnospiraceae*, *Bacteroidaceae* and *Prevotellaceae* (Brown et al., 2013). Additionally, during infection, the epithelial layer may become disrupted leading to blood vessel constriction and a reduction in oxygen flow. Hypoxia inducible factor 1 (HIF-1), a transcriptional factor important for cellular response to hypoxic stress, will begin to accumulate and promote angiogenesis and erythropoiesis (Wang and Semenza, 1993; Greijer et al., 2005). This will eventually result in a change in oxygen bioavailability. Due to this dynamic change in O_2 availability, bacterial pathogens must be able to sense oxygen levels and coordinate production of virulence factors and metabolic genes in the host.

Iron-Sulfur Clusters

Many proteins that sense oxygen and iron availability are associated with iron-sulfur clusters. Iron-sulfur clusters are commonly found as cofactors for a wide range of different proteins. Over 150 proteins in *E. coli* are believed to have an iron-sulfur cluster cofactor (Py and Barras, 2010). These proteins

serve functions ranging from general metabolism to gene regulation (Lill, 2009). Iron-sulfur clusters are normally found in the rhombic [2Fe-2S] state or the cubic [4Fe-4S] state, which are derived from ferrous/ferric iron and sulfide (Beinert, 2000). Three different iron-sulfur biogenesis systems have been identified in bacteria. These systems include NIF, ISC, and SUF, the latter two are also conserved in eukaryotes (Johnson et al., 2005). The NIF system was first identified in *Azotobacter vinelandii* and is dedicated to production of iron-sulfur clusters for nitrogenase, a key enzyme in bacteria that participate in nitrogen fixation (Jacobson et al., 1989). The ISC system is believed to be the housekeeping iron-sulfur biogenesis system, while SUF is hypothesized to be controlled via stress response and induced during iron limitation. The SUF system has been associated with stress response because the SUF system is less sensitive to destabilization by ROS, O₂ tension, and iron chelation compared to the ISC system (Blanc et al., 2014).

IscR in *E. coli*

The transcriptional regulator Iron Sulfur Cluster Regulator (IscR) was first characterized in *E. coli*, but has subsequently been linked to virulence in several pathogens (Schwartz et al., 2001; Lucchini et al., 2005; Choi et al., 2007; Lim and Choi, 2014; Miller et al., 2014; Vergnes et al., 2017). The gene *iscR* is part of an operon consisting of other proteins important for iron-sulfur biogenesis including IscS, IscU, and IscA. This operon also contains

the genes *hscBA* and *fdx*. The protein IscS is a cysteine desulfurase, which converts L-cysteine to L-alanine to obtain readily available sulfur atoms (Ollagnier-de Choudens et al., 2003). Eventually the extracted sulfur will be combined with iron to form an iron-sulfur cluster within a scaffold protein such as IscU (Blanc et al., 2015). Lastly the Fe-S clusters are transferred to proteins that utilize Fe-S clusters by a carrier protein such as IscA coupled with chaperones, HscBA. The IscR protein is the main regulator of this pathway. IscR has a winged helix-turn-helix (HTH) DNA binding domain which directly binds upstream of the *isc* operon and represses its expression (Santos et al., 2015). IscR is an example of a protein that utilizes Fe-S clusters. This transcriptional regulator controls the expression of more than 40 genes in *E. coli*, including the *isc* operon and other genes important for Fe-S cluster biogenesis such as *erpA*, *nfuA*, and the SUF operon (Giel et al., 2006). ChIP-seq analysis has revealed that IscR also directly regulates genes that are important for nitrate/nitrite reductase, iron transport, type-1 fimbriae production, flagellar biosynthesis, and biofilm formation (unpublished). Unlike the transcriptional regulator FNR (ferredoxin-NADP(+) oxidoreductase) that mainly relies on Fe-S cluster ligation to form dimers and bind DNA, IscR can bind DNA independent of Fe-S clusters. IscR exists in the holo form where it is bound to [2Fe-2S] or in the apo form, which is clusterless. In *E. coli*, IscR requires 3 conserved cysteine residues, which support ligation to Fe-S clusters. Both the apo and holo forms can bind

DNA. *In silico* analysis has revealed that IscR binds to two different DNA consensus sequences coined Type 1 sites and Type 2 sites (Figure 3B) (Giel et al., 2006). The holo form of IscR was shown to bind with a higher affinity towards Type 1 sites compared to the clusterless form of IscR (apo-IscR). An example of a conserved Type 1 site is located upstream of the *isc* operon, where holo-IscR represses the *isc* operon thus repressing Fe-S biogenesis (Figure 3A). On the other hand, both holo-IscR and apo-IscR have a similar affinity for Type 2 sites (Rajagopalan et al., 2013). An example of a conserved Type 2 site is found upstream the SUF operon promoter where both apo and holo forms of IscR can bind DNA and induce expression of SUF transcription. Crystallography studies have revealed that IscR differentiates between the two DNA binding motifs due to steric hindrance formed from a glutamate residue (E43). When this glutamate was substituted with an alanine, IscR no longer exhibited a preference for Type 1 and Type 2 DNA binding sites devoid of ligation to iron-sulfur clusters.

The levels of IscR are associated with iron and O₂ conditions. During normal aerobic conditions, Fe-S clusters are constantly degraded due to oxygen tension and result in a higher percentage of apo-IscR. This results in relieving repression of the *isc* operon because holo-IscR cannot inhibit transcription of the *isc* operon (Figure 3C). As a result, *isc* machinery is found in abundant levels under standard growth conditions (Py and Barras, 2010). On the other

hand, when *E. coli* is grown in anaerobic conditions, Fe-S clusters are stable resulting in a higher proportion of holo-IscR, which will repress the *isc* operon and reduce the amount of *isc* machinery. Fe-S clusters can also be destabilized by ROS, NO, iron depletion, or high levels of other metals, resulting in higher levels of apo-IscR. However the *isc* machinery responsible for Fe-S biogenesis can be inactivated by ROS and iron-deplete conditions (Jang and Imlay, 2010).

IscR in *Yersinia*

IscR was found to induce expression of the type III secretion system (T3SS) in *Yersinia pseudotuberculosis* (Miller et al., 2014). The T3SS is an important virulence factor for mammalian pathogens including *Shigella*, *Salmonella*, *Escherichia*, *Chlamydia*, *Vibrio*, *Pseudomonas*, and *Yersinia* (Troisfontaines and Cornelis, 2005; Coburn et al., 2007). The T3SS shuttles effector proteins from the bacterial cytoplasm to the host cytoplasm in order to dampen host defenses and to promote virulence. *Yersinia* IscR was identified in a forward genetic screen for genes involved in T3S, and shown to bind upstream of *IcrF*, the master regulator of the T3SS in *Yersinia*, and activate expression of *IcrF*. Bioinformatic analysis revealed a Type 2 site upstream of the *yscW-IcrF* operon. Binding assays confirmed that IscR binds the predicted Type 2 site. A deletion of *iscR* also led to a decrease in overall virulence compared to wild type *Yersinia* in a mouse infection model. A deletion of *iscR* is more

attenuated compared to a strain of *Yersinia* that lacks the T3SS. This suggests that IscR regulates other components critical for *Yersinia* virulence.

IscR regulon in Yersinia

To understand how IscR additionally contributes to overall pathogenesis, RNAseq was performed to compare the transcriptome of WT and Δ *iscR* in *Yersinia pseudotuberculosis*. A total of 134 genes were significantly up-regulated in the Δ *iscR* mutant while 92 genes were significantly downregulated compared to WT. Significance was scored by an average of ≥ 2 -fold change in reads per kilobase of transcript per million mapped reads (RPKM) between the WT strain and Δ *iscR* mutant. The genes that showed a significant change in transcript production between Δ *iscR* and WT include genes important for Fe-S cluster biogenesis, genes involved with T3SS, cellular detox genes, general metabolism genes, genes important for hemin transport/utilization, sulfur metabolism genes, and genes associated with virulence. As predicted, the *isc* operon was up-regulated in the Δ *iscR* mutant compared to WT, and the *SUF* operon was up-regulated in an apo locked mutant of IscR compared to both WT and Δ *iscR*. Many of the genes that were differentially expressed between WT and Δ *iscR* in the RNA-seq experiment have not been validated using follow up experiments such as q-RT-PCR or DNA binding assays.

According to the RNAseq analysis, IscR may play a role in repressing cellular detox genes in *Yersinia*. These cellular detox genes included *katY*, a catalase that breakdowns ROS, *tpx*, a thiol peroxidase which can degrade hydroperoxides and hydrogen peroxide, and *sodBC* a superoxide dismutase which can convert superoxide to less toxic substrates. All these genes were up-regulated in the Δ *iscR* mutant compared to WT suggesting IscR may repress cellular detoxifying genes. Both homologs of *katY* and *tpx* have been shown to be directly regulated by IscR in *Pseudomonas aeruginosa* (Kim et al., 2009; Somprasong et al., 2012). It is important to note that the deletion of *iscR* does not lead to increase in susceptibility to hydrogen peroxide. Therefore, it is not clear if IscR is important for expression of detox genes in *Yersinia*.

Genes involved with N-acetylglucosamine (GlcNAc) catabolism were also predicted to be regulated by IscR according to the RNAseq data. These genes involved with GlcNAc include the operon *nagBACD* and *nagE* which were all up-regulated in the Δ *iscR* mutant. GlcNAc is a key structural component of the bacterial cell wall. This sugar has been shown to be important for colonization of the host by *E. coli* and *Vibrio cholera*, while also controlling the production of virulence factors in *P. aeruginosa* and *Streptococcus mutans* (Chang et al., 2004; Ghosh et al., 2011; Korgaonkar and Whiteley, 2011; Kawada-Matsuo et al., 2012). Many studies have

focused on the relationship between GlcNAc abundance and the production of virulence factors in *E. coli*. GlcNAc down-regulates the production of type-1 fimbrial adhesins, which help promote host cell adhesion during urinary tract infections (Sohanpal et al., 2004). It has also been shown that GlcNAc lowers the production of curli fibers that are important for biofilm formation, adhesion, and overall internalization of *E. coli* by epithelial cells (Barnhart et al., 2006).

IscR may also regulate genes involved with virulence other than *lcrF*. For example, the gene encoding cytotoxic necrotizing factor (CNF γ) in *Yersinia*, was up-regulated in an *iscR* null mutant compared to WT. CNF γ has been shown to be promote effector protein translocation into neutrophils and macrophages (Schweer et al., 2013). A *cnf γ* knockout is severely attenuated in its ability to disseminate into the mesenteric lymph nodes, liver, and spleen. The overall production of CNF γ severely diminishes the recruitment of professional phagocytes and natural killer cells. IscR repressing CNF γ could benefit *Yersinia* virulence by allowing the bacteria to bypass the host immune response and only express CNF γ when warranted. IscR may also play a role in positively regulating the surface-associated protein Ail. This protein has been shown to be crucial for adhering to host cells by binding to laminin and fibronectin (Miller and Mekalanos, 1988; Yamashita et al., 2011). Tight attachment to host cells benefits *Yersinia* in translocating effector proteins

into host cells. Additionally Ail confers resistance against serum killing in all three mammalian pathogenic *Yersiniae* (Pierson and Falkow, 1993).

The small regulatory RNA's CsrB and CsrC are also suggested to be regulated by IscR due to being significantly up-regulated in the Δ *iscR* mutant according to RNA-seq analysis. These two siRNA's have been shown to play an important role in regulating InvA, the activator of primary cell entry in *Yersinia* (Heroven et al., 2012). InvA was not shown to be differentially expressed in the Δ *iscR* mutant according to the RNA-seq results, however this is mostly likely due to InvA being only expressed below 37°C while the RNA-seq experiment was performed using bacteria grown at 37°C. Csr/Rsm system has been shown to play a vital role in many other pathogens including *V. cholerae*, EPEC, *S. typhimurium*, *Legionella pneumophila*, and *P. aeruginosa* (Pessi et al., 2001; Fortune et al., 2006; Bhatt et al., 2009; Sahr et al., 2009; Jang et al., 2010). Lastly, IscR may also regulate virulence via regulation of the proteases ClpXP and Lon. These proteases share an operon with each other and were up-regulated in the *iscR* null mutant compared to WT. The protein YmoA forms a stable complex with the histone like protein, H-NS (Nieto et al., 2002). The YmoA/H-NS complex has been shown to repress both the T3SS and InvA via LcrF and RovA respectively (Cornelis, 1993; Ellison et al., 2003). YmoA was found to be a substrate of ClpXP and Lon thus leading to derepression of *lcrF* at 37°C when the proteases are more

enzymatically active (Jackson et al., 2004). If these proteases are indeed apart of the IscR regulon, then IscR may play a secondary role in regulating the T3SS via *IcrF* through YmoA.

IscR in *Vibrio vulnificus*

Vibrio vulnificus is an opportunistic Gram-negative pathogen that frequently contaminates oysters and causes gastroenteritis in humans. Less occasionally, this pathogen can also cause life-threatening septicemia (Strom and Paranjpye, 2000). IscR was shown to contribute to cytotoxic activity of *V. vulnificus* toward INT-407 human intestinal epithelial cells (Lim and Choi, 2014). Deletion of *iscR* in *V. vulnificus* resulted in a severely attenuated strain when mice were infected intragastrically compared to WT *V. vulnificus*. Microarray analysis was performed to understand what genes IscR potentially regulates. The microarray analysis predicted 67 genes to be regulated directly and indirectly by IscR, 52 genes were up-regulated and 15 genes were downregulated. The genes that were up-regulated in WT compared to Δ *iscR* consisted of genes important for transport, metabolism, energy production, motility, chemotaxis, oxidative stress, and virulence. A deletion of *iscR* led to a reduction in motility compared to WT. Also, an *iscR* mutant was severely attenuated in adhering to INT-407 cells. Furthermore, an *iscR* mutant was more susceptible to oxidative stress. A later study pointed out that IscR directly regulates Prx3, a protein that acts as an antioxidant that reduces

reactive oxygen species (ROS) such as H₂O₂ (Lim et al., 2014a). The IscR binding site upstream of *prx3* was determined to be a Type 2 site. This result suggests that when *V. vulnificus* encounters ROS, Fe-S clusters will be degraded shifting to an apo-IscR state and inducing *prx3* transcription via apo-IscR. The production of Prx3 and IscR may contribute to pathogenesis because bacteria will be less susceptible to ROS produced from the host immune response. Adding increasing concentrations of host cells also induced transcription of *iscR*, possibly as a result of ROS production by host cells. It was reported that *iscR* transcription in *Vibrio* is directly regulated by the master regulator of quorum sensing, AphA (Lim et al., 2014b). AphA is a PadR-family transcription factor that activates transcription of *tcpPH* resulting in the production of cholera toxin and toxin-coregulated pilus, two critical virulence factors in *Vibrio cholera* (Kovacikova and Skorupski, 1999; Kovacikova et al., 2004). IscR has also been shown to directly bind and induce transcription of *gfpA* (Jang et al., 2016). The gene *gfpA* encodes for a mucin binding protein, which has been shown to be important for virulence and the ability to colonize the intestinal tract of mice. Overall, IscR has been shown to be important for adhesion, cellular detox, and overall virulence in *Vibrio vulnificus*.

IscR in *Pseudomonas aeruginosa*

Pseudomonas aeruginosa is a Gram-negative bacterium that is an opportunistic pathogen. *Pseudomonas aeruginosa* can be found in soil, water, and other environmental habitats. This bacterium is considered an environmental pathogen because it is commonly found in the environment, but can also cause acute infections in hospitalized patients as well as cause chronic infections in cystic fibrosis patients. Many bacterial pathogens will be exposed to ROS during infection of the human host; ROS are secreted and can be found up to the millimolar levels inside phagosomal vesicles (Hasset and Cohen, 1989). One way the opportunistic pathogen *Pseudomonas aeruginosa* deals with oxidative stress is by expressing KatA, a catalase used to break down ROS. When investigating the main regulators of *katA* in *P. aeruginosa*, researchers found that IscR along with OxyR regulates transcription of this crucial enzyme (Choi et al., 2007). Deletion of *iscR* led to increased susceptibility to H₂O₂. Furthermore, Δ *iscR* mutants were severely attenuated in a peritonitis-sepsis-derived mouse infection compared to WT (Kim et al., 2009). IscR was also shown to directly repress *trx*, a thiol peroxidase homolog in *Pseudomonas aeruginosa* PAO1 (Somprasong et al., 2012). The protein Trx has been shown to degrade toxic peroxides such as hydroperoxides and hydrogen peroxide. In *P. aeruginosa*, *trx* expression can be induced via thiol-depleting agents and redox-cycling drugs. It was shown that a *trx* null mutant was more susceptible to submillimolar levels of H₂O₂

compared to the WT strain; however, there was no growth defect observed in the *trx* null mutant at millimolar levels of H₂O₂. It was also shown that *trx* does not contribute to virulence in the *C. elegans* infection model.

IscR in *Salmonella enterica*

Salmonella enterica serovar Typhimurium is an intracellular pathogen responsible for a wide range of infections including gastroenteritis and systemic infections. *Salmonella* utilizes two T3SS's termed Spi1 T3SS and Spi2 T3SS. It was recently shown that an *iscU* null mutant was found to be defective for epithelial cell invasion and for mouse infection (Vergnes et al., 2017). IscR was shown to directly repress *hilD* transcription. The gene *hilD* encodes for the master regulator of the Spi1 T3SS in *Salmonella*. Thus, IscR was responsible for repression of *hilD*, which controls the Spi1 T3SS. Furthermore, an *iscR* null mutant was hyperinvasive because of high expression of HilD.

IscR in *Shigella flexneri*

Shigella flexneri is a facultative intracellular pathogen that spends a significant portion of its life cycle within the epithelial cells lining the human colon. Transcriptional analysis of *S. flexneri* revealed that the SUF operon is induced during intracellular replication inside macrophages and epithelial cells (Runyen-Janecky and Payne, 2002; Lucchini et al., 2005). It is not clear if this

increase expression of the *SUF* operon is due to iron/oxygen conditions or due to detection of host. Furthermore, an *iscSUA* mutant was also shown to be more sensitive to H₂O₂ and phenazine methosulfate, a superoxide generator, compared to the parental strain (Runyen-Janecky et al., 2008). The *isc* biosynthesis operon was also shown to be essential to propagate plaque formation in Henle cell monolayers. Plaque formation is the result of bacterial invasion, lysis of the endocytic vacuole, bacterial multiplication within the host cell, and intracellular spread via actin polymerization. An Δ *isc* mutant was not able to invade host cells. Both the *isc* operon and *SUF* operon were shown to be induced intracellularly, presumably because of iron limitation.

FNR

The most studied transcription factor that senses oxygen starvation is the protein Fumarate Nitrate Regulator (FNR). In *E. coli*, FNR is divided into two domains, one domain that ligates to iron-sulfur clusters and the other that binds to DNA. The N-terminal domain contains four cysteine residues, which bind to the iron-sulfur cluster, while the C-terminal domain binds to specific FNR binding sites found in promoter regions (Beinert and Kiley, 1999). Under anaerobic conditions, FNR is ligated to a [4Fe-4S] cluster, which causes a conformational change that allows FNR to bind DNA and activate or repress gene expression (Green et al., 1996; Scott et al., 2003; Moore et al., 2006). FNR activates genes associated with anaerobic respiration, fermentation, and

virulence while also repressing genes associated with aerobic respiration. FNR has been shown to be important for virulence in *Pseudomonas aeruginosa*, *Shigella flexneri*, *Neisseria meningitidis*, *Salmonella enterica* serovar *Typhimurium*, and Uropathogenic *Escherichia coli* (UPEC) (Bartolini et al., 2006; Fink et al., 2007; Kuntumalla et al., 2011; Jackson et al., 2013; Barbieri et al., 2014). There is reason to believe crosstalk exists between FNR and IscR. A sRNA named FnrS is shown to be strictly dependent on FNR in *E. coli* (Boysen et al., 2010). This sRNA is induced during anaerobic conditions. FnrS binds upstream of *iscR* and prevents transcription of *iscR*, which adds a second layer of regulation during anaerobic growth (holo-IscR repressing *isc* operon and FnrS inhibits *iscR* transcription) (Wright et al., 2013). It is unclear whether FnrS plays a role in regulation of IscR in bacteria other than *E. coli*. This sRNA is 97% conserved in *Y. pseudotuberculosis* IP32953 while the putative FNR binding site upstream of FnrS is completely conserved.

OxyR

OxyR is a LysR family transcriptional factor found in many Gram-negative bacteria including *Proteobacteria*, *Bacteroidetes*, and *Actinobacteria* (Chiang and Schellhorn, 2012). OxyR has been shown to be important for cellular response to H₂O₂ (Dempfle and Amábile-Cuevas, 1991). The OxyR regulon can vary from 3 to 40 genes, with genes generally associated with cellular

detox and iron sequestration. OxyR activity is dependent on its oxidation/reduction state. When in the oxidized state, the DNA binding domain of OxyR can bind four major grooves of the DNA helix and affect gene expression. However, when OxyR is in the reduced state, OxyR can only bind to two major grooves of the DNA helix, which is generally less effective in regulating gene expression. Structural studies have demonstrated that two key residues, Cys199 and Cys208, form a disulfide bond during oxidizing conditions (Korgaonkar and Whiteley, 2011). Thus, in the presence of H₂O₂, this disulfide bridge forms and causes a conformational change that allows OxyR to cooperatively bind with RNA polymerase to regulate transcription of specific promoters. There is evidence pointing to cross-talk between IscR and OxyR, because both OxyR and IscR in *E. coli* activate the SUF operon (Lee et al., 2008). Activity of OxyR and IscR are similarly influenced by ROS and were shown to increase transcription of the SUF operon when exposed to H₂O₂.

OxyR was shown to activate the catalases KatAY in response to H₂O₂ in *Yersinia pestis* (Han et al., 2008). Due to this relationship OxyR may help *Yersinia* deal with reactive oxygen species when the pathogen encounters a phagocyte. OxyR was also shown to directly activate the T6SS-4 in *Yersinia pseudotuberculosis* (Wang et al., 2015). This secretion system was shown to be important to deal with oxidative stress in *Yersinia*.

T3SS regulation in Yersinia

All three *Yersinia* mammalian pathogens require the type III secretion system (T3SS) for virulence, including *Yersinia pestis*, which is the causative agent of bubonic and pneumonic plague, and *Yersinia enterocolitica* and *Yersinia pseudotuberculosis*, which cause self-limiting mesenteric lymphadenitis and gastroenteritis as well as serious disseminated infection in iron overload or immunocompromised individuals (Putzker et al., 2001). Human pathogenic *Yersinia* species share a virulence plasmid, which is approximately 70kb in size and contributes greatly to bacterial infection (Cornelis et al., 1998). This virulence plasmid is referred to as pCD1 in *Y. pestis* and pYV in *Y. pseudotuberculosis* and *Y. enterocolitica*. Genes encoded on the virulence plasmid include T3SS structural genes, T3SS effector proteins, T3SS chaperones, and genes that encode proteins which regulate the function and expression of the T3SS. The transcriptional factor LcrF (VirF in *Y. enterocolitica*) is the only characterized direct activator of T3SS genes in pathogenic *Yersinia* and activates many genes found on the virulence plasmid. LcrF contains two helix-turn-helix domains that allow LcrF to bind recognition sites near promoter regions of the LcrF regulon. LcrF expression is regulated both at the transcriptional level and translational level.

The *lcrF* gene has been demonstrated to be co-transcribed with the *yscW* gene, sharing a promoter with *yscW* (Figure 4) (Böhme et al., 2012). YmoA was shown to repress *yscW-lcrF* directly by binding downstream the promoter region of *yscW-lcrF* (Cornelis, 1993). YmoA is a histone like nucleoid structuring (H-NS) protein that interacts with H-NS. Band shift analysis revealed that YmoA co-purified with H-NS was able to interact with the *yscW-lcrF* promoter however H-NS alone was also able to interact with the *yscW-lcrF* promoter. The difference between H-NS alone and H-NS coupled with YmoA binding to this region and affecting expression remains unclear. YmoA is a substrate of the proteases Lon and ClpXP (Jackson et al., 2004). At 37°C Lon and ClpXP become more enzymatically active resulting in more degradation of YmoA. This degradation of YmoA leads to a derepression of *lcrF* transcription at host body temperature and contributes to thermoregulation of *lcrF* expression.

As stated earlier in this review, IscR was shown to directly activate the T3SS via binding upstream the promoter of *yscW-lcrF* in *Y. pseudotuberculosis* (Miller et al., 2014). Bioinformatic analysis revealed a Type 2 site upstream of the *yscW-lcrF* promoter, which can be bound to both holo-IscR and apo-IscR. This binding site is 100% conserved in *Y. pestis* and the residues that are required for binding are also conserved in *Y. enterocolitica* (Schwiesow et al.,

2016). This evidence suggests oxidative stress, oxygen limitation, and iron availability may contribute to expression of the T3SS via LcrF.

The response regulator RcsB was also shown to directly bind the *yscW-lcrF* promoter and activate transcription in *Y. pseudotuberculosis* (Li et al., 2015). The Rcs two-component signaling system has been shown to be important for capsulation, flagellar biosynthesis, motility, and biofilm formation in *Enterobacteriaceae* (Majdalani and Gottesman, 2005). This two component signaling system has also been shown to regulate the expression of the genome encoded T3SS in *Y. enterocolitica* and the T3SS in *Salmonella enterica* serotype *Typhi* (Arricau et al., 1998; Venecia and Young, 2005). RcsB was shown to interact with the *lcrF* promoter when in the phosphorylated state (Li et al., 2015). This suggests the expression of the T3SS in *Yersinia* is also regulated by environmental changes via RcsB. It was also shown that the response regulator CpxR inhibits expression of T3SS genes (Liu et al., 2012). However, it has not been demonstrated if CpxR directly affects T3SS via binding upstream of *yscW-lcrF*.

The T3SS in *Yersinia* is highly expressed at 37°C while repressed at moderate temperatures. *Yersinia* represses the T3SS at temperatures lower than the mammalian host body temperature because expression of the T3SS leads to growth arrest. One mechanism how *Yersinia* accomplishes

thermoregulation of the T3SS is through an RNA thermometer. The mRNA of *lcrF* forms a hairpin loop that sequesters the ribosome binding site and prevents translation of LcrF (Hoe and Goguen, 1993). This secondary structure is less stable at higher temperatures compared to lower temperatures. The hairpin loop is relieved at 37°C and allows for efficient translation of LcrF. Thus, LcrF is only expressed when *Yersinia* enters the human body or at 37°C *in vitro*. Variants of *lcrF* were engineered to either have an open mRNA state where the ribosome can be recruited at temperatures lower than 37°C, and a closed mutant where the mRNA would remain in a tight state where the ribosome would not have access to bind even at host body temperature (Böhme et al., 2012). Virulence studies showed that the closed *lcrF* mutant had a defect in dissemination to the Peyer's patches, liver, and spleen compared to WT. The closed mutant was also shown to be avirulent. The open mutant was attenuated in the YPIII background but was similar to WT in the IP32953 strain. Another example of virulence factor regulation when introduced to host conditions can be observed by virulence plasmid copy number control in *Yersinia*. A recent study showed that *Yersinia* increases copy number of the virulence plasmid when grow at 37°C in calcium deplete conditions compared to 26°C (Wang et al., 2016). The virulence plasmid copy number was also increased in bacteria recovered from Peyer's patches and the cecum 48 hours post infection. This regulation of copy number was also shown to be important for overall *Yersinia*

virulence in a mouse model. These results confirm coordination of virulence factor production when *Yersinia* encounters host conditions is crucial for pathogenicity.

ChIP Seq method

Chromatin immunoprecipitation followed by high-throughput sequencing (ChIP-seq) is a method that can identify protein-DNA binding sites (Myers et al., 2015). In bacteria a great deal of environmental response is regulated by transcription factors, and thus it may be important to determine a transcription factor's regulon. Although there are techniques such as electrophoretic mobility shift assay (EMSA) and DNase footprinting, which can identify if a transcription factor binds to a specific region of DNA, ChIP-seq allows for a more global approach in identifying where a transcription factor binds according to the genome.

ChIP-seq is performed by growing cells in the proper conditions, where the transcription factor will be expressed. The specific transcription factor can also be overexpressed using an inducible promoter if the specific transcription factor is normally expressed at a low level. However, overexpression of a transcription factor can lead to unspecific weak binding to degenerate binding sites. Proteins are then crosslinked to DNA by adding formaldehyde to the cells. The cells are then lysed to release the genomic-protein complexes and

the lysate is sonicated to fragment the DNA. The DNA-transcription factor complex is then immunoprecipitated (IP) with an antibody specific for the transcription factor. This antibody can be designed to bind to the native transcription factor, or the transcription factor can be fused to an affinity tag and be immunoprecipitated using an antibody designed for the affinity tag. If an affinity tag is used, the affinity tag should be designed to not affect activity or binding of the transcription factor. ChIP-qPCR can be utilized to test if an affinity tag affects binding of the transcription factor by performing qPCR following ChIP on genes that are known to be directly regulated by that specific transcription factor. There will also be a control sample called the input sample where the DNA-transcription complexes are not probed via an antibody. This sample represents the background signal of available chromatin for IP, which is not due to the transcription factor of interest. The DNA-transcription factor complexes are then denatured by heating, resulting in isolated DNA that was bound to the transcription factor of interest. This DNA is then ligated to adapter sequences and sequenced using a high-throughput method such as Illumina. The sequencing reads are then analyzed. First the sequencing reads go through quality control to determine the quality of the reads. Then the adapter sequences and poor reads are trimmed, and the remaining reads are aligned to the genome. Peaks of reads in the genome alignment are then called and assigned to a gene, which is determined to be bound to the specific transcription factor.

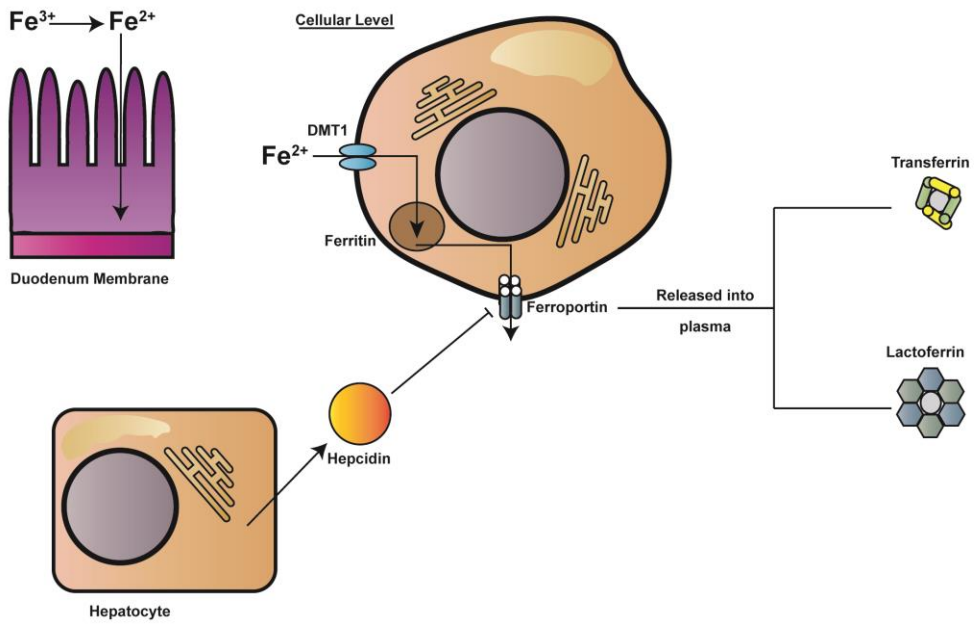


Figure 1. Iron trafficking in the mammalian host Ferric iron (Fe^{3+}) is converted to ferrous iron (Fe^{2+}) before being absorbed in the duodenum membrane. Ferrous iron can enter the cell via the transporter DMT1 and be stored as ferritin. This iron can be released from the cell into the plasma via the transporter ferroportin and will be coupled sequestered by transferrin or lactoferrin to prevent bacterial uptake of iron. Hepatocytes can produce hepcidin, which will result in degradation of ferroportin and thus less iron trafficking.

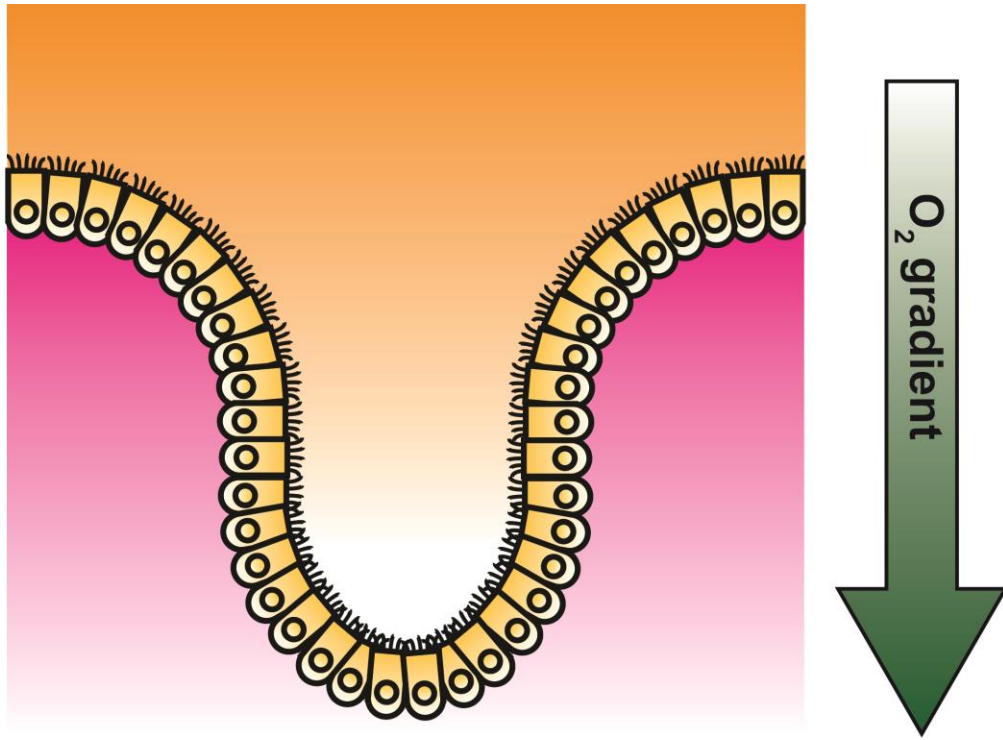


Figure 2. Oxygen gradient in the mammalian small intestine The concentration of oxygen becomes further increased in the villus compared to the intestinal lumen.

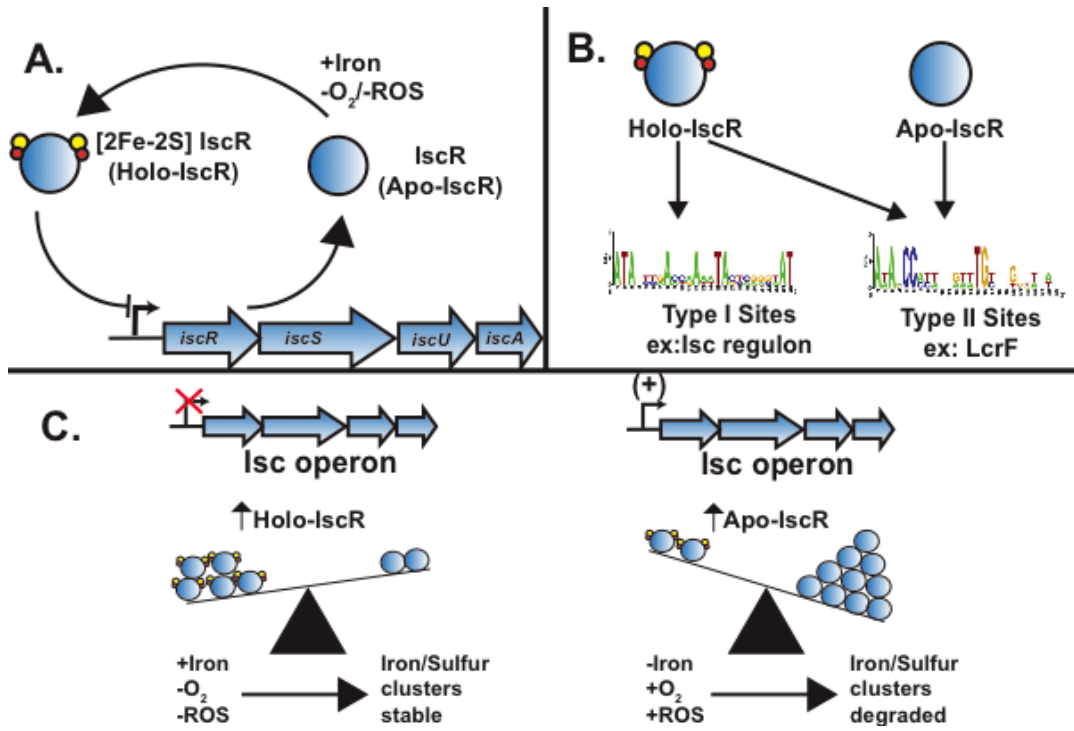


Figure 3. IscR regulates itself via a negative feedback loop and its activity is influenced by environmental conditions A. IscR participates in a negative feedback loop, where Holo-IscR binds upstream of the *isc* operon and prevents recruitment of RNA polymerase B. Holo-IscR can bind both type I and type II sites while Apo-IscR can only bind to type II sites. C. Environmental conditions such as oxygen tension and the bioavailability of iron affects if IscR is bound to Fe-S clusters or cluster-less, which ultimately affects expression of the *isc* operon.

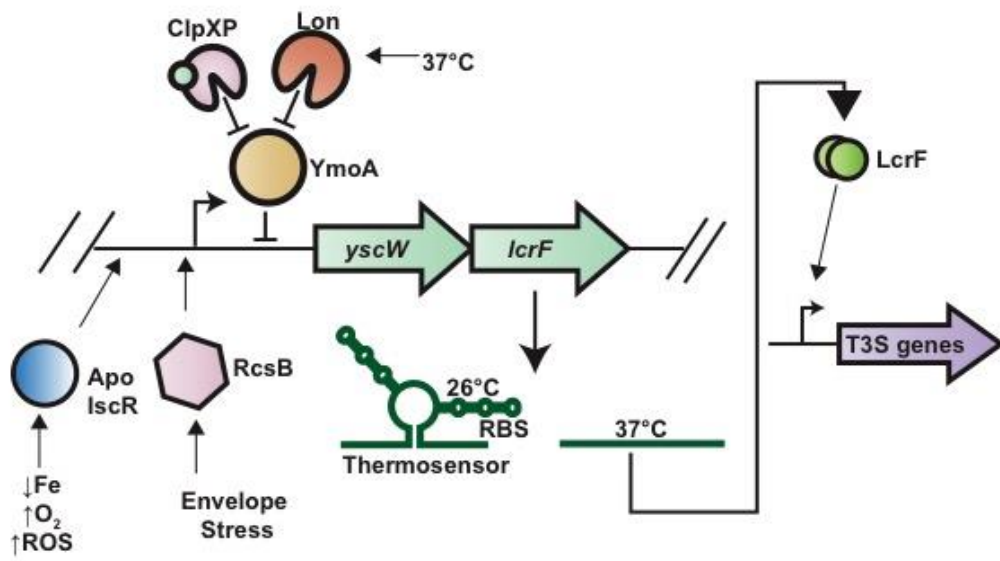


Figure 4. LcrF is regulated at both the transcriptional and post-transcriptional level Transcription of *lcrF* is blocked by the histone like protein YmoA. At host body temperature the proteases ClpXP and Lon become more enzymatically active and degrade YmoA leading to derepression of *lcrF* transcription. LcrF translation is also thermoregulated due to the presence of a thermosensor. This structure is also relieved at host body temperature allowing for recruitment of lcrF mRNA towards the ribosome to allow for translation.

References:

- Archibald, F. (1983). *Lactobacillus plantarum*, an organism not requiring iron. *FEMS Microbiol. Lett.* doi:10.1016/0378-1097(83)90353-1.
- Arezes, J., Jung, G., Gabayan, V., Valore, E., Ruchala, P., Gulig, P. A., et al. (2015). Hepcidin-induced hypoferremia is a critical host defense mechanism against the siderophilic bacterium *Vibrio vulnificus*. *Cell Host Microbe.* doi:10.1016/j.chom.2014.12.001.
- Arricau, N., Hermant, D., Waxin, H., Ecobichon, C., Duffey, P. S., and Popoff, M. Y. (1998). The RcsB-RcsC regulatory system of *Salmonella typhi* differentially modulates the expression of invasion proteins, flagellin and Vi antigen in response to osmolarity. *Mol. Microbiol.* doi:10.1046/j.1365-2958.1998.00976.x.
- Barbieri, N. L., Nicholson, B., Hussein, A., Cai, W., Wannemuehler, Y. M., Dell'Anna, G., et al. (2014). FNR regulates expression of important virulence factors contributing to pathogenicity of uropathogenic *Escherichia coli*. *Infect. Immun.* doi:10.1128/IAI.02315-14.
- Barnhart, M. M., Lynem, J., and Chapman, M. R. (2006). GlcNAc-6P levels modulate the expression of curli fibers by *Escherichia coli*. *J. Bacteriol.* doi:10.1128/JB.00234-06.
- Bartolini, E., Frigimelica, E., Giovinazzi, S., Galli, G., Shaik, Y., Genco, C., et al. (2006). Role of FNR and FNR-regulated, sugar fermentation genes in *Neisseria meningitidis* infection. *Mol. Microbiol.* doi:10.1111/j.1365-

2958.2006.05163.x.

- Beinert, H. (2000). Iron-sulfur proteins: Ancient structures, still full of surprises. *J. Biol. Inorg. Chem.* doi:10.1007/s007750050002.
- Beinert, H., and Kiley, P. J. (1999). Fe-S proteins in sensing and regulatory functions. *Curr. Opin. Chem. Biol.* doi:10.1016/S1367-5931(99)80027-1.
- Bhatt, S., Edwards, A. N., Nguyen, H. T. T., Merlin, D., Romeo, T., and Kalman, D. (2009). The RNA binding protein CsrA is a pleiotropic regulator of the locus of enterocyte effacement pathogenicity island of enteropathogenic *Escherichia coli*. *Infect. Immun.* doi:10.1128/IAI.00418-09.
- Blanc, B., Clémancey, M., Latour, J. M., Fontecave, M., and Ollagnier De Choudens, S. (2014). Molecular investigation of iron-sulfur cluster assembly scaffolds under stress. *Biochemistry.* doi:10.1021/bi5012496.
- Blanc, B., Gerez, C., and Ollagnier de Choudens, S. (2015). Assembly of Fe/S proteins in bacterial systems. Biochemistry of the bacterial ISC system. *Biochim. Biophys. Acta - Mol. Cell Res.* doi:10.1016/j.bbamcr.2014.12.009.
- Böhme, K., Steinmann, R., Kortmann, J., Seekircher, S., Heroven, A. K., Berger, E., et al. (2012). Concerted actions of a thermo-labile regulator and a unique intergenic RNA thermosensor control *Yersinia* virulence. *PLoS Pathog.* doi:10.1371/journal.ppat.1002518.
- Boysen, A., Møller-Jensen, J., Kallipolitis, B., Valentin-Hansen, P., and

- Overgaard, M. (2010). Translational regulation of gene expression by an anaerobically induced small non-coding RNA in *Escherichia coli*. *J. Biol. Chem.* doi:10.1074/jbc.M109.089755.
- Brown, E. M., Sadarangani, M., and Finlay, B. B. (2013). The role of the immune system in governing host-microbe interactions in the intestine. *Nat. Immunol.* doi:10.1038/ni.2611.
- Carreau, A., Hafny-Rahbi, B. El, Matejuk, A., Grillon, C., and Kieda, C. (2011). Why is the partial oxygen pressure of human tissues a crucial parameter? Small molecules and hypoxia. *J. Cell. Mol. Med.* doi:10.1111/j.1582-4934.2011.01258.x.
- Chang, D. E., Smalley, D. J., Tucker, D. L., Leatham, M. P., Norris, W. E., Stevenson, S. J., et al. (2004). Carbon nutrition of *Escherichia coli* in the mouse intestine. *Proc. Natl. Acad. Sci. U. S. A.* doi:10.1073/pnas.0307888101.
- Cherayil, B. J., Ellenbogen, S., and Shanmugam, N. N. (2011). Iron and intestinal immunity. *Curr. Opin. Gastroenterol.* doi:10.1097/MOG.0b013e32834a4cd1.
- Chiang, S. M., and Schellhorn, H. E. (2012). Regulators of oxidative stress response genes in *Escherichia coli* and their functional conservation in bacteria. *Arch. Biochem. Biophys.* doi:10.1016/j.abb.2012.02.007.
- Choi, J., Masaratana, P., Latunde-Dada, G. O., Arno, M., Simpson, R. J., and McKie, A. T. (2012). Duodenal reductase activity and spleen iron stores

- are reduced and erythropoiesis is abnormal in Dcytb knockout mice exposed to hypoxic conditions. *J. Nutr.* doi:10.3945/jn.112.160358.
- Choi, Y. S., Shin, D. H., Chung, I. Y., Kim, S. H., Heo, Y. J., and Cho, Y. H. (2007). Identification of *Pseudomonas aeruginosa* genes crucial for hydrogen peroxide resistance. *J. Microbiol. Biotechnol.*
- Coburn, B., Sekirov, I., and Finlay, B. B. (2007). Type III secretion systems and disease. *Clin. Microbiol. Rev.* doi:10.1128/CMR.00013-07.
- Cornelis, G. R. (1993). Role of the Transcription Activator VirF and the Histone-like Protein YmoA in the Thermoregulation of Virulence Functions in *Yersinia*. *Zentralblatt fur Bakteriologie*. doi:10.1016/S0934-8840(11)80833-9.
- Cornelis, G. R., Boland, A., Boyd, A. P., Geuijen, C., Iriarte, M., Neyt, C., et al. (1998). The Virulence Plasmid of *Yersinia*, an Antihost Genome. *Microbiol. Mol. Biol. Rev.* doi:10.1128/mmbr.62.4.1315-1352.1998.
- Demple, B., and Amábile-Cuevas, C. F. (1991). Redox redux: The control of oxidative stress responses. *Cell*. doi:10.1016/0092-8674(91)90355-3.
- DONOHUE, D. M., GABRIO, B. W., and FINCH, C. A. (1958). Quantitative measurement of hematopoietic cells of the marrow. *J. Clin. Invest.* doi:10.1172/JCI103749.
- Ellison, D. W., Young, B., Nelson, K., and Miller, V. L. (2003). YmoA Negatively Regulates Expression of Invasin from *Yersinia enterocolitica*. *J. Bacteriol.* doi:10.1128/JB.185.24.7153-7159.2003.

- Fang, F. C., and Weiss, G. (2014). Iron ERRs with Salmonella. *Cell Host Microbe*. doi:10.1016/j.chom.2014.04.012.
- Filip-Ciubotaru, F., Manciu, C., Stoleriu, G., and Foia, L. (2016). NADPH OXIDASE: STRUCTURE AND ACTIVATION MECHANISMS (REVIEW). NOTE I. *Rev. medico-chirurgicală a Soc. Medici și Nat. din Iași*.
- Fink, R. C., Evans, M. R., Porwollik, S., Vazquez-Torres, A., Jones-Carson, J., Troxell, B., et al. (2007). FNR is a global regulator of virulence and anaerobic metabolism in Salmonella enterica serovar typhimurium (ATCC 14028s). *J. Bacteriol.* doi:10.1128/JB.00726-06.
- Fisher, E. M., Khan, M., Salisbury, R., and Kuppusamy, P. (2013). Noninvasive Monitoring of Small Intestinal Oxygen in a Rat Model of Chronic Mesenteric Ischemia. *Cell Biochem. Biophys.* doi:10.1007/s12013-013-9611-y.
- Fortune, D. R., Suyemoto, M., and Altier, C. (2006). Identification of CsrC and characterization of its role in epithelial cell invasion in Salmonella enterica serovar typhimurium. *Infect. Immun.* doi:10.1128/IAI.74.1.331-339.2006.
- Ghosh, S., Rao, K. H., Sengupta, M., Bhattacharya, S. K., and Datta, A. (2011). Two gene clusters co-ordinate for a functional N-acetylglucosamine catabolic pathway in Vibrio cholerae. *Mol. Microbiol.* doi:10.1111/j.1365-2958.2011.07664.x.
- Giel, J. L., Rodionov, D., Liu, M., Blattner, F. R., and Kiley, P. J. (2006). IscR-

- dependent gene expression links iron-sulphur cluster assembly to the control of O₂-regulated genes in *Escherichia coli*. *Mol. Microbiol.* doi:10.1111/j.1365-2958.2006.05160.x.
- Green, J., Irvine, A. S., Meng, W., and Guest, J. R. (1996). FNR-DNA interactions at natural and semi-synthetic promoters. *Mol. Microbiol.* doi:10.1046/j.1365-2958.1996.353884.x.
- Greijer, A. E., van der Groep, P., Kemming, D., Shvarts, A., Semenza, G. L., Meijer, G. A., et al. (2005). Up-regulation of gene expression by hypoxia is mediated predominantly by hypoxia-inducible factor 1 (HIF-1). *J. Pathol.* doi:10.1002/path.1778.
- Gunshin, H., Mackenzie, B., Berger, U. V., Gunshin, Y., Romero, M. F., Boron, W. F., et al. (1997). Cloning and characterization of a mammalian proton-coupled metal-ion transporter. *Nature*. doi:10.1038/41343.
- Guzy, R. D., and Schumacker, P. T. (2006). Oxygen sensing by mitochondria at complex III: The paradox of increased reactive oxygen species during hypoxia. in *Experimental Physiology* doi:10.1113/expphysiol.2006.033506.
- Han, Y., Geng, J., Qiu, Y., Guo, Z., Zhou, D., Bi, Y., et al. (2008). Physiological and regulatory characterization of KatA and KatY in *Yersinia pestis*. *DNA Cell Biol.* doi:10.1089/dna.2007.0657.
- Hassett, D. J., and Cohen, M. S. (1989). Bacterial adaptation to oxidative stress: implications for pathogenesis and interaction with phagocytic

- cells. *FASEB J.* doi:10.1096/fasebj.3.14.2556311.
- Heroven, A. K., Böhme, K., and Dersch, P. (2012). The Csr/Rsm system of yersinia and related pathogens: A post-transcriptional strategy for managing virulence. *RNA Biol.* doi:10.4161/rna.19333.
- Hoe, N. P., and Goguen, J. D. (1993). Temperature sensing in *Yersinia pestis*: Translation of the LcrF activator protein is thermally regulated. *J. Bacteriol.* doi:10.1128/jb.175.24.7901-7909.1993.
- Imlay, J. A. (2003). Pathways of Oxidative Damage. *Annu. Rev. Microbiol.* doi:10.1146/annurev.micro.57.030502.090938.
- Jackson, A. A., Gross, M. J., Daniels, E. F., Hampton, T. H., Hammond, J. H., Vallet-Gely, I., et al. (2013). Anr and its activation by PlcH activity in *Pseudomonas aeruginosa* host colonization and virulence. *J. Bacteriol.* doi:10.1128/JB.02169-12.
- Jackson, M. W., Silva-Herzog, E., and Plano, G. V. (2004). The ATP-dependent ClpXP and Lon proteases regulate expression of the *Yersinia pestis* type III secretion system via regulated proteolysis of YmoA, a small histone-like protein. *Mol. Microbiol.* doi:10.1111/j.1365-2958.2004.04353.x.
- Jacobson, M. R., Cash, V. L., Weiss, M. C., Laird, N. F., Newton, W. E., and Dean, D. R. (1989). Biochemical and genetic analysis of the nifUSVWZM cluster from *Azotobacter vinelandii*. *MGG Mol. Gen. Genet.* doi:10.1007/BF00261156.

- Jang, J., Jung, K. T., Yoo, C. K., and Rhie, G. eun (2010). Regulation of hemagglutinin/protease expression by the VarS/VarA-CsrA/B/C/D system in *Vibrio cholerae*. *Microb. Pathog.* doi:10.1016/j.micpath.2010.03.003.
- Jang, K. K., Gil, S. Y., Lim, J. G., and Choi, S. H. (2016). Regulatory characteristics of *Vibrio vulnificus* gbpA gene encoding a mucin-binding protein essential for pathogenesis. *J. Biol. Chem.* doi:10.1074/jbc.M115.685321.
- Jang, S., and Imlay, J. A. (2010). Hydrogen peroxide inactivates the *Escherichia coli* Isc iron-sulphur assembly system, and OxyR induces the Suf system to compensate. *Mol. Microbiol.* doi:10.1111/j.1365-2958.2010.07418.x.
- Johnson, D. C., Dean, D. R., Smith, A. D., and Johnson, M. K. (2005). Structure, function, and formation of biological iron-sulfur clusters. *Annu. Rev. Biochem.* doi:10.1146/annurev.biochem.74.082803.133518.
- Kawada-Matsuo, M., Mazda, Y., Oogai, Y., Kajiya, M., Kawai, T., Yamada, S., et al. (2012). GlnS and NagB regulate amino sugar metabolism in opposing directions and affect *Streptococcus mutans* virulence. *PLoS One.* doi:10.1371/journal.pone.0033382.
- Kim, S. H., Lee, B. Y., Lau, G. W., and Cho, Y. H. (2009). IscR modulates catalase a (KatA) activity, peroxide resistance, and full virulence of *Pseudomonas aeruginosa* PA14. *J. Microbiol. Biotechnol.* doi:10.4014/jmb.0906.06028.

- Korgaonkar, A. K., and Whiteley, M. (2011). *Pseudomonas aeruginosa* enhances production of an antimicrobial in response to N-acetylglucosamine and peptidoglycan. *J. Bacteriol.* doi:10.1128/JB.01175-10.
- Kortman, G. A. M., Raffatellu, M., Swinkels, D. W., and Tjalsma, H. (2014). Nutritional iron turned inside out: Intestinal stress from a gut microbial perspective. *FEMS Microbiol. Rev.* doi:10.1111/1574-6976.12086.
- Kovacikova, G., Lin, W., and Skorupski, K. (2004). *Vibrio cholerae* AphA uses a novel mechanism for virulence gene activation that involves interaction with the LysR-type regulator AphB at the tcpPH promoter. *Mol. Microbiol.* doi:10.1111/j.1365-2958.2004.04121.x.
- Kovacikova, G., and Skorupski, K. (1999). A *Vibrio cholerae* LysR homolog, AphB, cooperates with AphA at the tcpPH promoter to activate expression of the ToxR virulence cascade. *J. Bacteriol.* doi:10.1128/jb.181.14.4250-4256.1999.
- Kuntumalla, S., Zhang, Q., Braisted, J. C., Fleischmann, R. D., Peterson, S. N., Donohue-Rolfe, A., et al. (2011). In vivo versus in vitro protein abundance analysis of *Shigella dysenteriae* type 1 reveals changes in the expression of proteins involved in virulence, stress and energy metabolism. *BMC Microbiol.* doi:10.1186/1471-2180-11-147.
- Lee, K. C., Yeo, W. S., and Roe, J. H. (2008). Oxidant-responsive induction of the suf operon, encoding a Fe-S assembly system, through Fur and IscR

- in *Escherichia coli*. *J. Bacteriol.* doi:10.1128/JB.01161-08.
- Li, Y., Hu, Y., Francis, M. S., and Chen, S. (2015). RcsB positively regulates the Yersinia Ysc-Yop type III secretion system by activating expression of the master transcriptional regulator LcrF. *Environ. Microbiol.* doi:10.1111/1462-2920.12556.
- Lill, R. (2009). Function and biogenesis of iron-sulphur proteins. *Nature.* doi:10.1038/nature08301.
- Lim, J. G., Bang, Y. J., and Choi, S. H. (2014a). Characterization of the vibrio vulnificus 1-Cys peroxiredoxin prx3 and regulation of its expression by the Fe-S cluster regulator IscR in response to oxidative stress and iron starvation. *J. Biol. Chem.* doi:10.1074/jbc.M114.611020.
- Lim, J. G., and Choi, S. H. (2014). IscR is a global regulator essential for pathogenesis of vibrio vulnificus and induced by host cells. *Infect. Immun.* doi:10.1128/IAI.01141-13.
- Lim, J. G., Park, J. H., and Choi, S. H. (2014b). Low cell density regulator AphA upregulates the expression of Vibrio vulnificus iscR gene encoding the Fe-S cluster regulator IscR. *J. Microbiol.* doi:10.1007/s12275-014-3592-4.
- Liu, J., Thanikkal, E. J., Obi, I. R., and Francis, M. S. (2012). Elevated CpxR~P levels repress the Ysc-Yop type III secretion system of Yersinia pseudotuberculosis. *Res. Microbiol.* doi:10.1016/j.resmic.2012.07.010.
- Lucchini, S., Liu, H., Jin, Q., Hinton, J. C. D., and Yu, J. (2005).

- Transcriptional adaptation of *Shigella flexneri* during infection of macrophages and epithelial cells: Insights into the strategies of a cytosolic bacterial pathogen. *Infect. Immun.* doi:10.1128/IAI.73.1.88-102.2005.
- Majdalani, N., and Gottesman, S. (2005). The Rcs phosphorelay: A complex signal transduction system. *Annu. Rev. Microbiol.* doi:10.1146/annurev.micro.59.050405.101230.
- Mazur, A., Feillet-Coudray, C., Romier, B., Bayle, D., Gueux, E., Ruivard, M., et al. (2003). Dietary iron regulates hepatic hepcidin 1 and 2 mRNAs in mice. *Metabolism.* doi:10.1016/S0026-0495(03)00277-4.
- McKie, A. T., Barrow, D., Latunde-Dada, G. O., Rolfs, A., Sager, G., Mudaly, E., et al. (2001). An iron-regulated ferric reductase associated with the absorption of dietary iron. *Science (80-.).* doi:10.1126/science.1057206.
- Miller, H. K., Kwuan, L., Schwiesow, L., Bernick, D. L., Mettert, E., Ramirez, H. A., et al. (2014). IscR Is Essential for *Yersinia pseudotuberculosis* Type III Secretion and Virulence. *PLoS Pathog.* doi:10.1371/journal.ppat.1004194.
- Miller, V. L., and Mekalanos, J. J. (1988). A novel suicide vector and its use in construction of insertion mutations: Osmoregulation of outer membrane proteins and virulence determinants in *Vibrio cholerae* requires *toxR*. *J. Bacteriol.* doi:10.1128/jb.170.6.2575-2583.1988.
- Moore, L. J., Mettert, E. L., and Kiley, P. J. (2006). Regulation of FNR

- dimerization by subunit charge repulsion. *J. Biol. Chem.*
doi:10.1074/jbc.M608331200.
- Myers, K. S., Park, D. M., Beauchene, N. A., and Kiley, P. J. (2015). Defining bacterial regulons using CHIP-seq. *Methods.*
doi:10.1016/j.ymeth.2015.05.022.
- Nairz, M., Haschka, D., Demetz, E., and Weiss, G. (2014). Iron at the interface of immunity and infection. *Front. Pharmacol.*
doi:10.3389/fphar.2014.00152.
- Nemeth, E., Tuttle, M. S., Powelson, J., Vaughn, M. D., Donovan, A., Ward, D. M. V., et al. (2004). Heparin regulates cellular iron efflux by binding to ferroportin and inducing its internalization. *Science (80-.).*
doi:10.1126/science.1104742.
- Nieto, J. M., Madrid, C., Miquelay, E., Parra, J. L., Rodríguez, S., and Juárez, A. (2002). Evidence for direct protein-protein interaction between members of the enterobacterial Hha/YmoA and H-NS families of proteins. *J. Bacteriol.* doi:10.1128/JB.184.3.629-635.2002.
- Ollagnier-de Choudens, S., Nachin, L., Sanakis, Y., Loiseau, L., Barras, F., and Fontecave, M. (2003). SufA from *Erwinia chrysanthemi*. Characterization of a scaffold protein required for iron-sulfur cluster assembly. *J. Biol. Chem.* doi:10.1074/jbc.M300285200.
- Paradkar, P. N., De Domenico, I., Durchfort, N., Zohn, I., Kaplan, J., and Ward, D. M. V. (2008). Iron depletion limits intracellular bacterial growth

- in macrophages. *Blood*. doi:10.1182/blood-2007-12-126854.
- Park, C. H., Valore, E. V., Waring, A. J., and Ganz, T. (2001). Hepsidin, a Urinary Antimicrobial Peptide Synthesized in the Liver. *J. Biol. Chem.* doi:10.1074/jbc.M008922200.
- Pessi, G., Williams, F., Hindle, Z., Heurlier, K., Holden, M. T. G., Cámara, M., et al. (2001). The global posttranscriptional regulator RsmA modulates production of virulence determinants and N-acylhomoserine lactones in *Pseudomonas aeruginosa*. *J. Bacteriol.* doi:10.1128/JB.183.22.6676-6683.2001.
- Pierson, D. E., and Falkow, S. (1993). The ail gene of *Yersinia enterocolitica* has a role in the ability of the organism to survive serum killing. *Infect. Immun.*
- Posey, J. E., and Gherardini, F. C. (2000). Lack of a role for iron in the Lyme disease pathogen. *Science (80-)*. doi:10.1126/science.288.5471.1651.
- Putzker, M., Sauer, H., and Sobe, D. (2001). Plague and other human infections caused by *Yersinia* species. *Clin. Lab.*
- Py, B., and Barras, F. (2010). Building Feg-S proteins: Bacterial strategies. *Nat. Rev. Microbiol.* doi:10.1038/nrmicro2356.
- Raida, M. K., and Buchmann, K. (2009). Innate immune response in rainbow trout (*Oncorhynchus mykiss*) against primary and secondary infections with *Yersinia ruckeri* O1. *Dev. Comp. Immunol.* doi:10.1016/j.dci.2008.07.001.

- Rajagopalan, S., Teter, S. J., Zwart, P. H., Brennan, R. G., Phillips, K. J., and Kiley, P. J. (2013). Studies of IscR reveal a unique mechanism for metal-dependent regulation of DNA binding specificity. *Nat. Struct. Mol. Biol.* doi:10.1038/nsmb.2568.
- Runyen-Janecky, L., Daugherty, A., Lloyd, B., Wellington, C., Eskandarian, H., and Sgransky, M. (2008). Role and regulation of iron-sulfur cluster biosynthesis genes in *Shigella flexneri* virulence. *Infect. Immun.* doi:10.1128/IAI.01211-07.
- Runyen-Janecky, L. J., and Payne, S. M. (2002). Identification of chromosomal *Shigella flexneri* genes induced by the eukaryotic intracellular environment. *Infect. Immun.* doi:10.1128/IAI.70.8.4379-4388.2002.
- Sahr, T., Brüggemann, H., Jules, M., Lomma, M., Albert-Weissenberger, C., Cazalet, C., et al. (2009). Two small ncRNAs jointly govern virulence and transmission in *Legionella pneumophila*. *Mol. Microbiol.* doi:10.1111/j.1365-2958.2009.06677.x.
- Santos, J. A., Pereira, P. J. B., and Macedo-Ribeiro, S. (2015). What a difference a cluster makes: The multifaceted roles of IscR in gene regulation and DNA recognition. *Biochim. Biophys. Acta - Proteins Proteomics.* doi:10.1016/j.bbapap.2015.01.010.
- Schwartz, C. J., Giel, J. L., Patschkowski, T., Luther, C., Ruzicka, F. J., Beinert, H., et al. (2001). IscR, an Fe-S cluster-containing transcription

- factor, represses expression of escherichia coli genes encoding Fe-S cluster assembly proteins. *Proc. Natl. Acad. Sci. U. S. A.*
doi:10.1073/pnas.251550898.
- Schweer, J., Kulkarni, D., Kochut, A., Pezoldt, J., Pisano, F., Pils, M. C., et al. (2013). The Cytotoxic Necrotizing Factor of *Yersinia pseudotuberculosis* (CNFY) Enhances Inflammation and Yop Delivery during Infection by Activation of Rho GTPases. *PLoS Pathog.*
doi:10.1371/journal.ppat.1003746.
- Schwiesow, L., Lam, H., Dersch, P., and Auerbuch, V. (2016). *Yersinia* type III secretion system master regulator LcrF. *J. Bacteriol.*
doi:10.1128/JB.00686-15.
- Scott, C., Partridge, J. D., Stephenson, J. R., and Green, J. (2003). DNA target sequence and FNR-dependent gene expression. *FEBS Lett.*
doi:10.1016/S0014-5793(03)00312-0.
- Sohanpal, B. K., El-Labany, S., Lahooti, M., Plumbridge, J. A., and Blomfield, I. C. (2004). Integrated regulatory responses of fimB to N-acetylneuraminic (sialic) acid and GlcNAc in *Escherichia coli* K-12. *Proc. Natl. Acad. Sci. U. S. A.* doi:10.1073/pnas.0405821101.
- Somprasong, N., Jittawuttiyapoka, T., Duang-Nkern, J., Romsang, A., Chaiyen, P., Schweizer, H. P., et al. (2012). *Pseudomonas aeruginosa* Thiol Peroxidase Protects against Hydrogen Peroxide Toxicity and Displays Atypical Patterns of Gene Regulation. *J. Bacteriol.*

doi:10.1128/JB.00347-12.

Strom, M. S., and Paranjpye, R. N. (2000). Epidemiology and pathogenesis of *Vibrio vulnificus*. *Microbes Infect.* doi:10.1016/S1286-4579(00)00270-7.

Taylor, C. T., and Colgan, S. P. (2007). Hypoxia and gastrointestinal disease. *J. Mol. Med.* doi:10.1007/s00109-007-0277-z.

Troisfontaines, P., and Cornelis, G. R. (2005). Type III secretion: More systems than you think. *Physiology.* doi:10.1152/physiol.00011.2005.

Venecia, K., and Young, G. M. (2005). Environmental regulation and virulence attributes of the Ysa type III secretion system of *Yersinia enterocolitica* biovar 1B. *Infect. Immun.* doi:10.1128/IAI.73.9.5961-5977.2005.

Vergnes, A., Viala, J. P. M., Ouadah-Tsabet, R., Pocachard, B., Loiseau, L., Méresse, S., et al. (2017). The iron–sulfur cluster sensor IscR is a negative regulator of Spi1 type III secretion system in *Salmonella enterica*. *Cell. Microbiol.* doi:10.1111/cmi.12680.

Von Drygalski, A., and Adamson, J. W. (2013). Iron metabolism in man. *J. Parenter. Enter. Nutr.* doi:10.1177/0148607112459648.

Vulpe, C. D., Kuo, Y. M., Murphy, T. L., Cowley, L., Askwith, C., Libina, N., et al. (1999). Hephaestin, a ceruloplasmin homologue implicated in intestinal iron transport, is defective in the sla mouse. *Nat. Genet.* doi:10.1038/5979.

Wang, G. L., and Semenza, G. L. (1993). General involvement of hypoxia-

- inducible factor 1 in transcriptional response to hypoxia. *Proc. Natl. Acad. Sci. U. S. A.* doi:10.1073/pnas.90.9.4304.
- Wang, H., Avican, K., Fahlgren, A., Erttmann, S. F., Nuss, A. M., Dersch, P., et al. (2016). Increased plasmid copy number is essential for Yersinia T3SS function and virulence. *Science (80-.)*. doi:10.1126/science.aaf7501.
- Wang, T., Si, M., Song, Y., Zhu, W., Gao, F., Wang, Y., et al. (2015). Type VI Secretion System Transports Zn²⁺ to Combat Multiple Stresses and Host Immunity. *PLoS Pathog.* doi:10.1371/journal.ppat.1005020.
- Wright, P. R., Richter, A. S., Papenfort, K., Mann, M., Vogel, J., Hess, W. R., et al. (2013). Comparative genomics boosts target prediction for bacterial small RNAs. *Proc. Natl. Acad. Sci. U. S. A.* doi:10.1073/pnas.1303248110.
- Wu, H. J., Wang, A. H. J., and Jennings, M. P. (2008). Discovery of virulence factors of pathogenic bacteria. *Curr. Opin. Chem. Biol.* doi:10.1016/j.cbpa.2008.01.023.
- Yamashita, S., Lukacik, P., Barnard, T. J., Noinaj, N., Felek, S., Tsang, T. M., et al. (2011). Structural insights into ail-mediated adhesion in Yersinia pestis. *Structure*. doi:10.1016/j.str.2011.08.010.

Chapter 2

Genomic scale analysis reveals IscR directly and indirectly regulates virulence factor genes in pathogenic Yersinia

By David Balderas, Erin Mettert, Hanh N. Lam, Rajdeep Banerjee, Tomas
Gverzdys, Pablo Alvarez, Geetha Saarunya, Natasha Tanner, Adam Zoubedi,
Yahan Wei, Patricia J. Kiley, Victoria Auerbuch

Abstract

The iron-sulfur cluster coordinating transcription factor IscR is important for the virulence of *Yersinia pseudotuberculosis* and a number of other bacterial pathogens. However, the IscR regulon has not yet been defined in any organism. To determine the *Yersinia* IscR regulon and identify IscR-dependent functions important for virulence, we employed chromatin immunoprecipitation sequencing (ChIP-Seq) and RNA sequencing (RNA-Seq) of *Y. pseudotuberculosis* expressing or lacking *iscR* following iron starvation conditions, such as those encountered during infection. We found that IscR binds to the promoters of genes involved in iron homeostasis, reactive oxygen species metabolism, and cell envelope remodeling, and regulates expression of these genes in response to iron depletion. Consistent with our previous work, we also found that IscR binds *in vivo* to the promoter of the Ysc type III secretion system (T3SS) master regulator LcrF, leading to regulation of T3SS genes. Interestingly, comparative genomic analysis suggested over 93% of IscR binding sites were conserved between *Y. pseudotuberculosis* and the related plague agent *Yersinia pestis*. Surprisingly, we found that the IscR positively-regulated *sufABCDSE* Fe-S cluster biogenesis pathway was required for T3SS activity. These data suggest that IscR regulates the T3SS in *Yersinia* through maturation of an Fe-S cluster protein critical for type III secretion, in addition to its known role in activating T3SS genes through LcrF. Altogether, our study shows that iron starvation

triggers IscR to co-regulate multiple, distinct pathways relevant to promoting bacterial survival during infection.

Importance

How bacteria adapt to the changing environment within the host is critical for their ability to survive and cause disease. For example, the mammalian host severely restricts iron availability to limit bacterial growth, referred to as nutritional immunity. Here we show that pathogenic *Yersinia* use the Iron-sulfur (Fe-S) cluster Regulator IscR, a factor critical for pathogenesis, to sense iron availability and regulate multiple pathways known or predicted to contribute to virulence. Under low iron conditions that mimic those *Yersinia* encounter during infection, IscR levels increase, leading to modulation of genes involved in iron metabolism, stress resistance, cell envelope remodeling, and subversion of host defenses. These data suggest that IscR senses nutritional immunity to coordinate processes important for bacterial survival within the mammalian host.

Introduction

Iron is an important cofactor for many proteins involved in respiration, oxidative stress resistance, gene regulation, and other processes (Heroven and Dersch, 2014). Most bacteria require $\sim 10^{-6}$ M iron to support optimal growth. Yet in the mammalian host the level of free iron is only 10^{-18} M due to the concerted action of mammalian iron storage and carrier proteins (Litwin and Calderwood, 1993; Carpenter and Payne, 2014). During infection, the amount of available iron decreases even further as a result of nutritional immunity, a process through which inflammatory mediators lead to further sequestration of iron (Rohmer et al., 2011). *Y. pseudotuberculosis* and the related enteropathogen *Y. enterocolitica* cause self-limiting mesenteric lymphadenitis and gastroenteritis in immunocompetent people as well as serious disseminated infection in iron overloaded individuals (Putzker et al., 2001; Dube, 2009). The plague agent *Y. pestis* is closely related to *Y. pseudotuberculosis*, emerging as a distinct species $\sim 1,500$ - $6,400$ years ago (Sun et al., 2014). The elevated susceptibility of iron overloaded individuals to disseminated *Yersinia* infection underscores the low iron bioavailability experienced by *Yersinia* in mammalian tissues other than the intestinal lumen, despite expression of multiple iron uptake systems (Quenee et al., 2012; Miller et al., 2016; Hooker-Romero et al., 2019). *In vitro*, enteropathogenic *Yersinia* can utilize both inorganic and heme iron sources through a number of iron uptake systems typical of many pathogens

(Stojiljkovic and Hantke, 1992; Thompson et al., 1999; Perry et al., 2015; Schwiesow et al., 2018). Although the importance of iron availability in *Yersinia* infection is well accepted, the transcription regulatory networks that operate under iron starvation conditions have not been firmly established.

In many pathogenic bacteria, expression of iron uptake systems and virulence factors is controlled by the conserved global iron regulator Fur (Troxell and Hassan, 2013). Although multiple iron uptake systems are controlled by Fur in *Yersinia* including yersiniabactin, the key siderophore in pathogenic *Yersinia*, Fur has not been shown to directly regulate known virulence factors other than those involved in metal acquisition (Gao et al., 2008; Perry and Fetherston, 2011). Rather, we discovered that expression of a key virulence factor, the *Yersinia* secretion (Ysc) type III secretion system (T3SS), encoded on a 70 kb virulence plasmid pYV/pCD1 (Gemski et al., 1980), was controlled by a different iron-regulated transcription factor, IscR (Miller et al., 2014; Hooker-Romero et al., 2019). Subsequently, IscR has been shown to coordinate virulence factor expression in multiple pathogens (Choi et al., 2007, 2020; Jones-Carson et al., 2008; Lim and Choi, 2014; Vergnes et al., 2017).

In *E. coli* where IscR was discovered, DNA binding is regulated by ligation of an Fe-S cluster (Schwartz et al., 2001a), providing a linkage between iron

availability and activity of this transcription factor. *E. coli* IscR controls the expression of more than 40 genes, including anaerobic metabolism and respiration, and the Isc and Suf Fe-S cofactor biogenesis systems (Giel et al., 2006). IscR exists in either a holo form, when it is bound to a [2Fe-2S] cluster, or in an apo form, which is clusterless (Ruzicka et al., 2002). While holo-IscR binds to so-called type I motif sequences with a significantly higher affinity than apo-IscR, both holo-IscR and apo-IscR can bind to type II motif sequences (Ruzicka et al., 2002; Nesbit et al., 2009; Rajagopalan et al., 2013). IscR can both activate and repress transcription depending on the position of its binding site relative to a promoter. Bioavailability of iron, oxygen tension, and reactive oxygen species have all been inferred to affect the relative ratio of holo- to apo-IscR (Schwartz et al., 2001b; Zheng et al., 2001; Outten et al., 2004; Imlay, 2006; Yeo et al., 2006; Py et al., 2011; Giel et al., 2013; Miller and Auerbuch, 2015). In turn, holo-IscR negatively regulates *iscR* transcription through two type I motif sequences in the *isc* operon promoter, leading to an increase in overall IscR levels under aerobic and/or iron-starved conditions (Schwartz et al., 2001b; Hooker-Romero et al., 2019), and derepression of the Isc and Suf biogenesis pathways to maintain Fe-S cluster homeostasis (Schwartz et al., 2001a; Giel et al., 2006).

In *Yersinia*, IscR binds to a type II motif in the promoter of the gene encoding LcrF, the master regulator of the Ysc T3SS (Miller et al., 2014; Hooker-

Romero et al., 2019). IscR, and subsequently LcrF, levels increase with oxygen tension through derepression of the *isc* operon, driving T3SS expression (Hooker-Romero et al., 2019) . While the T3SS is important for *Yersinia* virulence, *Y. pseudotuberculosis* lacking T3SS expression can still colonize the intestinal lumen as well as the mesenteric lymph nodes (Simonet et al., 1984; Balada-Llasat and Meccas, 2006; Crimmins et al., 2012; Hooker-Romero et al., 2019). In contrast, *Y. pseudotuberculosis* lacking *iscR* is defective in colonization of all mouse tissues tested (Miller et al., 2014; Hooker-Romero et al., 2019). This suggests that IscR regulates additional virulence factors in *Yersinia*. In order to assess further how IscR contributes to *Yersinia* virulence, we used whole transcriptome RNA sequencing (RNA-Seq) and chromatin immunoprecipitation with massively parallel DNA sequencing (ChIP-Seq) to identify genes directly regulated by IscR following iron starvation, which *Yersinia* experiences during disseminated infection. Interestingly, comparative genomics revealed very high predicted conservation of the IscR regulon in *Y. pestis*. One highly conserved IscR binding site was found in the promoter of the *suf* Fe-S cluster biogenesis operon. Surprisingly, our data shows that IscR direct regulation of the *Y. pseudotuberculosis* *suf* operon is critical for T3SS activity under iron depleted conditions.

Results

Identification of IscR and iron regulated genes in *Y. pseudotuberculosis*

Yersinia experience iron starvation during extraintestinal infection (Sebbane et al., 2006; Nuss et al., 2017). Since IscR levels and activity are regulated by iron, we chose to assess the bacterial transcriptional response following iron starvation. Wildtype and $\Delta iscR$ *Y. pseudotuberculosis* were starved for iron using previously published methods (see Materials and Methods)(Schwiesow et al., 2018). Cultures either remained iron limited (no iron added back to Chelex-treated media) or were supplemented with organic iron (5 μ M hemin) or inorganic iron (3.6 μ M FeSO₄), which can both be utilized by *Yersinia* via distinct uptake systems (Stojiljkovic and Hantke, 1992; Thompson et al., 1999; Perry et al., 2015; Schwiesow et al., 2018) , and incubated for three hours at 37°C. RNA-Seq analysis showed that levels of IscR mRNA and protein were highest following prolonged iron starvation compared to after iron supplementation (Fig 1A-C). As holo-IscR negatively regulates *isc* operon transcription, these data are consistent with a decrease in holo-IscR activity following iron starvation and suggest that these growth conditions modulate IscR-regulated gene expression and provide a mimic of conditions found in the host. Indeed, we previously found that even adding back only 0.036 μ M FeSO₄ prevented de-repression of *iscR* expression (Hooker-Romero et al., 2019).

Global RNA-Seq analysis revealed a number of genes that respond to iron availability. We used clustering analysis to sort these differentially expressed genes into seven groups based on the relative changes in expression following prolonged iron starvation compared to supplementation with inorganic iron or heme. The two largest clusters were either genes that were downregulated (Cluster VI) or upregulated (Cluster II) in response to iron limitation. (Fig 2; Supplemental Dataset 1). Cluster VI and II genes also showed similar expression between the two iron sources. Cluster II genes contained *iscR* in addition to genes involved in iron uptake (*ex-hemPR*, *hmuSTUV*, *iutA/iucABCD*, *feoB*), iron sulfur cluster biogenesis (*sufABCDS*), LPS biosynthesis and modification (*arnABCDE*, *lpxABDTL*, *rfaQ*, *pagP*), lipoprotein and outer membrane protein targeting (*lolCDE*, *bamA*, *surA*, *skp*), cell wall remodeling and defense, the *dusB-fis* virulence-associated operon, and the T3SS. Upregulation of iron uptake genes and the *suf* operon in response to iron starvation was expected given previous studies (Outten et al., 2004; Perry et al., 2015; Schwiesow et al., 2018), but regulation of LPS modification, periplasmic protein targeting, and cell wall remodeling by iron has not been previously reported in *Yersinia*. Cluster VI included genes involved in energy metabolism (*sucABCD*, *fdoGHI*, *dmsAD*), antioxidants (*sodB*, *katAG*, *ompW*), and the AI-2 autoinducer pathway (*IsrR* regulator and *Isr* operon). Altogether, these results suggest that *Y. pseudotuberculosis* increases iron metabolism and cell envelope remodeling during iron

starvation, a condition known to be experienced by *Yersinia* during extraintestinal infection (Sebbane et al., 2006; Nuss et al., 2017).

Genes that are differentially regulated in response to changes in iron availability may be controlled by IscR, Fur, and possibly other transcription factors, or may be indirectly regulated by these factors. In order to determine which genes are affected by IscR, we carried out the same RNA-Seq analysis as above with the $\Delta iscR$ mutant. Under prolonged iron starvation (Chelex condition), when IscR levels are highest in the WT strain, a total of 324 genes were differentially expressed in the wildtype versus the $\Delta iscR$ strains (Fig 3; Supplemental Dataset 1). Of the 127 genes whose expression was greater in wildtype compared to $\Delta iscR$, 48 (~38%) were pYV-encoded and were among the genes with the largest fold changes between wildtype and $\Delta iscR$. As our previous data showed that apo-IscR directly regulates the T3SS master regulator LcrF, the majority of these pYV-encoded genes are likely to be indirectly regulated by IscR. In iron limited conditions, such as those encountered by *Yersinia* during extraintestinal infection, the dominant form of IscR is predicted to be apo-IscR. Genes induced by apo-IscR would be expected to be more highly expressed during iron starvation compared to after iron supplementation as well as have decreased expression upon deletion of *iscR*. Genes whose expression patterns were consistent with apo-IscR induction of their promoters included the T3SS genes *yscCDEFGHK*, the

sufABCDSE operon, metal transport genes *iucABCDiutA*, *alcC*, *cirA*, *fhuC_1*, and *oprC*, and cell envelope biosynthesis and remodeling genes *pagP*, *amiD*, and *ydhO* (Fig 4A, Supplementary Dataset 1). As expected, the 197 genes expressed at lower levels in wildtype compared to the Δ *iscR* strain under prolonged iron starvation included those in the *isc* operon. Genes repressed by apo-IscR would be expected to have higher mRNA levels following iron supplementation compared to iron starvation in wildtype bacteria as well as have increased expression upon deletion of *iscR*. Genes whose expression patterns are consistent with apo-IscR repression include *sodB*, *katA*, *ompW*, and the [4Fe-4S] cluster protein *napF* (Fig 4B).

ChIP-Seq analysis of *in vivo* IscR binding in *Y. pseudotuberculosis*

In order to identify the genes directly regulated by IscR, we carried out *in vivo* genome-wide detection of IscR binding sites via ChIP-Seq, using an anti-FLAG antibody and a *Y. pseudotuberculosis* strain expressing FLAG-tagged IscR (Fig S1; see Materials and Methods). Wild-type *Y. pseudotuberculosis* was used as a negative control since the FLAG antibody should not pull down IscR-DNA complexes in the absence of the affinity tag. A total of 295 unique regions of the genome were enriched during the FLAG pulldown (Fig 5AB). Of these ChIP-Seq peaks, 176 fell within 500 nucleotides upstream of an open reading frame (ORF) start codon and no more than 100 nucleotides downstream of a start codon, potentially within a regulatory region controlling

transcription. Out of these 176 peaks, 173 are found on the chromosome and three on the pYV virulence plasmid. A total of 37 peaks fell in between divergent genes and such ChIP-Seq peaks were assigned to both genes (encoded on the sense and antisense strands) for our preliminary analysis. Therefore, the 176 identified peaks fell within the predicted regulatory regions of 213 TU's encoding 401 individual genes (Supplemental Dataset 2). Of these 213 TU's, 46 contain genes found in Cluster II (upregulated by iron starvation) and 40 in cluster VI and VII (downregulated by iron starvation). The remaining 127 transcription units associated with a ChIP-Seq peak were not found in our cluster analysis, as they were not differentially expressed in response to iron. These data show that 40% of the IscR binding sites identified by our ChIP-Seq analysis were upstream of genes responsive to iron under aerobic conditions.

The most well documented IscR binding site in *Yersinia* is the type II site found 367 nucleotides upstream of the *yscW* start codon (Miller et al., 2014). A ChIP-Seq peak was detected in this region, with the pinnacle of the peak centering 364 nucleotides upstream of *yscW-lcrF* (Fig 5C). We used MEME-suite tools to probe for over-represented sequences near the center of ChIP-Seq peaks (Bailey et al., 2009). MEME analysis revealed identifiable IscR type II binding sequences in 175 out of the 176 ChIP-Seq peaks positioned within a putative regulatory region, with the predicted binding sequences

highly correlated with the center of the ChIP-Seq peak (CentriMo p-value, $8.4E-10^{28}$; Fig 5D). The over-represented sequence from these IscR-enriched sites strongly resembles the consensus IscR type II site from *E. coli* (Fig 5E)(Nesbit et al., 2009). No significant ChIP-Seq peaks were detected upstream of predicted IscR type I sites in *Yersinia* (Fig S2AB). This may be because holo-IscR does not crosslink as well or bind with high enough affinity as apo-IscR, and the resulting peaks are difficult to detect over the signals of apo-IscR binding. Taken together, these data indicate that our 3xFLAG-IscR ChIP was able to enrich for IscR type II binding sites, but not type I binding sites, under the conditions used. Importantly, genes driven by type II motif-containing promoters are predicted to be regulated by IscR under iron limited and aerobic conditions, such as those encountered by *Yersinia* during disseminated infection and therefore potential virulence factors.

In order to validate our *in vivo* IscR binding results, we carried out *in vitro* binding studies on the identified IscR binding sites upstream of the *katA* and *sodB* antioxidants as well as the known virulence genes *fis* and *ail* (Fig 6A). IscR has been shown to regulate antioxidant genes in other bacterial pathogens (Jones-Carson et al., 2008; Kim et al., 2009; Somprasong et al., 2012). The gene *fis*, which is part of the *dusB-fis* operon, encodes a nucleoid-associated protein involved in resistance to oxidative stress (Green et al., 2016). The protein Ail is important for tight attachment to host cells, type III

secretion, and resistance against serum killing (Pierson and Falkow, 1993; Yamashita et al., 2011). Although, unlike the *katA* and *sodB* genes, expression of *fis* and *ail* was not responsive to iron, we included them in our analysis because of their known roles in extraintestinal infection (Pierson and Falkow, 1993; Green et al., 2016). Since the promoters of these IscR targets are predicted to encode an IscR type II site, we used purified IscR-C92A (apo-locked IscR) to assess binding *in vitro*. *In vitro* electrophoretic mobility shift assays showed that apo-IscR binds to these promoters, although the binding to the *ail* promoter appeared weaker (Fig 6B). Indeed, the binding site predicted upstream of *ail* is missing key residues known to be important for IscR binding. A very large band shift was observed when assessing IscR binding to the *katA* promoter fragment (unpublished observations), indicating the possibility of more than one IscR binding site in this region. Indeed, when the *katA* promoter fragment was split into two, each with a bioinformatically identifiable IscR type II motif, binding to both fragments was observed. Collectively, these data demonstrate that IscR binds both *in vitro* and *in vivo* to the promoters of genes known or predicted to be involved in virulence.

IscR binding sites are conserved in human pathogenic *Yersinia*

We previously showed that IscR regulated the T3SS in both *Y. pestis* and *Y. pseudotuberculosis*, suggesting conservation of IscR regulation between these two species (Hooker-Romero et al., 2019). To assess the degree of

conservation of the identified IscR binding sites in the human pathogenic *Yersinia* species, we carried out a comparative genomics analysis. We first searched for orthologs of the first gene of each of the 213 TU's containing an upstream IscR *in vivo* binding site in *Y. pseudotuberculosis* IP2666 (Supplemental Dataset 3). Out of these 213 TU's, we could identify 203 orthologs of the first gene in each TU in *Y. pseudotuberculosis* IP32953, 203 in *Y. pestis* CO92, and 152 in *Y. enterocolitica* 8081 (Fig 7A), which is more distantly related to *Y. pseudotuberculosis* compared to *Y. pestis*. In order to assess conservation of IscR binding sites among these four strains, MEME-suite was utilized to assess the similarity of identified IscR binding motifs to the IscR type II consensus motif generated from this study (Fig 5E). Of the TU's for which an ortholog could be identified in at least one of the other *Yersinia* strains, the majority contained an upstream identifiable IscR type II binding motif. If orthologous type II motif sequences in two different *Yersinia* strains are functionally conserved in terms of IscR regulatory control, then the distance between the motif and the downstream gene should be similar between the two species. Indeed, the predicted IscR binding site for orthologous genes were of similar distance from the downstream start codon, with more similarity among the *Y. pseudotuberculosis* and *Y. pestis* strains, than between *Y. pseudotuberculosis* and *Y. enterocolitica* (Fig S3A). In addition, the IscR binding sites overall are highly conserved among IP2666, IP32953, and CO92, although many diverge in 8081 (Fig S3B). In order to

visualize the conservation of IscR type II motifs in *Yersinia*, a heatmap was generated illustrating the retainment of critical nucleotides that have been shown to be important for IscR binding (Fig 7B)(Nesbit et al., 2009). Importantly, there was very high conservation of IscR type II motifs between *Y. pseudotuberculosis* and *Y. pestis*. Out of the 203 transcription units whose putative regulatory regions were bound by IscR in *Y. pseudotuberculosis* IP2666 and conserved in *Y. pestis* CO92, 173 (~85%) had IscR type II motif sequences in their promoters that were 100% conserved between IP2666 and CO92, while 17 (~8%) only contained differences in nucleotides not critical for IscR binding. Interestingly, the IscR binding sites that were among the most conserved between all three *Yersinia* species included those within the promoters of *sodB*, *katA*, the *suf* operon, *pagP*, *ompW*, *yscW-IcrF*, *dusB-fis*, and *ail*.

Integration of transcriptome profiling with identified IscR binding sites

To determine which genes are directly regulated by IscR in *Y. pseudotuberculosis*, we collated the ChIP-Seq results with our published RNA-Seq data carried out under the same aerobic, non-iron starved conditions used for the IscR chromatin precipitation (Miller et al., 2014)(Supplemental Dataset 2). Under this condition, only 18 out of the 213 putative IscR regulatory sites found to be associated with an IscR binding site drove IscR dependent changes in expression of predicted transcription units.

Three of these 18 TU's, DN756_21815-DN756_21820, *yscW-lcrF*, and *yscIJKL*, are encoded on the pYV virulence plasmid and were downregulated in the *iscR* mutant. We have extensively validated direct regulation of the *yscW-lcrF* operon by IscR (Miller et al., 2014; Hooker-Romero et al., 2019)(Figs 5C). The *yscIJKL* T3SS genes are encoded within the virC operon, *yscABCDEFGHIJKL* (Michiels et al., 1991), which is controlled by the T3SS master regulator LcrF (Schwiesow et al., 2016). Since *lcrF* transcription is directly regulated by IscR (Miller et al., 2014), further experiments are needed to determine if alternative transcriptional start sites that are regulated by LcrF or IscR exist for the virC operon. DN756_21815 and DN756_21820 are a hypothetical gene and pseudogene, respectively, and are encoded on the pYV virulence plasmid. Interestingly, deletion of DN756_21815 and DN756_21820 had a small but significant effect on secretion of the T3SS effector protein YopE into culture supernatant (Fig S4). The remaining 15 TU's are encoded on the chromosome and include *sodB*, *ail*, and *fis*. A number of ChIP-Seq studies have shown that transcription factors exhibit binding to promoters whose genes are differentially regulated by the transcription factor under some but not all conditions tested, including the condition used for ChIP-Seq (Kleinman et al., 2017; Choudhary et al., 2020). Therefore, it was not surprising to see limited overlap between the ChIP-Seq data and RNA-Seq from only one culture condition.

We assessed whether our transcriptome analysis of iron-starved *Yersinia* might reveal additional genes associated with *in vivo* IscR binding whose expression is regulated by IscR. Indeed, 86 TU's with an upstream IscR binding site were found to contain genes differentially expressed in the presence and absence of IscR under at least one of the RNA-Seq conditions (Supplementary Dataset 2). We carried out a COG analysis on genes of the IscR direct regulon whose promoters contain an IscR enrichment site (Fig S5A), functional regulon genes associated with a ChIP-Seq peak that showed differential expression by IscR in at least one condition tested (Fig S5B), and the indirect regulon whose expression depends on IscR but are not associated with a ChIP-Seq peak (Fig S5C). The direct regulon was enriched for coenzyme and lipid metabolism as well as inorganic iron uptake compared to the indirect regulon, while the indirect regulon was enriched for biosynthesis, energy production, and the T3SS. Included in the functional regulon were genes whose expression patterns are consistent with apo-IscR induction or repression in our RNA-Seq analysis and are therefore predicted to be directly controlled by IscR during disseminated infection: the *suf* operon; the metal transporters *iucABCDiutA*, *alcC*, *cirA*, *fhuC_1*, *oprC*, and *yiuA*; the cell envelope enzymes *pagP*, *amiD*, and *ydhO*; and the oxidative stress associated *sodB*, *katA*, and *ompW*. However, many genes within the functional regulon did not display an expression pattern consistent with apo-IscR activation or repression, yet showed differential expression in response

to IscR under at least one RNA-Seq condition. This is consistent with other reports that identified ChIP-Seq peaks for genes differentially regulated by their respective transcription factors only under certain environmental conditions (Kleinman et al., 2017; Choudhary et al., 2020).

IscR directly regulates the *suf* operon, which contributes to type III secretion under iron-limiting conditions

The validated IscR binding site in the *suf* promoter exhibited 100% conservation among all human pathogenic *Yersinia* (Fig 7B), yet the role of the *suf* operon has never been studied in *Yersinia*. We observed a ChIP-Seq peak in the *suf* promoter with an identifiable IscR type II binding motif (Fig 8A), as well as *in vitro* binding of IscR to the *suf* promoter using EMSA (Fig 8B). Furthermore, the *suf* operon was differentially expressed by IscR following iron starvation (Fig S6), when IscR levels are high and Fur repression is predicted to decrease (Lee et al., 2003, 2008). Indeed, *sufABCDSE* were found to be expressed 3-11-fold more in wildtype *Y. pseudotuberculosis* compared to the Δ *iscR* mutant during iron starvation (Fig 8C, Fig S6). Together, these data strongly suggest that apo-IscR binds to a type II binding motif sequence in the *suf* promoter, activating *suf* operon expression.

We constructed a Δ *sufABCDSE* *Y. pseudotuberculosis* mutant, which exhibited normal growth and motility (Fig S7AB). Surprisingly, this mutant had

a significant type III secretion defect under aerobic conditions, when the Suf system is the dominant Fe-S cluster biogenesis pathway (Fig 8DE). These data suggest that an Fe-S cluster containing protein is important for T3SS expression or activity. As the *suf* mutant did not exhibit a defect in T3SS gene expression (Fig S7C), these data indicate that the Suf pathway contributes to type III secretion in a post-translational manner. The Isc pathway is the dominant Fe-S cluster biogenesis pathway under anaerobic conditions. However, we were unable to test whether the Isc pathway was required for type III secretion under anaerobic conditions because we were unsuccessful in deleting *iscSUA*, suggesting these are essential genes. Together, these data suggest that IscR regulates the *Yersinia* T3SS in two distinct ways: through direct control of the LcrF T3SS master regulator and through direct control of the Suf pathway that matures an Fe-S cluster protein critical for T3SS activity.

Discussion

IscR and iron are both critical factors in the pathogenesis of *Yersinia* and a number of other bacteria (Perry et al., 2015; Palmer and Skaar, 2016; Vergnes et al., 2017; Hooker-Romero et al., 2019; Choi et al., 2020). In this study, we present the first characterization of the IscR direct regulon. We used ChIP-Seq and RNA-Seq analysis to identify *Yersinia* genes directly regulated by IscR in response to changes in iron availability. Our data

suggest that IscR allows *Yersinia* to couple sensing of iron starvation, a condition experienced by the bacterium during extraintestinal infection, to control of genes involved in iron homeostasis, cell envelope modification, oxidative stress response, as well as T3SS expression and activity (Fig 9). Over 93% of *in vivo* IscR binding sites identified in *Y. pseudotuberculosis* were conserved in *Y. pestis*, suggesting that *Y. pestis* retained IscR as an important regulator after its evolution from food-borne pathogen to plague agent.

In this study we show that complete iron starvation induces IscR mRNA and protein levels in *Yersinia* under aerobic conditions. Previously, iron limitation was shown to induce IscR levels in both *E. coli* and *Vibrio vulnificus* (Outten et al., 2004; Lim et al., 2014). Iron starvation not only limits the amount of free iron that can incorporate into Fe-S cofactors, but can also affect the function of the Fe-S cluster biogenesis machinery (Santos et al., 2015). Ultimately, iron starvation leads to a reduction of Fe-S cluster availability causing a shift to more apo-IscR compared to holo-IscR (Fig 9). Since holo-IscR represses transcription of the *isc* operon, this shift leads to derepression of the *isc* operon under iron starved conditions (Giel et al., 2013). We previously found that supplementing *Yersinia* with as little as 0.036 μM FeSO_4 prevented this derepression of *iscR*, suggesting why in our earlier study IscR levels were not iron responsive under aerobic conditions (Hooker-Romero et al., 2019).

However, we show here that following prolonged iron starvation, IscR and IscR target genes are indeed responsive to either inorganic or heme iron. These data suggest that during infection, when the availability of free iron is vanishingly low and is further reduced by inflammatory pathways (Sebbane et al., 2006; Nuss et al., 2017), IscR levels should fluctuate in response to the ability of *Yersinia* to scavenge iron.

Two important categories of genes found to be regulated by iron and IscR were involved in cell envelope modification and the oxidative stress response. *Yersinia* modifies its LPS during growth at 37°C such that its LPS is less stimulatory to the endotoxin receptor TLR4 (Krasikova et al., 1995; Kawahara et al., 2002; Montminy et al., 2006; Rebeil et al., 2006). Interestingly, we found in this study that a number of *Yersinia* LPS biosynthesis and modification enzymes genes are upregulated upon iron starvation. Of these genes, only *pagP*, which encodes an outer membrane lipid A palmitoyltransferase, was found to be directly regulated by IscR. The *pagP* promoter contained an IscR type II motif that bound to IscR *in vivo* and *pagP* expression was consistent with induction by apo-IscR. *Salmonella* PagP, which is regulated by magnesium through the PhoP/Q regulatory system (Dalebroux and Miller, 2014), enables production of LPS lipid A that is less stimulatory to TLR4 (Bishop et al., 2000; Kawasaki et al., 2004; Bishop, 2005). In contrast, *Y. pestis* has an inactive *pagP* allele, but when the *Y.*

pseudotuberculosis functional *pagP* gene is inserted into *Y. pestis*, the LPS that is produced is more immunostimulatory (Chandler et al., 2020).

Therefore, how IscR affects LPS stimulation of TLR4 and other LPS sensors remains to be determined. To our knowledge, iron availability has not been previously shown to affect *Yersinia* LPS gene expression nor has IscR been shown to regulate LPS modifying genes in other bacterial species. In contrast, IscR has been implicated in controlling genes involved in the response to free radical stress in *Vibrio vulnificus*, *Pseudomonas aeruginosa*, and *Burkholderia mallei* (Choi et al., 2007, 2020; Jones-Carson et al., 2008; Kim et al., 2009; Lim et al., 2014). The *Yersinia* T3SS, which is positively regulated by IscR, inhibits phagocytic cell oxidative burst. Therefore, IscR induction of the T3SS should lead to a decrease in the amount of reactive oxygen species (ROS) encountered by *Yersinia* during infection. In this study, we also found that IscR directly repressed the genes encoding catalase, *katA*, superoxide dismutase, *sodB*, and the oxidative stress-associated OmpW (Zhang et al., 2020). It is possible that IscR upregulation of the T3SS may be coupled to lower expression of KatA and SodB, since the bacteria would be less likely to encounter ROS stress when the T3SS is active.

We showed that IscR binds to the *sufABCDSE* promoter both *in vitro* and *in vivo*, and that *suf* expression is consistent with apo-IscR induction of the *suf* promoter. This is in line with a previous study showing that IscR activates the

E. coli *suf* operon upon exposure to the iron chelator dipyrityl (Outten et al., 2004). However, surprisingly, our data also showed that deletion of the *suf* operon leads to reduced Ysc T3SS activity. Loss of the *suf* operon did not affect T3SS gene expression or protein levels, but instead affected secretion of T3SS cargo. This phenotype was observed under standard aerobic non-iron starved conditions (data not shown), and was even more pronounced under iron limited conditions where the *suf* operon becomes more important for synthesizing Fe-S clusters. Loss of the *suf* operon may affect the electron transport chain and lead to a proton motive force defect, which is required for T3SS activity (Wilharm et al., 2004). However, the *suf* mutant had no motility defect, which also requires the proton motive force. Under anaerobic iron replete conditions, when the Isc pathway mediates Fe-S cluster biogenesis for the cell, the *suf* mutant displays normal type III secretion. Collectively, these results suggest that a *Yersinia* Fe-S cluster protein, matured by the Suf pathway under aerobic conditions, promotes T3SS activity. Interestingly, the *Salmonella* Isc pathway, but not the Suf pathway, was shown to be important for IscR-mediated repression of the SPI-1 T3SS and for virulence following oral infection. In contrast to the *Yersinia* T3SS, *Salmonella* expresses its SPI-1 T3SS in the intestine where it is required for entry into intestinal epithelial cells (Vergnes et al., 2017).

IscR positively regulates the T3SS master regulator LcrF, and type III secretion only occurs under anaerobic conditions in the absence, not the presence, of iron (Miller et al., 2014; Hooker-Romero et al., 2019). Therefore, it was surprising that only the *virC* structural operon (*yscCDEFGHKL*), but no other LcrF-regulated genes were significantly upregulated under our aerobic iron starvation conditions. Indeed, while mRNA levels of the *yscW-lcrF* operon trended up in the absence of iron, this difference was not statistically significant. In fact, some T3SS effector protein and chaperone genes (*yopO*, *yopK*, *yopH*, *yopJ*, *sycDH*), the *yscM* T3SS regulatory gene, and the needle tip protein *lcrV* were expressed ~2-4-fold *more* after iron supplementation. However, importantly, most of these genes were downregulated ~10-50-fold by deletion of *iscR*, demonstrating that the presence of an *iscR* gene had a much stronger effect on T3SS gene expression than changes in iron availability under aerobic conditions. *Y. pseudotuberculosis* transits from the small intestine to lymph tissue and vital organs during infection. In the intestines, *Yersinia* experiences an anaerobic iron replete environment where it does not require its T3SS (Jacobi et al., 2001; Avican et al., 2015; Zheng et al., 2015). In contrast, once *Yersinia* crosses the intestinal barrier and the T3SS becomes important for virulence, oxygen tension increases and host iron sequestration causes a drastically lower amount of bioavailable iron. Collectively, our data show that IscR represses the *Yersinia* T3SS in the intestines and induces the T3SS once *Yersinia* disseminate.

Only about 40% of genes associated with an IscR binding site were found to be differentially regulated by IscR in at least one condition tested, and even fewer had expression patterns consistent with apo-IscR activation or repression. However, a recent study examining the regulons associated with five different two component regulatory systems in *E. coli* noted the existence of genes whose promoters directly bound a transcription factor (TF), but that only showed differential expression by that TF under certain conditions (Choudhary et al., 2020). The authors speculated that this is due to other regulators controlling such promoters and referred to these genes as exhibiting “hypothetical functional binding” by the TF, as other studies have also suggested (Sastry et al., 2019). We postulate that *ail* and *dusB-fis* may fall into this category, as they are differentially expressed by IscR only under non-iron starved conditions but show IscR binding to their promoters *in vitro* and *in vivo*. Ail encodes an adhesin that contributes to delivery of T3SS effector proteins into target host cells and mediates complement resistance (Miller and Falkow, 1988; Pierson and Falkow, 1993; Kirjavainen et al., 2008; Yamashita et al., 2011). The Factor for Inversion (Fis) nucleoid-associated protein influences the topological state of DNA and affects gene expression (Duprey et al., 2014). Fis regulates virulence in a number of pathogens, including *Y. pseudotuberculosis* (Green et al., 2016). In some organisms, Fis expression is regulated by growth phase while in others it is regulated by

specific environmental signals (Duprey et al., 2014). For example, *Salmonella* Fis regulates the supercoiling of DNA encoding the SPI-1 and SPI-2 T3SSs in an opposite manner in response to oxygen (Ó Cróinín et al., 2006; Cróinín and Dorman, 2007). In our study, we show that the *Yersinia fis* gene is expressed at higher levels under iron starvation compared to after iron supplementation. In *Y. pseudotuberculosis*, Fis has been shown to be crucial for resistance to oxidative stress and colonization of the murine spleen and liver (Green et al., 2016). Additional environmental signals, such as oxygen tension, should be examined for their ability to regulate *Yersinia ail* and *fis* to explore whether IscR regulation of these genes may be important under anaerobic conditions such as those found in the intestinal lumen.

The remaining 60% of genes associated with an IscR binding site were not found to be differentially expressed by IscR under any condition tested. Choudhary et al categorized such genes as having “potentially non-functional binding” of the TF (Choudhary et al., 2020). The *in vivo* IscR binding associated with these genes either represents spurious, non-functional binding, or another regulator is preventing IscR from exerting an effect on gene expression under the conditions tested. Indeed, there is evidence that IscR regulates promoters also targeted by other TFs. For example, out of the 213 TUs targeted by IscR, 65 had a predicted Fur box in their corresponding regulatory region (unpublished observations). Additional RNA-Seq analysis of WT and $\Delta iscR$ *Yersinia* will help determine whether the “potentially non-

functional binding” genes identified in this study are differentially expressed under certain conditions, for example anaerobic iron replete conditions that mimic those encountered by *Yersinia* in the intestinal lumen where IscR is also necessary for colonization.

Fur in uropathogenic *E. coli* (UPEC) regulates genes found in pathogenicity islands and siderophores not present in commensal *E. coli* K-12 strain MG1655 (Banerjee et al., 2020). This difference in Fur regulon members from the two species could be due to the lack of the pathogenicity islands in commensal *E. coli*. Interestingly, UPEC Fur directly regulated genes that were also present in commensal *E. coli*, yet only UPEC Fur directly regulated this subset of genes. These data suggest that as species evolve and find new niches, regulons and transcription regulatory networks change to adapt to the environment. Current models suggest that *Y. pestis* evolved as recently as ~1500 years ago from *Y. pseudotuberculosis* through a series of DNA element acquisitions along with gene loss (McNally et al., 2016), making *Yersinia* an interesting model to study the IscR regulon. These genomic changes enabled a previously facultative food-borne pathogen to colonize and be transmitted through a flea vector. However, once inside the host, both *Y. pseudotuberculosis* and *Y. pestis* colonize lymph nodes and spread to deeper tissues (Putzker et al., 2001; Balada-Llasat and Mecsas, 2006). In addition, while the two pathogens exhibit very different life cycles, there is

evidence that, within lymph nodes, they both experience iron starvation (Sebbane et al., 2006; Nuss et al., 2017). For example, *Y. pseudotuberculosis* in the Peyer's patches upregulate metal acquisition genes such as *hmuR*, *alcC*, *znuABC*, *mntH* as well as others (Nuss et al., 2017). These same genes are upregulated in our transcriptomic data upon iron starvation. Our comparative genomic analysis suggests that the IscR regulon is highly conserved in *Y. pseudotuberculosis* and *Y. pestis*. We speculate that IscR control of genes involved in iron homeostasis, virulence, stress response, and other pathways has provided a fitness benefit to *Y. pestis* during its evolution as the plague agent and was therefore retained. Furthermore, as a number of the IscR binding sites identified in *Y. pseudotuberculosis* are conserved in the *Y. enterocolitica* genome, we also speculate that IscR regulated genes important for pathogenesis in the shared ancestor of *Y. enterocolitica* and *Y. pseudotuberculosis*/*Y. pestis*.

Materials and Methods

Bacterial strains, plasmids, and growth conditions

All strains used in this study are listed in Table 1. *Y. pseudotuberculosis* strains were grown in M9 minimal media supplemented with casamino acids, referred to here as M9+3.6 μM FeSO_4 , at 26°C with shaking at 250 rpm, unless otherwise indicated (Cheng et al., 1997). Non-iron starved conditions were achieved by subculturing an M9+3.6 μM FeSO_4 overnight culture to an

optical density at 600 nm (OD_{600}) of 0.2 in fresh M9+3.6 μM FeSO_4 , and shaking for 3 hrs at 37°C.

Iron starvation was achieved by growing *Y. pseudotuberculosis* aerobically in M9 media lacking iron treated with Chelex 100 resin to remove all traces of iron in acid-washed glassware, as previously described (Schwiesow et al., 2018; Hooker-Romero et al., 2019). Specifically, iron-replete overnight cultures (M9+3.6 μM FeSO_4) grown at 26°C aerobically were diluted to an OD_{600} of 0.1 into Chelex-treated M9 media and grown for 8 hrs at 26°C aerobically with agitation. Cultures were then sub-cultured a second time to OD_{600} of 0.1 in fresh Chelex-treated M9 and grown for 12 hrs at 26°C with agitation. Cultures were then sub-cultured to OD_{600} of 0.1 into 20 mL Chelex treated M9 media with either no iron, 5 μM hemin, or 3.6 μM FeSO_4 and grown for 3 hrs at 37°C with agitation.

Construction of *Yersinia* mutant strains

A 3xFLAG affinity tag was placed at the C-terminus of IscR encoded at the native *iscR* chromosomal locus to facilitate detection of IscR with FLAG monoclonal antibody (Fig S1A). The 3xFLAG affinity tag was chromosomally added to the C-terminus of *iscR* through splicing by overlap extension (Warrens et al., 1997). Primer pair *FiscR_cds/RiscR_cds* (Table 2) was used to amplify ~500bp upstream of *iscR* plus the *iscR* coding region excluding the

stop codon. Primer pair F3xFLAG/R3xFLAG was used to amplify the 3xFLAG tag. Primer pair F3'*iscR*/R3'*iscR* was used to amplify the ~500 bp downstream region of *iscR* including the stop codon. These amplified PCR fragments were cloned into a BamHI and SacI digested pSR47s suicide plasmid [λ pir-dependent replicon, kanamycin resistant (Kan^R), *sacB* gene conferring sucrose sensitivity] using the NEBuilder HiFi DNA Assembly kit (New England Biolabs, Inc). Recombinant plasmids were transformed into *E. coli* S17-1 λ pir competent cells and later introduced into *Y. pseudotuberculosis* IP2666 via conjugation. The resulting Kan^R, *irgansan*^R (*Yersinia* selective antibiotic) integrants were grown in the absence of antibiotics and plated on sucrose-containing media to select for clones that had lost *sacB* (and by inference, the linked plasmid DNA). Kan^S, sucrose^R, congo red-positive colonies were screened by PCR and sequenced. *Yersinia* carrying only the 3xFLAG-IscR allele secreted similar levels of YopE compared to the wild-type strain, suggesting that the 3xFLAG tag does not affect the ability of IscR to regulate T3SS gene expression (Fig S1B). In addition, derepression of *iscS* mRNA was not observed in the 3xFLAG-IscR strain, suggesting the 3xFLAG-IscR retains the ability to repress *iscS* (Ruzicka et al., 2002) (Fig S1C). These data demonstrate that the 3xFLAG affinity tag does alter IscR function and thus is suitable for CHIP-Seq experiments.

Generation of The Δ *sufABCDSE* and Δ *DN756_21815-21820* mutants were generated via splicing by overlap extension (Warrens et al., 1997). Primer pairs F5/R5 Δ *sufABCDSE* and F5/R5 Δ *DN756_21815-21820* (Table 2) were used to amplify ~1000 bp 5' of *sufA* and *DN756_21815*, respectively. Primer pair F3/R3 Δ *sufABCDSE* and F3/R3 Δ *DN756_21815-21820* were used to amplify ~1000 bp 3' of *sufE* and *DN756_21820*, respectively. Amplified PCR fragments were cloned into a BamHI- and SacI-digested pSR47s suicide plasmid (λ pir-dependent replicon, kanamycin^R, *sacB* gene conferring sucrose sensitivity) using the NEBuilder HiFi DNA Assembly kit (New England Biolabs, Inc). Mutant strains were generated as described for the 3xFLAG-IscR strain above.

Chromatin immunoprecipitation followed by high-throughput sequencing

ChIP-Seq experiments were performed in the IscR-3xFLAG strain and the parental wildtype IP2666 strain after growth at 37°C for 3 hrs in M9+3.6 μ M FeSO₄, using the IP2666pIB1 genome (NCBI CP032566.1 and CP032567.1) for analysis. ChIP assays were performed as previously described (Myers et al., 2013) using a monoclonal mouse anti-FLAG antibody (Sigma-Aldrich) that enriched for IscR-3XFLAG. Immunoprecipitated DNA was sheared to 200-500 base pairs via probe-based sonication. DNA quantification was carried out using both Agilent High Sensitivity DNA kit and Invitrogen Qubit dsDNA HS

Assay Kit once DNA was immunoprecipitated and purified. For ChIP-Seq experiments, 10 ng of immunoprecipitated and purified DNA fragments from IscR-3XFLAG (three biological replicates) and WT non-FLAG tagged IscR (one biological replicate), along with 10 ng of input control, were used to generate libraries using Illumina TruSeq ChIP Library Preparation Kit. This kit was used following manufacturer's instructions, except that the purification of the ligation products was performed using an Invitrogen E-Gel Power Snap System with Invitrogen E-Gel Size Select II 2% Agarose Gels. Final library validation was performed using the Qubit and Bioanalyzer. This resulted in eight libraries for sequencing: triplicate immunoprecipitated samples and a single negative control sample, each with a paired input sample. Libraries were sequenced by the University of Wisconsin at Madison Biotechnology Center DNA Sequencing Facility on an Illumina HiSeq to produce 51 bp single-end reads.

Initial quality control checks were performed on FASTQ files with FastQC v0.11.5(Andrews, 2015). Trimmomatic v0.36(Bolger et al., 2014) was used to remove low quality reads from the FASTQ files and to also remove Illumina adapters. The reference files for the *Y. pseudotuberculosis* IP26666pIB1 chromosome and plasmid were downloaded from the NCBI (GenBank CP032566.1 and CP032567.1) and concatenated into a single file. The trimmed FASTQ files were then aligned to the *Y. pseudotuberculosis* genome

using Bowtie2 v2.3.3.1 (Langmead and Salzberg, 2012b) with the default settings to generate SAM files. To remove all unaligned reads and all reads which aligned ambiguously, the SAM files were filtered with Samtools v1.6 (Li et al., 2009) with the flags “view -q 10”.

Sequences associated with IscR enrichment following precipitation, or “peaks”, were identified using three separate programs: QuEST v2.4 (Valouev et al., 2008), MOSAiCS v2.18.0 (Kuan et al., 2011), and MACS2 (Zhang et al., 2008). QuEST was run according to the manual with the following options: perform FDR analysis, search for punctate peaks (option 1), and use relaxed peak calling criteria (option 3). QuEST was run separately for each of the three immunoprecipitated samples and the negative control sample using the paired input sample as a background file. From the generated output, the ‘max_pos’ of each identified enriched region was used at the peak summit. Wiggle files were outputted as a default function of QuEST. MOSAiCS was run as a two-sample analysis as described in the vignette (version May 2, 2019) chapters 3 and 5.1 with the same sample pairs as used with QuEST. During the use of MOSAiCS, a fragment and bin size of 175 nucleotides was used. This number was derived by multiplying the average peakshift, as calculated by QuEST from the immunoprecipitated samples, by two. Peak summits and wiggle files were outputted by MOSAiCS as the last steps of the

analysis. MACS2 was run according to the manual with a criteria cutoff of FDR value $<E-5$, p-Value $<-\log_{10}70$.

Sequences with IscR enrichment following immunoprecipitation were considered *bona fide* ChIP-Seq peaks if, for each peak-calling program, a peak was called in at least two of three samples. Peaks were considered to be the same if their summits fell within 175 bp of each other. At every location where a negative control peak overlapped an immunoprecipitated sample peak, we manually examined the negative control data to determine if the peak should be removed from our analysis. Specifically, we visually looked for negative peaks which were centered on the immunoprecipitated sample peaks and also confirmed that the negative peaks were composed of both forward and reverse mapping reads. MochiView (Homann and Johnson, 2010) and Tablet (Milne et al., 2013) were used to visualize the Wig files and binary SAM (BAM) files, respectively. Peaks confirmed to be arising from background noise were removed from our analysis. The average position of the immunoprecipitated sample peak summits was used as the new peak summit moving forward. This process was repeated for each peak calling program independently, thus yielding three lists of confirmed peak summits. Finally, confirm peak summits were clustered as above. All peaks which were identified by at least two of three peak calling programs were marked as *bone fide* peaks and other peaks discarded. Each peak in the final list was

examined by eye with MochiView, and particular care taken to confirm the validity of peaks called by only two of three algorithms. For visualization and graphing purposes, BAM files were displayed on tracks with Integrative Genomics Viewer using BAMCoverage from DeepTools2 (Ramírez et al., 2016). Of the 295 peaks, 80% were called by all three peak calling programs.

RNA Isolation and RNA-Seq

For RNA isolated from samples subjected to iron starvation, *Y. pseudotuberculosis* WT and $\Delta iscR$ strains were grown in 5 mL of M9+3.6 μM FeSO_4 overnight. Cultures were then diluted to OD_{600} of 0.1 in 20 mL of M9 media lacking iron treated with Chelex (Bio-Rad) to remove trace amounts of iron and allowed to grow for 8 hrs at 26°C (Schwiesow et al., 2018). The cultures were then diluted again to OD_{600} 0.1 into 20 mL Chelex-treated M9 media and allowed to grow for 12 hrs at 26°C. Cultures were then diluted to OD_{600} of 0.1 into 20 mL Chelex-treated M9 media with either no iron, 5 μM hemin, or 3.6 μM FeSO_4 . Stock hemin solutions were Chelex-treated overnight. After 3 hrs of growth at 37°C, 5 mL of culture from each condition was pelleted by centrifugation for 5 minutes at 4,000 rpm. The supernatant was removed, and pellets resuspended in 500 μL media and treated with 1 mL Bacterial RNA Protect Reagent (Qiagen) according to the manufacturer's protocol. Total RNA was isolated using the RNeasy Mini Kit (Qiagen) per the manufacturer's protocol. Contaminating DNA was removed using the TURBO

DNA-free Kit (Life Technologies/Thermo Fischer). rRNA was removed using the RiboMinus Transcriptome Isolation Kit bacteria (Invitrogen). The cDNA library was prepared using the NEB Ultra Directional RNA Library Prep Kit for Illumina. Quality of RNA and cDNA libraries were assessed using an Agilent 2000 Bioanalyzer. Libraries were sequenced using the HiSeq2500 Illumina sequencing platform for 50 bp single reads (UC Davis Genome Center).

Trimmomatic (Bolger et al., 2014) version 0.36 was used to trim off low-quality bases and adapter sequences. Trimmed reads were then aligned to a concatenated chromosome (CP032566.1) and virulence plasmid (CP032567.1) through Bowtie2 (Langmead and Salzberg, 2012a). Low quality aligned reads were removed by filtering out mapped reads with a mapQC score <10 . The BAM file with the aligned reads with a mapQC score >10 was then split to separate chromosomal mapped reads from virulence plasmid mapped reads. Mapped reads were then normalized to TMM and differential expression analysis was performed using EdgeR (Robinson et al., 2009). Genes were called differentially expressed if the \log_2FC was ≥ 1 or ≤ -1 with an FDR value <0.01 .

Motif Identification and *in silico* Search

IscR binding motif analyses was carried out using MEME tool from the MEME software suite with default settings (Bailey et al., 2009). The *E. coli* IscR type I

and type II binding motifs were compiled from a training set consisting of known IscR binding sites in *E. coli* (Ruzicka et al., 2002; Nesbit et al., 2009). FIMO tool from the MEME software suite was then used to search for an IscR type I binding motif upstream *Yersinia iscRSUA*, *cysE*, *erpA*, and *nfuA*.

In order to identify a *Yersinia* IscR consensus binding site from sequences enriched during IscR-FLAG immunoprecipitation, 50 nucleotides within the center of all 176 enriched DNA regions were extracted and MEME suite used to generate a *Yersinia* IscR type II motif. CentiMo tool from MEME-suite was utilized to assess if the predicted IscR type II consensus motif was often found near the center of each IscR ChIP-Seq peak.

Western blot analysis

Bacterial pellets were resuspended in final sample buffer plus 0.2 M dithiothreitol (FSBS+DTT) and boiled for 15 min. At the time of loading, samples were normalized to the same number of cells by OD₆₀₀. Protein samples were run on a 12.5% SDS-PAGE gel and transferred to a blotting membrane (Immobilon-P) with a wet mini trans-blot cell (Bio-Rad). Blots were blocked for an hour in Tris-buffered saline with Tween 20 and 5% skim milk, and probed with rabbit anti-IscR (Nesbit et al., 2009), rabbit anti-YopD (gift from Alison Davis and Joan Mecsas), goat anti-YopE (Santa Cruz Biotechnology), rabbit anti-RpoA (gift from Melanie Marketon), and

horseradish peroxidase-conjugated secondary antibodies (Santa Cruz Biotech). Gels were imaged by Image Lab software (Bio-Rad).

Type III secretion assay under non-iron starved conditions

Visualization of T3SS cargo secreted in broth culture was performed as previously described (Kwuan et al., 2013). For standard *Y. pseudotuberculosis* T3SS induction (Fig S1B and Fig S4C) bacteria were grown overnight in LB media, subcultured in LB plus 20 mM sodium oxalate (to chelate calcium and induce type III secretion) and 20 mM MgCl₂ to an OD₆₀₀ of 0.2, grown at 26°C for 1.5 hrs followed by 37°C for another 1.5 hrs. Cultures were normalized by OD₆₀₀ and pelleted at 13,200 rpm for 10 min at room temperature. Supernatants were removed and proteins precipitated by addition of trichloroacetic acid (TCA) to a final concentration of 10%. Samples were incubated on ice for 20 min and pelleted at 13,200 rpm for 15 min at 4°C. Resulting pellets were washed twice with ice-cold 100% acetone and subsequently resuspended in FSB+DTT. Samples were boiled for 5 min prior to running on a 12.5% SDS PAGE gel.

Type III secretion assay under iron starved aerobic or anaerobic conditions

We previously found that small amounts of iron are needed to get sufficient *Yersinia* growth under anaerobic conditions to detect T3SS activity (Hooker-

Romero et al., 2019); therefore, we added 0.036 μ M to the “low iron” samples for these experiments rather than continuing to iron starve them. Cultures were grown aerobically in Chelex-treated M9 minimal media plus 0.9% glucose in acid-washed glassware, as previously described (Hooker-Romero et al., 2019). Specifically, iron-replete overnight cultures (M9+3.6 μ M FeSO₄) grown at 26°C aerobically were sub-cultured to an OD₆₀₀ of 0.1 into Chelex-treated M9 media plus 0.9% glucose and grown for 8 hrs at 26°C aerobically with agitation. Cultures were then sub-cultured a second time to OD₆₀₀ 0.1 in fresh Chelex-treated M9 media plus 0.9% glucose and grown for 12 hrs at 26°C with agitation. Subsequently, cultures were then sub-cultured a third time to OD₆₀₀ 0.2 in M9 media plus 0.9% glucose supplemented with 3.6 μ M FeSO₄ (iron-replete) or with 0.036 μ M FeSO₄ (iron limitation), grown for 2 hrs at 26°C with agitation, and then shifted to 37°C for 4 hrs with agitation to induce type III secretion. For anaerobic cultures, the cultures were instead diluted a second time to OD₆₀₀ 0.1 in M9 media plus 0.9% glucose supplemented with 3.6 μ M FeSO₄ (iron-replete) or with 0.036 μ M FeSO₄ (iron limitation), and transferred to a vinyl anaerobic chamber where they were grown at 26°C for 12 hrs. Cultures were then shifted to 37°C for another 4 hrs to induce type III secretion. Samples were then processed as for standard secretion assay conditions, above.

Quantitative PCR (qPCR) analysis.

A total of 5 mL of culture from each condition were pelleted by centrifugation for 5 minutes at 4 krpm. The supernatant was removed, and pellets were resuspended in 500 μ L of media and treated with 1 mL Bacterial RNA Protect Reagent (Qiagen) according to the manufacturer's protocol. Total RNA was isolated using the RNeasy Mini Kit (Qiagen) per the manufacturer's protocol. After harvesting total RNA, genomic DNA was removed via the TURBO-DNA-free kit (Life Technologies/Thermo Fisher). cDNA was generated for each sample by using the M-MLV Reverse Transcriptase (Invitrogen) according to the manufacturer's instructions, as we previously described (Miller et al., 2014). Power SYBR Green PCR master mix (Thermo Fisher Scientific), and primers (Table 2) with optimized concentrations were used to measure target gene levels. The expression levels of each target gene were normalized to that of 16S rRNA present in each sample and calculated by the $\Delta\Delta$ Ct method. Three independent biological replicates were collected for each tested condition. For each target transcript, significant differential expression between different bacterial strains were defined by p-value <0.05 of two-way analysis of variance (one-way ANOVA with Tukey post-test).

Cluster of Orthologous Groups (COG) analysis

The gene bank file of the *Y. pseudotuberculosis* chromosome (CP032566.1) and virulence plasmid (CP032567.1) were downloaded from NCBI. These files were opened using the Artemis Genome Browser (Carver et al., 2012),

where the proteome was exported to a FASTA file. EggNOG 4.5.1 (Huerta-Cepas et al., 2016) was used to determine the following gene information based on ortholog databases: preferred gene name, COG category, and gene function.

Cluster Analysis

Cluster analysis was used to cluster gene expression data from the RNA-Seq experiments. The elbow method was first used to determine the appropriate number of clusters. Gene expression data was inputted as normalized reads (TMM) values. These gene expression values were then scaled by gene. R-package pheatmap was used to create clusters dependent on Euclidean distances and a complete method.

Protein purification and electrophoretic mobility shift assays (EMSAs)

The *iscR* coding sequence was PCR amplified from the *E. coli* K12 MG1655 chromosome using primers that incorporated a NdeI restriction site at the 5' end of the gene, and a BamHI site and His₆-tag (order listed in 5'-3' direction) at the 3' end. The NdeI and BamHI digested fragment was cloned into pET11a to generate pPK14263, which was subsequently transformed into strain PK7878 (Rajagopalan et al., 2013). IscR-C92A-His₆ was purified as previously described for untagged IscR (Giel et al., 2006; Nesbit et al., 2009). DNA fragments containing the predicted IscR binding region for *ail* [-

386 to +14 bp relative to the +1 transcription start site (TSS)], *dusB-fis* (-447 to -247 bp relative to the +1 TSS), *sodB* (-116 to +84 bp relative to the +1 TSS), *katA1* (-240 to -93 bp relative to the +1 TSS), *katA2* (-92 to +1 bp relative to the +1 TSS), and *sufA* (-144 to +56 bp relative to the +1 TSS) were amplified from *Y. pseudotuberculosis* genomic DNA using primers (Table 2). Amplified products were digested with XhoI and BamHI and subsequently ligated into the pPK7179 plasmid. DNA templates for EMSAs were isolated from plasmid DNA after restriction digest with XhoI and BamHI. These fragments and linearized plasmid (which served as competitor DNA in the EMSAs) were purified using the QIAquick PCR purification kit (Qiagen). IscR-C92A was incubated with DNA fragments (~5–10 nM) for 30 min at 37°C in 40 mM Tris (pH 7.9), 30 mM KCl, 100 µg/mL bovine serum albumin (BSA), and 1 mM DTT. Glycerol was added to 10% and samples were loaded onto a non-denaturing 6% polyacrylamide gel in 0.5x Tris-borate-EDTA (TBE) buffer and run at 200 V for 3.5 hours. The gel was stained with SYBR Green EMSA nucleic acid gel stain (Molecular Probes) and visualized using a Typhoon FLA 900 imager (GE).

Comparative Genomics

Orthologs of the 213 IscR targets were determined in *Y. pseudotuberculosis* IP32953 (NC_006155.1), *Y. pestis* CO92 (NC_003143.1), and *Y. enterocolitica* 8081 (NC_008800.1) through a combination of BLAST and

Mauve, a multiple genome alignment tool (Darling et al., 2004). Paralogs were avoided by using Mauve. For all orthologs, 1000 nucleotides upstream and downstream of the start codon were extracted. An IscR binding site was predicted using MEME-suite tools, and was compared to the known IscR binding site in *Y. pseudotuberculosis* IP2666. The orthologous IscR binding site was identified based off sequence similarity and distance of the IscR binding site from the start codon. Sequence similarity was calculated by computing the absolute distance between logMEME-FIMO-pvalue in *Y. pseudotuberculosis* IP2666 (known IscR binding site) compared to logMEME-FIMO-pvalue of orthologous binding site in the indicated strain of *Yersinia* (binding site in question).

Motility Assay

A total of 1 μ l *Y. pseudotuberculosis* overnight culture was spotted onto motility medium containing 1% tryptone/0.25% agar. The plates were incubated at 26°C for 24 hrs or 48 hrs before the diameter of the motile colony was measured.

Microbial Genome Browser

Both ChIP-Seq and RNA-Seq tracks were deposited to the UCSC Microbial Genome browser. For RNA-Seq data, final BAM file alignments were

converted to bigwig files using bamCoverage-deepTools (Ramírez et al., 2016). Chromosomal alignments were normalized by counts per million mapped reads (CPM) while alignments to the virulence plasmid were not normalized due to the known increase in plasmid copy number at 37°C relative to the chromosome (Wang et al., 2016). For ChIP-Seq data, both BAM files that were mapped to the chromosome or virulence plasmid were normalized by CPM. The RNA-Seq and ChIP-Seq data is available for viewing and the track hub data can be found at <http://zam.soe.ucsc.edu/hubs/StoneYersinia/hub.txt>.

Acknowledgments

This study was supported by National Institutes of Health (www.nih.gov) grant R01AI119082 (to VA and PJK). DAB and PA received support from the National Human Genome Research Institute of the National Institutes of Health under Award Number 4R25HG006836. DHR received support from the Ford Foundation (www.fordfoundation.org). We thank Patricia Chan and Todd Lowe for assistance with the Microbial Genome Browser. The funders had no role in study design, data collection and analysis, decision to publish, or preparation of the manuscript.

References

- Andrews, S. (2015). FASTQC A Quality Control tool for High Throughput Sequence Data. *Babraham Inst.*
- Avican, K., Fahlgren, A., Huss, M., Heroven, A. K., Beckstette, M., Dersch, P., et al. (2015). Reprogramming of *Yersinia* from Virulent to Persistent Mode Revealed by Complex In Vivo RNA-seq Analysis. *PLoS Pathog.* doi:10.1371/journal.ppat.1004600.
- Bailey, T. L., Boden, M., Buske, F. A., Frith, M., Grant, C. E., Clementi, L., et al. (2009). MEME Suite: Tools for motif discovery and searching. *Nucleic Acids Res.* doi:10.1093/nar/gkp335.
- Balada-Llasat, J. M., and Mecsas, J. (2006). *Yersinia* has a tropism for B and T cell zones of lymph nodes that is independent of the type III secretion system. *PLoS Pathog.* doi:10.1371/journal.ppat.0020086.
- Banerjee, R., Weisenhorn, E., Schwartz, K. J., Myers, K. S., Glasner, J. D., Perna, N. T., et al. (2020). Tailoring a global iron regulon to a uropathogen. *MBio.* doi:10.1128/mBio.00351-20.
- Bishop, R. E. (2005). The lipid A palmitoyltransferase PagP: Molecular mechanisms and role in bacterial pathogenesis. *Mol. Microbiol.* doi:10.1111/j.1365-2958.2005.04711.x.
- Bishop, R. E., Gibbons, H. S., Guina, T., Trent, M. S., Miller, S. I., and Raetz, C. R. H. (2000). Transfer of palmitate from phospholipids to lipid A in outer membranes of Gram-negative bacteria. *EMBO J.*

doi:10.1093/emboj/19.19.5071.

- Bliska, J. B., Guan, K., Dixon, J. E., and Falkow, S. (1991). Tyrosine phosphate hydrolysis of host proteins by an essential *Yersinia* virulence determinant. *Proc. Natl. Acad. Sci. U. S. A.* doi:10.1073/pnas.88.4.1187.
- Bolger, A. M., Lohse, M., and Usadel, B. (2014). Trimmomatic: A flexible trimmer for Illumina sequence data. *Bioinformatics*. doi:10.1093/bioinformatics/btu170.
- Carpenter, C., and Payne, S. M. (2014). Regulation of iron transport systems in Enterobacteriaceae in response to oxygen and iron availability. *J. Inorg. Biochem.* doi:10.1016/j.jinorgbio.2014.01.007.
- Carver, T., Harris, S. R., Berriman, M., Parkhill, J., and McQuillan, J. A. (2012). Artemis: An integrated platform for visualization and analysis of high-throughput sequence-based experimental data. *Bioinformatics*. doi:10.1093/bioinformatics/btr703.
- Chandler, C. E., Harberts, E. M., Pelletier, M. R., Thaipisuttikul, I., Jones, J. W., Hajjar, A. M., et al. (2020). Early evolutionary loss of the lipid A modifying enzyme PagP resulting in innate immune evasion in *Yersinia pestis*. *Proc. Natl. Acad. Sci. U. S. A.* doi:10.1073/pnas.1917504117.
- Cheng, L. W., Anderson, D. M., and Schneewind, O. (1997). Two independent type III secretion mechanisms for YopE in *Yersinia enterocolitica*. *Mol. Microbiol.* doi:10.1046/j.1365-2958.1997.3831750.x.
- Choi, G., Jang, K. K., Lim, J. G., Lee, Z. W., Im, H., and Choi, S. H. (2020).

- The transcriptional regulator IscR integrates host-derived nitrosative stress and iron starvation in activation of the *vvhBA* operon in *Vibrio vulnificus*. *J. Biol. Chem.* doi:10.1074/jbc.RA120.012724.
- Choi, Y. S., Shin, D. H., Chung, I. Y., Kim, S. H., Heo, Y. J., and Cho, Y. H. (2007). Identification of *Pseudomonas aeruginosa* genes crucial for hydrogen peroxide resistance. *J. Microbiol. Biotechnol.*
- Choudhary, K. S., Kleinmanns, J. A., Decker, K., Sastry, A. V., Gao, Y., Szubin, R., et al. (2020). Elucidation of Regulatory Modes for Five Two-Component Systems in *Escherichia coli* Reveals Novel Relationships. *mSystems*. doi:10.1128/msystems.00980-20.
- Crimmins, G. T., Mohammadi, S., Green, E. R., Bergman, M. A., Isberg, R. R., and Mecsas, J. (2012). Identification of MrtAB, an ABC Transporter Specifically Required for *Yersinia pseudotuberculosis* to Colonize the Mesenteric Lymph Nodes. *PLoS Pathog.* doi:10.1371/journal.ppat.1002828.
- Cróinín, T. Ó., and Dorman, C. J. (2007). Expression of the Fis protein is sustained in late-exponential- and stationary-phase cultures of *Salmonella enterica* serovar Typhimurium grown in the absence of aeration. *Mol. Microbiol.* doi:10.1111/j.1365-2958.2007.05916.x.
- Dalebroux, Z. D., and Miller, S. I. (2014). *Salmonellae* PhoPQ regulation of the outer membrane to resist innate immunity. *Curr. Opin. Microbiol.* doi:10.1016/j.mib.2013.12.005.

- Darling, A. C. E., Mau, B., Blattner, F. R., and Perna, N. T. (2004). Mauve: Multiple alignment of conserved genomic sequence with rearrangements. *Genome Res.* doi:10.1101/gr.2289704.
- Dube, P. (2009). Interaction of Yersinia with the Gut: Mechanisms of pathogenesis and immune evasion. *Curr. Top. Microbiol. Immunol.* doi:10.1007/978-3-642-01846-6-3.
- Duprey, A., Reverchon, S., and Nasser, W. (2014). Bacterial virulence and Fis: Adapting regulatory networks to the host environment. *Trends Microbiol.* doi:10.1016/j.tim.2013.11.008.
- Gao, H., Zhou, D., Li, Y., Guo, Z., Han, Y., Song, Y., et al. (2008). The iron-responsive fur regulon in Yersinia pestis. *J. Bacteriol.* doi:10.1128/JB.01910-07.
- Gemski, P., Lazere, J. R., Casey, T., and Wohlhieter, J. A. (1980). Presence of a virulence-associated plasmid in Yersinia pseudotuberculosis. *Infect. Immun.*
- Giel, J. L., Nesbit, A. D., Mettert, E. L., Fleischhacker, A. S., Wanta, B. T., and Kiley, P. J. (2013). Regulation of iron-sulphur cluster homeostasis through transcriptional control of the Isc pathway by [2Fe-2S]-IscR in Escherichia coli. *Mol. Microbiol.* doi:10.1111/mmi.12052.
- Giel, J. L., Rodionov, D., Liu, M., Blattner, F. R., and Kiley, P. J. (2006). IscR-dependent gene expression links iron-sulphur cluster assembly to the control of O₂-regulated genes in Escherichia coli. *Mol. Microbiol.*

doi:10.1111/j.1365-2958.2006.05160.x.

Green, E. R., Clark, S., Crimmins, G. T., Mack, M., Kumamoto, C. A., and Meccas, J. (2016). Fis Is Essential for *Yersinia pseudotuberculosis* Virulence and Protects against Reactive Oxygen Species Produced by Phagocytic Cells during Infection. *PLoS Pathog.*

doi:10.1371/journal.ppat.1005898.

Heroven, A. K., and Dersch, P. (2014). Coregulation of host-adapted metabolism and virulence by pathogenic yersiniae. *Front. Cell. Infect. Microbiol.* doi:10.3389/fcimb.2014.00146.

Homann, O. R., and Johnson, A. D. (2010). MochiView: Versatile software for genome browsing and DNA motif analysis. *BMC Biol.*

doi:10.1186/1741-7007-8-49.

Hooker-Romero, D., Mettert, E., Schwiesow, L., Balderas, D., Alvarez, P. A., Kicin, A., et al. (2019). Iron availability and oxygen tension regulate the *Yersinia* Ysc type III secretion system to enable disseminated infection. *PLoS Pathog.* doi:10.1371/journal.ppat.1008001.

Huerta-Cepas, J., Szklarczyk, D., Forslund, K., Cook, H., Heller, D., Walter, M. C., et al. (2016). EGGNOG 4.5: A hierarchical orthology framework with improved functional annotations for eukaryotic, prokaryotic and viral sequences. *Nucleic Acids Res.* doi:10.1093/nar/gkv1248.

Imlay, J. A. (2006). Iron-sulphur clusters and the problem with oxygen. *Mol. Microbiol.* doi:10.1111/j.1365-2958.2006.05028.x.

- Jacobi, C. A., Gregor, S., Rakin, A., and Heesemann, J. (2001). Expression analysis of the yersiniabactin receptor gene *fyuA* and the heme receptor *hemR* of *Yersinia enterocolitica* in vitro and in vivo using the reporter genes for green fluorescent protein and luciferase. *Infect. Immun.* doi:10.1128/IAI.69.12.7772-7782.2001.
- Jones-Carson, J., Laughlin, J., Hamad, M. A., Stewart, A. L., Voskuil, M. I., and Vázquez-Torres, A. (2008). Inactivation of [Fe-S] metalloproteins mediates nitric oxide-dependent killing of *Burkholderia mallei*. *PLoS One.* doi:10.1371/journal.pone.0001976.
- Kawahara, K., Tsukano, H., Watanabe, H., Lindner, B., and Matsuura, M. (2002). Modification of the structure and activity of lipid A in *Yersinia pestis* lipopolysaccharide by growth temperature. *Infect. Immun.* doi:10.1128/IAI.70.8.4092-4098.2002.
- Kawasaki, K., Ernst, R. K., and Miller, S. I. (2004). Deacylation and palmitoylation of lipid A by *Salmonellae* outer membrane enzymes modulate host signaling through Toll-like receptor 4. *J. Endotoxin Res.* doi:10.1179/096805104225006264.
- Kim, S. H., Lee, B. Y., Lau, G. W., and Cho, Y. H. (2009). IscR modulates catalase a (*KatA*) activity, peroxide resistance, and full virulence of *Pseudomonas aeruginosa* PA14. *J. Microbiol. Biotechnol.* doi:10.4014/jmb.0906.06028.
- Kirjavainen, V., Jarva, H., Biedzka-Sarek, M., Blom, A. M., Skurnik, M., and

- Meri, S. (2008). Yersinia enterocolitica serum resistance proteins YadA and ail bind the complement regulator C4b-binding protein. *PLoS Pathog.* doi:10.1371/journal.ppat.1000140.
- Kleinman, C. L., Sycz, G., Bonomi, H. R., Rodriguez, R. M., Zorreguieta, A., and Sieira, R. (2017). ChIP-seq analysis of the LuxR-type regulator VjbR reveals novel insights into the Brucella virulence gene expression network. *Nucleic Acids Res.* doi:10.1093/nar/gkx165.
- Krasikova, I. N., Khotimchenko, S. V., Solov'eva, T. F., and Ovodov, Y. S. (1995). Mutual influence of plasmid profile and growth temperature on the lipid composition of Yersinia pseudotuberculosis bacteria. *Biochim. Biophys. Acta (BBA)/Lipids Lipid Metab.* doi:10.1016/0005-2760(95)00061-G.
- Kuan, P. F., Chung, D., Pan, G., Thomson, J. A., Stewart, R., and Keleş, S. (2011). A statistical framework for the analysis of ChIP-Seq data. *J. Am. Stat. Assoc.* doi:10.1198/jasa.2011.ap09706.
- Kwuan, L., Adams, W., and Auerbuch, V. (2013). Impact of host membrane pore formation by the Yersinia pseudotuberculosis type III secretion system on the macrophage innate immune response. *Infect. Immun.* doi:10.1128/IAI.01014-12.
- Langmead, B., and Salzberg, S. L. (2012a). Fast gapped-read alignment with Bowtie 2. *Nat. Methods.* doi:10.1038/nmeth.1923.
- Langmead, B., and Salzberg, S. L. (2012b). Fast gapped-read alignment

- with Bowtie 2. *Nat. Methods*. doi:10.1038/nmeth.1923.
- Lee, J. H., Yeo, W. S., and Roe, J. H. (2003). Regulation of the sufABCDSE operon by Fur. *J. Microbiol.*
- Lee, K. C., Yeo, W. S., and Roe, J. H. (2008). Oxidant-responsive induction of the suf operon, encoding a Fe-S assembly system, through Fur and IscR in Escherichia coli. *J. Bacteriol.* doi:10.1128/JB.01161-08.
- Li, H., Handsaker, B., Wysoker, A., Fennell, T., Ruan, J., Homer, N., et al. (2009). The Sequence Alignment/Map format and SAMtools. *Bioinformatics*. doi:10.1093/bioinformatics/btp352.
- Lim, J. G., Bang, Y. J., and Choi, S. H. (2014). Characterization of the vibrio vulnificus 1-Cys peroxiredoxin prx3 and regulation of its expression by the Fe-S cluster regulator IscR in response to oxidative stress and iron starvation. *J. Biol. Chem.* doi:10.1074/jbc.M114.611020.
- Lim, J. G., and Choi, S. H. (2014). IscR is a global regulator essential for pathogenesis of vibrio vulnificus and induced by host cells. *Infect. Immun.* doi:10.1128/IAI.01141-13.
- Litwin, C. M., and Calderwood, S. B. (1993). Role of iron in regulation of virulence genes. *Clin. Microbiol. Rev.* doi:10.1128/CMR.6.2.137.
- McNally, A., Thomson, N. R., Reuter, S., and Wren, B. W. (2016). “Add, stir and reduce”: Yersinia spp. as model bacteria for pathogen evolution. *Nat. Rev. Microbiol.* doi:10.1038/nrmicro.2015.29.
- Michiels, T., Vanooteghem, J. C., Lambert de Rouvroit, C., China, B., Gustin,

- A., Boudry, P., et al. (1991). Analysis of virC, an operon involved in the secretion of Yop proteins by *Yersinia enterocolitica*. *J. Bacteriol.*
doi:10.1128/jb.173.16.4994-5009.1991.
- Miller, H. K., and Auerbuch, V. (2015). Bacterial iron-sulfur cluster sensors in mammalian pathogens. *Metallomics*. doi:10.1039/c5mt00012b.
- Miller, H. K., Kwuan, L., Schwiesow, L., Bernick, D. L., Mettert, E., Ramirez, H. A., et al. (2014). IscR Is Essential for *Yersinia pseudotuberculosis* Type III Secretion and Virulence. *PLoS Pathog.*
doi:10.1371/journal.ppat.1004194.
- Miller, H. K., Schwiesow, L., Au-Yeung, W., and Auerbuch, V. (2016). Hereditary hemochromatosis predisposes mice to *Yersinia pseudotuberculosis* infection even in the absence of the type III secretion system. *Front. Cell. Infect. Microbiol.*
doi:10.3389/fcimb.2016.00069.
- Miller, V. L., and Falkow, S. (1988). Evidence for two genetic loci in *Yersinia enterocolitica* that can promote invasion of epithelial cells. *Infect. Immun.*
- Milne, I., Stephen, G., Bayer, M., Cock, P. J. A., Pritchard, L., Cardle, L., et al. (2013). Using tablet for visual exploration of second-generation sequencing data. *Brief. Bioinform.* doi:10.1093/bib/bbs012.
- Montminy, S. W., Khan, N., McGrath, S., Walkowicz, M. J., Sharp, F., Conlon, J. E., et al. (2006). Virulence factors of *Yersinia pestis* are

- overcome by a strong lipopolysaccharide response. *Nat. Immunol.*
doi:10.1038/ni1386.
- Morgan, J. M., Duncan, M. C., Johnson, K. S., Diepold, A., Lam, H., Dupzyk, A. J., et al. (2017). Piericidin A1 Blocks Yersinia Ysc Type III Secretion System Needle Assembly. *mSphere*. doi:10.1128/msphere.00030-17.
- Myers, K. S., Yan, H., Ong, I. M., Chung, D., Liang, K., Tran, F., et al. (2013). Genome-scale Analysis of Escherichia coli FNR Reveals Complex Features of Transcription Factor Binding. *PLoS Genet.*
doi:10.1371/journal.pgen.1003565.
- Nesbit, A. D., Giel, J. L., Rose, J. C., and Kiley, P. J. (2009). Sequence-Specific Binding to a Subset of IscR-Regulated Promoters Does Not Require IscR Fe-S Cluster Ligation. *J. Mol. Biol.*
doi:10.1016/j.jmb.2009.01.055.
- Nuss, A. M., Beckstette, M., Pimenova, M., Schmühl, C., Opitz, W., Pisano, F., et al. (2017). Tissue dual RNA-seq allows fast discovery of infection-specific functions and riboregulators shaping host-pathogen transcriptomes. *Proc. Natl. Acad. Sci. U. S. A.*
doi:10.1073/pnas.1613405114.
- Ó Cróinín, T., Carroll, R. K., Kelly, A., and Dorman, C. J. (2006). Roles for DNA supercoiling and the Fis protein in modulating expression of virulence genes during intracellular growth of *Salmonella enterica* serovar Typhimurium. *Mol. Microbiol.* doi:10.1111/j.1365-

2958.2006.05416.x.

Outten, F. W., Djaman, O., and Storz, G. (2004). A suf operon requirement for Fe-S cluster assembly during iron starvation in *Escherichia coli*. *Mol. Microbiol.* doi:10.1111/j.1365-2958.2004.04025.x.

Palmer, L. D., and Skaar, E. P. (2016). Transition Metals and Virulence in Bacteria. *Annu. Rev. Genet.* doi:10.1146/annurev-genet-120215-035146.

Perry, R. D., Bobrov, A. G., and Fetherston, J. D. (2015). The role of transition metal transporters for iron, zinc, manganese, and copper in the pathogenesis of *Yersinia pestis*. *Metallomics.* doi:10.1039/c4mt00332b.

Perry, R. D., and Fetherston, J. D. (2011). Yersiniabactin iron uptake: Mechanisms and role in *Yersinia pestis* pathogenesis. *Microbes Infect.* doi:10.1016/j.micinf.2011.04.008.

Pierson, D. E., and Falkow, S. (1993). The ail gene of *Yersinia enterocolitica* has a role in the ability of the organism to survive serum killing. *Infect. Immun.*

Putzker, M., Sauer, H., and Sobe, D. (2001). Plague and other human infections caused by *Yersinia* species. *Clin. Lab.*

Py, B., Moreau, P. L., and Barras, F. (2011). Fe-S clusters, fragile sentinels of the cell. *Curr. Opin. Microbiol.* doi:10.1016/j.mib.2011.01.004.

Quenee, L. E., Hermanas, T. M., Ciletti, N., Louvel, H., Miller, N. C., Elli, D.,

- et al. (2012). Hereditary hemochromatosis restores the virulence of plague vaccine strains. *J. Infect. Dis.* doi:10.1093/infdis/jis433.
- Rajagopalan, S., Teter, S. J., Zwart, P. H., Brennan, R. G., Phillips, K. J., and Kiley, P. J. (2013). Studies of IscR reveal a unique mechanism for metal-dependent regulation of DNA binding specificity. *Nat. Struct. Mol. Biol.* doi:10.1038/nsmb.2568.
- Ramírez, F., Ryan, D. P., Grüning, B., Bhardwaj, V., Kilpert, F., Richter, A. S., et al. (2016). deepTools2: a next generation web server for deep-sequencing data analysis. *Nucleic Acids Res.* doi:10.1093/nar/gkw257.
- Rebeil, R., Ernst, R. K., Jarrett, C. O., Adams, K. N., Miller, S. I., and Hinnebusch, B. J. (2006). Characterization of late acyltransferase genes of *Yersinia pestis* and their role in temperature-dependent lipid A variation. *J. Bacteriol.* doi:10.1128/JB.188.4.1381-1388.2006.
- Robinson, M. D., McCarthy, D. J., and Smyth, G. K. (2009). edgeR: A Bioconductor package for differential expression analysis of digital gene expression data. *Bioinformatics.* doi:10.1093/bioinformatics/btp616.
- Rohmer, L., Hocquet, D., and Miller, S. I. (2011). Are pathogenic bacteria just looking for food? Metabolism and microbial pathogenesis. *Trends Microbiol.* doi:10.1016/j.tim.2011.04.003.
- Ruzicka, F. J., Beinert, H., Schwartz, C. J., Patschkowski, T., Giel, J. L., Kiley, P. J., et al. (2002). IscR, an Fe-S cluster-containing transcription factor, represses expression of *Escherichia coli* genes encoding Fe-S

cluster assembly proteins. *Proc. Natl. Acad. Sci.*

doi:10.1073/pnas.251550898.

Santos, J. A., Pereira, P. J. B., and Macedo-Ribeiro, S. (2015). What a difference a cluster makes: The multifaceted roles of IscR in gene regulation and DNA recognition. *Biochim. Biophys. Acta - Proteins Proteomics*. doi:10.1016/j.bbapap.2015.01.010.

Sastry, A. V., Gao, Y., Szubin, R., Hefner, Y., Xu, S., Kim, D., et al. (2019). The Escherichia coli transcriptome mostly consists of independently regulated modules. *Nat. Commun.* doi:10.1038/s41467-019-13483-w.

Schwartz, C. J., Giel, J. L., Patschkowski, T., Luther, C., Ruzicka, F. J., Beinert, H., et al. (2001a). IscR, an Fe-S cluster-containing transcription factor, represses expression of escherichia coli genes encoding Fe-S cluster assembly proteins. *Proc. Natl. Acad. Sci. U. S. A.* doi:10.1073/pnas.251550898.

Schwartz, C. J., Giel, J. L., Patschkowski, T., Luther, C., Ruzicka, F. J., Beinert, H., et al. (2001b). IscR, an Fe-S cluster-containing transcription factor, represses expression of Escherichia coli genes encoding Fe-S cluster assembly proteins. *Proc. Natl. Acad. Sci.* doi:10.1073/pnas.251550898.

Schwiesow, L., Lam, H., Dersch, P., and Auerbuch, V. (2016). Yersinia type III secretion system master regulator LcrF. *J. Bacteriol.* doi:10.1128/JB.00686-15.

- Schwiesow, L., Mettert, E., Wei, Y., Miller, H. K., Herrera, N. G., Balderas, D., et al. (2018). Control of hmu heme uptake genes in *Yersinia pseudotuberculosis* in response to iron sources. *Front. Cell. Infect. Microbiol.* doi:<http://dx.doi.org/10.3389/fcimb.2018.00047>.
- Sebbane, F., Lemaître, N., Sturdevant, D. E., Rebeil, R., Virtaneva, K., Porcella, S. F., et al. (2006). Adaptive response of *Yersinia pestis* to extracellular effectors of innate immunity during bubonic plague. *Proc. Natl. Acad. Sci. U. S. A.* doi:[10.1073/pnas.0601182103](https://doi.org/10.1073/pnas.0601182103).
- Simonet, M., Mazigh, D., and Berche, P. (1984). Growth of *Yersinia pseudotuberculosis* in mouse spleen despite loss of a virulence plasmid of mol. wt 47 x 10⁶. *J. Med. Microbiol.* doi:[10.1099/00222615-18-3-371](https://doi.org/10.1099/00222615-18-3-371).
- Somprasong, N., Jittawuttipoka, T., Duang-Nkern, J., Romsang, A., Chaiyen, P., Schweizer, H. P., et al. (2012). *Pseudomonas aeruginosa* Thiol Peroxidase Protects against Hydrogen Peroxide Toxicity and Displays Atypical Patterns of Gene Regulation. *J. Bacteriol.* doi:[10.1128/JB.00347-12](https://doi.org/10.1128/JB.00347-12).
- Stojiljkovic, I., and Hantke, K. (1992). Hemin uptake system of *Yersinia enterocolitica*: similarities with other TonB-dependent systems in gram-negative bacteria. *EMBO J.* doi:[10.1002/j.1460-2075.1992.tb05535.x](https://doi.org/10.1002/j.1460-2075.1992.tb05535.x).
- Sun, Y. C., Jarrett, C. O., Bosio, C. F., and Hinnebusch, B. J. (2014). Retracing the evolutionary path that led to flea-borne transmission of *Yersinia pestis*. *Cell Host Microbe.* doi:[10.1016/j.chom.2014.04.003](https://doi.org/10.1016/j.chom.2014.04.003).

- Thompson, J. M., Jones, H. A., and Perry, R. D. (1999). Molecular characterization of the hemin uptake locus (hmu) from *Yersinia pestis* and analysis of hmu mutants for hemin and hemoprotein utilization. *Infect. Immun.* doi:10.1128/iai.67.8.3879-3892.1999.
- Troxell, B., and Hassan, H. M. (2013). Transcriptional regulation by Ferric Uptake Regulator (Fur) in pathogenic bacteria. *Front. Cell. Infect. Microbiol.* doi:10.3389/fcimb.2013.00059.
- Valouev, A., Johnson, D. S., Sundquist, A., Medina, C., Anton, E., Batzoglou, S., et al. (2008). Genome-wide analysis of transcription factor binding sites based on ChIP-Seq data. *Nat. Methods.* doi:10.1038/nmeth.1246.
- Vergnes, A., Viala, J. P. M., Ouadah-Tsabet, R., Pocachard, B., Loiseau, L., Méresse, S., et al. (2017). The iron–sulfur cluster sensor IscR is a negative regulator of Spi1 type III secretion system in *Salmonella enterica*. *Cell. Microbiol.* doi:10.1111/cmi.12680.
- Wang, H., Avican, K., Fahlgren, A., Erttmann, S. F., Nuss, A. M., Dersch, P., et al. (2016). Increased plasmid copy number is essential for *Yersinia* T3SS function and virulence. *Science* (80-). doi:10.1126/science.aaf7501.
- Warrens, A. N., Jones, M. D., and Lechler, R. I. (1997). Splicing by over-lap extension by PCR using asymmetric amplification: An improved technique for the generation of hybrid proteins of immunological interest. *Gene.* doi:10.1016/S0378-1119(96)00674-9.

- Wilharm, G., Lehmann, V., Krauss, K., Lehnert, B., Richter, S., Ruckdeschel, K., et al. (2004). *Yersinia enterocolitica* type III secretion depends on the proton motive force but not on the flagellar motor components MotA and MotB. *Infect. Immun.* doi:10.1128/IAI.72.7.4004-4009.2004.
- Yamashita, S., Lukacik, P., Barnard, T. J., Noinaj, N., Felek, S., Tsang, T. M., et al. (2011). Structural insights into ail-mediated adhesion in *Yersinia pestis*. *Structure.* doi:10.1016/j.str.2011.08.010.
- Yeo, W. S., Lee, J. H., Lee, K. C., and Roe, J. H. (2006). IscR acts as an activator in response to oxidative stress for the suf operon encoding Fe-S assembly proteins. *Mol. Microbiol.* doi:10.1111/j.1365-2958.2006.05220.x.
- Zhang, P., Ye, Z., Ye, C., Zou, H., Gao, Z., and Pan, J. (2020). OmpW is positively regulated by iron via Fur, and negatively regulated by SoxS contribution to oxidative stress resistance in *Escherichia coli*. *Microb. Pathog.* doi:10.1016/j.micpath.2019.103808.
- Zhang, Y., Liu, T., Meyer, C. A., Eeckhoute, J., Johnson, D. S., Bernstein, B. E., et al. (2008). Model-based analysis of ChIP-Seq (MACS). *Genome Biol.* doi:10.1186/gb-2008-9-9-r137.
- Zheng, L., Kelly, C. J., and Colgan, S. P. (2015). Physiologic hypoxia and oxygen homeostasis in the healthy intestine. A review in the theme: Cellular responses to hypoxia. *Am. J. Physiol. - Cell Physiol.* doi:10.1152/ajpcell.00191.2015.

Zheng, M., Wang, X., Templeton, L. J., Smulski, D. R., LaRossa, R. A., and Storz, G. (2001). DNA microarray-mediated transcriptional profiling of the *Escherichia coli* response to hydrogen peroxide. *J. Bacteriol.* doi:10.1128/JB.183.15.4562-4570.2001.

Table 1. Strains used in this study.

Strain	Relevant Genotype	Source or References
IP2666/(WT)	Naturally lacks full-length YopT	(Bliska et al., 1991)
IP2666/(Δ <i>iscR</i>)	<i>iscR</i> in frame deletion of codons 2 to 156	(Miller et al., 2014)
IP2666/(IscR 3xFLAG)	In frame C-terminus 3xFLAG tag of chromosomal <i>IscR</i>	This work
IP2666/(Δ <i>sufABCDSE</i>)	<i>sufABCDSE</i> in frame deletion retains first 10 codons of <i>SufA</i> and last 20 codons of <i>SufE</i>	This work
IP2666/(Δ <i>DN756</i> <i>DN756_21815-DN756_21820</i>)	<i>DN756_21815-DN756_21820</i> in frame deletion retains first 10 codons of <i>DN756_21815</i> and last 10 codons of <i>DN756_21820</i>	This work
IP2666/(Apo-locked <i>IscR</i>)	<i>IscR</i> -C92A/C98A/C104A	(Miller et al., 2014)
IP2666/(Δ <i>flhD</i>)	WT strain with inactive <i>flhDC</i> from <i>Yersinia pestis</i>	(Miller et al., 2014)

Table 2. *Y. pseudotuberculosis* primers used in this study.

Name	Primer Sequence ^a	References
<i>FiscR_cds</i>	gatatcgaattcctgcagcccggggGCTCCTTAAATTTA GCCATGGC	This work
<i>RiscR_cds</i>	ggtctttgtagtcTGCGCGCAGATTGACGTTAATC	This work
F3xFLAG	cgtcaatctgcgcgcaGACTACAAAGACCATGAC	This work
R3xFLAG	ccgcaaattctgcttaCTCGAGTCCACCTTTATC	This work
F3' <i>iscR</i>	agtgaggactcgagTAAGCAGAATTTGCGGAATTTT AC	This work
R3' <i>iscR</i>	ggtggcggccgctctagaactagtgCCTTCAACATAGT TGAAGC	This work
F5' Δ <i>sufABCDS</i>	cgaattcctgcagcccggggTCAATCCTCGTTTTGCG	This work
<i>E</i>	C	
R5' Δ <i>sufABCDS</i>	cctccagaccAGAAAATGTCCCAACTGATTC	This work
<i>E</i>		
F5' Δ DN756_21	cgaattcctgcagcccggggGTTGAGTTCTGAAAGAA	This work
815- DN756_21820	CAATTGTG	
R5' Δ DN756_21	ggcgaccttcTTTGCGGTTGGCTTCGATG	This work
815_21820		
F3' Δ <i>sufABCDS</i>	gacatttctGGTCTGGAGGCGATGATC	This work
<i>E</i>		

R3' Δ <i>sufABCDS</i>	agggaaacaaaagctggagctATAGTCAGTACTGACC	This work
<i>E</i>	CCG	
F3' Δ <i>DN756_21</i>	caaccgcaaaGAAGGTCGCCTCGATAAAG	This work
815-21820		
R3' Δ <i>DN756_21</i>	agggaaacaaaagctggagctTTAACTGATCTGCCAG	This work
815_21820	AATTAC	
qPCR_ <i>lcrF</i> _F	GGAGTGATTTTCCGTCAGTA	(8)
qPCR_ <i>lcrF</i> _R	CTCCATAAATTTTTGCAACC	(8)
		(Hooker-
qPCR_ <i>iscR</i> _F	CAGGGCGGAAATCGCTGCCT	Romero et
		al., 2019)
		(Hooker-
qPCR_ <i>iscR</i> _R	ATTAGCCGTTGCGGCGCCTAT	Romero et
		al., 2019)
qPCR_ <i>sufA</i> _F	CGCAAATTACGCGGCTTATGC	This work
qPCR_ <i>sufA</i> _R	GGCAGGCTCTTTAGCCATATC	This work
		(Miller et
qPCR_ <i>iscS</i> _F	CGACGCCAGTAGATCCGCGT	al., 2014)
		(Miller et
qPCR_ <i>iscS</i> _R	ACGAGGGTCTGCACCCACCA	al., 2014)
		(Morgan et
qPCR_ <i>yopE</i> _F	CCATAAACCGGTGGTGAC	al., 2017)

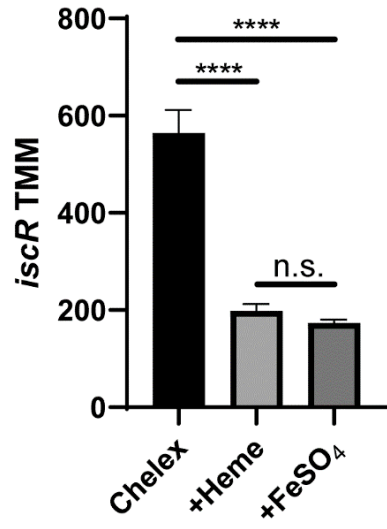
qPCR_ypjE_R	CTTGGCATTGAGTGATACTG	(Morgan et al., 2017)
qPCR_16s_F	AGCCAGCGGACCACATAAAG	(32)
qPCR_16s_R	AGTTGCAGACTCCAATCCGG	(32)
EMSA_suf_F	tttt <u>CTCGAGG</u> GAGTGTTTTTTCTTTTAGACC	This work
EMSA_suf_R	tttt <u>GGATCC</u> TAAACGTTTTTCAGGTTGAA	This work
EMSA_dusBfis_F	tttt <u>CTCGAGG</u> TATCGATAATATTTTCAGTATTAA	This work
	C	
EMSA_dusBfis_R	tttt <u>GGATCC</u> GTAGAAATATATCTGTCACACAT	This work
	C	
EMSA_ail_F	tttt <u>CTCGAGC</u> TGTCACCGTCCTGG	This work
EMSA_ail_R	tttt <u>GGATCC</u> GACTAAAGTGGCCAGCC	This work
EMSA_sodB_F	tttt <u>CTCGAG</u> TAACTGACGGTCCG	This work
EMSA_sodB_R	tttt <u>GGATCC</u> GGTGTGGGGTGAA	This work
EMSA_katA1_F	ccg <u>CTCGAG</u> TATTGCTCTCTCATTGTTTCGTTA TG	This work
EMSA_katA1_R	cgc <u>GGATCC</u> ATTTGAAATTATGATCATTGAA ATACTGTGC	This work
EMSA_katA2_F	ccg <u>CTCGAGG</u> ATCGTCAGTTCCCACAG	This work
EMSA_katA2_R	cgc <u>GGATCC</u> CCCCACTAGTTGTAGTCG	This work
NdeI-iscR_F	GGAATTCCATATGAGACTGACATCTAAAGGG CGC	This work

BamHI-His6-	GCGGGATCCTTAGTGGTGGTGGTGGTGGTG	This work
IscR_R	AGCGCGTAACTTAACGTCGATCGC	

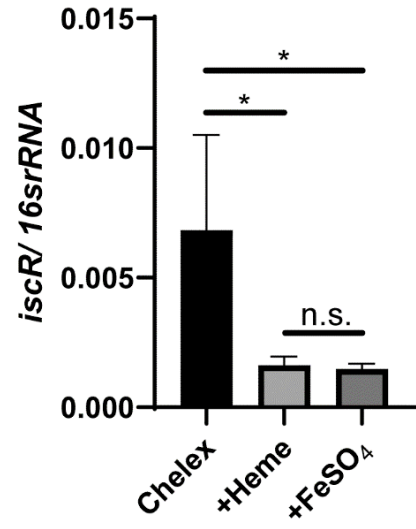
^a Uppercase specifies primer that anneals to target for molecular cloning,
lowercase is complementary sequence for NEB Gibson Assembly or extra
nucleotides to facilitate efficient restriction digest

^b Underline specifies XhoI and BamHI restriction sites

A.



B.



C.

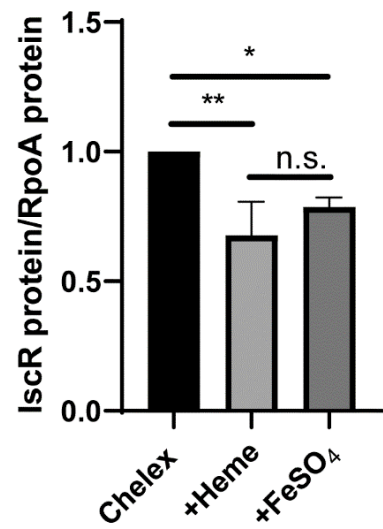
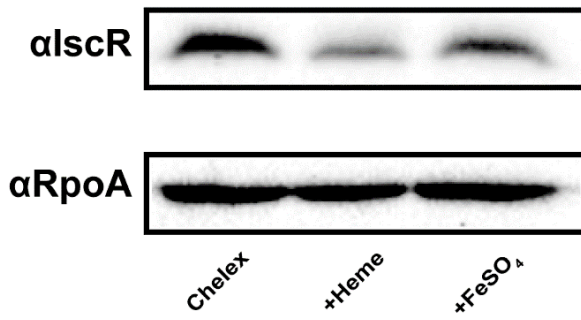


Figure 1. IscR mRNA and protein levels decrease upon iron

supplementation. (A) Expression of *iscR* in *Y. pseudotuberculosis* under varying iron conditions, as measured by RNA-Seq. Reads are represented by Trimmed Mean of M-values (TMM) of WT in Chelex-treated M9 minimal media with no iron source added back (Chelex), supplemented with 5 μ M hemin (+Heme), or supplemented with 3.6 μ M FeSO₄ (+FeSO₄).

****p<0.0001; n.s. non-significant (EdgeR with a corrected FDR post-hoc

test). **(B)** Expression of *iscR* mRNA relative to 16s rRNA, as measured by

qRT-PCR. *p<0.05 (one way ANOVA with Dunnett's post-hoc test). **(C)** IscR

protein levels in whole cell extracts from WT *Y. pseudotuberculosis*, as

detected using an anti-IscR antibody. RpoA served as a loading control.

Shown is the average of three biological replicates \pm standard deviation.

**p<0.01; *p<0.05 (one way ANOVA with Dunnett's post-hoc test).

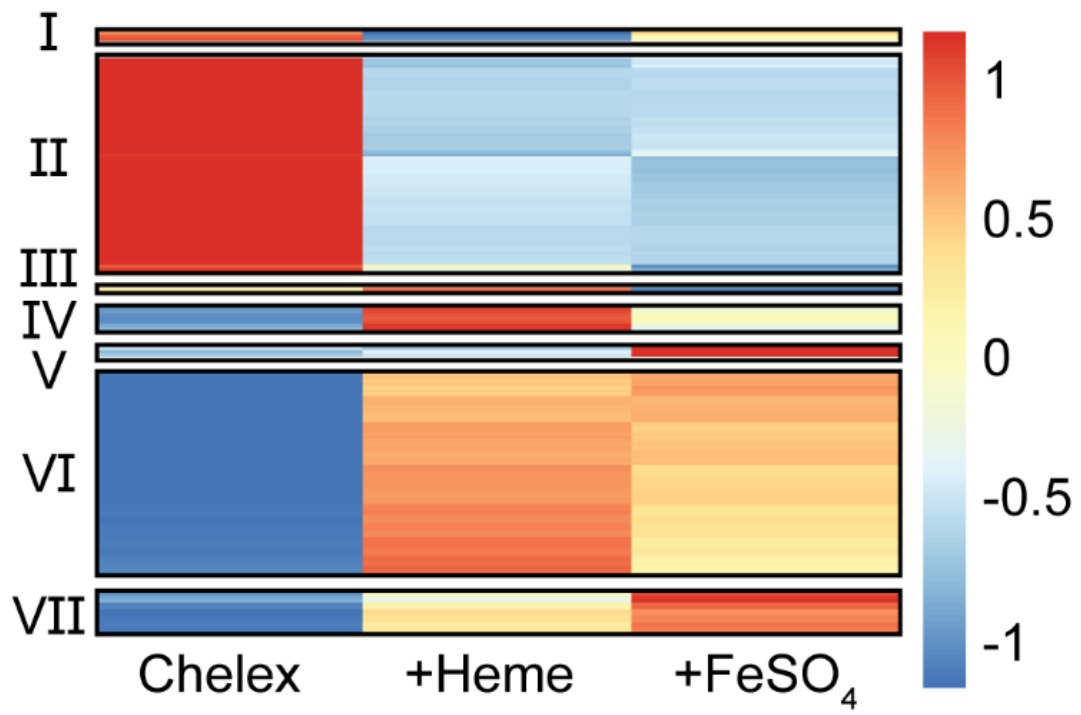


Figure 2. Iron supplementation modulates the expression of 1373 genes in *Yersinia*. RNA-Seq was carried out in WT *Y. pseudotuberculosis* after iron starvation (Chelex), or followed by supplementation with heme or FeSO₄, as in Figure 1. Cluster analysis was performed on the average RNA-Seq reads normalized by Trimmed Mean of M-values (TMM) for all 1373 differentially expressed genes. Expression values were transformed and scaled by gene before cluster analysis. Color bar represent relative gene expression.

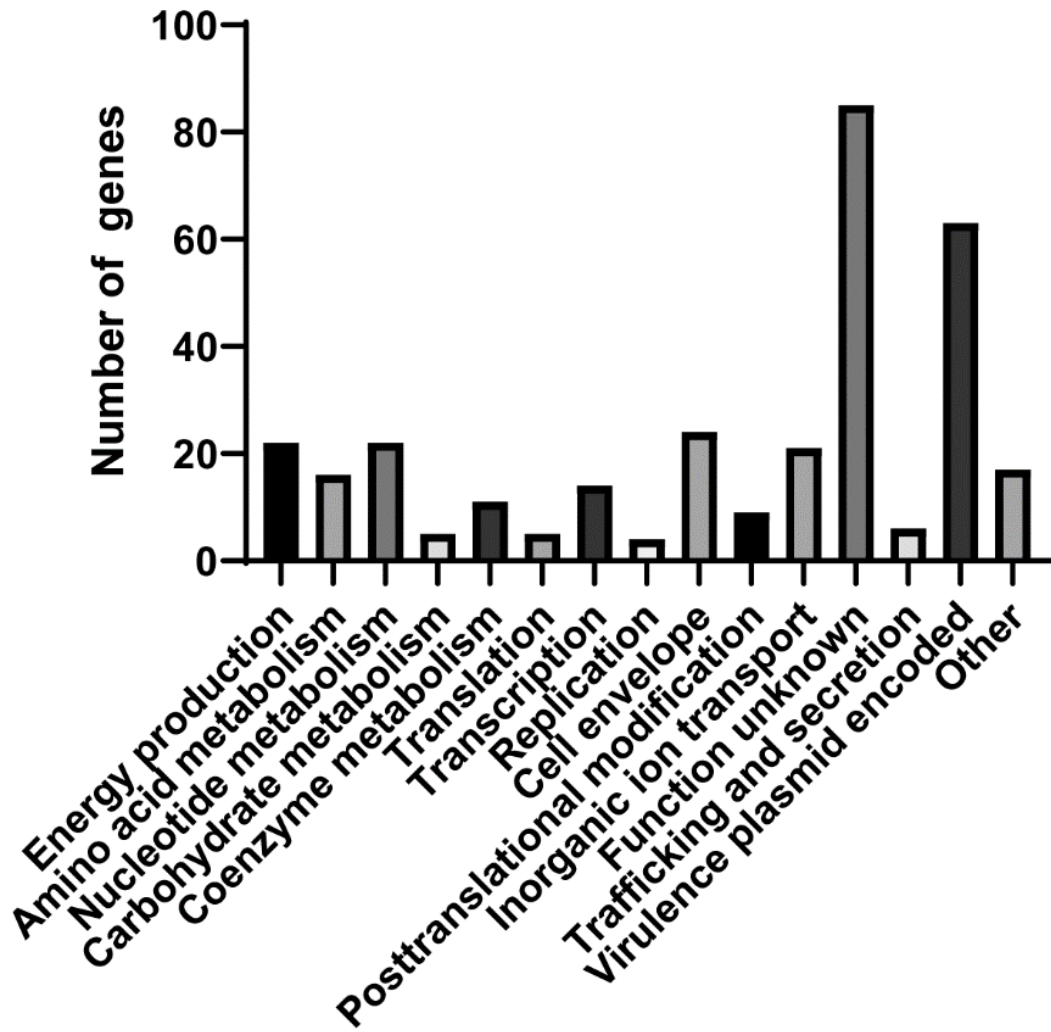
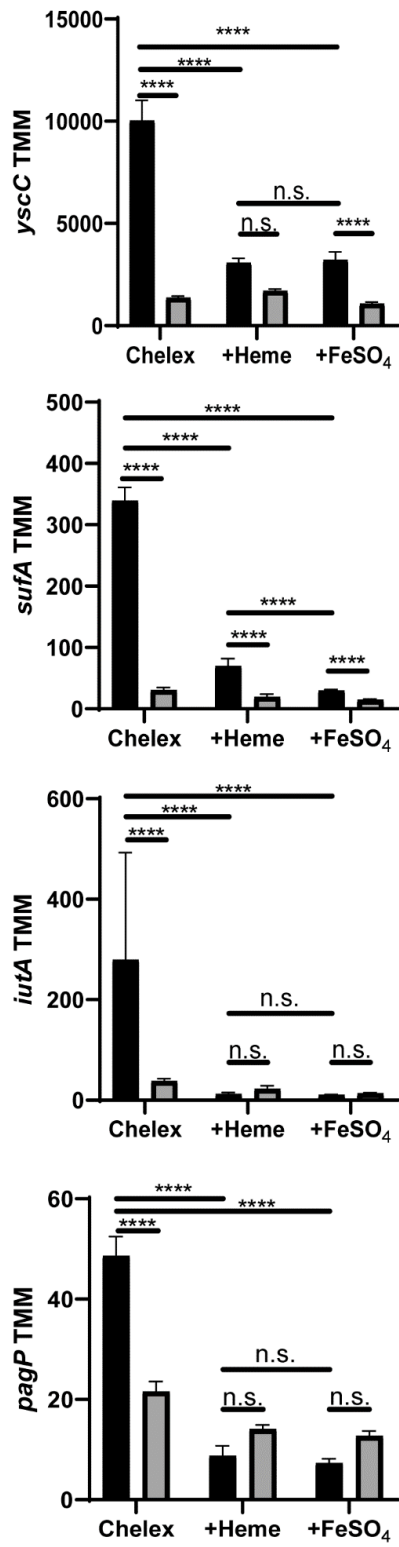


Figure 3. Deletion of *iscR* leads to expression changes in genes involved in virulence, ion transport, cell envelope, and other processes following prolonged iron starvation. Clusters of Orthologous Groups of proteins (COG) analysis of genes differentially expressed between the WT and $\Delta*iscR*$ strains following iron starvation.

A.



B.

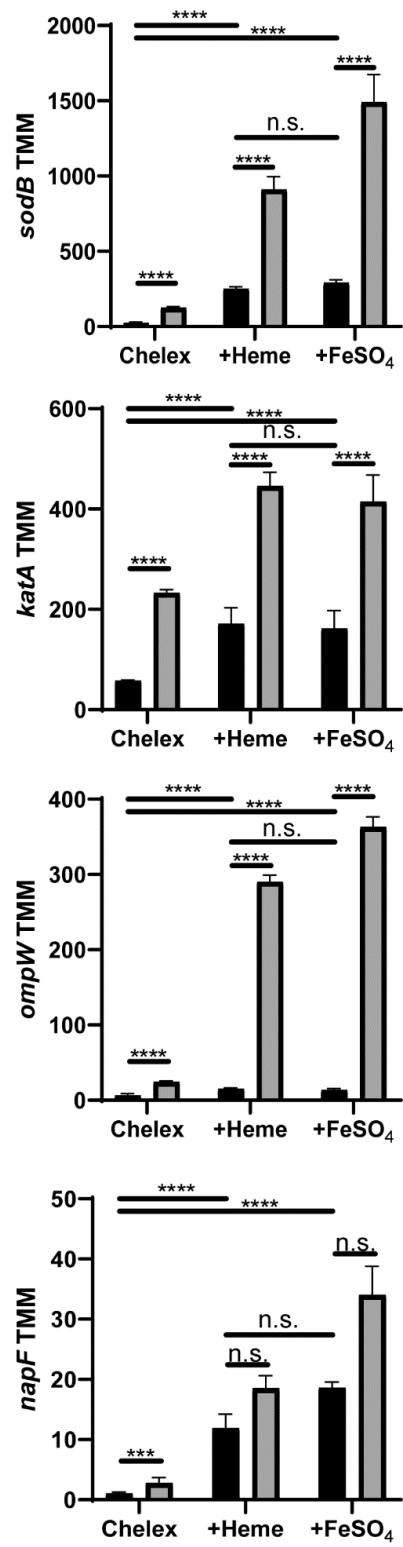


Figure 4. Several *Yersinia* genes follow expression patterns consistent with activation or repression by apo-IscR Expression of various genes as measured by RNA-Seq. Reads are represented by Trimmed Mean of M-values (TMM) of WT (black) and Δ *iscR* strains (grey).****p<0.0001; n.s. non-significant (EdgeR with a corrected FDR post-hoc test). **(A)** Genes predicted to be activated by apo-IscR. **(B)** Genes predicted to be repressed by apo-IscR.

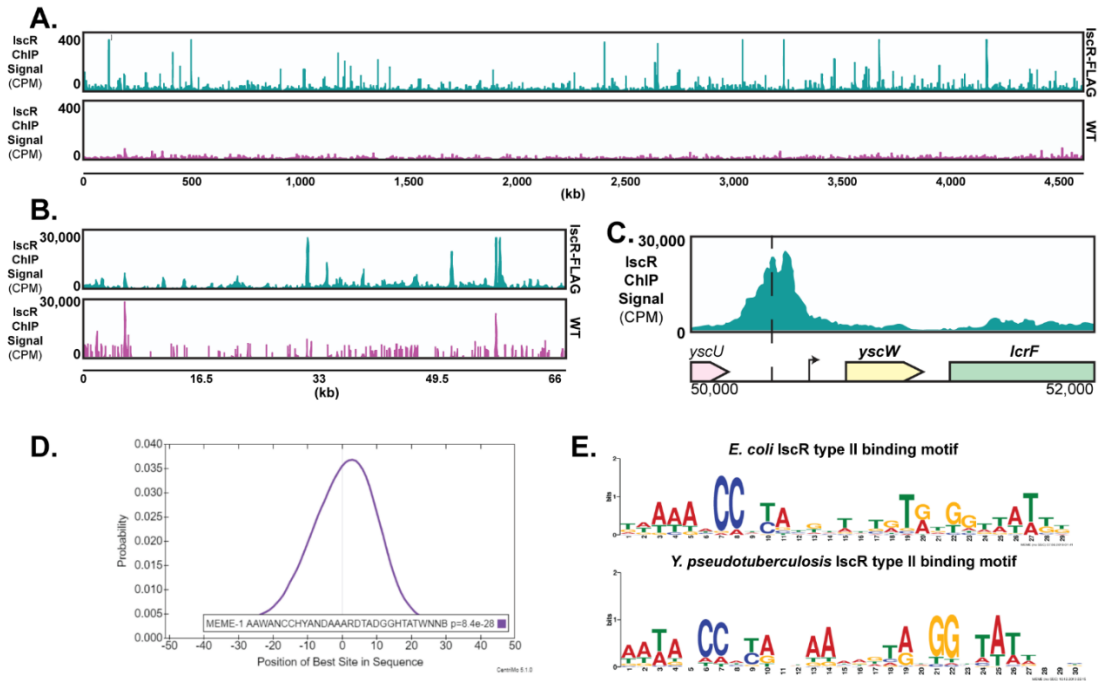
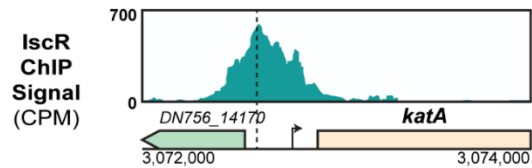
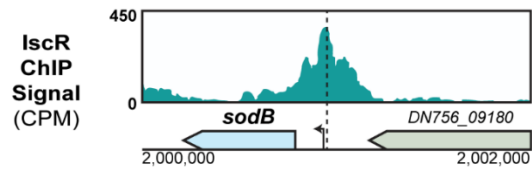
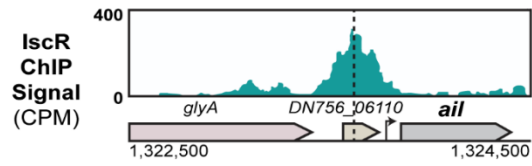
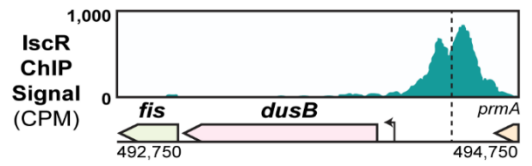


Figure 5. ChIP-Seq reveals IscR to be a global regulator in *Yersinia*. (A)

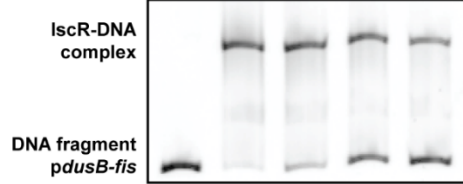
ChIP-Seq analysis reveals enrichment of IscR binding sites throughout the genome following anti-FLAG pulldown. First track (blue) represents read coverage of IscR-bound sequences throughout the *Y. pseudotuberculosis* IscR-3-xFLAG chromosome from three biological replicates, shown as count per million reads (CPM). The second track (pink) represents sequencing reads from WT *Y. pseudotuberculosis* (negative control). **(B)** ChIP-Seq plots illustrating read coverage of the pYV virulence plasmid (not scaled to size of genome). Y-axis for the pYV plasmid is significantly higher than for the chromosome because pYV copy number is expected to be high under these conditions (Wang et al., 2016). **(C)** ChIP-Seq sequence read peaks mapped to the *yscW-lcrF* promoter. The x-axis indicates the genomic position of the ChIP-Seq peaks. Dashed lines correspond to the center of the known 30 bp IscR type II binding site. Arrow indicates transcriptional start site (Nuss et al., 2017). **(D)** Motif that is over-represented within 100 nucleotides of the zenith of IscR ChIP-Seq sequence read peaks. This motif was identified in 175 peaks out of 176 peaks. The motif representing the type II characterized in *E. coli* K12 MG1655 is shown as reference. **(E)** The motif illustrated in Fig 5D has a high probability of being located at or near the peak summit (Centri-Mo).

A.



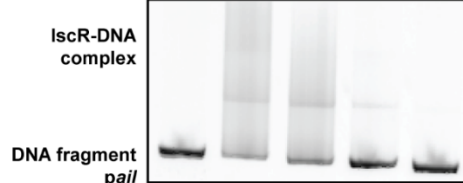
B.

nM IscR-C92A: 0 250 125 62.5 31.25



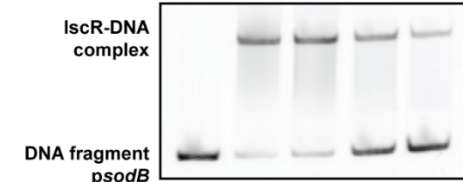
TATTCCATAGTAAAATCATGGGTATG

nM IscR-C92A: 0 250 125 62.5 31.25



CTGGTCGCCAAGGTCAATGGGGCTATT

nM IscR-C92A: 0 250 125 62.5 31.25



CAATACCCCAATTAACTGTATGGTTAT

nM IscR-C92A: 0 250 125 62.5 31.25



TATTCCATAGTAAAATCATGGGTATG

nM IscR-C92A: 0 250 125 62.5 31.25



ATTACCCATGTTACAATAAGGCATAC

Figure 6. IscR binds to the promoters of *dusB-fis*, *ail*, *sodB*, and *katA* in vivo and in vitro. (A) IscR-enriched sequence reads located within the promoter regions of *dusB-fis*, *ail*, *sodB*, and *katA*. The y-axis indicates read count, while the x-axis indicates the genomic position of the ChIP-Seq peaks. Dashed lines correspond to the identified 30 base pair IscR type II motif sequence. Arrows indicate previously identified transcriptional start sites (Nuss et al., 2017). **(B)** Purified *E. coli* IscR-C92A was used for electrophoretic mobility shift assays (EMSAs) using DNA from the promoter regions of *dusB-fis*, *ail*, *sodB*, and *katA*. The predicted IscR type II binding site is noted below each EMSA and critical nucleotides are highlighted in color. Note the *katA* promoter template was split into two distinct fragments.

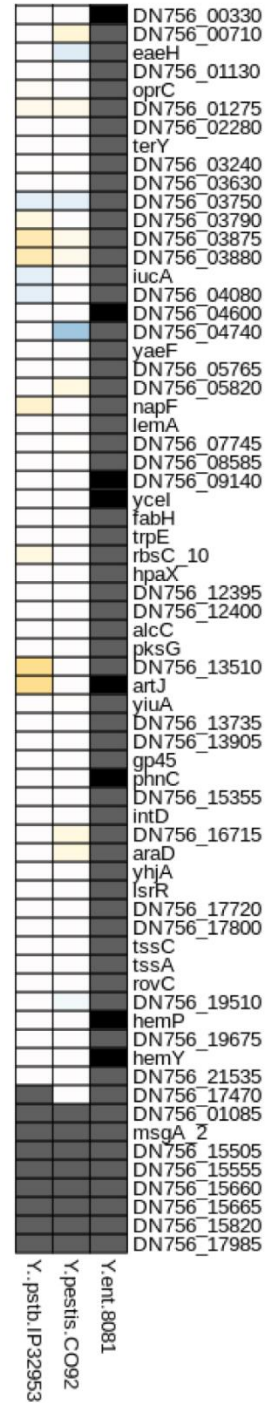
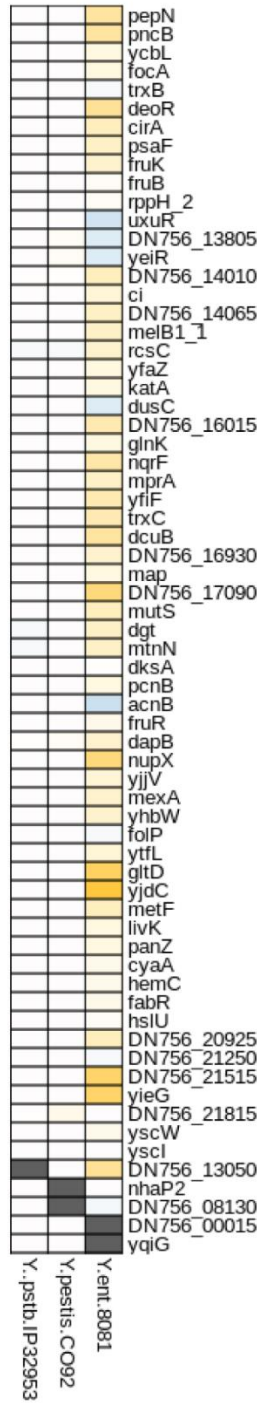
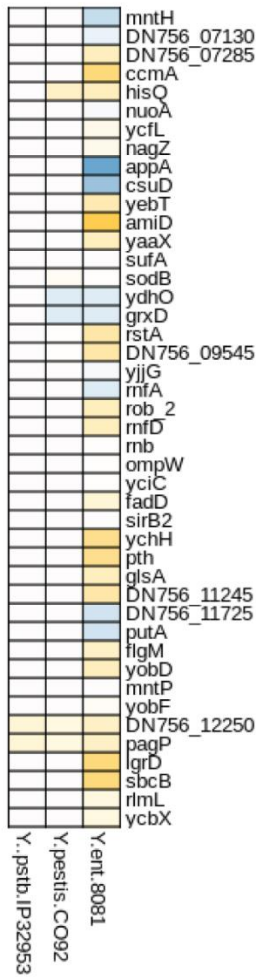
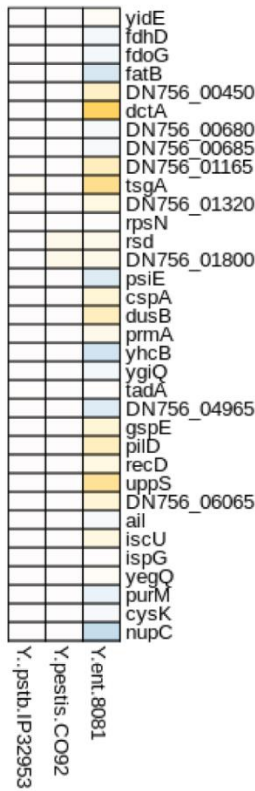
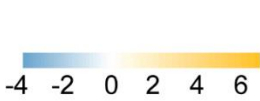
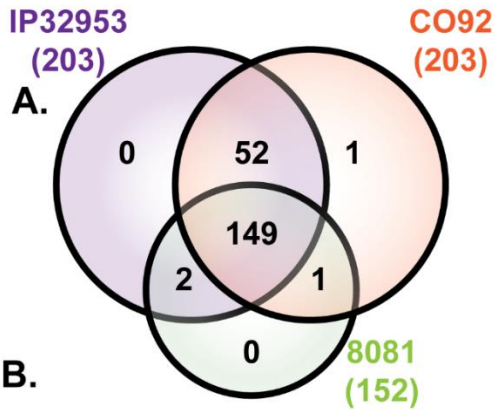


Figure 7. IscR binding site sequences are highly conserved in human pathogenic *Yersinia*. **(A)** The first gene of the 213 transcription units identified in this study as being targets of IscR in *Y. pseudotuberculosis* IP2666 were used to identify orthologs in *Y. pseudotuberculosis* IP32953, *Yersinia pestis* CO92, and *Yersinia enterocolitica* 8081. **(B)** Heatmap showing similarity of IscR binding sites in *Y. pseudotuberculosis* IP32953, *Y. pestis* CO92, and *Y. enterocolitica* 8081 compared to *Y. pseudotuberculosis* IP2666, in the promoter of the 213 IscR transcription units. Blue boxes indicate a bioinformatically-identified IscR type II binding motif predicted to enable stronger binding in the IP32953, CO92, or 8081 strain compared to the IP2666 strain. Yellow boxes indicate a motif predicted to bind IscR more weakly in IP32953, CO92, or 8081 compared to IP2666. White boxes indicate the predicted IscR binding site is similar in IP32953, CO92, or 8081 compared to IP2666. Grey boxes indicate no ortholog was found in the strain. Black boxes indicate an ortholog was identified but no IscR binding site was predicted by MEME-suite tools. Values represent absolute log difference between MEME-FIMO-pvalue of known IscR binding site to orthologous IscR binding site.

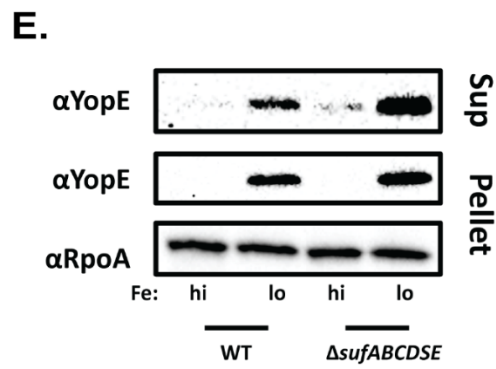
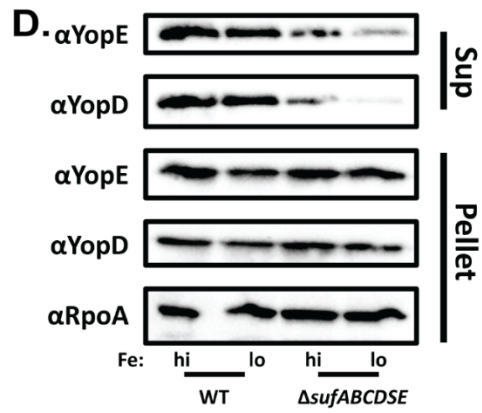
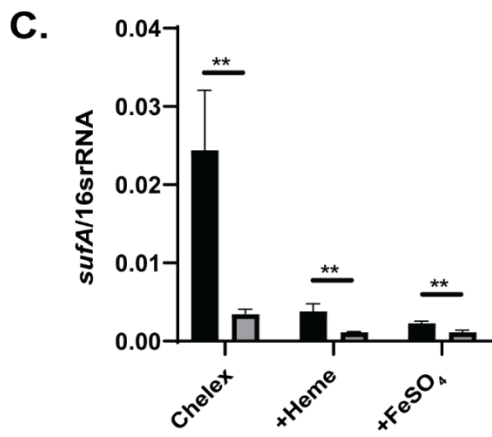
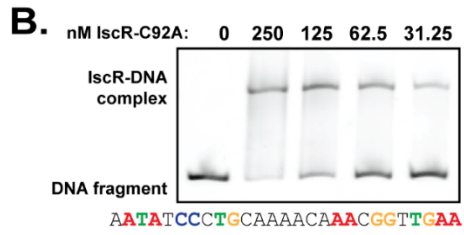
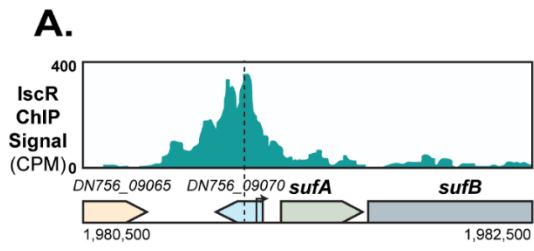


Figure 8. IscR directly regulates the Suf Fe-S cluster biogenesis pathway, which is important for type III secretion activity specifically under aerobic conditions. (A) IscR-enriched sequence reads located within the promoter regions of *sufABCDSE*. The y-axis indicates read count, while the x-axis indicates the genomic position of the ChIP-Seq peaks. Dashed lines correspond to the identified 30 base pair IscR type II motif sequence. Arrows indicate previously identified transcriptional start site (Nuss et al., 2017). **(B)** Purified *E. coli* IscR-C92A was used for electrophoretic mobility shift assays (EMSAs) using DNA from the promoter regions of *sufABCDSE*. The predicted IscR type II binding site is noted below the EMSA and critical nucleotides are highlighted in color. **(C)** Expression of *sufA* relative to 16s rRNA as measured by qRT-PCR of WT (black) and $\Delta iscR$ strains (grey). ** $p < 0.01$; (one way ANOVA with Dunnett's post-hoc test). Average of three independent experiments \pm standard deviation is shown. **(D-E)** WT and $\Delta sufABCDSE$ cultures were iron starved in chelex-treated M9 minimal media and supplemented with either 3.6 μM FeSO_4 (hi) or 0.036 μM FeSO_4 (lo) before type III secretion was induced under aerobic **(D)** or anaerobic **(E)** conditions. Proteins secreted into culture supernatant and precipitated with trichloroacetic acid were probed with antibodies for YopE and YopD T3SS cargo proteins. Cell lysates were probed with antibodies for RpoA, YopE, and YopD. One representative experiment out of three biological replicates is shown.

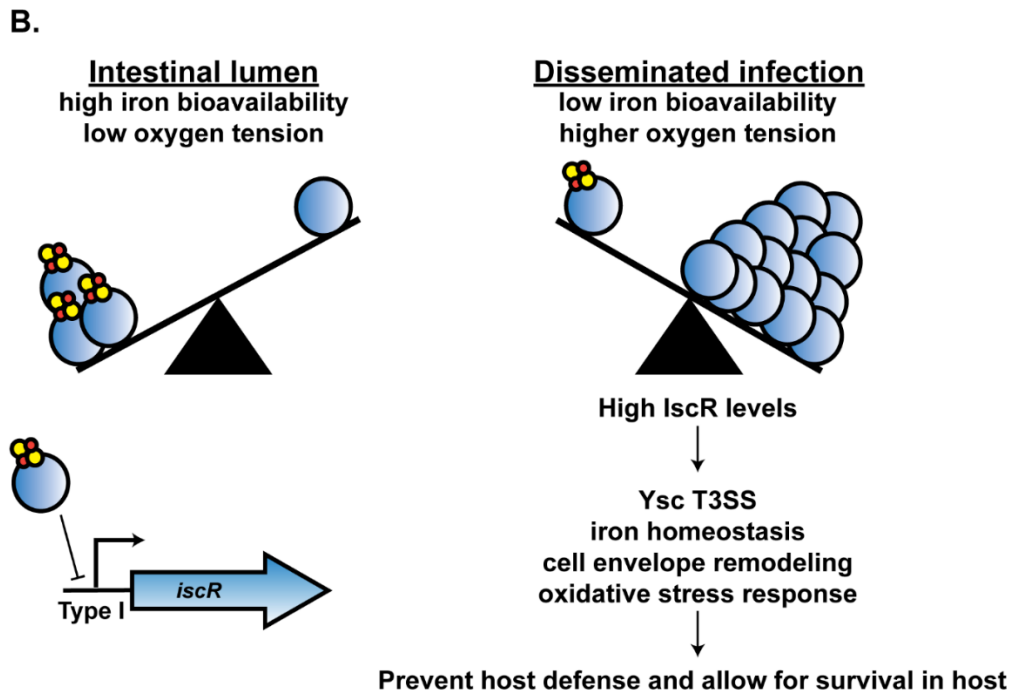
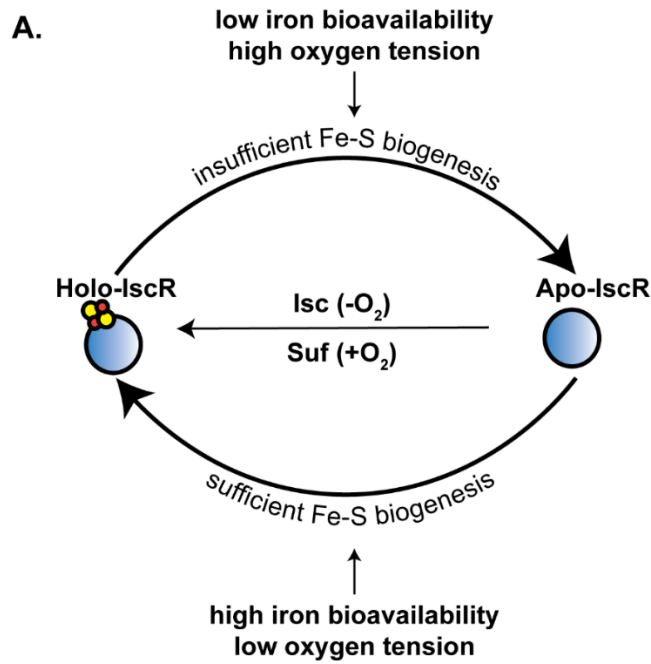


Figure 9. Model of how iron modulates IscR levels and leads to differential expression of IscR dependent virulence factors. (A) The Suf system loads Fe-S clusters onto IscR under aerobic conditions while the Isc system is more active under anaerobic conditions. Iron bioavailability and oxygen tension affect the holo-/apo-IscR ratio. (B) Low iron and oxidative stress, which are encountered by *Yersinia* during disseminated infection, lead to increased Fe-S cluster demand. This leads to a decrease in holo-IscR, subsequent derepression of the overall IscR expression, and an increase in apo-IscR levels. Apo-IscR directly regulates genes involved in the T3SS, oxidative stress resistance, cell envelope remodeling, iron homeostasis, and other genes, enabling virulence.

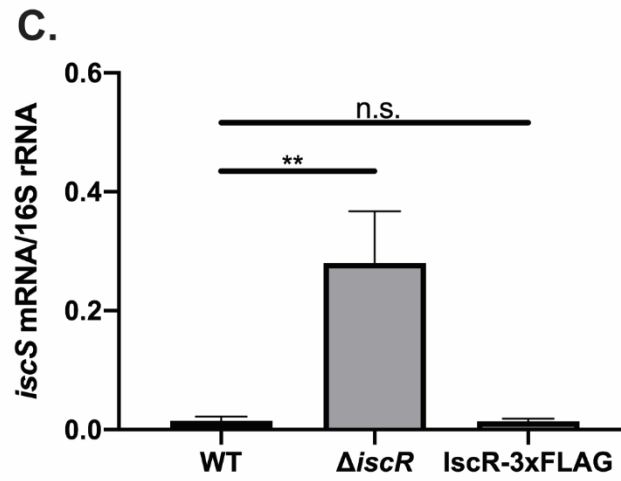
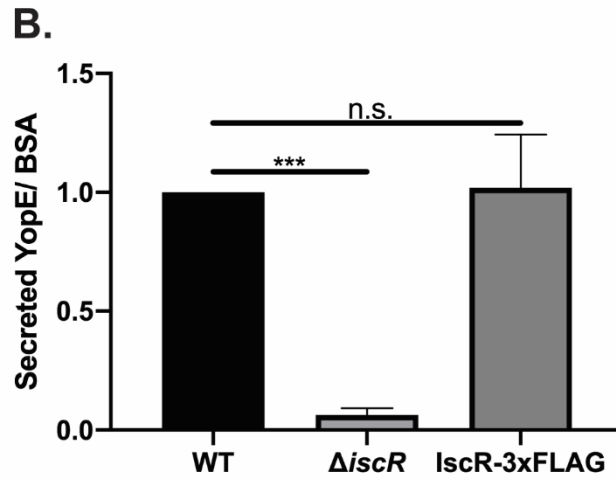
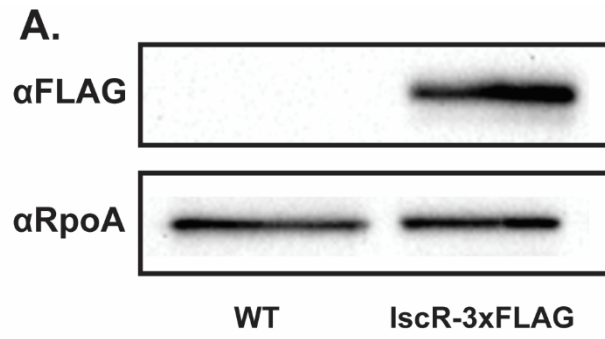
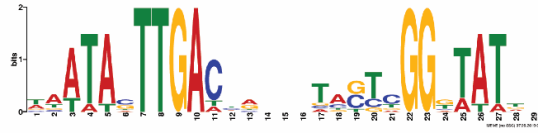


Figure S1. 3xFLAG-tagged IscR rescues an *iscR* deletion. (A) Whole cell extracts from WT *Y. pseudotuberculosis* or a strain harboring a chromosomally-encoded 3xFLAG tagged IscR were visualized using anti-FLAG or anti-RpoA antibodies. **(B)** To measure the relative efficiency of the Ysc T3SS, *Yersinia* strains were grown under T3SS-inducing conditions and secreted proteins precipitated by trichloroacetic acid were visualized using Coomassie blue. Relative amounts of the T3SS effector protein YopE were quantified by densitometry compared to a spiked in BSA protein control. The average of three biological replicates \pm standard deviation is shown. **(C)** *Yersinia* strains were grown under T3SS inducing conditions and relative *iscS* mRNA levels evaluated by qPCR and normalized to 16s rRNA. The average of three biological replicates \pm standard deviation is shown. *** $p < 0.001$; ** $p < 0.01$; n.s. non-significant (one-way ANOVA with Dunnett's *post-hoc* test).

A.



nfuA CAATAGTTGACTACTCTTGTCGGTTATAA
iscR TAATAGTTGAGTGAATTACTAGGTAAAT
erpA GAGTACTTGAAATGAAATACTCAGGTATTA
cysE CAACACTTGATAAATTTGTTTCAGTTATTG

B.

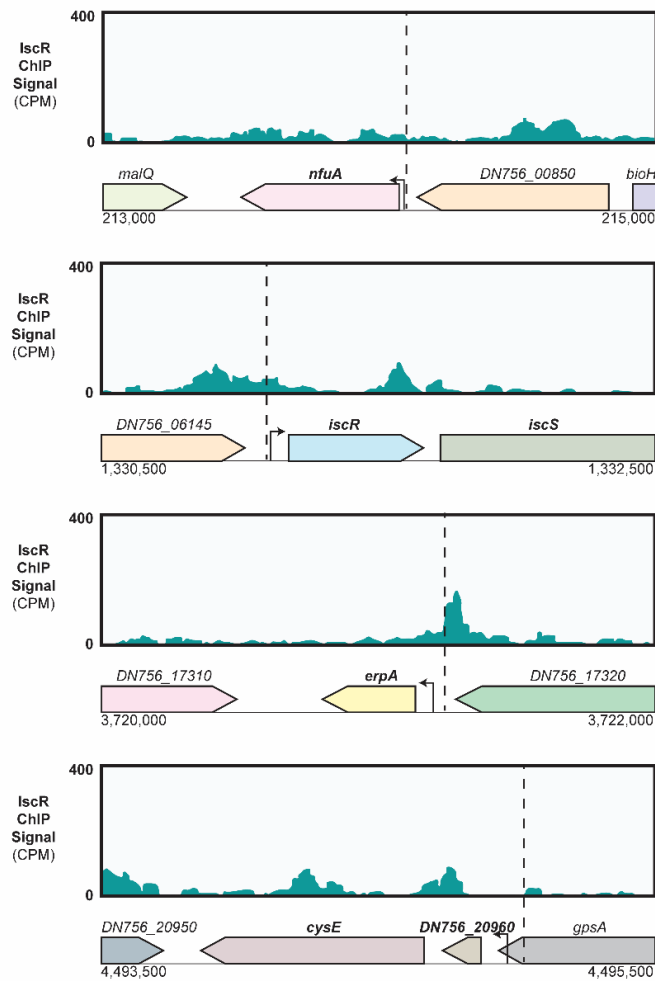


Figure S2. Global IscR ChIP-seq analysis fails to identify predicted IscR

Type I sites. (A) Known *E. coli* IscR type I binding sites were used to generate a IscR type I binding motif using MEME-suite tools. The *Y. pseudotuberculosis* IP2666 genome was scanned for IscR type I sites using FIMO specifically upstream of the *nfuA*, *iscRSUA*, *erpA*, and *DN756_20960_cysE* promoters. The predicted sequences were aligned to the *E. coli* consensus IscR type I binding motif. **(B)** IscR ChIP-seq plots illustrating read coverage of IscR-binding peaks assigned to the promoter of *nfuA*, *iscRSUA*, *erpA*, and *DN756_20960_cysE* from all three replicates combined. Dashed lines correspond to the zenith of the predicted 29 bp IscR type I motifs.

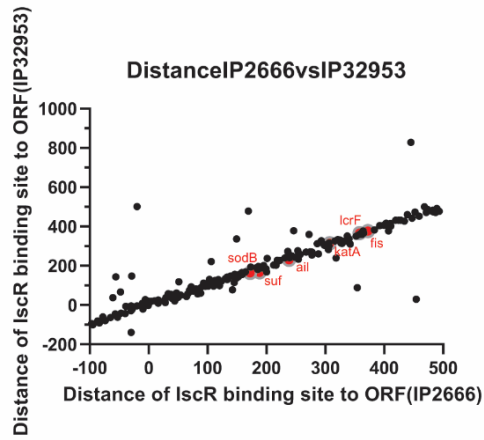
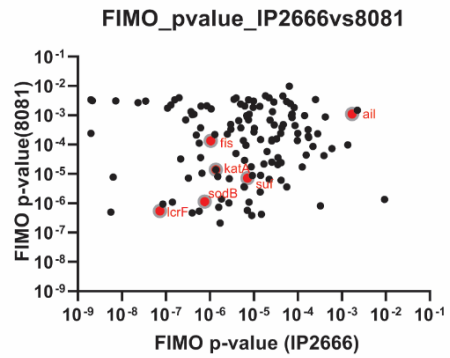
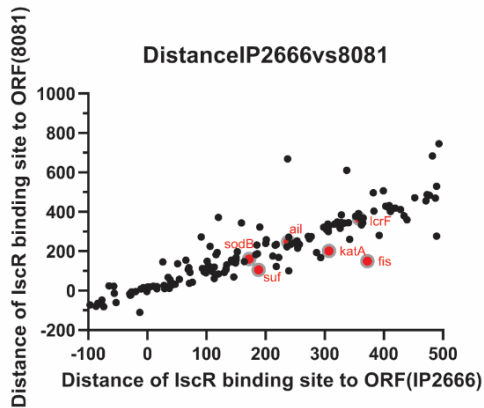
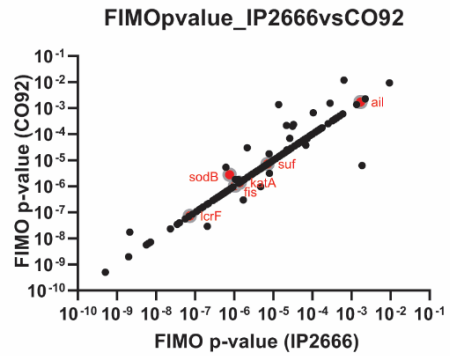
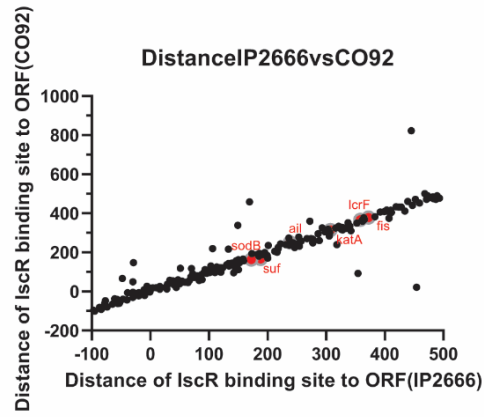
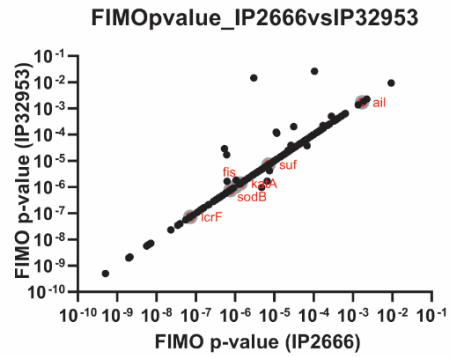
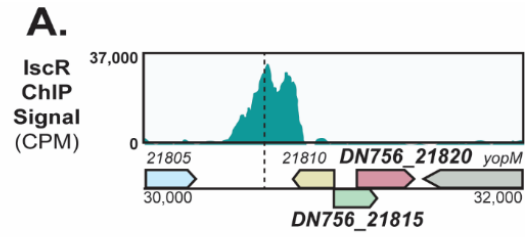
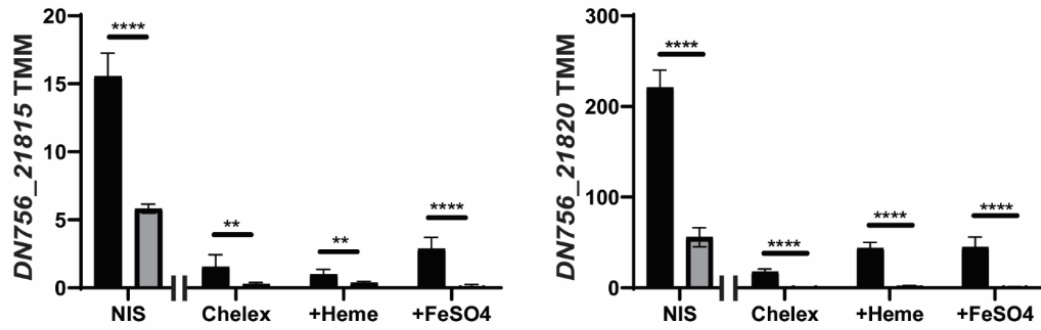
A.**B.**

Figure S3. Conservation of IscR binding sites in *Y. pseudotuberculosis* (IP2666, IP32953), *Y. pestis* (CO92), and *Y. enterocolitica* (8081). (A)

Distance of the identified IscR binding site in *Y. pseudotuberculosis* (IP2666) from the start codon of each transcription unit member of the IscR regulon is plotted versus the distance of the predicted IscR binding site from the start codon of the identified ortholog in *Y. pseudotuberculosis* (IP32953), *Y. pestis* (CO92), or *Y. enterocolitica* (8081). **(B)** The \log_{10} FIMO p-value of the identified IscR binding site in *Y. pseudotuberculosis* (IP2666) is plotted versus the \log_{10} FIMO p-value of the predicted IscR binding site upstream of identified orthologs in *Y. pseudotuberculosis* (IP32953), *Y. pestis* (CO92), or *Y. enterocolitica* (8081).



B.



C.

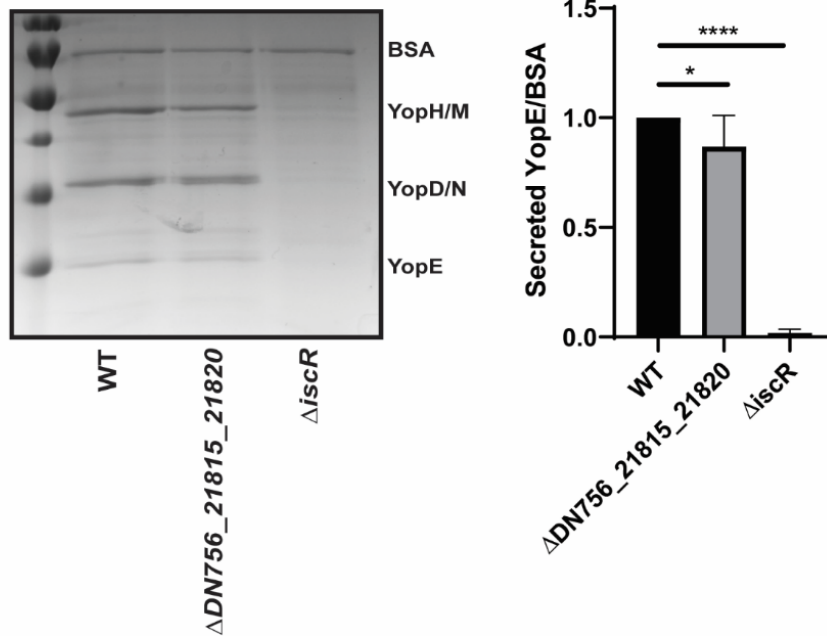


Figure S4. Deletion of DN756_21815 and DN756_21820, identified gene targets of IscR, results in a small but significant decrease in type III secretion. (A) Read coverage of IscR-binding peaks proximal to *DN756_21815_DN756_21820*. Counts per million reads (CPM) are plotted versus the genomic position. Dashed lines correspond to the predicted 30 bp IscR type II motif. Arrows indicate transcriptional start sites (50). **(B)** Expression of *DN756_21815*, and *DN756_21820* genes under varying iron conditions as measured by RNA-seq. Reads are represented by Trimmed Mean of M-values (TMM) of WT (black) and Δ *iscR* strains (grey) grown in M9 minimal media containing FeSO₄ (non-iron starved, NIS), iron starved in chelex-treated M9 minimal media with no iron source added back (Chelex), supplemented with 5 mM hemin (+Heme), or supplemented with FeSO₄ (+FeSO₄). **p<0.01; ***p<0.001; ****p<0.0001 (EdgeR with a corrected FDR post-hoc test). **(C)** *Yersinia* strains were grown under rich media, T3SS inducing conditions. The secretome of these cultures was visualized with Coomassie blue. The effector protein, YopE, was quantified by densitometry relative to the WT control to measure the relative efficiency of the Ysc T3SS. The average of 5 biological replicates \pm standard deviation is shown. ****p<0.0001; *p<0.05 (one way ANOVA with Dunnett's post-hoc test).

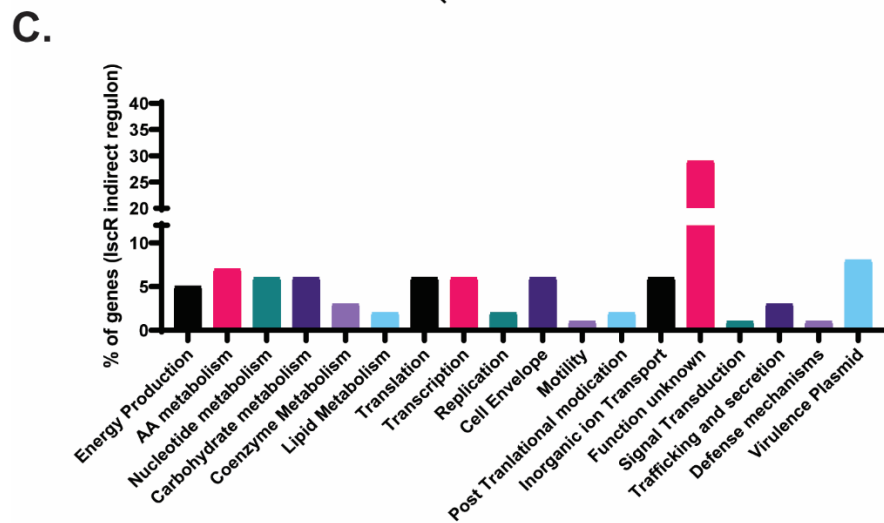
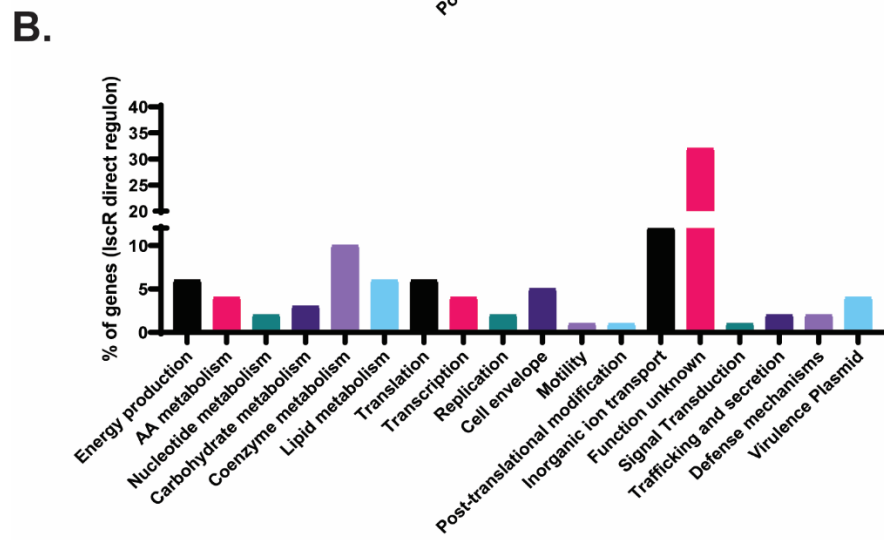
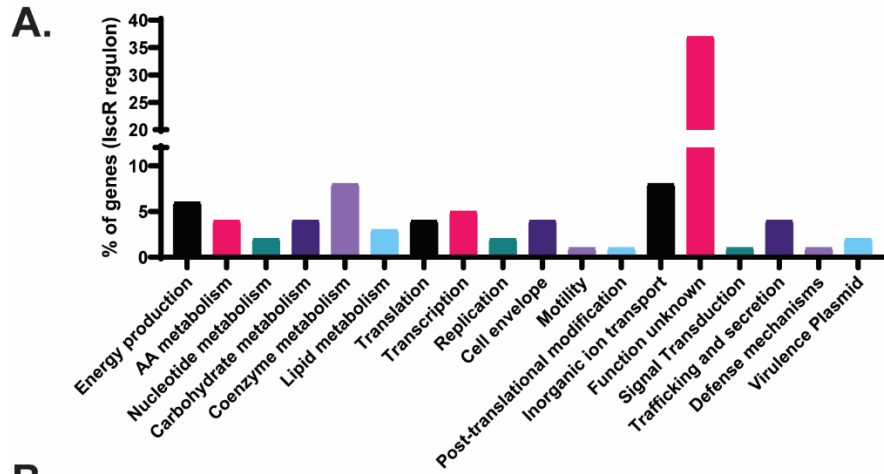


Figure S5. COG analysis of the IscR regulon, functional regulon, and indirect regulon. Clusters of Orthologous Groups of proteins (COG) analysis of genes with a IscR CHIP-Seq peak **(A)**, genes with a IscR CHIP-Seq peak and are differentially expressed between WT and the *iscR* mutant under at least one tested condition **(B)**, and genes differentially expressed between WT and the *iscR* mutant but have no IscR CHIP-Seq peak **(C)**.

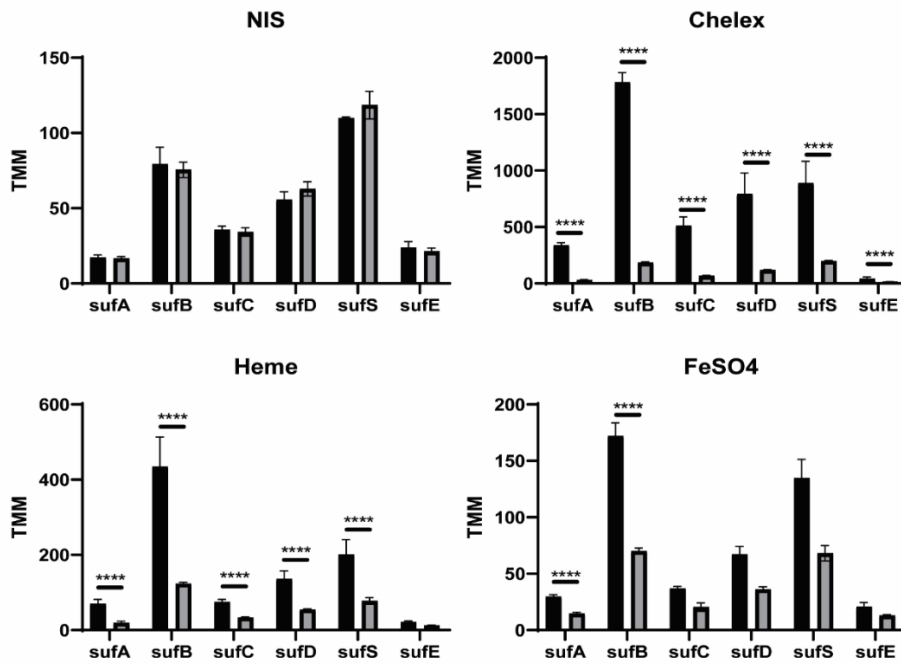


Figure S6. Expression of the *suf* operon is modulated by iron and requires IscR . Expression of *sufA*, *sufB*, *sufC*, *sufD*, *sufS*, and *sufE* genes under varying iron conditions as measured by RNA-seq. Reads are represented by Trimmed Mean of M-values (TMM) of WT (black) and Δ *iscR* strains (grey) grown in M9 minimal media containing 3.6 μ M FeSO₄ (non-iron starved, NIS), iron starved in chelex-treated M9 minimal media with no iron source added back (Chelex), supplemented with 5 mM hemin (+Heme), or supplemented with 3.6 μ M FeSO₄ (+FeSO₄). **p<0.01; ***p<0.001; ****p<0.0001 (EdgeR with a corrected FDR post-hoc test).

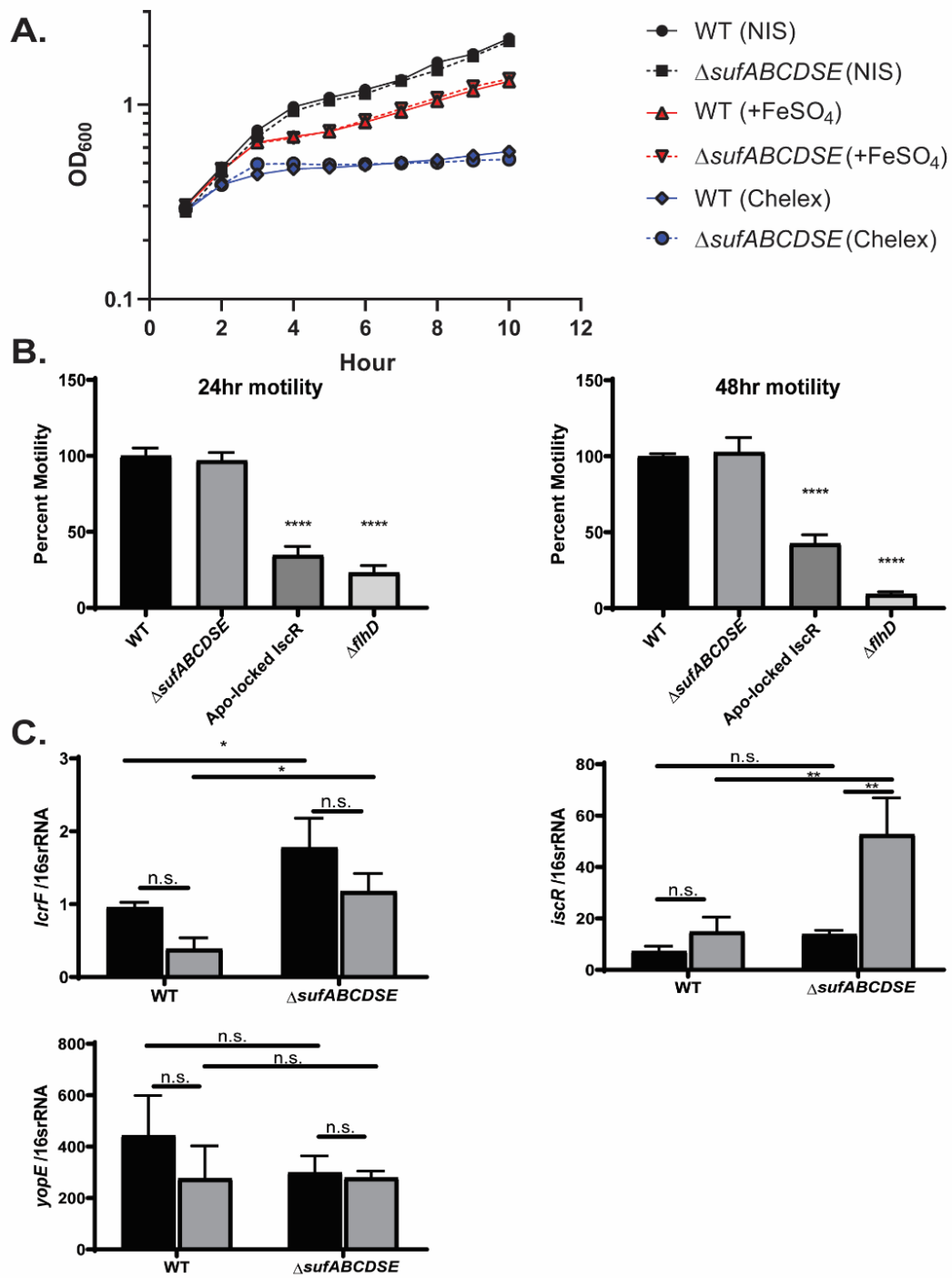


Figure S7. The Suf pathway does not affect motility or growth. (A) Iron starved *Y. pseudotuberculosis* were either kept in iron starved chelex-treated M9 minimal media with no iron source added back (Chelex), or supplemented with 3.6 μM FeSO_4 (+ FeSO_4). Cultures were grown at 26°C for 10 hr and optical density at 600 nm measured every hour. Non-iron starved (NIS) samples were never exposed to chelex-treated M9. **(B)** The indicated strains were spotted onto Motility agar (1% Tryptone 0.25% Agar) and were grown at 26°C. The diameters of the colonies were measured 24 hr and 48 hr later and used to calculate percent motility. Graphs represent three biological replicates. **** $p < 0.0001$ (one way ANOVA with Dunnett's post-hoc test). **(C)** Expression of *IcrF*, *iscR*, and *yopE*, relative to 16s rRNA, following iron starved conditions in M9 minimal media at 37°C, as measured by qPCR. Black bars represent cultures which were iron starved and supplemented with 3.6 μM FeSO_4 before induction of the type III secretion system, while grey bars represent cultures that received 0.036 μM FeSO_4 before induction of the type III secretion system. Average of three independent experiments \pm standard deviation is shown. *** $p < 0.001$; ** $p < 0.01$; * $p < 0.05$ (one way ANOVA with Dunnett's post-hoc test).

Chapter 3

IscR promotes Yersinia type III secretion system activity by antagonizing the repressive H-NS-YmoA complex at the IcrF promoter

By David Balderas, Pablo Alvarez, Mané Ohanyan, Erin Mettert, Natasha
Tanner, Patricia J. Kiley, Victoria Auerbuch

Abstract

The type III secretion system (T3SS) is a bacterial appendage used by many pathogens, such as pathogenic *Yersinia*, to subvert host defenses. However, because the T3SS is energetically costly and immunogenic, it must be tightly regulated to enable survival in the host. *Yersinia* Ysc T3SS gene expression is controlled at the transcriptional level by the master regulator LcrF. LcrF transcription is predicted to be repressed by the YmoA/H-NS complex and is induced by IscR under aerobic conditions or iron starvation. H-NS is a histone-like protein that controls gene expression by binding to specific DNA sequences and altering DNA topology, while YmoA is a non-DNA-binding, thermoregulated protein that binds H-NS and modulates its activity on a subset of promoters. Although IscR has been shown to bind the *lcrF* promoter, IscR fails to directly enhance *lcrF* transcription *in vitro*. These data suggest a complex underlying mechanism. In this study, we show that in a *ymoA* mutant, IscR is not required for LcrF expression/T3SS activity. Additionally, a mutation in YmoA that prevents H-NS binding (*ymoA*^{D43N}) rescues the T3SS defect of an Δ *iscR* mutant. Furthermore, H-NS is enriched at the *lcrF* promoter at environmental temperatures, while IscR is enriched at this promoter at mammalian body temperature under aerobic conditions. Importantly, CRISPRi knockdown of H-NS leads to increased *lcrF* transcription. Collectively, our data suggest that as IscR levels rise with iron limitation and oxidative stress, conditions *Yersinia* experiences during

extraintestinal infection, IscR antagonizes YmoA/H-NS-mediated repression of *lcrF* transcription to drive T3SS and manipulate host defense mechanisms.

Significance Statement

Facultative pathogens have the ability to silence genes important for causing virulence in environmental conditions, while also being able to upregulate these same genes when in the host. The ability to sense temperature, oxygen, pH, trace minerals, and other host specific signals allows bacteria to distinguish the host environment and upregulate virulence genes. In this study we show that the type III secretion system, a major virulence factor found in Gram-negative facultative pathogens, is regulated by an antagonization molecular mechanism. Under lower temperatures, the proteins H-NS-YmoA repress expression of this virulence factor. However, mammalian body temperature decreases H-NS regulation and aerobic conditions promote the transcription factor IscR which can antagonize H-NS-YmoA leading to upregulation of the type III secretion system.

Introduction

Virulence factors are critical components that allow pathogens to establish or sustain infections within a given host. One common bacterial virulence factor is a needle-like apparatus, known as the type III secretion system (T3SS) (Cornelis, 2006; Deng et al., 2017). Enteropathogenic *Yersinia pseudotuberculosis* is one of three human pathogenic *Yersinia spp.* that use the T3SS to inject effector proteins into host cells that dampen host immune responses, facilitating extracellular growth (Navarro et al., 2005; Viboud and Bliska, 2005; Pha, 2016; Schubert et al., 2020). Members of human pathogenic *Yersinia spp.* include *Yersinia pestis*, the causative agent of plague, and the enteropathogens *Yersinia enterocolitica* and *Yersinia pseudotuberculosis*. While the T3SS is critical for infection, this apparatus appears to be metabolically burdensome since constitutive expression of the T3SS leads to growth arrest (Brubaker, 1983; Milne-Davies et al., 2019). In addition, the Ysc T3SS is associated with pathogen-associated molecular patterns (PAMPs) recognized by several innate immune receptors, and some of these T3SS-associated PAMPs have evolved under selective evolutionary pressure by the ensuing immune response (Brodsky and Medzhitov, 2008; Schubert et al., 2020). Without tight regulation of T3SS expression and deployment, these metabolic and immunological burdens would decrease the chance of *Yersinia* survival in the host.

The Ysc T3SS is encoded on a 70 kb plasmid for *Yersinia* Virulence, known as pYV or pCD1 (Cornelis et al., 1998). Transcriptional regulation of T3SS genes is maintained by a master regulator called LcrF/VirF (Yother et al., 1986; Hoe et al., 1992; Schwiesow et al., 2016; Liu et al., 2021). LcrF itself is also encoded on pYV, within the *yscW-lcrF* operon, and is highly conserved among all three human pathogenic *Yersinia* species. LcrF is part of a larger family of AraC-like transcriptional regulators, and orthologs exist in other T3SS-encoding pathogens, such as ExsA in the nosocomial pathogen *Pseudomonas aeruginosa* (King et al., 2013). The *yscW-lcrF* operon is regulated at various stages in response to different environmental stimuli, including temperature, oxygen, and iron availability (Böhme et al., 2012; Hooker-Romero et al., 2019). For example, an RNA thermometer blocks the ribosome binding site of *lcrF* at room temperature, but melts at mammalian body temperature, allowing *lcrF* translation (Böhme et al., 2012).

In addition, transcriptional control of *yscW-lcrF* has been predicted to be mediated by the Histone-like Nucleoid structuring protein, H-NS (Böhme et al., 2012). H-NS contains an N-terminal oligomerization domain and a C-terminal DNA minor-groove binding domain separated by a flexible linker (Shindo et al., 1999; Gordon et al., 2011). H-NS preferentially binds AT rich regions of DNA (Navarre et al., 2006; Gordon et al., 2011). Once H-NS binds a high-affinity site, H-NS oligomerizes on the DNA (Dame et al., 2000, 2005).

H-NS oligomers can either form a nucleoprotein filament on a contiguous stretch of DNA, or H-NS can form DNA bridges when multiple discrete H-NS binding regions are brought together, either way leading to transcriptional silencing of that particular gene (Liu et al., 2010). Interestingly, H-NS in multiple bacterial pathogens has been shown to silence certain gene targets during growth outside of the mammalian host (20-30°C), but fails to silence these same targets when exposed to mammalian body temperature (37°C) (Ono et al., 2005; Yang et al., 2005; Picker and Wing, 2016). This suggests H-NS may play a role in repressing virulence factors outside host organisms in facultative pathogens. However, H-NS has been suggested to be an essential gene in pathogenic *Yersinia* (Heroven et al., 2004; Ellison and Miller, 2006), making it challenging to definitively test the role of H-NS in regulating gene expression in these organisms. However, YmoA (“*Yersinia* modulator”) in *Y. pseudotuberculosis*, an *E. coli* Hha (“high hemolysin activity”) ortholog, has been suggested to modulate H-NS repression of a subset of promoters and deletion of *ymoA* in *Yersinia* leads to changes in gene expression of putative H-NS targets (Cornelis, 1993; Jackson et al., 2004; Madrid et al., 2007; Böhme et al., 2012). YmoA and Hha lack a DNA binding domain; instead, these proteins form a heterocomplex with H-NS or H-NS paralogs (Nieto et al., 2002; Paytubi et al., 2004; García et al., 2006; Ali et al., 2013). Recent data has suggested that Hha contributes to H-NS silencing by aiding in H-NS bridging (Boudreau et al., 2018).

In the plague agent *Yersinia pestis*, YmoA is suggested to have a higher turnover rate at 37°C compared to environmental temperatures (Jackson et al., 2004). While YmoA alone cannot bind the *yscW-lcrF* promoter, H-NS alone or the YmoA/H-NS complex can (Böhme et al., 2012). Current models suggest that degradation of YmoA and therefore a reduction in the YmoA/H-NS complex at 37°C relieves repression of *yscW-lcrF* (Jackson et al., 2004). Yet, *ymoA* deletion mutants exhibit even higher levels of T3SS expression at 37°C compared to a parental strain in all three pathogenic *Yersinia* species (Cornelis, 1993; Jackson et al., 2004; Böhme et al., 2012), suggesting that some YmoA is present even at 37°C during mammalian infection.

The Iron Sulfur Cluster Regulator IscR is a critical positive regulator of *lcrF* (Miller et al., 2014; Hooker-Romero et al., 2019). IscR belongs to the Rrf2 family of winged helix-turn-helix transcription factors (Rodionov et al., 2006; Shepard et al., 2011). IscR was first characterized in *E. coli* where it exists in two forms: holo-IscR bound to a [2Fe-2S] cluster, and cluster-less apo-IscR (Schwartz et al., 2001a; Giel et al., 2006; Nesbit et al., 2009; Fleischhacker et al., 2012). Both forms of IscR bind DNA, but while both apo-IscR and holo-IscR bind to so-called type II motif sequences, only holo-IscR binds type I motifs (Giel et al., 2006; Nesbit et al., 2009). Holo-IscR represses its own expression through binding two type I motifs in the *isc* promoter (Schwartz et al., 2001b). Thus, conditions that increase iron-sulfur cluster demand, such as

iron starvation or oxidative stress, lead to a lower holo- to apo-IscR ratio and higher overall IscR levels. *E. coli* IscR has been shown to activate or repress transcription of target genes *in vitro* and *in vivo* (Giel et al., 2006). We have previously shown that low iron and oxidative stress lead to upregulation of IscR in *Yersinia*, and subsequently upregulation of *lcrF* transcription and T3SS expression (Miller et al., 2014; Hooker-Romero et al., 2019). Although we have shown IscR must bind upstream the *yscW-lcrF* promoter to promote *lcrF* expression, we did not know how IscR promotes *lcrF* transcription mechanistically.

In this study, we perform *in vitro* transcription assays with the *yscW-lcrF* promoter and show no enhanced transcription of *yscW-lcrF* mRNA by IscR. Therefore, how IscR potentiates LcrF expression and type III secretion remain unclear. We use CRISPRi knockdown of H-NS and a YmoA mutant that cannot bind H-NS to suggest that YmoA and H-NS form a repressive complex at the *yscW-lcrF* promoter. Furthermore, we show that IscR regulates transcription of the *yscW-lcrF* promoter by antagonizing YmoA/H-NS repression.

Materials and Methods

Bacterial strains and growth conditions

Bacterial strains used in this paper are listed in Table 1.1. *Y. pseudotuberculosis* were grown, unless otherwise specified, in LB (Luria Broth) at 26°C shaking overnight. To induce the T3SS, overnight cultures were diluted into low calcium LB medium (LB plus 20 mM sodium oxalate and 20 mM MgCl₂) to an optical density (OD₆₀₀) of 0.2 and grown for 1.5 h at 26°C shaking followed by 1.5 h at 37°C to induce Yop synthesis, depending on the assay, as previously described (Auerbuch et al., 2009).

For growing *Yersinia* under various oxygen conditions casamino acid-supplemented M9 media, referred to as M9 below, was used (Cheng et al., 1997). Growth of cultures to vary oxygen tension was achieved by first diluting 26°C overnight aerobic cultures of *Y. pseudotuberculosis* to an OD₆₀₀ of 0.1 in fresh M9 minimal media supplemented with 0.9% glucose to maximize growth rate and energy production under anaerobic conditions, and incubating for 12 hrs under either aerobic or anaerobic conditions at 26°C. Both aerobic and anaerobic cultures were diluted to an OD₆₀₀ of 0.1, grown for 2 hrs at 26°C, and then shifted to 37°C for 4 hrs.

Construction of *Yersinia* mutant strains

A 3xFLAG affinity tag was placed at the C-terminus of H-NS encoded at the native *h-ns* chromosomal locus to facilitate detection of H-NS with FLAG monoclonal antibody. The 3xFLAG affinity tag was chromosomally added to the C-terminus of *hns* through splicing by overlap extension (Warrens et al.,

1997). Primer pair *Fhns_cds/Rhns_cds* (Table 2) was used to amplify ~500bp upstream of *hns* plus the *hns* coding region excluding the stop codon. Primer pair F3xFLAG/R3xFLAG was used to amplify the 3xFLAG tag. Primer pair F3'*hns*/R3'*hns* was used to amplify the ~500 bp downstream region of *hns* including the stop codon. These amplified PCR fragments were cloned into a BamHI and SacI digested pSR47s suicide plasmid [λ pir-dependent replicon, kanamycin resistant (Kan^R), *sacB* gene conferring sucrose sensitivity] using the NEBuilder HiFi DNA Assembly kit (New England Biolabs, Inc). Recombinant plasmids were transformed into *E. coli* S17-1 λ pir competent cells and later introduced into *Y. pseudotuberculosis* IP2666 via conjugation. The resulting Kan^R, irgansan^R (*Yersinia* selective antibiotic) integrants were grown in the absence of antibiotics and plated on sucrose-containing media to select for clones that had lost *sacB* (and by inference, the linked plasmid DNA). Kan^S, sucrose^R, congo red-positive colonies were screened by PCR and sequenced.

The *ymoA* mutants were generated via splicing by overlap extension (Warrens et al., 1997). Primer pairs F5/R5 Δ *ymoA* (Table 2) were used to amplify ~1000 bp 5' of *ymoA*. Primer pair F3/R3 Δ *ymoA* were used to amplify ~1000 bp 3' of *ymoA*. Amplified PCR fragments were cloned into a BamHI- and SacI-digested pSR47s suicide plasmid (λ pir-dependent replicon, Kanamycin^R, *sacB* gene conferring sucrose sensitivity) using the NEBuilder

HiFi DNA Assembly kit (New England Biolabs, Inc). Mutant strains were generated as described for the 3xFLAG-H-NS strain above.

To generate the *ymoA*^{D43N} mutant primer pairs pUC19_YmoA_F and pUC19_YmoA_R were used to amplify 250 bp upstream *ymoA* to 250 bp downstream the *ymoA* start codon. These amplified PCR fragments were cloned into a BamHI and SacI digested pUC19 plasmid (AMP^R), using the NEBuilder HiFi DNA Assembly kit (New England Biolabs, Inc). Q5 site directed mutagenesis was performed using primer pairs *ymoA*^{D43N}_F and *ymoA*^{D43N}_R with pUC19 YmoA serving as the template DNA. The resulting plasmid, pUC19 *ymoA*^{D43N}, was digested with BamHI and SacI and the resulting fragment was ligated into the suicide plasmid pSR47s. Mutant strains were generated as described above.

In order to generate *lacZ* promoter constructs of *ymoBA* and *hns*, primer pairs pFU99a_ymoA_F/pFU99a_ymoA_R and pFU99a_hns_F/pFU99a_hns_R were used to amplify ~500 bp upstream *ymoA* and *hns* respectively which included the first ten amino acids of *ymoA* and *hns*. These promoters and first ten amino acids of YmoA and H-NS were fused in frame to *lacZ* and cloned into a BamHI- and Sall-digested pFU99a using the NEBuilder HiFi DNA Assembly kit (New England Biolabs, Inc). These reporter plasmids were

electroporated into wildtype *Y. pseudotuberculosis* and the *iscR* mutant to measure *ymoA* and *hns* promoter activity.

In order to generate *lacZ* promoter constructs of *yscW-lcrF*, the reverse primer pFU99a_yscWlcrF_R was used with the following forward primers pFU99a_yscWlcrF_p1 (promoter construct 1/ -505 to +294 of *yscW*), pFU99a_yscWlcrF_p2 (promoter construct 2/ -309 to +294 of *yscW*), pFU99a_yscWlcrF_p3 (promoter construct 3/ -166 to +294 of *yscW*), pFU99a_yscWlcrF_p4 (promoter construct 4/ -47 to +294 of *yscW*), and pFU99a_yscWlcrF_p5 (promoter construct 5/ +101 to +294 of *yscW*). These promoter fragments were cloned into a BamHI- and Sall-digested pFU99a using the NEBuilder HiFi DNA Assembly kit (New England Biolabs, Inc). These reporter plasmids were electroporated into *Y. pseudotuberculosis*.

***In vitro* transcription assay**

The DNA template used to assess if IscR could directly promote transcription of the *yscW-lcrF* promoter contained the -206 to +12 bp relative to the +1 transcription start site of *yscW*. The effect of IscR-C92A on σ 70-dependent promoter activity from the *yscW-lcrF* promoter regions was determined by incubating IscR-C92A with 2 nM supercoiled pPK12778 [purified with the QIAfilter Maxi kit (Qiagen)], 0.25 μ Ci of [α -³²P]UTP (3,000 μ Ci/mmol; Perkin Elmer), 20 μ M UTP, and 500 μ M each of ATP, GTP, and CTP for 30 min at

37°C in 40 mM Tris (pH 7.9), 30 mM KCl, 10 mM MgCl₂, 100 µg/mL bovine serum albumin (BSA), and 1 mM DTT. Purified apo-IscR was used since the IscR binding site upstream *yscW-lcrF* has been characterized to be an IscR type II site, which apo-IscR is capable of binding (Miller et al., 2014; Hooker-Romero et al., 2019). Eσ70 RNA polymerase (NEB) was added to a final concentration of 50 nM and the reaction was terminated after 5 min by addition of Stop Solution (USB Scientific). Samples were heated for 60 s at 90°C, and loaded onto a 7 M urea-8% polyacrylamide gel in 0.5× Tris-borate-EDTA (TBE) buffer. The reaction products were visualized by phosphorimaging.

Type III secretion system assays

Visualization of T3SS cargo secreted in broth culture was performed as previously described (Kwuan et al., 2013). Briefly, *Y. pseudotuberculosis* in LB low calcium media (LB plus 20 mM sodium oxalate and 20 mM MgCl₂) was grown for 1.5 h at 26°C followed by growth at 37°C for 1.5 h. Cultures were normalized by OD₆₀₀ and pelleted at 13,200 rpm for 10 min at room temperature. Supernatants were removed and proteins precipitated by addition of trichloroacetic acid (TCA) at a final concentration of 10%. Samples were incubated on ice for at least 1 hr and pelleted at 13,200 rpm for 15 min at 4°C. Resulting pellets were washed twice with ice-cold 100% Acetone and subsequently resuspended in final sample buffer (FSB) containing 0.2 M

dithiothreitol (DTT). Samples were boiled for 5 min prior to separating on a 12.5% SDS PAGE gel. Coomassie stained gels were imaged using Bio-Rad Image Lab Software Quantity and Analysis tools. YopE bands were quantified using this software and normalized to the BSA loading control.

Western Blot Analysis

In some experiments cell pellets were also collected and resuspended in FSB plus 0.2 M DTT, and were boiled for fifteen minutes. At the time of loading, supernatants and cell pellets were normalized to the same number of cells. After separation on a 12.5% SDS PAGE gel, proteins were transferred onto a blotting membrane (Immobilon-P) with a wet mini trans-blot cell (Bio-Rad). Blots were blocked for an hour in Tris-buffered saline with Tween 20 and 5% skim milk, and probed with the rabbit anti-RpoA (gift from Melanie Marketon), rabbit anti-LcrF (Böhme et al., 2012), rabbit anti-IscR (Nesbit et al., 2009), rabbit anti-YmoA (gift from Gregory Plano), rabbit anti H-NS (gift from Robert Landick), mouse M2 anti-FLAG (Sigma), goat anti-YopE (Santa Cruz Biotech), and horseradish peroxidase-conjugated secondary antibodies (Santa Cruz Biotech). Following visualization, quantification of the bands was performed with Image Lab software (Bio-Rad).

RT-qPCR Sample Preparation

Cultures were pelleted by centrifugation for 5 minutes at 4,000 rpm. The supernatant was removed, and pellets were resuspended in 500 μ L of media and treated with 1 mL Bacterial RNA Protect Reagent (Qiagen) according to the manufacturer's protocol. Total RNA was isolated using the RNeasy Mini Kit (Qiagen) per the manufacturer's protocol. After harvesting total RNA, genomic DNA was removed via the TURBO-DNA-free kit (Life Technologies/Thermo Fisher). cDNA was generated for each sample by using the M-MLV Reverse Transcriptase (Invitrogen) according to the manufacturer's instructions, as previously described (Schwiesow et al., 2018). Each 15 μ l qPCR assay contained 7.5 μ l of 1:10 diluted cDNA sample, 7.5 μ l of Power SYBR Green PCR master mix (Thermo Fisher Scientific), and primers (Table 2) with optimized concentrations. The expression levels of each target gene were normalized to that of 16S rRNA present in each sample and calculated by utilization of a standard curve. At least three independent biological replicates were analyzed for each condition.

Beta-galactosidase Assays

Y. pseudotuberculosis harboring promoter-*lacZ* fusion plasmids were grown in LB low calcium media (LB plus 20 mM sodium oxalate and 20 mM MgCl₂) for 1.5 h at 26°C followed by growth at 37°C for 1.5 h. β -galactosidase assays were carried out by stopping protein expression by incubating cells on ice for 20 minutes. Cultures were spun down and resuspended in Z Buffer (Miller,

1972). Culture concentration was measured by OD600, and samples were permeabilized using chloroform and 0.1% sodium dodecyl sulfate. Samples were incubated with 0.8 mg/mL ONPG and β -galactosidase enzymatic activity was terminated by the addition of 1M sodium bicarbonate. The β -galactosidase activity per cell was reported as Miller units.

CRISPRi knockdown

Knockdown of H-NS via CRISPRi methods was adapted from (Wang et al., 2019). In order to generate the pgRNA-tetO-JTetR-H-NS plasmid, a protospacer-adjacent motif (PAM) was located near the promoter of *hns* (Hsu et al., 2014). Two oligonucleotides (*hns_gRNA_F* and *hns_gRNA_R*) consisting of 20-nt targeting the *hns* promoter region with BbsI cohesive ends were synthesized and annealed before being cloned into pgRNA-*tetO*-JTetR by Golden Gate assembly. The plasmids pdCas9-bacteria and pgRNA-*tetO*-JTetR-H-NS were transformed into WT *Y. pseudotuberculosis* sequentially. These plasmids induce expression of dCas9 and gRNA-H-NS when exposed to anhydrotetracycline. *Y. pseudotuberculosis* cultures carrying these plasmids were sub-cultured to OD 0.2 and incubated at 26°C for 3 hrs in the presence or absence of 1 μ g/mL anhydrotetracycline, and then transferred to 37°C for 1.5 hrs to induce the T3SS. Samples were collected, and RNA was isolated for qRT-PCR analysis.

Bioinformatic prediction of YmoA/H-NS binding sites

A training set of known H-NS binding sites in *E. coli* K-12 substr. MG1655 was used from RegulonDB (Santos-Zavaleta et al., 2019). This training set was used to generate a H-NS binding motif using MEME from MEME-suite 5.1.1 tools (Bailey et al., 2009). FIMO was then used to scan for a H-NS binding site near the regulatory region of the *yscW-lcrF* promoter.

ChIP-qPCR

Cells were grown for 3hrs at 26°C or 37°C with shaking at 250 rpm and protein/nucleic acids were crosslinked using 1% formaldehyde at 26°C or 37°C for 10 min. Crosslinking was quenched with the addition of ice cold 0.1 M glycine and incubated at 4°C for 30 min. 32 OD_{600s} of cells were harvested for each replicate and cell pellets were stored at -80°C. DNA was fragmented by resuspending samples using IP buffer (100mM Tris-HCl, pH 8, 300mM NaCl, 1% Triton X-100, 1 mM PMSF) and sonicated at 25% Amplitude 15s on/ 59s off for a total of 8 cycles per sample. After sonication, lysates were treated with micrococcal nuclease and RNase-A for 1hr at 4°C. Lysates were clarified via centrifugation at 13,000 rpm for 15 min at 4°C. FLAG-tagged proteins. Lysates were pre-cleared using Dynabeads Protein A/G for 3hr at 4°C. Immunoprecipitation was performed by adding Sigma monoclonal mouse anti-FLAG M2 antibody to samples and incubated overnight at 4°C (IscR was tagged C-terminally reference? and H-NS was tagged C-

terminally). Dynabeads Protein A/G were added to samples and washes were performed to remove non-specific binding. After H-NS-DNA or IscR-DNA complexes were eluted, samples were placed at 65°C for 5hr to reverse crosslinks. DNA was then purified using Qiagen PCR purification kit and input samples were diluted 1:100 while samples treated with antibody or control samples not treated with the antibody were diluted 1:5 and q-PCR was performed to assess IscR/H-NS binding to promoters of interest. Percent input was calculated by the following equation $100 * 2^{CT_{input} - CT_{+AB}}$.

Results

IscR does not promote *lcrF* transcription *in vitro*

IscR has previously been shown to enhance transcription by directly activating transcription by RNA polymerase or by antagonizing transcriptional repressors (Giel et al., 2006; Choi et al., 2020). To determine the molecular mechanism by which IscR potentiates transcription of *yscW-lcrF*, we performed an *in vitro* transcription assay with a DNA fragment containing the wild-type *Y. pseudotuberculosis yscW-lcrF* promoter (-206 to +12 bp relative to the +1 transcription start site). Surprisingly, no change in *yscW-lcrF* transcription was observed after addition of apo-IscR (Fig 1). These data suggest that IscR does not enhance *yscW-lcrF* transcription by regulating RNA polymerase directly. We therefore hypothesized that IscR promotes *yscW-lcrF* expression by antagonizing a repressor.

IscR is not required for LcrF expression or type III secretion in the absence of YmoA

Loss of *iscR* leads to a profound defect in T3SS activity while disruption of *ymoA* causes enhanced T3SS activity (Cornells et al., 1991; de Rouvroit et al., 1992; Böhme et al., 2012; Miller et al., 2014; Hooker-Romero et al., 2019).

We therefore hypothesized that IscR antagonizes YmoA-dependent repression of the T3SS. To test this, we assessed T3SS activity of *Y. pseudotuberculosis* expressing or lacking *iscR* and/or *ymoA*. Consistent with previous studies, we observed ~18-fold decrease in secretion of the T3SS effector protein YopE upon *iscR* deletion, while *ymoA* deletion led to ~6-fold increase in YopE secretion (Fig 2). As expected for this transcriptional circuit, the effect of YmoA on T3SS activity required LcrF, the direct regulator of T3SS (Fig S1). Importantly, YopE secretion in the Δ *iscR*/ Δ *ymoA* double mutant was similar to Δ *ymoA* mutant, suggesting that IscR is dispensable for T3SS activity in the absence of YmoA (Fig 2).

Proteins of the YmoA family lack a DNA binding domain and are thought to affect transcription by its interaction with the histone like protein H-NS (Madrid et al., 2007; Boudreau et al., 2018). Previous work has shown that a complex of YmoA/H-NS, but not YmoA alone, binds the *yscW-lcrF* promoter (Böhme et al., 2012). To test the requirement for a YmoA/H-NS complex in regulation of YopE secretion by IscR we made use of a YmoA D43N mutant, which cannot

interact with H-NS *in vitro* (Cordeiro et al., 2015) and which we showed was produced in *Y. pseudotuberculosis* (Fig S2). Indeed, a *ymoA*^{D43N} mutant exhibited ~6-fold increase in YopE secretion similar to a *ymoA* deletion (Fig 2). This suggests that YmoA represses *yscW-lcrF* through its interaction with H-NS. Furthermore, there was no difference in YopE secretion between the *ymoA*^{D43N} mutant and the *iscR ymoA*^{D43N} double mutant. These effects on YopE secretion are most easily explained by changes in *lcrF* transcription and accordingly, LcrF protein levels. Indeed, while the Δ *iscR* mutant had a ~5-fold reduction in *lcrF* mRNA compared to wildtype and the Δ *ymoA* and *ymoA*^{D43N} mutants displayed ~10-fold elevated *lcrF*, we observed no difference in *lcrF* mRNA levels between the Δ *ymoA* and Δ *iscR*/ Δ *ymoA* mutants (Fig 3A). Accordingly, we observed no difference in LcrF protein levels when *iscR* was deleted from the *ymoA* mutants (Fig 3B). Collectively, these data suggest that YmoA requires H-NS binding to inhibit *lcrF* transcription, and that IscR only exerts its positive effect on *lcrF* transcription in the presence of the YmoA/H-NS complex.

IscR does not indirectly regulate LcrF through modulation of YmoA or H-NS expression

To test whether IscR indirectly effects *lcrF* transcription through regulation of YmoA or H-NS expression, we fused the promoters of *ymoBA* or *hns* to *lacZ* and measured promoter activity comparing the *iscR* mutant and the wildtype

strain (Fig 4A). Deletion of *iscR* did not influence promoter activity of *ymoBA* and only slightly downregulated promoter activity of *hns*. Consistent with this observation deletion of *iscR* did not influence *ymoA* and *hns* mRNA levels (Fig 4B). YmoA was previously found to be degraded at 37°C by ClpXP/Lon proteases in *Y. pestis* (Jackson et al., 2004), yet residual YmoA is functional at 37°C since deletion of *ymoA* or the YmoA-D43N mutation that eliminates H-NS binding leads to derepressed T3SS activity at 37°C. As expected, YmoA protein levels were reduced at 37°C compared to 26°C, but were, importantly, still detectable by Western blot. In contrast, IscR and H-NS levels were not temperature dependent, nor did IscR affect YmoA or H-NS expression (Fig 4C). Furthermore, while YmoA levels are temperature dependent, YmoA protein is still detectable at 37°C. These data show that IscR does not indirectly regulate *yscW-lcrF* through regulation of YmoA or H-NS expression.

IscR binding to the *yscW-lcrF* promoter is critical for LcrF expression only in the presence of YmoA

As IscR did not modulate YmoA or H-NS expression, we hypothesized that IscR must bind the *yscW-lcrF* promoter to antagonize YmoA/H-NS-mediated repression. To test whether IscR binding to the *yscW-lcrF* promoter is important for regulating LcrF expression in the presence of YmoA, we used a previously characterized DNA site mutant (*lcrF^{Null}*) that ablates IscR binding

to the *yscW-lcrF* promoter but expresses wildtype IscR by mutating the IscR binding site upstream *yscW-lcrF* (Hooker-Romero et al., 2019). As expected, the *lcrF*^{ΔNull} and Δ *iscR* mutants exhibited a ~5-fold reduction in *lcrF* mRNA compared to the wildtype strain and LcrF protein was completely undetectable in these two mutants (Fig 5AB). However, in the absence of *ymoA* this reduction in LcrF expression or T3SS activity by the *lcrF*^{ΔNull} mutation was eliminated (Fig 5A-C). Taken together, these data suggest that IscR dependent activation of LcrF expression in the presence of YmoA requires direct binding of IscR to the *yscW-lcrF* promoter.

Knockdown of H-NS leads to derepression of LcrF

We next examined the role of H-NS regulation of *lcrF*. H-NS has been proposed to be essential in both *Y. pseudotuberculosis* and *Y. enterocolitica* (Heroven et al., 2004; Ellison and Miller, 2006). To test whether reducing H-NS occupancy at the *yscW-lcrF* promoter affects LcrF expression, we used CRISPRi to knockdown H-NS expression in wildtype *Y. pseudotuberculosis* and measured *lcrF* expression levels. For this CRISPRi system pioneered in *Yersinia pestis* (Wang et al., 2019), target gene guide RNAs and dCas9 can be induced in the presence of anhydrotetracycline (aTC). CRISPRi knockdown led to a ~6-fold decrease in H-NS transcription when exposed to aTC (Fig 6A). Importantly, this reduction of H-NS expression led to a ~31-fold increase in *lcrF* mRNA, suggesting H-NS represses LcrF transcription (Fig

6B). Knockdown of H-NS did not affect expression of *gyrA*, a housekeeping gene (Fig 6C). These data support the model that H-NS negatively influences LcrF expression.

Two H-NS binding sites are required to repress *yscW-lcrF* promoter activity

H-NS and YmoA/H-NS complexes bind the *yscW-lcrF* promoter between the -2 to the +272 position relative to the transcriptional start site (Böhme et al., 2012). However, the exact H-NS binding site was not identified. We used FIMO-MEME suite tools to predict putative H-NS binding sites upstream of *yscW-lcrF* and identified three predicted H-NS binding sites (p-value < 10⁻³; Fig 7A). These data suggested that H-NS may form a DNA bridge at this locus (Ayala et al., 2015; Chaparian et al., 2020). To characterize which regions of the *yscW-lcrF* promoter allow for H-NS-YmoA repression and IscR activation, we systematically truncated the *yscW-lcrF* promoter and fused the truncated promoters to *lacZ* and tested promoter activity in the wildtype, Δ *iscR*, Δ *ymoA*, and Δ *iscR*/ Δ *ymoA* backgrounds at 37°C (Fig 7A). As expected, deletion of *ymoA* led to an increase in activity of the longest promoter construct, while *iscR* deletion led to a decrease in promoter activity compared to the wildtype strain (Fig 7B). In addition, deletion of *iscR* in a Δ *ymoA* background did not inhibit the derepressed promoter activity seen in the Δ *ymoA* background. Eliminating the most upstream predicted H-NS binding site did not affect

promoter activity (promoter 1 compared to promoter 2). However, additional truncation of the second H-NS binding site led to an increase in promoter activity in the wildtype and $\Delta iscR$ backgrounds, but not in the backgrounds lacking *ymoA* (promoter 2 compared to promoter 3) suggesting that some of the repressive effect by H-NS/YmoA had been lost. Importantly, further truncation to eliminate the IscR binding site led to deregulated promoter activity that was independent of IscR and YmoA (promoter 4). These data suggest that IscR is required to disrupt YmoA/H-NS repressive activity explaining why it is dispensable in the absence of YmoA/H-NS. Lastly, truncation to eliminate the -35 and -10 promoter elements led to a complete lack of promoter activity (promoter 5). Taken together, these data suggest that IscR binding to the *ycsW-lcrF* promoter antagonizes YmoA/H-NS repression.

To test whether H-NS binds to these predicted sites, we carried out ChIP-qPCR analysis to assess H-NS occupancy at the I, II, and III putative binding regions *in vivo*. In order to immunoprecipitate H-NS-DNA complexes, we used a chromosomally-encoded 3xFLAG tagged H-NS allele. This FLAG tag did not affect the ability of H-NS to repress *LcrF* expression (Fig S3). Surprisingly, we could not detect H-NS binding at any of these predicted sites even though repression by H-NS was detectable under the same conditions (37°C). Interestingly, previous reports have shown that H-NS in other facultative

pathogens represses the expression of certain virulence genes under environmental temperatures (<30°C) but exhibits decreased binding and repressive activity at mammalian body temperature (37°C) (Prosseda et al., 1998; Ono et al., 2005; Picker and Wing, 2016). On this note, we did observe enrichment of H-NS-FLAG at all three predicted sites in the *yscW-lcrF* promoter when bacteria were cultured at 26°C, but not at a control pYV-encoded promoter that was not predicted to bind H-NS (DN756_21750) (Fig 8A). YmoA is predicted to affect the repressive ability of H-NS but was not shown to affect H-NS binding to the *yscW-lcrF* promoter (Böhme et al., 2012). To test if YmoA influenced H-NS binding to the *yscW-lcrF* promoter *in vivo*, we carried out our ChIP-qPCR analysis in the absence of *ymoA*. This experiment was performed at 26°C since YmoA is highly degraded at 37°C and because H-NS binding to the *yscW-lcrF* promoter is near the limit of detection at 37°C. No difference in H-NS binding was observed in the *ymoA* mutant compared to the parental strain at 26°C (Fig 8B), suggesting that YmoA does not affect H-NS occupancy at the *yscW-lcrF* promoter at this temperature. Next to determine if IscR antagonizes H-NS binding to the *yscW-lcrF* promoter we performed ChIP-qPCR in the absence of *iscR*. Likewise, there was no difference in H-NS enrichment at the *yscW-lcrF* promoter between the *iscR* mutant and the wildtype strain at 26 °C or 37 °C (Fig 8BC). It is possible that H-NS binds to the *yscW-lcrF* promoter at 37°C, but this is at the limit of detection for ChIP experiments. This data would

suggest that H-NS occupies the *yscW-lcrF* promoter to a higher degree under environmental temperatures compared to mammalian body temperature.

We also measured IscR enrichment at the *yscW-lcrF* promoter *in vivo*. We used a chromosomal 3xFLAG tagged IscR allele previously shown not to affect IscR activity (ref). Interestingly, IscR enrichment at the *yscW-lcrF* promoter was ~3-fold higher at 37°C compared to 26°C (Fig 8D). This increase in IscR binding is not due to increased IscR levels since we do not observe higher levels of IscR protein when cultured at 37°C compared to 26°C (Fig 4C), nor do we see increased binding of IscR at the promoter of another known IscR target, the *suf* operon (Fig S4). In addition, deletion of *ymoA* did not affect IscR occupancy at the *yscW-lcrF* promoter at 26°C or 37°C. These data suggest that at environmental temperatures, H-NS binds to and represses the *yscW-lcrF* promoter, while at mammalian body temperature IscR binding to the *yscW-lcrF* promoter antagonizes YmoA/H-NS repression.

Environmental cues that increase IscR levels enable derepression of the *yscW-lcrF* promoter

We previously showed that low iron and high oxidative stress lead to elevated IscR levels, which then activate the T3SS through upregulation of LcrF (Hooker-Romero et al., 2019). The data shown here suggest that this increase in IscR levels may be necessary to antagonize repressive YmoA-H-

NS-activity at the *yscW-lcrF* promoter. To test this model, we measured *lcrF* mRNA levels in $\Delta iscR$ and $\Delta ymoA$ mutants under aerobic or anaerobic conditions. As expected, under aerobic conditions *iscR* mRNA levels were increased ~4-fold compared to anaerobic conditions (Fig 9A). This upregulation of *iscR* levels led to a ~12-fold induction in wildtype *lcrF* levels (Fig 9B). Interestingly *lcrF* mRNA and protein levels were not affected by oxygen in the $\Delta ymoA$ and $\Delta iscR/\Delta ymoA$ mutants (Fig 9A, 9C). These data suggest that environmental conditions that increase IscR levels (such as aerobic conditions) allow YmoA/H-NS-mediated derepression of *lcrF* expression.

Discussion

Our data suggest IscR activates transcription of *yscW-lcrF* by antagonizing repressive activity of YmoA-H-NS (Fig 10). Knockdown of *hns* expression by CRISPRi revealed that H-NS, a putative essential gene in *Yersinia*, is required for repression of *yscW-lcrF*. Furthermore, YmoA must interact with H-NS to repress *yscW-lcrF* transcription and overall T3SS activity at 37°C. Importantly, IscR promotes *yscW-lcrF* expression and T3SS activity only in the presence of YmoA-H-NS repression. Our data point to a model where H-NS occupies the *yscW-lcrF* promoter at environmental temperatures independently of YmoA and IscR, but at mammalian body temperature YmoA binding to H-NS represses the *yscW-lcrF* promoter only when IscR levels are

low (Fig 10). *Y. pseudotuberculosis* IscR levels are thought to be kept low in the intestinal lumen, under anaerobic iron-replete conditions. Under these conditions, where the T3SS is not required for colonization, YmoA and H-NS cooperate to repress LcrF expression. Once *Yersinia* cross the intestinal barrier, oxygen tension increases and iron is scarce, allowing elevated IscR levels that antagonize YmoA/H-NS activity to allow LcrF expression and type III secretion, which is required for extraintestinal infection (He et al., 1999; Balada-Llasat and Mecsas, 2006; Cassat and Skaar, 2013; Rivera-Chávez et al., 2017). This suggests that YmoA/H-NS and IscR work together to allow temperature and oxygen tension/iron availability to limit T3SS activity not just to only inside the host organism, but to only in extraintestinal tissue. Given that IscR is essential for T3SS activity in the related plague agent *Y. pestis* that does not enter the intestinal tract (Hooker-Romero et al., 2019), we predict that in the flea vector that maintains temperatures lower than the mammalian host, H-NS represses LcrF expression. Then upon entry into the mammalian host bloodstream, the elevated temperature leads to decreased occupancy of YmoA/H-NS at the *yscW-lcrF* promoter such that IscR antagonizes YmoA/H-NS repression and facilitates the T3SS activity required for early stages of plague (Cornelis, 2000; Plano and Schesser, 2013).

Previous reports have suggested that H-NS targets a subset of genes under environmental conditions, but no longer represses those same genes under

mammalian body temperature. For example in the facultative intracellular pathogen *Shigella flexneri*, *virF* encodes a AraC transcriptional regulator that activates expression of several operons that are critical for invasion and contribute to virulence (Schroeder and Hilbi, 2008; Di Martino et al., 2016). The transcription factor VirF promotes VirB, which ultimately activates the *Shigella* T3SS (Beloin et al., 2002). The *Shigella* T3SS is only expressed under mammalian body temperature and this is controlled by preventing expression of VirF at environmental temperatures. Interestingly, H-NS was shown to directly repress *virF* transcription by binding to the *virF* promoter (Prosseda et al., 1998). Later studies found that H-NS binds to two distinct sites upstream of *virF* leading to the formation of a DNA bridge (Falconi et al., 1998). This study also found that H-NS binds to a higher degree at the *virF* promoter under lower temperatures (<30°C) compared to mammalian body temperature (37°C). Thus H-NS was shown to repress promoter activity of *virF* at both lower temperatures (<30°C) and mammalian body temperature (37°C), however H-NS has a stronger effect on repression of *virF* under lower temperatures (Prosseda et al., 1998). This molecular mechanism is similar to what we report here, where H-NS occupies the *yscW-lcrF* promoter at environmental conditions and is below the limit of detection by ChIP-qPCR at 37°C. However, *Yersinia* H-NS repression of LcrF still occurs at 37°C unless IscR levels increase sufficiently to antagonize this repression.

YmoA was previously shown to bind to H-NS and the YmoA/H-NS complex was proposed to regulate LcrF expression (Böhme et al., 2012; Cordeiro et al., 2015). However, YmoA was not shown to affect H-NS binding to the *yscW-lcrF* promoter *in vitro* (Böhme et al., 2012), and our ChIP-qPCR analysis did not find a change in H-NS *yscW-lcrF* promoter occupancy at 26°C. H-NS occupancy was below the limit of detection by ChIP-qPCR at 37°C, so we could not rule out H-NS or YmoA/H-NS binding to the *yscW-lcrF* promoter at this temperature. Indeed, deletion of *ymoA* or knockdown of *h-ns* both caused elevated LcrF expression at 37°C, indicating that both proteins are needed to repress the *yscW-lcrF* promoter at mammalian body temperature. *E. coli* Hha, the YmoA homolog, influences H-NS bridging and promotes H-NS silencing of target genes (Boudreau et al., 2018). Whether YmoA can repress genes independently of H-NS or other nucleoid-associated proteins such as StpA has been debated. Although YmoA/Hha have been shown to bind DNA *in vitro*, YmoA and Hha lack a DNA binding domain and most likely purification of YmoA/Hha leads to copurification of H-NS or other H-NS paralogs. This may explain why YmoA has been shown to interact with specific segments of DNA *in vitro*. Our data further support that YmoA influences H-NS repressive activity on *lcrF* transcription.

The mechanism by which IscR promotes or represses transcription of target genes varies. For example, elevated transcription of the *suf* iron-sulfur cluster

biogenesis operon in *E. coli* is thought to be driven by direct interaction between RNA polymerase and IscR (Giel et al., 2006). However, IscR has also been shown to activate transcription of other target genes by antagonizing a repressor (Choi et al., 2020). For example, in *Vibrio vulnificus* IscR promotes expression of the *vvhBA* operon, which encodes an extracellular pore-forming toxin essential for its hemolytic activity (Gray and Kreger, 1985; Jeong and Satchell, 2012; Choi et al., 2020), while the *vvhBA* operon is repressed by H-NS (Elgaml and Miyoshi, 2015). In *V. vulnificus*, nitrosative stress and iron starvation lead to upregulation of IscR (Choi et al., 2020). This increase in IscR leads to upregulation of *vvhBA* by increasing IscR levels and antagonizing H-NS repression of *vvhBA*. This molecular mechanism is very similar to what we observe here for IscR and H-NS in *Yersinia*, where aerobic conditions promote high IscR levels that antagonize H-NS repressive activity at the *yscW-lcrF* promoter.

Conflict of Interest

The authors declare that the research was conducted in the absence of any commercial or financial relationships that could be construed as a potential conflict of interest.

Author Contributions

VA, DB, and PK designed the study. DB, PA, EM, NT, and MO performed the experiments. DB, PA, EM, NT, and MO performed data analysis. DB, PA, VA, and PK wrote the paper.

Funding

This study was supported by National Institutes of Health (www.NIH.gov) grant R01AI119082 (to VA and PJK). DAB and PA received support from the National Human Genome Research Institute of the National Institutes of Health under Award Number 4R25HG006836. The funders had no role in study design, data collection and analysis, decision to publish, or preparation of the manuscript.

Acknowledgments

We thank Gregory V. Plano from University of Miami Health System for providing the YmoA antibody, and Robert Landick from University of Wisconsin, Madison for providing the H-NS antibody.

References

Ali, S. S., Whitney, J. C., Stevenson, J., Robinson, H., Howell, P. L., and Navarre, W. W. (2013). Structural insights into the regulation of foreign genes in salmonella by the Hha/H-NS complex. *J. Biol. Chem.* doi:10.1074/jbc.M113.455378.

- Auerbuch, V., Golenbock, D. T., and Isberg, R. R. (2009). Innate immune recognition of *Yersinia pseudotuberculosis* type III secretion. *PLoS Pathog.* doi:10.1371/journal.ppat.1000686.
- Ayala, J. C., Wang, H., Silva, A. J., and Benitez, J. A. (2015). Repression by H-NS of genes required for the biosynthesis of the *Vibrio cholerae* biofilm matrix is modulated by the second messenger cyclic diguanylic acid. *Mol. Microbiol.* doi:10.1111/mmi.13058.
- Bailey, T. L., Boden, M., Buske, F. A., Frith, M., Grant, C. E., Clementi, L., et al. (2009). MEME Suite: Tools for motif discovery and searching. *Nucleic Acids Res.* doi:10.1093/nar/gkp335.
- Balada-Llasat, J. M., and Meccas, J. (2006). *Yersinia* has a tropism for B and T cell zones of lymph nodes that is independent of the type III secretion system. *PLoS Pathog.* doi:10.1371/journal.ppat.0020086.
- Beloin, C., McKenna, S., and Dorman, C. J. (2002). Molecular dissection of VirB, a key regulator of the virulence cascade of *Shigella flexneri*. *J. Biol. Chem.* doi:10.1074/jbc.M111429200.
- Bliska, J. B., Guan, K., Dixon, J. E., and Falkow, S. (1991). Tyrosine phosphate hydrolysis of host proteins by an essential *Yersinia* virulence determinant. *Proc. Natl. Acad. Sci. U. S. A.* doi:10.1073/pnas.88.4.1187.
- Böhme, K., Steinmann, R., Kortmann, J., Seekircher, S., Heroven, A. K., Berger, E., et al. (2012). Concerted actions of a thermo-labile regulator and a unique intergenic RNA thermosensor control *Yersinia* virulence.

- PLoS Pathog.* doi:10.1371/journal.ppat.1002518.
- Boudreau, B. A., Hron, D. R., Qin, L., Van Der Valk, R. A., Kotlajich, M. V., Dame, R. T., et al. (2018). StpA and Hha stimulate pausing by RNA polymerase by promoting DNA-DNA bridging of H-NS filaments. *Nucleic Acids Res.* doi:10.1093/nar/gky265.
- Brodsky, I. E., and Medzhitov, R. (2008). Reduced secretion of YopJ by *Yersinia* limits in vivo cell death but enhances bacterial virulence. *PLoS Pathog.* doi:10.1371/journal.ppat.1000067.
- Brubaker, R. R. (1983). The Vwa+ virulence factor of yersiniae: the molecular basis of the attendant nutritional requirement for Ca⁺⁺. *Rev. Infect. Dis.* doi:10.1093/clinids/5.supplement_4.s748.
- Cassat, J. E., and Skaar, E. P. (2013). Iron in infection and immunity. *Cell Host Microbe.* doi:10.1016/j.chom.2013.04.010.
- Chaparian, R. R., Tran, M. L. N., Miller Conrad, L. C., Rusch, D. B., and Van Kessel, J. C. (2020). Global H-NS counter-silencing by LuxR activates quorum sensing gene expression. *Nucleic Acids Res.* doi:10.1093/nar/gkz1089.
- Cheng, L. W., Anderson, D. M., and Schneewind, O. (1997). Two independent type III secretion mechanisms for YopE in *Yersinia enterocolitica*. *Mol. Microbiol.* doi:10.1046/j.1365-2958.1997.3831750.x.
- Choi, G., Jang, K. K., Lim, J. G., Lee, Z. W., Im, H., and Choi, S. H. (2020). The transcriptional regulator IscR integrates host-derived nitrosative

- stress and iron starvation in activation of the *vvhBA* operon in *Vibrio vulnificus*. *J. Biol. Chem.* doi:10.1074/jbc.RA120.012724.
- Cordeiro, T. N., García, J., Bernadó, P., Millet, O., and Pons, M. (2015). A three-protein charge zipper stabilizes a complex modulating bacterial gene silencing. *J. Biol. Chem.* doi:10.1074/jbc.M114.630400.
- Cornelis, G. R. (1993). Role of the Transcription Activator VirF and the Histone-like Protein YmoA in the Thermoregulation of Virulence Functions in *Yersinia*. *Zentralblatt fur Bakteriologie*. doi:10.1016/S0934-8840(11)80833-9.
- Cornelis, G. R. (2000). Molecular and cell biology aspects of plague. *Proc. Natl. Acad. Sci. U. S. A.* doi:10.1073/pnas.97.16.8778.
- Cornelis, G. R. (2006). The type III secretion injectisome. *Nat. Rev. Microbiol.* doi:10.1038/nrmicro1526.
- Cornelis, G. R., Boland, A., Boyd, A. P., Geuijen, C., Iriarte, M., Neyt, C., et al. (1998). The Virulence Plasmid of *Yersinia*, an Antihost Genome. *Microbiol. Mol. Biol. Rev.* doi:10.1128/mmbr.62.4.1315-1352.1998.
- Cornelis, G. R., Sluiter, C., Delor, I., Geib, D., Kaniga, K., de Rouvoit, C. L., et al. (1991). *ymoA*, a *Yersinia enterocolitica* chromosomal gene modulating the expression of virulence functions. *Mol. Microbiol.* doi:10.1111/j.1365-2958.1991.tb01875.x.
- Dame, R. T., Luijsterburg, M. S., Krin, E., Bertin, P. N., Wagner, R., and Wuite, G. J. L. (2005). DNA bridging: A property shared among H-NS-like

- proteins. *J. Bacteriol.* doi:10.1128/JB.187.5.1845-1848.2005.
- Dame, R. T., Wyman, C., and Goosen, N. (2000). H-NS mediated compaction of DNA visualised by atomic force microscopy. *Nucleic Acids Res.* doi:10.1093/nar/28.18.3504.
- Davis, K. M., Mohammadi, S., and Isberg, R. R. (2015). Community Behavior and Spatial Regulation within a Bacterial Microcolony in Deep Tissue Sites Serves to Protect against Host Attack. *Cell Host Microbe.* doi:10.1016/j.chom.2014.11.008.
- de Rouvroit, C. L., Sluiter, C., and Cornelis, G. R. (1992). Role of the transcriptional activator, VirF, and temperature in the expression of the pYV plasmid genes of *Yersinia enterocolitica*. *Mol. Microbiol.* doi:10.1111/j.1365-2958.1992.tb01483.x.
- Deng, W., Marshall, N. C., Rowland, J. L., McCoy, J. M., Worrall, L. J., Santos, A. S., et al. (2017). Assembly, structure, function and regulation of type III secretion systems. *Nat. Rev. Microbiol.* doi:10.1038/nrmicro.2017.20.
- Di Martino, M. L., Falconi, M., Micheli, G., Colonna, B., and Prosseda, G. (2016). The multifaceted activity of the VirF regulatory protein in the *Shigella* Lifestyle. *Front. Mol. Biosci.* doi:10.3389/fmolb.2016.00061.
- Elgaml, A., and Miyoshi, S. I. (2015). Role of the histone-like nucleoid structuring protein H-NS in the regulation of virulence factor expression and stress response in *Vibrio vulnificus*. *Biocontrol Sci.*

doi:10.4265/bio.20.263.

Ellison, D. W., and Miller, V. L. (2006). H-NS represses *inv* transcription in *Yersinia enterocolitica* through competition with RovA and interaction with YmoA. *J. Bacteriol.* doi:10.1128/JB.00862-05.

Falconi, M., Colonna, B., Prosseda, G., Micheli, G., and Gualerzi, C. O. (1998). Thermoregulation of *Shigella* and *Escherichia coli* EIEC pathogenicity. A temperature-dependent structural transition of DNA modulates accessibility of *virF* promoter to transcriptional repressor H-NS. *EMBO J.* doi:10.1093/emboj/17.23.7033.

Fleischhacker, A. S., Stubna, A., Hsueh, K. L., Guo, Y., Teter, S. J., Rose, J. C., et al. (2012). Characterization of the [2Fe-2S] cluster of *Escherichia coli* transcription factor IscR. *Biochemistry.* doi:10.1021/bi3003204.

García, J., Madrid, C., Juárez, A., and Pons, M. (2006). New Roles for Key Residues in Helices H1 and H2 of the *Escherichia coli* H-NS N-terminal Domain: H-NS Dimer Stabilization and Hha Binding. *J. Mol. Biol.* doi:10.1016/j.jmb.2006.03.059.

Garrity-Ryan, L. K., Kim, O. K., Balada-Llasat, J. M., Bartlett, V. J., Verma, A. K., Fisher, M. L., et al. (2010). Small molecule inhibitors of LcrF, a *Yersinia pseudotuberculosis* transcription factor, attenuate virulence and limit infection in a murine pneumonia model. *Infect. Immun.* doi:10.1128/IAI.01305-09.

Giel, J. L., Rodionov, D., Liu, M., Blattner, F. R., and Kiley, P. J. (2006). IscR-

- dependent gene expression links iron-sulphur cluster assembly to the control of O₂-regulated genes in *Escherichia coli*. *Mol. Microbiol.*
doi:10.1111/j.1365-2958.2006.05160.x.
- Gordon, B. R. G., Li, Y., Cote, A., Weirauch, M. T., Ding, P., Hughes, T. R., et al. (2011). Structural basis for recognition of AT-rich DNA by unrelated xenogeneic silencing proteins. *Proc. Natl. Acad. Sci. U. S. A.*
doi:10.1073/pnas.1102544108.
- Gray, L. D., and Kreger, A. S. (1985). Purification and characterization of an extracellular cytolysin produced by *Vibrio vulnificus*. *Infect. Immun.*
doi:10.1128/iai.48.1.62-72.1985.
- He, G., Shankar, R. A., Chzhan, M., Samouilov, A., Kuppusamy, P., and Zweier, J. L. (1999). Noninvasive measurement of anatomic structure and intraluminal oxygenation in the gastrointestinal tract of living mice with spatial and spectral EPR imaging. *Proc. Natl. Acad. Sci. U. S. A.*
doi:10.1073/pnas.96.8.4586.
- Heroven, A. K., Nagel, G., Tran, H. J., Parr, S., and Dersch, P. (2004). RovA is autoregulated and antagonizes H-NS-mediated silencing of invasins and rovA expression in *Yersinia pseudotuberculosis*. *Mol. Microbiol.*
doi:10.1111/j.1365-2958.2004.04162.x.
- Hoe, N. P., Minion, F. C., and Goguen, J. D. (1992). Temperature sensing in *Yersinia pestis*: Regulation of yopE transcription by lcrF. *J. Bacteriol.*
doi:10.1128/jb.174.13.4275-4286.1992.

- Hooker-Romero, D., Mettert, E., Schwiesow, L., Balderas, D., Alvarez, P. A., Kicin, A., et al. (2019). Iron availability and oxygen tension regulate the Yersinia Ysc type III secretion system to enable disseminated infection. *PLoS Pathog.* doi:10.1371/journal.ppat.1008001.
- Hsu, P. D., Lander, E. S., and Zhang, F. (2014). Development and applications of CRISPR-Cas9 for genome engineering. *Cell.* doi:10.1016/j.cell.2014.05.010.
- Jackson, M. W., Silva-Herzog, E., and Plano, G. V. (2004). The ATP-dependent ClpXP and Lon proteases regulate expression of the Yersinia pestis type III secretion system via regulated proteolysis of YmoA, a small histone-like protein. *Mol. Microbiol.* doi:10.1111/j.1365-2958.2004.04353.x.
- Jeong, H. G., and Satchell, K. J. F. (2012). Additive function of vibrio vulnificus MARTXVv and VvhA cytolysins promotes rapid growth and epithelial tissue necrosis during intestinal infection. *PLoS Pathog.* doi:10.1371/journal.ppat.1002581.
- King, J. M., Bartra, S. S., Plano, G., and Yahr, T. L. (2013). ExsA and LcrF recognize similar consensus binding sites, but differences in their oligomeric state influence interactions with promoter DNA. *J. Bacteriol.* doi:10.1128/JB.00990-13.
- Kwuan, L., Adams, W., and Auerbuch, V. (2013). Impact of host membrane pore formation by the Yersinia pseudotuberculosis type III secretion

- system on the macrophage innate immune response. *Infect. Immun.*
doi:10.1128/IAI.01014-12.
- Liu, L., Huang, S., Fei, K., Zhou, W., Chen, S., and Hu, Y. (2021).
Characterization of the binding motif for the T3SS master regulator LcrF
in *Yersinia pseudotuberculosis*. *FEMS Microbiol. Lett.*
doi:10.1093/femsle/fnab031.
- Liu, Y., Chen, H., Kenney, L. J., and Yan, J. (2010). A divalent switch drives
H-NS/DNA-binding conformations between stiffening and bridging
modes. *Genes Dev.* doi:10.1101/gad.1883510.
- Madrid, C., Balsalobre, C., García, J., and Juárez, A. (2007). The novel
Hha/YmoA family of nucleoid-associated proteins: Use of structural
mimicry to modulate the activity of the H-NS family of proteins. *Mol.*
Microbiol. doi:10.1111/j.1365-2958.2006.05497.x.
- Miller, H. K., Kwuan, L., Schwiesow, L., Bernick, D. L., Mettert, E., Ramirez,
H. A., et al. (2014). IscR Is Essential for *Yersinia pseudotuberculosis*
Type III Secretion and Virulence. *PLoS Pathog.*
doi:10.1371/journal.ppat.1004194.
- Miller, J. H. (1972). Experiments in Molecular Genetics. *Cold Spring Harb.*
Lab. Press.
- Milne-Davies, B., Helbig, C., Wimmi, S., Cheng, D. W. C., Paczia, N., and
Diepold, A. (2019). Life After Secretion—*Yersinia enterocolitica* Rapidly
Toggles Effector Secretion and Can Resume Cell Division in Response

- to Changing External Conditions. *Front. Microbiol.*
doi:10.3389/fmicb.2019.02128.
- Navarre, W. W., Porwollik, S., Wang, Y., McClelland, M., Rosen, H., Libby, S. J., et al. (2006). Selective silencing of foreign DNA with low GC content by the H-NS protein in Salmonella. *Science* (80-.).
doi:10.1126/science.1128794.
- Navarro, L., Alto, N. M., and Dixon, J. E. (2005). Functions of the Yersinia effector proteins in inhibiting host immune responses. *Curr. Opin. Microbiol.* doi:10.1016/j.mib.2004.12.014.
- Nesbit, A. D., Giel, J. L., Rose, J. C., and Kiley, P. J. (2009). Sequence-Specific Binding to a Subset of IscR-Regulated Promoters Does Not Require IscR Fe-S Cluster Ligation. *J. Mol. Biol.*
doi:10.1016/j.jmb.2009.01.055.
- Nieto, J. M., Madrid, C., Miquelay, E., Parra, J. L., Rodríguez, S., and Juárez, A. (2002). Evidence for direct protein-protein interaction between members of the enterobacterial Hha/YmoA and H-NS families of proteins. *J. Bacteriol.* doi:10.1128/JB.184.3.629-635.2002.
- Ono, S., Goldberg, M. D., Olsson, T., Esposito, D., Hinton, J. C. D., and Ladbury, J. E. (2005). H-NS is a part of a thermally controlled mechanism for bacterial gene regulation. *Biochem. J.* doi:10.1042/BJ20050453.
- Paytubi, S., Madrid, C., Forns, N., Nieto, J. M., Balsalobre, C., Uhlin, B. E., et al. (2004). YdgT, the Hha paralogue in Escherichia coli, forms

- heteromeric complexes with H-NS and StpA. *Mol. Microbiol.*
doi:10.1111/j.1365-2958.2004.04268.x.
- Pha, K. (2016). Yersinia type III effectors perturb host innate immune responses. *World J. Biol. Chem.* doi:10.4331/wjbc.v7.i1.1.
- Picker, M. A., and Wing, H. J. (2016). H-NS, its family members and their regulation of virulence genes in Shigella species. *Genes (Basel)*.
doi:10.3390/genes7120112.
- Plano, G. V., and Schesser, K. (2013). The Yersinia pestis type III secretion system: Expression, assembly and role in the evasion of host defenses. *Immunol. Res.* doi:10.1007/s12026-013-8454-3.
- Prosseda, G., Fradiani, P. A., Di Lorenzo, M., Falconi, M., Micheli, G., Casalino, M., et al. (1998). A role for H-NS in the regulation of the virF gene of Shigella and enteroinvasive Escherichia coli. *Res. Microbiol.*
doi:10.1016/S0923-2508(97)83619-4.
- Qi, L. S., Larson, M. H., Gilbert, L. A., Doudna, J. A., Weissman, J. S., Arkin, A. P., et al. (2013). Repurposing CRISPR as an RNA-guided platform for sequence-specific control of gene expression. *Cell*.
doi:10.1016/j.cell.2013.02.022.
- Rivera-Chávez, F., Lopez, C. A., and Bäumlér, A. J. (2017). Oxygen as a driver of gut dysbiosis. *Free Radic. Biol. Med.*
doi:10.1016/j.freeradbiomed.2016.09.022.
- Rodionov, D. A., Gelfand, M. S., Todd, J. D., Curson, A. R. J., and Johnston,

- A. W. B. (2006). Computational reconstruction of iron- and manganese-responsive transcriptional networks in α -proteobacteria. *PLoS Comput. Biol.* doi:10.1371/journal.pcbi.0020163.
- Santos-Zavaleta, A., Salgado, H., Gama-Castro, S., Sánchez-Pérez, M., Gómez-Romero, L., Ledezma-Tejeida, D., et al. (2019). RegulonDB v 10.5: Tackling challenges to unify classic and high throughput knowledge of gene regulation in *E. coli* K-12. *Nucleic Acids Res.* doi:10.1093/nar/gky1077.
- Schroeder, G. N., and Hilbi, H. (2008). Molecular pathogenesis of *Shigella* spp.: Controlling host cell signaling, invasion, and death by type III secretion. *Clin. Microbiol. Rev.* doi:10.1128/CMR.00032-07.
- Schubert, K. A., Xu, Y., Shao, F., and Auerbuch, V. (2020). The *Yersinia* Type III Secretion System as a Tool for Studying Cytosolic Innate Immune Surveillance. *Annu. Rev. Microbiol.* doi:10.1146/annurev-micro-020518-120221.
- Schwartz, C. J., Giel, J. L., Patschkowski, T., Luther, C., Ruzicka, F. J., Beinert, H., et al. (2001a). IscR, an Fe-S cluster-containing transcription factor, represses expression of *Escherichia coli* genes encoding Fe-S cluster assembly proteins. *Proc. Natl. Acad. Sci. U. S. A.* doi:10.1073/pnas.251550898.
- Schwartz, C. J., Giel, J. L., Patschkowski, T., Luther, C., Ruzicka, F. J., Beinert, H., et al. (2001b). IscR, an Fe-S cluster-containing transcription

- factor, represses expression of Escherichia coli genes encoding Fe-S cluster assembly proteins. *Proc. Natl. Acad. Sci.*
doi:10.1073/pnas.251550898.
- Schwiesow, L., Lam, H., Dersch, P., and Auerbuch, V. (2016). Yersinia type III secretion system master regulator LcrF. *J. Bacteriol.*
doi:10.1128/JB.00686-15.
- Schwiesow, L., Mettert, E., Wei, Y., Miller, H. K., Herrera, N. G., Balderas, D., et al. (2018). Control of hmu heme uptake genes in Yersinia pseudotuberculosis in response to iron sources. *Front. Cell. Infect. Microbiol.* doi:http://dx.doi.org/10.3389/fcimb.2018.00047.
- Shepard, W., Soutourina, O., Courtois, E., England, P., Haouz, A., and Martin-Verstraete, I. (2011). Insights into the Rrf2 repressor family - The structure of CymR, the global cysteine regulator of Bacillus subtilis. *FEBS J.* doi:10.1111/j.1742-4658.2011.08195.x.
- Shindo, H., Ohnuki, A., Ginba, H., Katoh, E., Ueguchi, C., Mizuno, T., et al. (1999). Identification of the DNA binding surface of H-NS protein from Escherichia coli by heteronuclear NMR spectroscopy. *FEBS Lett.*
doi:10.1016/S0014-5793(99)00862-5.
- Viboud, G. I., and Bliska, J. B. (2005). Yersinia outer proteins: Role in modulation of host cell signaling responses and pathogenesis. *Annu. Rev. Microbiol.* doi:10.1146/annurev.micro.59.030804.121320.
- Wang, T., Wang, M., Zhang, Q., Cao, S., Li, X., Qi, Z., et al. (2019).

- Reversible gene expression control in *Yersinia pestis* by using an optimized CRISPR interference system. *Appl. Environ. Microbiol.* doi:10.1128/AEM.00097-19.
- Warrens, A. N., Jones, M. D., and Lechler, R. I. (1997). Splicing by over-lap extension by PCR using asymmetric amplification: An improved technique for the generation of hybrid proteins of immunological interest. *Gene.* doi:10.1016/S0378-1119(96)00674-9.
- Yang, J., Tauschek, M., Strugnell, R., and Robins-Browne, R. M. (2005). The H-NS protein represses transcription of the eltAB operon, which encodes heat-labile enterotoxin in enterotoxigenic *Escherichia coli*, by binding to regions downstream of the promoter. *Microbiology.* doi:10.1099/mic.0.27734-0.
- Yang, Y., Merriam, J. J., Mueller, J. P., and Isberg, R. R. (1996). The psa locus is responsible for thermoinducible binding of *Yersinia pseudotuberculosis* to cultured cells. *Infect. Immun.* doi:10.1128/iai.64.7.2483-2489.1996.
- Yother, J., Chamness, T. W., and Goguen, J. D. (1986). Temperature-controlled plasmid regulon associated with low calcium response in *Yersinia pestis*. *J. Bacteriol.* doi:10.1128/jb.165.2.443-447.1986.

Table 1. Strains used in this study.

Strain	Relevant Genotype	Source or References
IP2666/(WT)	Naturally lacks full-length YopT	(Bliska et al., 1991)
IP2666/(Δ <i>iscR</i>)	<i>iscR</i> in frame deletion of codons 2 to 156	(Miller et al., 2014)
IP2666/(IscR 3xFLAG)	In frame C-terminus 3xFLAG tag of chromosomal <i>IscR</i>	(REF)
IP2666/(H-NS 3xFLAG)	In frame C-terminus 3xFLAG tag of chromosomal H-NS	This work
IP2666/(Δ <i>ymoA</i>)	<i>ymoA</i> in frame full deletion	(Böhme et al., 2012)

IP2666/(Δ <i>iscR</i> Δ <i>ymoA</i>)	Double deletion mutant of <i>iscR</i> and <i>ymoA</i>	This work
IP2666/(<i>ymoA</i> ^{D43N})	Single residue mutation of D43N YmoA	This work
IP2666/(Δ <i>iscR</i> <i>ymoA</i> ^{D43N})	<i>iscR</i> in frame deletion in YmoA D43N mutant	This work
IP2666/(<i>lcrF</i> ^{pNull})	Point mutations in IscR binding site upstream <i>yscW-lcrF</i>	(Hooker-Romero et al., 2019)
IP2666/(Δ <i>ymoA</i> <i>lcrF</i> ^{pNull})	<i>ymoA</i> in frame deletion in <i>lcrF</i> ^{pNull} mutant	This work (Garrity-
IP2666/(Δ <i>lcrF</i>)	<i>lcrF</i> in frame full deletion	Ryan et al., 2010)
IP2666/(Δ <i>lcrF</i> Δ <i>ymoA</i>)	<i>ymoA</i> in frame deletion in <i>lcrF</i> mutant	This work

Table 2. *Y. pseudotuberculosis* primers used in this study.

Name	Primer Sequence ^a	References
qPCR_16s_F	AGCCAGCGGACCACATAAAG	(Yang et al., 1996)
qPCR_16s_R	AGTTGCAGACTCCAATCCGG	(Yang et al., 1996)
qPCR_1crF_F	GGAGTGATTTTCCGTCAGTA	(Miller et al., 2014)
qPCR_1crF_R	CTCCATAAATTTTGTCAACC	(Miller et al., 2014)
qPCR_iscR_F	CAGGGCGGAAATCGCTGCCT	(Hooker-Romero et al., 2019)
qPCR_iscR_R	ATTAGCCGTTGCGGCGCCTAT	(Hooker-Romero et al., 2019)

		al., 2019)
qPCR_ <i>hns</i> _F	TGCAACAATACCGTGAAATG	This work
qPCR_ <i>hns</i> _R	AGCACGTTTTGCTTTACCAG	This work
qPCR_ <i>gyrA</i> _F	GGGGAAGTGGTGCTGAATAA	(Davis et al., 2015)
qPCR_ <i>gyrA</i> _R	AAAATGGTACGGCGAGTCAC	(Davis et al., 2015)
qPCR_ <i>cpxR</i> _F	TTGATGATGACCGTGAAGT	This work
qPCR_ <i>cpxR</i> _R	ATCATAGGCGACCACAACAT	This work
qPCR_ <i>rcsB</i> _F	GCAAATTGAATGGGTAAACG	This work
qPCR_ <i>rcsB</i> _R	TAATTAGCACGTTGGCATCA	This work
qPCR_ <i>ymoA</i> _F	CCTGATGCGTTTAAGAAAATG	This work
qPCR_ <i>ymoA</i> _R	GATGGTCTGCAGCTGAGTAAA	This work
<i>Fhns_cds</i>	cgaattcctgcagcccggggAGATGAGCACCATAAA TG	This work
<i>Rhns_cds</i>	aacccccatCAACAGGAAGTCATCCAG	This work
F3xFLAG	cttcctgttgATGGGGGGTTCTGACTAC	This work
R3xFLAG	aataaaactaTCAACCTTTATCGTCGTCATC	This work
F3' <i>hns</i>	taaaggtgaTAGTTTTATTTCTTTAGCTATTACT ATCG	This work
R3' <i>hns</i>	aggaacaaaagctggagctCGCCTAAATAGTCGTG GG	This work

F5' Δ <i>ymoA</i>	cgaattcctgcagccccggggGATAGACAGCTGTATTT ATATGAC	This work
R5' Δ <i>ymoA</i>	gcgctaagcaGGTTTTTCTTCTCGATATACAAAT TAATATTG	This work
F3' Δ <i>ymoA</i>	aagaaaaaccTGCTTAGCGCTGGTTAAG	This work
R3' Δ <i>ymoA</i>	agggaacaaaagctggagctCCTGTATTATCACTTT CCTGC	This work
pUC19- YmoA_F	acggccagtgattcgagctcTTCATTTGTGATGAGTT TTAAAATAAAATAC	This work
pUC19-YmoA-R	cctgcaggtcgactctagaggatccAGAGGGCTGAATT TGAATG	This work
<i>ymoA</i> ^{D43N} _F	CTCAGCTGCAaACCATCGCCT	This work
<i>ymoA</i> ^{D43N} _R	TAAAACAATTCCAGTTCATCATCAGAAAGTTC G	This work
pFU99a_ <i>ymoA</i> _F	ccttcgtcttcacctcgagTAATTGGTATATTTTCAAT GCTTGTTTGGATATCAATAC	This work
pFU99a_ <i>ymoA</i> _R	tcatttttaattcctcctgGTCATGCCGCTTAGGCGAG	This work
pFU99a_ <i>hns</i> _F	ccttcgtcttcacctcgagATTGTACATAACGATACA GAAAC	This work
pFU99a_ <i>hns</i> _R	tcatttttaattcctcctgGTTGTTAAGAATTTTAAACG CTTC	This work

<i>hns_gRNA_F</i>	GCACTCCTAGTCTCAAATTATAAT	This work
<i>hns_gRNA_R</i>	AAACATTATAATTTGAGACTAGGA	This work
<i>hnsChIP_site1_F</i>	GCCCGTGCTCTTTATTGGG	This work
<i>hnsChIP_site1_R</i>	CACTTCAGCTGTGGCCTCTA	This work
<i>hnsChIP_site2_F</i>	TGGGGTGATTAACACCGG	This work
<i>hnsChIP_site2_R</i>	ATATAAGTGAACCTCTTGTTGGTTAAC	This work
<i>hnsChIP_site3_F</i>	TTATATGCGCAAGGTGTGATATTG	This work
<i>hnsChIP_site3_R</i>	TTCCCAATTATCTCAACGGGT	This work
<i>hnsChIP_controI_F</i>	TGACGTCGGCAGTC	This work
<i>hnsChIP_controI_R</i>	TCACCCCTTCGCAATAC	This work
<i>iscRChIP_lcrF_F</i>	CGATATGGTTAACCAACAAGAGGTTC	This work
<i>iscRChIP_lcrF_R</i>	GCACAGGAGAAATACAATTACCATAC	This work

iscRChIP_suf_FCTTTTAGACCTCCTTGGGTATCGC This work

iscRChIP_suf_
R CCGTTTGTTTTGCAGGGATATTAGG This work

iscRChIP_hpt_FGCATGATGCTGGGCTTTAC This work

iscRChIP_hpt_
R ATAACAAAAATGCGCAGTGG This work

pFU99a_yscWlcttcattttaattcctcctgAGAAATGATGAGTGCTATAA
This work

rF_R TACG

pFU99a_yscWlc
rF_p1 ccttcgtcttcacctcgagCAAGTTCAGACTGTGCGC This work

pFU99a_yscWlc
rF_p2 ccttcgtcttcacctcgagAGGCTGCAATGTAAGTAG This work

pFU99a_yscWlcccttcgtcttcacctcgagATGGTTAACCAACAAGAG
rF_p3 G This work

pFU99a_yscWlcccttcgtcttcacctcgagAATTAGGATTAATCTCTTG
rF_p4 ACTTTTTTTTG This work

pFU99a_yscWlc
rF_p5 ccttcgtcttcacctcgagGGCTTTATATGCGCAAGG This work

^a Uppercase specifies primer that anneals to target for molecular cloning,
lowercase is complementary sequence for NEB Gibson Assembly or extra
nucleotides to facilitate efficient restriction digest

Table 3. Plasmids used in this study.

Name	Description	References
pPK7179- <i>yscW-lcrF</i>	Promoter template for in vitro transcription, Amp ^R	(Hooker-Romero et al., 2019)
pSR47S Δ <i>ymoA</i>	Suicide vector for <i>ymoA</i> deletion, Kan ^R	This work
pUC19 <i>YmoA</i>	Vector with CDS of <i>YmoA</i> , Amp ^R	This work
pUC19 <i>ymoA</i> ^{D43N}	Vector with CDS of <i>YmoA</i> with <i>ymoA</i> ^{D43N} mutation, Amp ^R	This work
pSR47S <i>ymoA</i> ^{D43N}	Suicide vector for <i>ymoA</i> ^{D43N} mutation, Kan ^R	This work
pdCas9-bacteria	Expressing dCas9 protein under the control of an ATc-inducible promoter with a TetR cassette, Cm ^R	(Qi et al., 2013)
pgRNA-tetO-JTetR	Expressing TetR driven by promoter J23119 and sgRNA driven by PL2tetO. Amp ^R	(Wang et al., 2019)
pgRNA-tetO-JTetR-H-NS	20-bp targeting sequence for <i>hns</i> gene was inserted into pgRNA-tetO-JTetR, Amp ^R	This work
pFU99a	Empty vector carrying promoter-less <i>lacZ</i>	This work

fusion, Cm^R

pFU99a p <i>ymoBA</i> :: <i>lacZ</i>	The promoter of <i>ymoBA</i> fused to <i>lacZ</i> , Cm ^R	This work
pFU99a p <i>hns</i> :: <i>lacZ</i>	The promoter of <i>hns</i> fused to <i>lacZ</i> , Cm ^R	This work
pFU99a p <i>yscW</i> - <i>lcrF</i> :: <i>lacZ</i> p1	The promoter of <i>yscW-lcrF</i> (-505 - +294) fused to <i>lacZ</i> , Cm ^R	This work
pFU99a p <i>yscW</i> - <i>lcrF</i> :: <i>lacZ</i> p2	The promoter of <i>yscW-lcrF</i> (-309 - +294) fused to <i>lacZ</i> , Cm ^R	This work
pFU99a p <i>yscW</i> - <i>lcrF</i> :: <i>lacZ</i> p3	The promoter of <i>yscW-lcrF</i> (-166 - +294) fused to <i>lacZ</i> , Cm ^R	This work
pFU99a p <i>yscW</i> - <i>lcrF</i> :: <i>lacZ</i> p4	The promoter of <i>yscW-lcrF</i> (-47 - +294) fused to <i>lacZ</i> , Cm ^R	This work
pFU99a p <i>yscW</i> - <i>lcrF</i> :: <i>lacZ</i> p5	The promoter of <i>yscW-lcrF</i> (+101 - +294) fused to <i>lacZ</i> , Cm ^R	This work

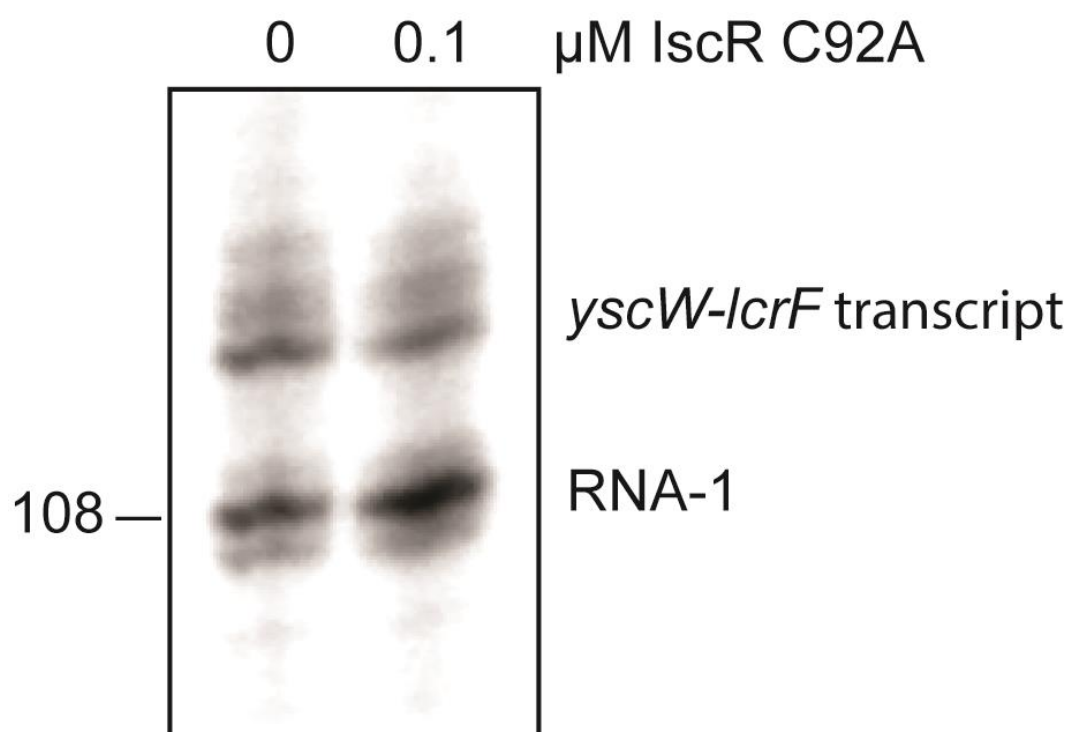


Figure 1 IscR does not directly promote transcription of *yscW-lcrF* in vitro. *In vitro* transcription reactions containing the pPK7179 plasmid encoding the promoter of *yscW-lcrF*, E σ 70 RNA polymerase, and, where indicated, 0.1 μ M IscR C92A protein lacking iron sulfur cluster coordination were incubated and analyzed. Numbers indicate the size of the transcripts and transcripts from the control RNA-1 promoter are indicated.

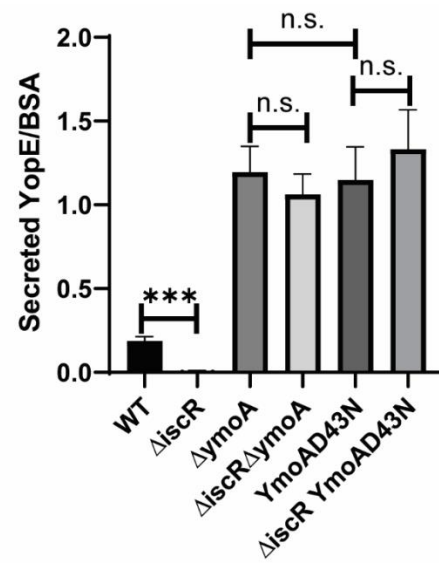
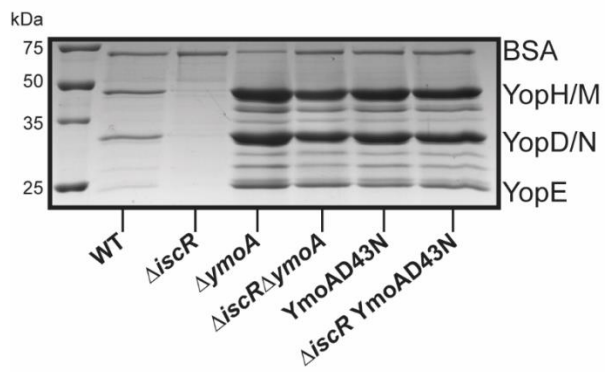


Figure 2. Deletion of *iscR* is dispensable for type III secretion in the $\Delta ymoA$ mutant background. *Yersinia* strains were grown under T3SS-inducing conditions (low calcium at 37°C) and precipitated secreted proteins visualized by SDS-PAGE followed by Coomassie blue staining. Bovine serum albumin (BSA) was used as a loading control. Densitometry was used to measure the relative amount of secreted YopE T3SS effector protein versus BSA control. The average of four independent replicates \pm standard deviation is shown, and statistical analysis was performed using an unpaired Student's t-test (**p < .001, and n.s. non-significant).

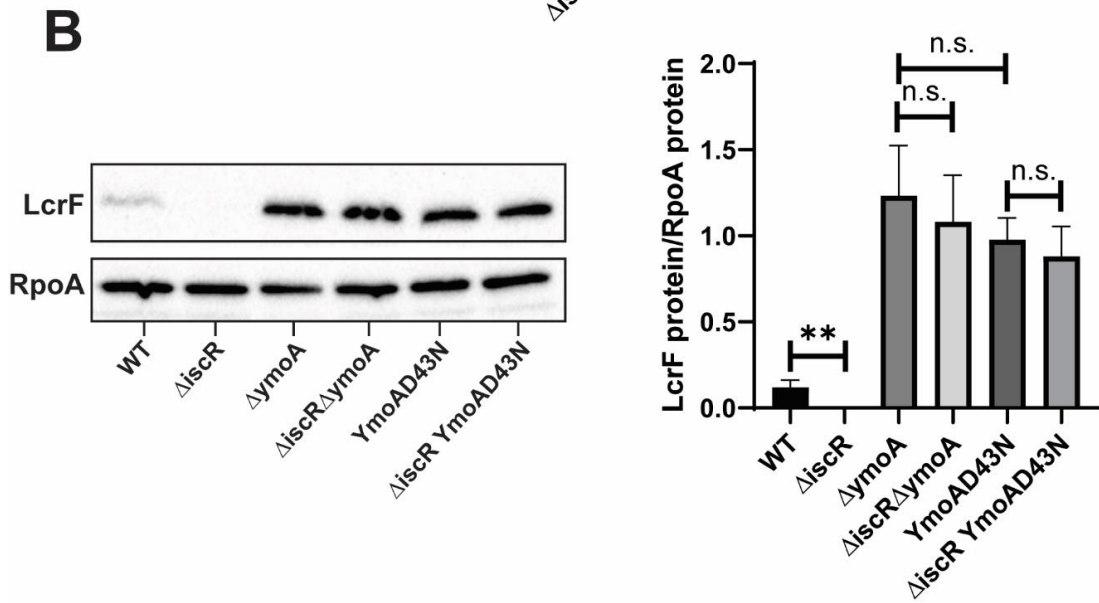
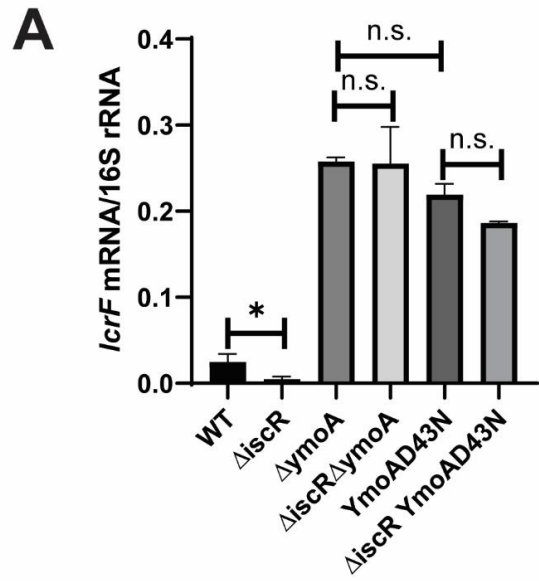


Figure 3. YmoA is epistatic to IscR with respect to *lcrF* transcriptional regulation. *Yersinia* strains grown under T3SS-inducing conditions. **(A)** RNA was extracted, and reverse transcriptase quantitative PCR (RT-qPCR) was used to measure relative levels of *lcrF* mRNA normalized to 16S rRNA. The average of at least three biological replicates are shown \pm standard deviation. **(B)** LcrF protein levels were determined by Western blotting and densitometry relative to the RpoA loading control. Shown is the average of four independent replicates \pm standard deviation. Statistical analysis was performed using an unpaired Student's t-test (* $p < .05$, ** $p < .01$, and n.s. non-significant).

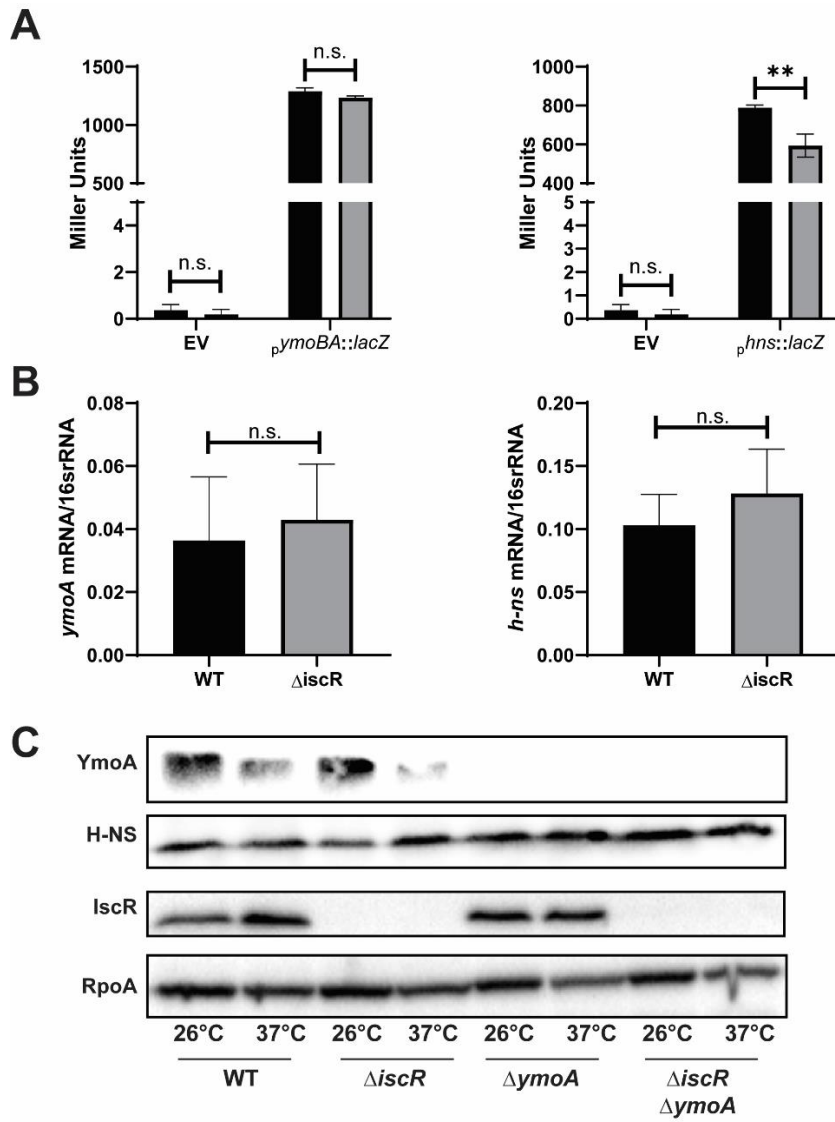


Figure 4. IscR does not regulate YmoA or H-NS expression. (A) *Yersinia* strains harboring either an empty pFU99a plasmid (EV) or a pFU99a plasmid encoding the *ymoBA* or *hns* promoters fused to *lacZ* were grown under T3SS inducing conditions and β -Galactosidase activity determined in Miller units. Black bars represent WT background and grey bars represent the *iscR* mutant background. The average of three biological replicates are shown \pm standard deviation. **(B)** RNA was extracted from *Yersinia* strains grown under T3SS-inducing conditions and RT-qPCR used to measure relative *ymoA* and *hns* mRNA levels normalized to 16S rRNA. Black bars represent WT background and grey bars represent the *iscR* mutant background. The average of at least three biological replicates are shown \pm standard deviation. **(C)** *Yersinia* strains were grown in low calcium LB at 26°C or 37°C for 3 hours. Equal amounts of cell lysates were probed for RpoA, IscR, H-NS, and YmoA by Western blotting. One representative experiment out of three biological replicates is shown. Statistical analysis was performed using an unpaired Student's t-test (n.s. non-significant).

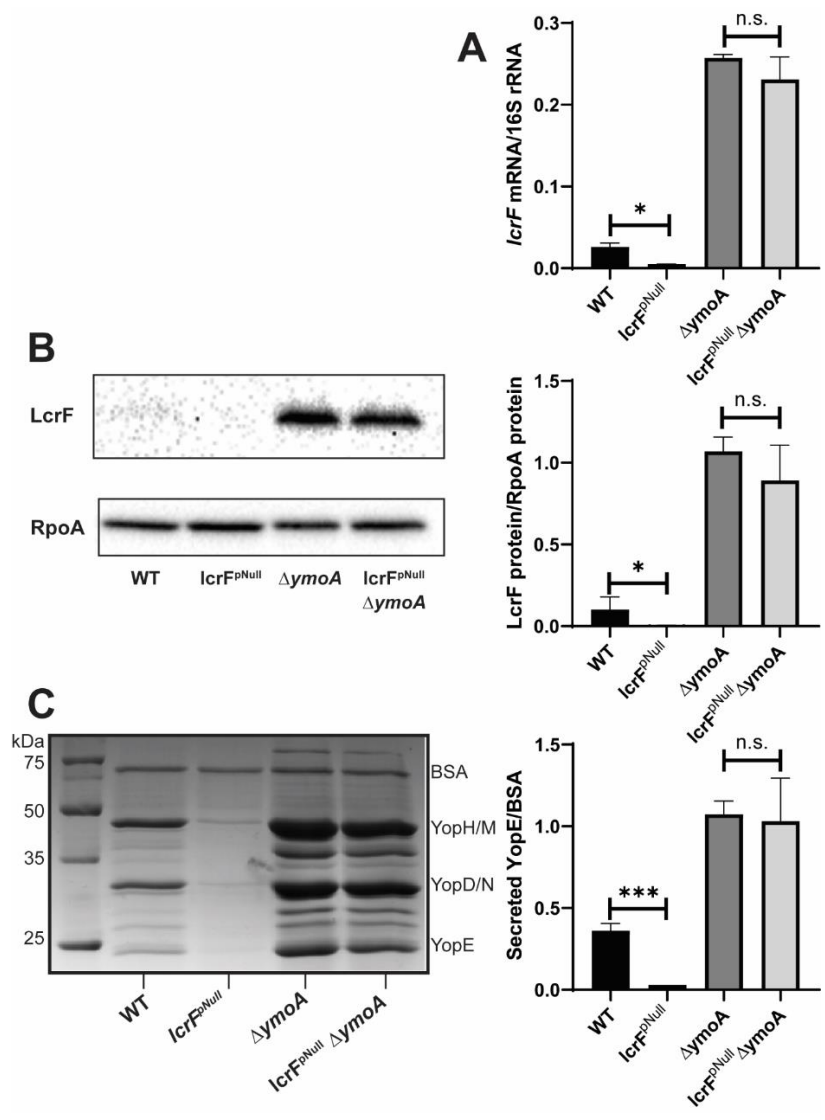


Figure 5. IscR binding to the *yscW-lcrF* promoter is dispensable in the absence of *ymoA*. *Yersinia* strains were grown under T3SS-inducing conditions. **(A)** Levels of *lcrF* mRNA were measured and normalized to 16S rRNA using RT-qPCR. The average of at least three biological replicates are shown \pm standard deviation. **(B)** LcrF protein levels were measured relative to the RpoA loading control by Western blotting and densitometry. Shown is the average of four biological replicates \pm standard deviation. **(C)** Secreted proteins were precipitated and visualized by SDS-PAGE followed by Coomassie blue staining. The YopE bands were normalized to the BSA loading control. The average of three biological replicates \pm standard deviations are shown. Statistical analysis was performed using an unpaired Student's t-test (* $p < .05$, *** $p < .001$, and n.s. non-significant).

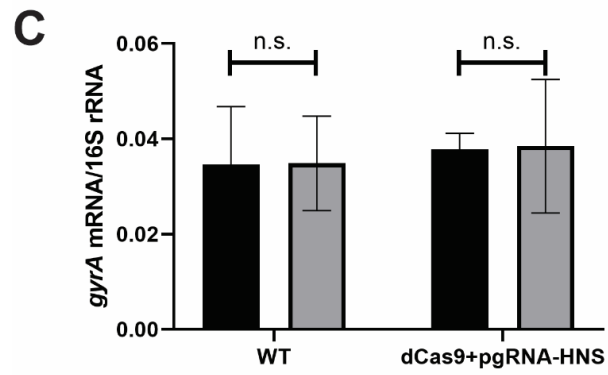
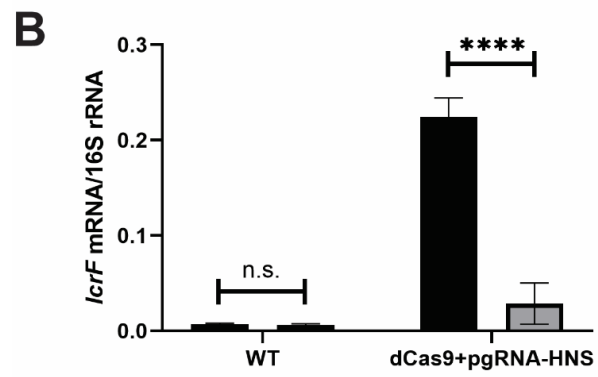
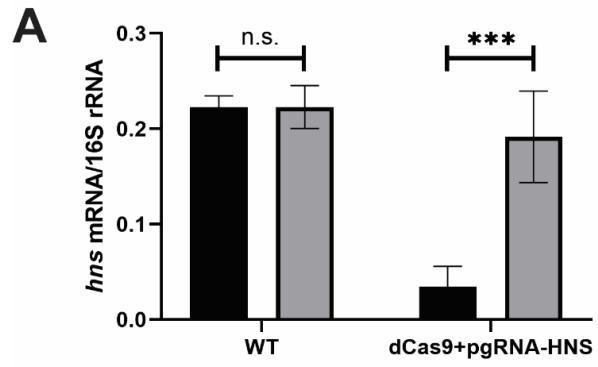


Figure 6. Knockdown of H-NS leads to derepression of LcrF. *Y.*

pseudotuberculosis expressing pdCas9-bacteria and pgRNA-H-NS were grown under T3SS-inducing conditions and supplemented with anhydrotetracycline to induce expression of guide RNA and dCas9 or were left uninduced. *Yersinia* were grown in low calcium LB in the absence (grey bars) or presence (black bars) of 1 µg/mL anhydrotetracycline for 3 hrs at 26°C and transferred to 37°C (T3SS inducing conditions) for 1.5 hrs. RNA was analyzed by qPCR using qPCR for *h-ns* (A), *lcrF* (B), or *gyrA* (C) mRNA level normalized to 16S rRNA. The average of three biological replicates are shown ± standard deviation. Statistical analysis was performed using an unpaired Student's t-test (**p<.001, ****p<.0001, and n.s. non-significant).

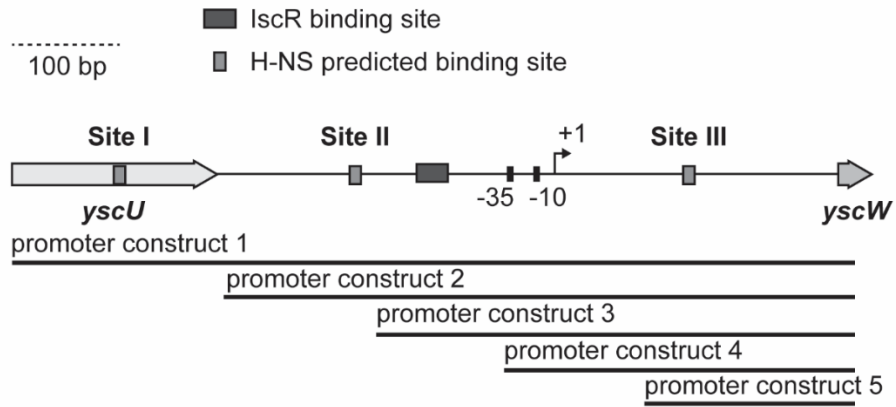
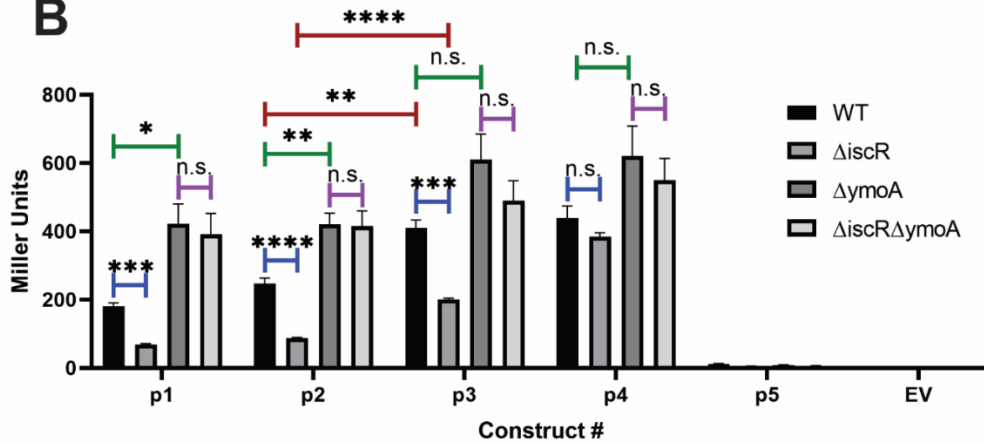
A**B**

Figure 7. Analysis of IscR and H-NS-YmoA regulated segments of *pyscW-lcrF* (A) Diagram of *yycW-lcrF* promoter (800 bp). The characterized IscR binding site is illustrated by the dark grey box. MEME-suite FIMO predicted three H-NS binding sites referred to as Site I, Site II, and Site III. Arrow indicates the previously characterized transcriptional start site. Schematic of *pyscW-lcrF::lacZ* fusions. Five promoter constructs were used to assess which segment of *pyscW-lcrF* allows for H-NS-YmoA repression and IscR activation. (B) *Yersinia* harboring the various *pyscW-lcrF::lacZ* plasmids were grown under T3SS-inducing conditions (low calcium LB at 37°C) for 1.5 hrs and β -Galactosidase activity determined in Miller units. The average of at least three biological replicates are shown \pm standard deviation. Statistical analysis was performed using an unpaired Student's t-test (* $p < .05$, ** $p < .01$, *** $p < .001$, **** $p < .0001$, and n.s. non-significant).

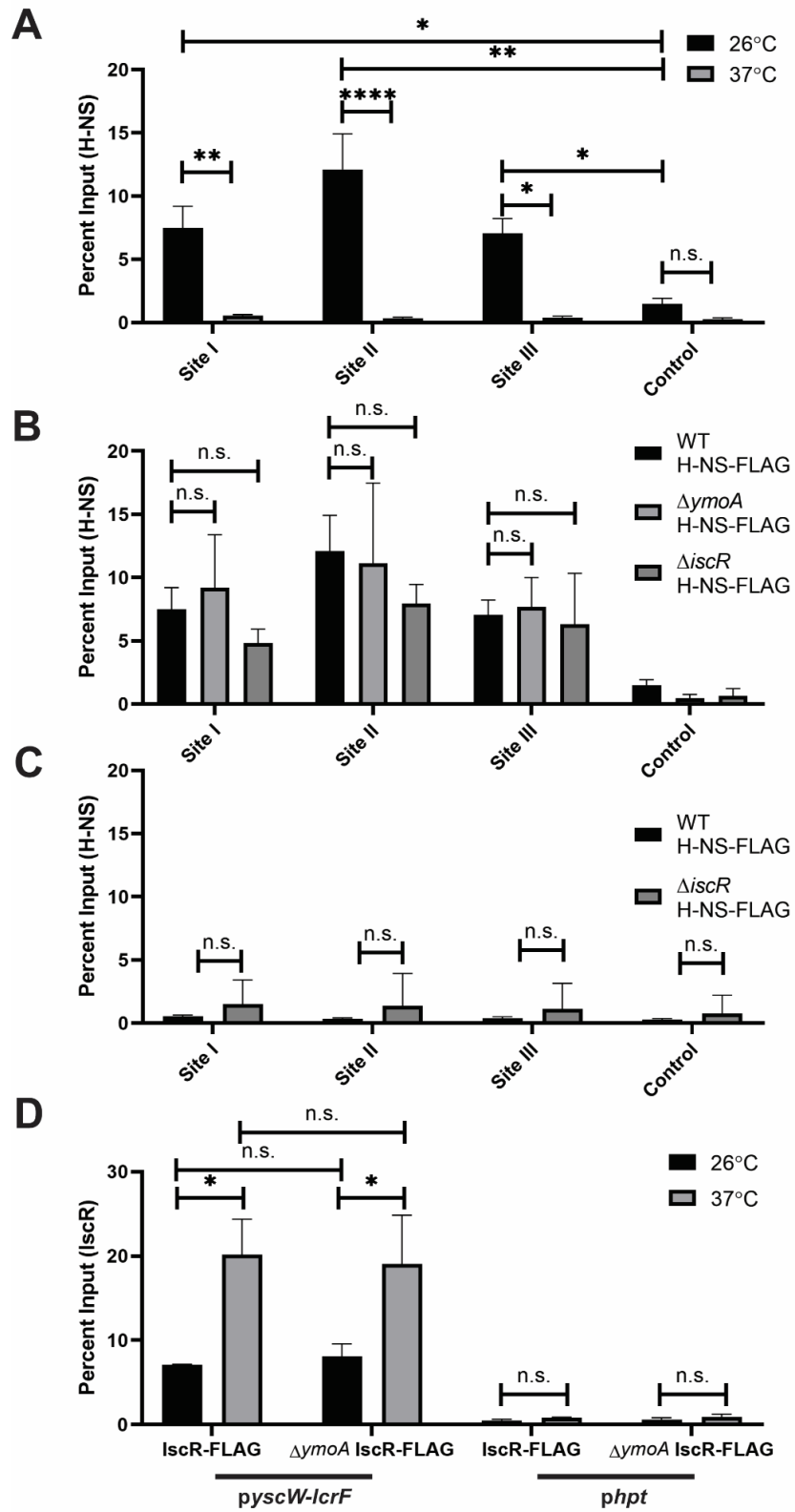


Figure 8. H-NS and IscR bind to the *yscW-lcrF* promoter at different temperatures **(A)** The relative enrichment (percent input) of Site I, Site II, and Site III promoter DNA as analyzed by anti-FLAG ChIP-qPCR in *Yersinia* expressing the H-NS-FLAG allele. ChIP-qPCR was performed with bacteria grown at 26°C (black bars) or 37°C (grey bars) in low calcium LB for 3 hrs. ChIP-qPCR was also performed on a control promoter (DN756_21750) which H-NS is not predicted to bind. The average of at least three biological replicates \pm standard deviation is shown. **(B)** ChIP-qPCR was performed with the H-NS-FLAG allele in the wildtype, $\Delta ymoA$, or $\Delta iscR$ mutant background at 26°C. The average of at least three biological replicates \pm standard deviation is shown. **(C)** ChIP-qPCR was performed with the H-NS-FLAG allele in the wildtype or $\Delta iscR$ mutant background at 37°C. The average of at least three biological replicates \pm standard deviation is shown **(D)** ChIP-qPCR was performed with the IscR-FLAG allele in the wildtype or $\Delta ymoA$ mutant background at 26°C (black bars) or 37°C (grey bars). The *hpt* control promoter, which IscR is not predicted to bind, was used. The average of at least three biological replicates \pm standard deviation is shown, and statistical analysis was performed using Two-way ANOVA (* $p < .05$, ** $p < .01$, *** $p < .001$, **** $p < .0001$ and n.s. non-significant).

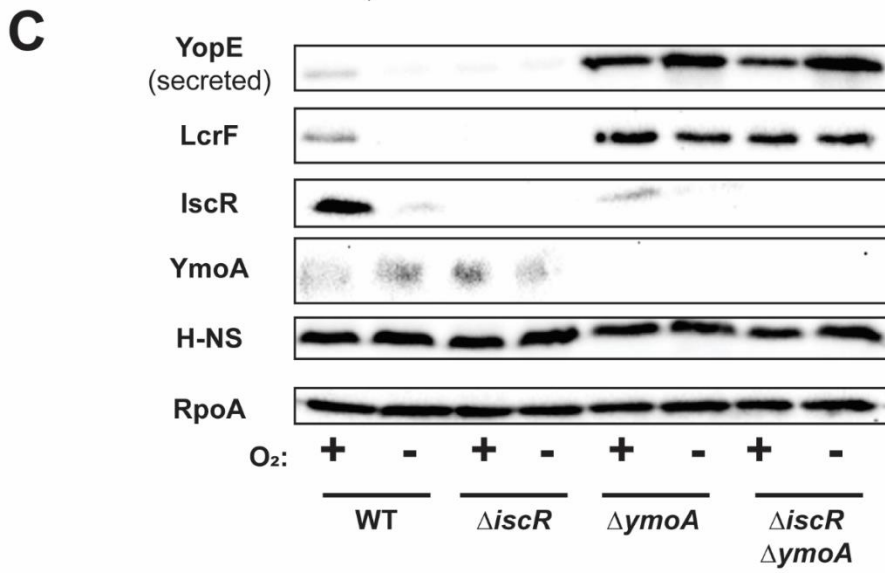
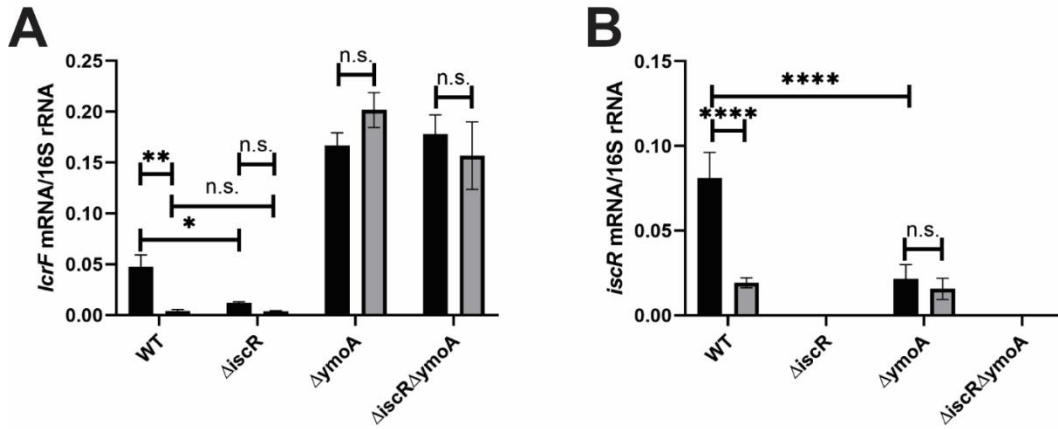


Figure 9. Oxygen does not influence *lcrF* levels in *ymoA* mutants

Yersinia strains were cultured under T3SS inducing conditions under aerobic (black bars) or anaerobic (grey bars) conditions. Levels of *lcrF* **(A)** and *iscR* **(B)** mRNA levels were measured by qPCR and normalized to 16S rRNA. The average of at three biological replicates are shown \pm standard deviation. **(C)** *Yersinia* strains were grown under similar conditions as stated above and whole cell extracts were probed for RpoA, IscR, H-NS, LcrF, YopE, and YmoA by Western blotting. One representative experiment out of three biological replicates is shown. Statistical analysis was performed using a one-way ANOVA with Tukey multiple comparisons (* $p < .05$, ** $p < .01$, **** $p < .0001$, and n.s. non-significant).

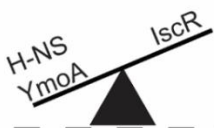
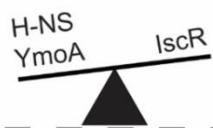
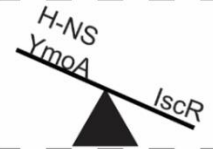
	Environment	Intestinal Lumen	Disseminated Infection
Conditions:	Temp: <30°C Iron availability varies Oxygen tension varies	Temp: 37°C Iron replete Anaerobic	Temp: 37°C Iron starvation Aerobic/microaerophilic
YmoA Levels:	High	Low	Low
IscR Levels:	Varies	Low	High
<i>pyscW-IsrF</i> occupancy:			
LcrF transcription:	Off	Off	On

Figure 10. Proposed model for activation of *yscW-lcrF* via IscR (A) At environmental conditions (26°C, low oxidative stress, high iron), H-NS occupancy at the *yscW-lcrF* promoter is high and LcrF expression and T3SS activity is repressed. **(B)** When *Y. pseudotuberculosis* becomes ingested, it travels to the intestinal lumen. YmoA protein levels decrease due to ClpXP/Lon protease activity at 37°C, but sufficient levels remain to potentiate H-NS-mediated repression of *yscW-lcrF* and prevent type III secretion. This is because IscR levels are kept low by the anaerobic and iron replete conditions. **(C)** Once *Y. pseudotuberculosis* crosses the intestinal barrier, it encounters high oxygen tension and low iron availability, causing an increase in IscR protein levels that can antagonize YmoA/H-NS repression of *yscW-lcrF* and allow for LcrF expression and T3SS activity.

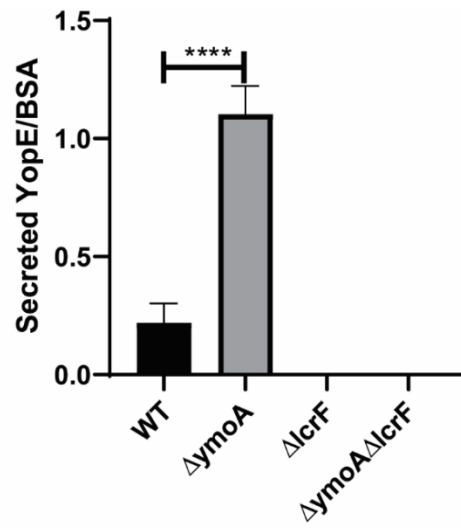
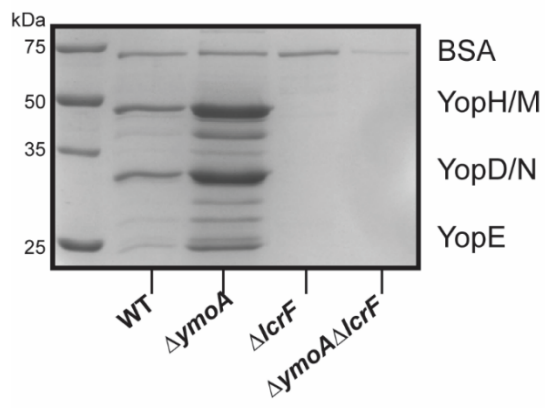


Figure S1. YmoA affects type III secretion activity dependent on LcrF.

Yersinia strains were grown in low calcium LB for 1.5 hrs at 26°C and transferred to 37°C (T3SS inducing conditions) for 1.5 hrs. The supernatant was harvested and separated on a 12.5% SDS polyacrylamide gel, and subsequently stained with Coomassie blue. Bovine serum albumin (BSA) was used as a loading control. Gel bands were quantified by using Bio-Rad Image Lab Software Quantity and Analysis tools. YopE bands were normalized to the BSA loading control. The average of 3 biological replicates \pm standard deviation is shown, and statistical significance is represented through Statistical analysis was performed using an unpaired Student's t-test. Statistical values indicated are (**** $p < .0001$).

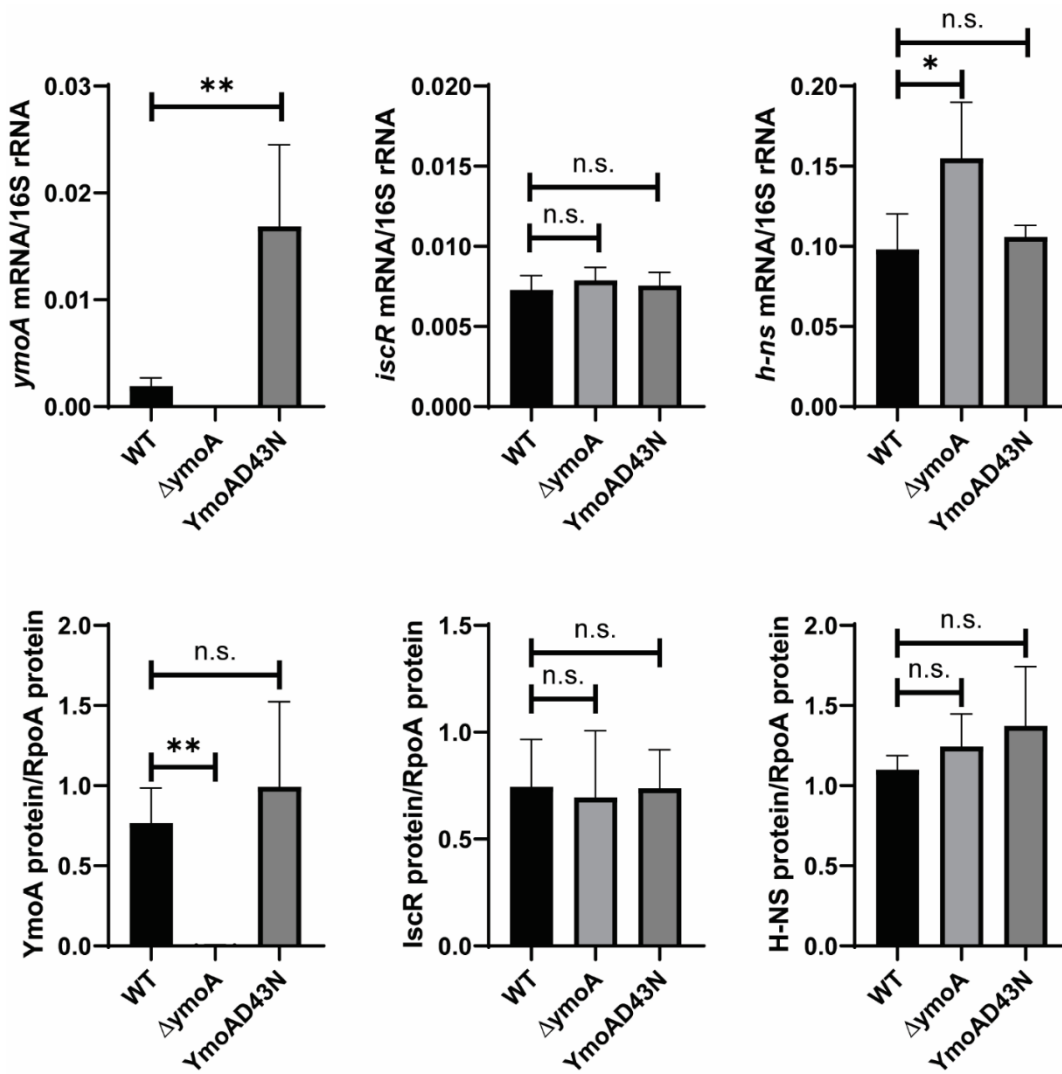


Figure S2. YmoA mutations do not affect mRNA levels of known transcriptional regulators of *IcrF* RNA and whole cell extracts were extracted from *Yersinia* strains grown in low calcium LB for 1.5 hrs at 26°C and transferred to 37°C (T3SS inducing conditions) for 1.5 hrs. Complementary DNA was generated from extracted RNA, and *ymoA*, *iscR*, and *h-ns* mRNA expression was evaluated by qPCR. mRNA levels were normalized to 16S rRNA. The average of at least three biological replicates are shown with standard deviation. For western blots, proteins were visualized using anti-YmoA, anti-IscR, and anti-H-NS antibodies. Proteins were quantified by densitometry using BioRad Image Lab. The average of three biological replicates are shown with standard deviation. Statistical analysis was performed using an unpaired Student's t-test. Statistical values indicated are (*p<.05, **p<.01, and n.s. non-significant).

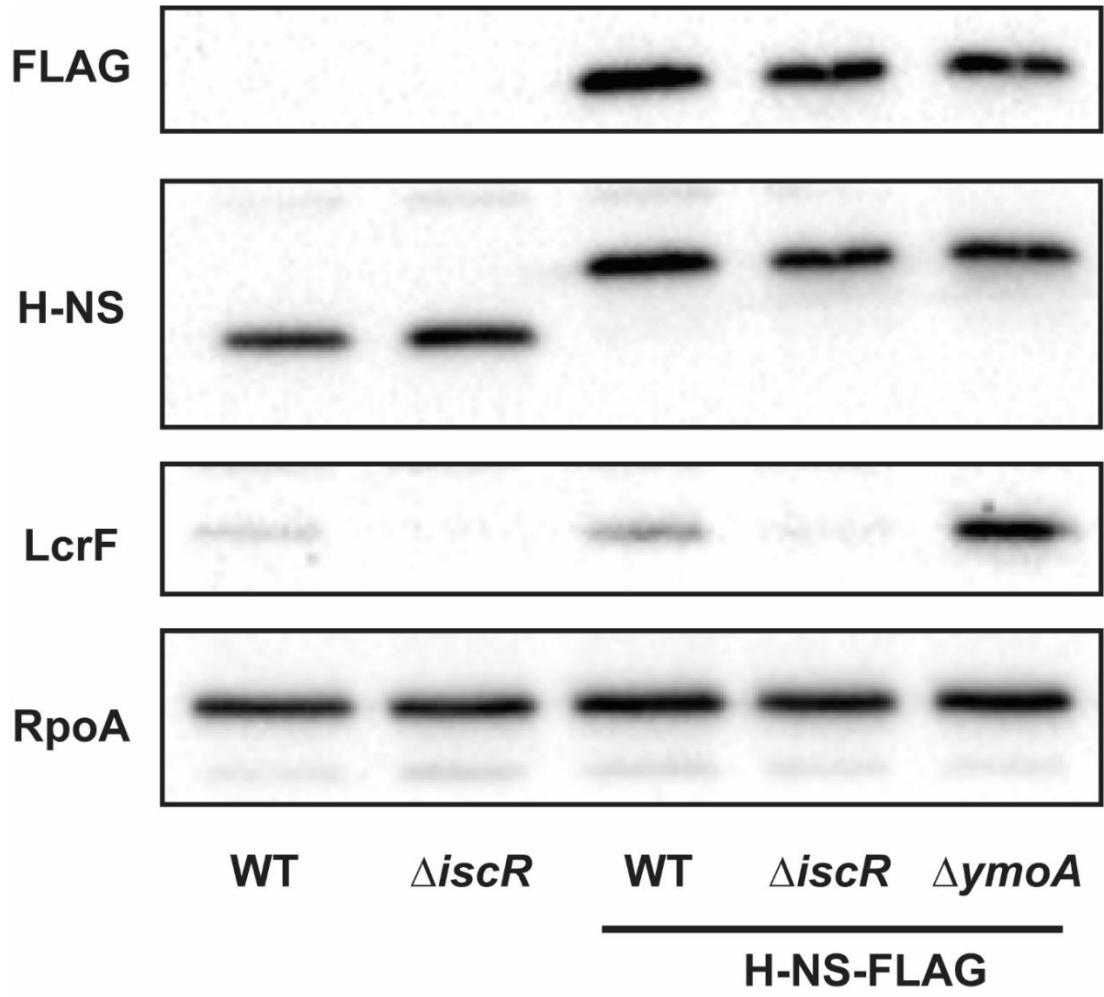


Figure S3. 3xFLAG tag allows for detection of H-NS using FLAG antibody (A) Whole cell extracts from WT *Y. pseudotuberculosis* or a strain harboring a chromosomally-encoded 3xFLAG tagged H-NS were visualized using anti-FLAG, anti-HNS, anti-LcrF, or anti-RpoA antibodies. One representative experiment out of three biological replicates is shown.

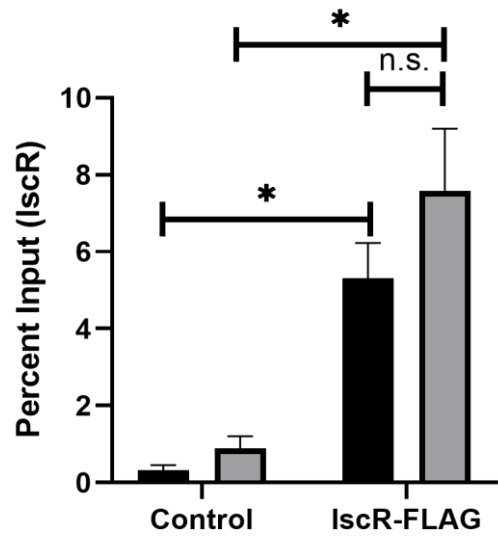


Figure S4. IscR enrichment at the *suf* promoter is not influence by temperature The relative enrichment (percent input) of *suf* promoter DNA analyzed by CHIP-qPCR with the IscR-FLAG strain or the control strain (WT; non-FLAG tagged IscR). CHIP-qPCR was performed with bacteria grown at 26°C (black bars) or 37°C (grey bars). The average of 3 biological replicates ± standard deviation is shown, and statistical significance is represented through Statistical analysis was performed using an unpaired Student's t-test. Statistical values indicated are (*p<.05, and n.s. non-significant).

Chapter 4

The CpxRA two-component regulatory system modulates the Yersinia T3SS through regulation of the YmoA repressor

By David Balderas, Natasha Tanner, Pablo Alvarez, Erin Mettert, Patricia J.

Kiley & Victoria Auerbuch

Abstract

The type III secretion system (T3SS) is a crucial virulence factor in many Gram-negative pathogens. The two-component regulatory system, CpxRA, regulates expression of the type III secretion system in multiple pathogens including *Yersinia pseudotuberculosis*. The CpxRA two-component regulatory system consists of a histidine kinase, CpxA, and a cognate response regulator, CpxR. In the presence of extracytoplasmic stress, CpxA undergoes autophosphorylation and phosphorylates CpxR, which activates the CpxR transcription factor. Previous data suggests that CpxR directly inhibits transcription of *LcrF*, the master regulator of the Ysc type III secretion system. In this study, we show that purified CpxR does not bind to the *lcrF* promoter, suggesting CpxR does not directly regulate *lcrF*. Instead, a predicted CpxR binding site was identified upstream of the *ymoA* promoter. YmoA is a histone-like protein that represses *lcrF* transcription through its interaction with N-HS and thus represses expression of the T3SS in *Yersinia*. Indeed, CpxR activates *ymoA* promoter activity in a transcriptional reporter assays. Lastly, deletion of *ymoA* in *cpx* mutants restores T3SS activity, implying that CpxRA requires YmoA to repress *lcrF*. We propose that the CpxRA two-component regulatory system represses *lcrF* transcription and overall T3SS activity by promoting expression of the YmoA repressor. As other pathogens use YmoA (Hha) and CpxR orthologues to repress the T3SS, this may

represent a conserved mechanism for regulating expression of this large cell envelope-embedded structure in response to extracytoplasmic stress.

Introduction

Bacteria are found in a wide array of environmental niches and adapt to changes in pH, salinity, oxygen tension, and many other environmental conditions. Bacteria sense and respond to environmental stimuli, allowing them to adapt to changing conditions. One of the most common ways bacteria sense and respond to environmental stimuli is through two-component regulatory systems (Groisman, 2016). Two-component regulatory systems allow bacteria to acclimate to environmental stimuli by modulating bacterial physiology usually mediated through changes in gene expression. A canonical two- component regulatory system consists of a histidine kinase and response regulator. Upon recognition of a certain signal/stimuli, the histidine kinase autophosphorylates and can transfer the phosphoryl group to a cognate response regulator. Phosphorylation of a response regulator modulates the activity of the response regulator, and most often when the response regulator is a transcription factor, phosphorylation causes the response regulator to influence gene expression of certain target genes.

One common environmental stimulus that bacteria respond to is cell envelope stress. The bacterial envelope separates the bacterial cytosol from the

environment, and is the site for respiration, nutrient/ion transport, as well as assembly of adhesion proteins or other virulence structures (Rowley et al., 2006; Hews et al., 2019). A cell envelope stress response can be instigated by chemical stressors (detergent, pH), physical stressors (temperature, osmolarity), or biological stressors (adhesion, infection). Multiple bacterial pathways have evolved to mitigate the negative consequences of envelope stress.

One pathway that responds to envelope stress is the two-component regulatory system CpxRA (Raffa and Raivio, 2002). This pathway is found in numerous γ -proteobacteria including *Escherichia coli* and consists of an inner membrane histidine kinase, CpxA, and a cognate response regulator, CpxR (Raivio, 2014). In the absence of envelope stress, a periplasmic protein CpxP interacts with CpxA and prevents autophosphorylation of CpxA (Raivio and Silhavy, 1997). In this condition, CpxA acts as a phosphatase to remove phosphoryl groups from CpxR. Upon exposure to envelope stress, CpxP binds misfolded proteins and no longer interacts with CpxA which undergoes autophosphorylation and can activate CpxR through phosphorylation. CpxR encodes a transcription factor that can both activate or repress transcription of specific gene targets in the phosphorylated state. CpxR is predicted to directly regulate over 60 genes/operons in *E. coli*, which range in function from protein folding/degradation, pilus adherence, copper response,

motility/chemotaxis, and biofilm production (De Wulf et al., 2002; Price and Raivio, 2009; Santos-Zavaleta et al., 2019). Interestingly, the CpxRA system has been shown to affect virulence in multiple bacterial pathogens including *Legionella pneumophila*, *Salmonella enterica*, Enterohemorrhagic *E. coli*, Uropathogenic *E. coli*, *Neisseria gonorrhoeae*, *Shigella sonnei*, and *Yersinia pseudotuberculosis* (Nakayama and Watanabe, 1998; Gal-Mor and Segal, 2003; Carlsson et al., 2007b; De la Cruz et al., 2015, 2016; Gangaiah et al., 2017; Dbeibo et al., 2018).

Yersinia pseudotuberculosis is an enteric pathogen that is closely related to the causative agent of plague, *Yersinia pestis*. Both pathogens rely on the Ysc type III secretion system (T3SS) to ensure survival inside the host. The Ysc T3SS is encoded on a ~70 kb virulence plasmid, and most genes on this plasmid are activated by the transcriptional factor, LcrF (Cornelis et al., 1998; Schwiesow et al., 2016). The transcription factor LcrF is co-transcribed with YscW, the Ysc pilotin (Burghout et al., 2004). These genes are highly regulated at the transcriptional level to prevent expression of the T3SS when not in the host (Schwiesow et al., 2016). One characterized repressor of *yscW-lcrF* transcription is CpxR (Carlsson et al., 2007b; Liu et al., 2012). In the absence of *cpxA*, CpxR becomes hyperphosphorylated and prevents expression of the Ysc T3SS (Liu et al., 2012). It was proposed that phosphorylated CpxR directly represses *yscW-lcrF* transcription, but purified

CpxR protein was shown to bind an intergenic region between *yscW* and *lcrF* that is not predicted to affect *lcrF* mRNA levels.

In this study, we show evidence that CpxR does not bind to the promoter of *yscW-lcrF* and thus does not directly repress type III secretion through LcrF. Instead, we provide data to suggest that phosphorylated CpxR directly activates a characterized repressor of *yscW-lcrF*, YmoA. Our data illustrates that phosphorylated CpxR induces expression of YmoA and that CpxR is predicted to bind the *ymoA* promoter. The protein YmoA has been shown to interact with H-NS and YmoA-H-NS are predicted to be direct repressors of *yscW-lcrF* transcription (Böhme et al., 2012; Cordeiro et al., 2015). We show that the *cpxA* mutant does not affect type III secretion in the absence of YmoA, and thus phosphorylated CpxR requires YmoA to inhibit T3SS activity. This model suggests the CpxRA two-component regulatory system, which responds to envelope stress, can repress the T3SS through YmoA-dependent repression of *yscW-lcrF*.

Results

Purified CpxR binds to a non-regulatory region of *yscW-lcrF*

Purified phosphorylated CpxR was previously shown to bind the *yscW-lcrF* genomic locus in *Yersinia pseudotuberculosis* (Liu et al., 2012). This previous study demonstrated that CpxR binds to an intergenic region in between

yscW-lcrF (Fig 1A). Since then, the *yscW-lcrF* transcription unit has been further characterized and shown that *yscW-lcrF* has one transcriptional start site upstream of *yscW* (Böhme et al., 2012). Thus, CpxR binding to an intergenic region between the *yscW* and *lcrF* open reading frames most likely does not impact transcription of *yscW-lcrF*. We tested if purified CpxR can bind to the promoter of *yscW-lcrF* by using a DNA template that includes the *yscW-lcrF* promoter. This yielded nonspecific binding to the DNA template, suggesting CpxR does not bind to the promoter of *yscW-lcrF* at least *in vitro* (Fig 1B). As a positive control, we showed that CpxR bound to its own promoter (a known target) at low nanomolar concentrations (Fig 1C). These data suggest that CpxR does not influence type III secretion by directly repressing *yscW-lcrF* transcription and suggests that CpxR influences *yscW-lcrF* transcription and type III secretion through a different mechanism.

CpxR is predicted to bind to the promoter of *ymoBA*

To determine how CpxR affects T3SS activity, we assessed whether CpxR affected known regulators of *yscW-lcrF*. Interestingly, in *E. coli*, CpxR positively regulates the YmoB and YmoA orthologs *tomB* and *hha*, respectively (Yamamoto and Ishihama, 2006; Price and Raivio, 2009). The genes *ymoB-ymoA* or *tomB-hha* are expressed in an operon in *Yersinia* and *E. coli*, respectively. Thus, one possibility for how CpxR modulates T3SS activity is that activation of CpxR leads to upregulation of YmoA, which can

repress *yscW-lcrF* transcription. To determine if CpxR directly regulates *Yersinia* YmoBA, we scanned for a CpxR binding site near the promoter of *ymoB-ymoA* (Fig 2). We identified a predicted CpxR binding site 42 nucleotides upstream of the transcriptional start site of *ymoBA*. This suggests that *Yersinia* CpxR may directly regulate YmoA, a known repressor of LcrF.

CpxR influences YmoA expression levels

To test if CpxR regulates *ymoBA*, we tested whether *cpxR* and *cpxA* mutations affect *ymoB-ymoA* promoter activity and mRNA levels. Loss of *cpxA* leads to hyper-phosphorylation of CpxR, and increases CpxR activity (Liu et al., 2012). To test if the CpxRA system affects YmoBA levels, we fused the promoter of *ymoB-ymoA* to *lacZ* and measured the promoter activity in wildtype, $\Delta cpxA$, and $\Delta cpxR$ mutant strain. Interestingly loss of *cpxA* resulted in a ~3-fold increase of *ymoB-ymoA* promoter activity compared to the wildtype strain (Fig 3A). Furthermore, loss of *cpxR* led to a ~2.7-fold decrease in *ymoB-ymoA* promoter activity compared to the wildtype strain. This suggests that high levels of phosphorylated CpxR increase *ymoB-ymoA* promoter activity, while lower levels of phosphorylated CpxR lead to lower *ymoB-ymoA* promoter activity. Next, we performed qRT-PCR to measure *ymoA* transcript levels in the wildtype and the *cpxA* deletion mutant (Fig 3B). This experiment showed that *cpxA* deletion leads to a ~2-fold induction of

ymoA mRNA levels compared to the wildtype strain. These data suggest that CpxRA play a role in directly activating expression of YmoA.

The CpxRA pathway influences T3SS activity dependent on YmoA

Since the *cpxA* deletion mutant in *Yersinia* leads a decrease in T3SS activity, we wanted to test if this is through a YmoA-mediated mechanism. In *Yersinia*, YmoA has been shown to repress type III secretion (Cornells et al., 1991). We therefore proposed that deletion of *cpxA* leads to increased phosphorylated CpxR, which induces YmoA transcription and that this increase in YmoA represses T3SS activity. To test this model, we determined if YmoA is essential for the *cpxA* mutant to repress type III secretion. As has been previously demonstrated the *cpxA* mutant secreted less effector proteins, such as YopE, compared to the wildtype strain (Fig 4AB). Deletion of *ymoA* led to an increase in YopE secretion compared to the wildtype strain. Furthermore, deletion of *ymoA* in the *cpxA* mutant led to an increase in YopE secretion, suggesting *cpxA* requires YmoA to repress T3SS activity. These data suggest a model where CpxR promotes *ymoA* transcription, which has the capacity to block *lcrF* transcription and reduce type III secretion.

Discussion

Previous models suggest the *Yersinia* two component regulatory system CpxRA represses T3SS activity (Carlsson et al., 2007a; Liu et al., 2012).

Although it is known that CpxRA negatively influences LcrF and the T3SS, the molecular mechanism of how CpxRA represses LcrF and the T3SS was not clear. Originally, it was proposed that phosphorylated CpxR can bind to the intergenic region between *yscW* and *lcrF* (Liu et al., 2012). However, the only identified promoter for *lcrF* is located upstream of *yscW* (Böhme et al., 2012). Furthermore, we could find no evidence that phosphorylated CpxR can bind to the promoter region of *yscW-lcrF*, suggesting that CpxR regulates LcrF through an indirect mechanism. We show here that CpxR activates transcription of *ymoA*, a small histone-like protein, which has been shown to repress LcrF expression and therefore T3SS activity (Cornells et al., 1991; Cornelis, 1993; Böhme et al., 2012). This regulation seems to be direct since a predicted CpxR binding site was identified upstream the *ymoA* promoter (see below). This points to a model where activated CpxR induces transcription of YmoA, which represses LcrF transcription and decreases type III secretion (Fig 5).

The homologs of YmoB and YmoA in *E. coli* K12 MG1655 are TomB/YbaJ and Hha, respectively. These genes are encoded as an operon, *ymoBA* or *tomB-hha*. The *tomB(ybaJ)-hha* operon has been shown to be activated by CpxR in *E. coli* K12 (Yamamoto and Ishihama, 2006). This study showed that CpxR directly binds to a CpxR binding motif (TTTAC-[N]₄₋₈-TTTAC) found a few nucleotides upstream of the -35 element of *tomB-hha* operon. Likewise,

we identified a CpxR binding motif upstream of the *ymoB-ymoA* operon in *Yersinia*, a few nucleotides upstream of the -35 element. This suggests that the *ymoB-ymoA* operon is a conserved target of the CpxR regulon. Furthermore, the study that originally identified *tomB-hha* to be a target of *E. coli* CpxR also showed that exposure to copper caused an increase in *tomB* transcription that was dependent through CpxR (Yamamoto and Ishihama, 2006). Future experiments should be performed to assess if copper exposure leads to upregulation of *Yersinia* YmoA through a CpxR dependent mechanism.

Interestingly, Hha and CpxR have been shown to regulate type III secretion in multiple pathogens. For example, Hha and H-NS directly repress HilD, HilC, and RtsA, which promote expression of the SPI-1 T3SS in *Salmonella enterica* (Boddicker et al., 2003; Olekhovich and Kadner, 2007).

Interestingly, CpxR was also shown to negatively inhibit the SPI-1 T3SS in *S. enterica* (Nakayama et al., 2003; De la Cruz et al., 2015). This study described that deletion of *cpxA* in *S. enterica* led to a loss of SPI-1 type III secretion and that phosphorylated CpxR negatively influenced the SPI-1 T3SS. This observation is similar to what is observed in *Yersinia*, where an H-NS-YmoA complex represses LcrF expression (Chapter 3), and CpxR plays a repressive role on T3SS activity (Carlsson et al., 2007a; Liu et al., 2012).

Future experiments should address whether CpxR affects Hha levels in *Salmonella* to determine how CpxR influences the SPI-1 T3SS.

New data suggests that mis localized lipoproteins may act as a signal to induce the CpxRA two-component regulatory system. Lipoproteins are proteins found in the periplasm that can be anchored to the inner or outer membrane by a lipid moiety (Szewczyk and Collet, 2016). Overexpression of the lipoprotein NlpE or artificial mislocalization of NlpE leads to activation of the CpxRA two-component regulatory system (Snyder et al., 1995; Miyadai et al., 2004; Delhaye et al., 2016). NlpE is a outer-membrane lipoprotein and overexpression of NlpE leads to mislocalization of NlpE to the inner membrane. Interestingly overexpression of YafY, an inner membrane anchored lipoprotein, also leads to activation of the CpxRA two-component regulatory system (Miyadai et al., 2004). This could suggest that misfolding or errors in lipoprotein trafficking can act as a signal to induce the CpxRA pathway and lead to downregulation of the T3SS. Interestingly, the Ysc T3SS requires a lipoprotein, YscJ/SctJ, to assemble the basal body of the T3SS. Future studies should be carried out to test if mislocalization of YscJ influences the CpxRA pathway.

It remains unclear which signals the CpxRA two-component regulatory system responds to in the host. A recent study showed that the

neurotransmitter, serotonin, mitigates virulence of enterohemorrhagic *E. coli* and *Citrobacter rodentium* (Kumar et al., 2020). Both these pathogens rely on their T3SSs as a virulence factor to initiate attachment and form effacement lesions on epithelial cells to cause disease. Serotonin is primarily synthesized in enterochromaffin cells, and secreted into the lamina propria or the intestinal lumen (Camilleri, 2009). Both enterohemorrhagic *E. coli* and *Citrobacter rodentium* will be exposed to serotonin in the gut lumen before initiating attachment through the T3SS. Kumar et al showed that serotonin antagonizes phosphorylation of the CpxRA system through a direct mechanism. Thus, one of the host signals the CpxRA system may respond to is gut-derived serotonin.

In this study we provided a mechanism for how the two-component regulatory system CpxRA inhibits type III secretion in *Yersinia*. We show that the response regulator, CpxR, does not directly regulate LcrF, the main transcriptional activator of the type III secretion system. Rather, CpxR activates repression of YmoA, a characterized inhibitor of LcrF and type III secretion (Cornells et al., 1991; Cornelis, 1993; Böhme et al., 2012). Future studies should be carried out to determine if CpxR binds to the *ymoA* promoter both *in vitro* and *in vivo* and determine what signals govern CpxR regulation of the T3SS.

Materials and Methods

Bacterial strains and growth conditions

Bacterial strains used in this paper are listed in Table 1.1. *Y. pseudotuberculosis* were grown, unless otherwise specified, in LB (Luria broth) at 26°C shaking overnight. In order to induce the T3SS, overnight cultures were diluted into low calcium medium (LB plus 20 mM sodium oxalate and 20 mM MgCl₂) to an optical density (OD₆₀₀) of 0.2 and grown for 1.5 h at 26°C shaking followed by 1.5 h at 37°C to induce Yop synthesis, depending on the assay, as previously described (Auerbuch et al., 2009).

Construction of *Yersinia* mutant strains

Generation of The $\Delta ymoA$, $\Delta cpxA$, and $\Delta cpxR$ mutants were generated via splicing by overlap extension (Warrens et al., 1997). Primer pairs F5/R5 $\Delta ymoA$, F5/R5 $\Delta cpxA$, and F5/R5 $\Delta cpxR$ (Table 2) were used to amplify ~1000 bp 5' of *ymoA*, *cpxA*, and *cpxR*, respectively. Primer pair F3/R3 $\Delta ymoA$, F3/R3 $\Delta cpxA$, and F3/R3 $\Delta cpxR$ were used to amplify ~1000 bp 3' of *ymoA*, *cpxA*, and *cpxR*, respectively. Amplified PCR fragments were cloned into a BamHI- and SacI-digested pSR47s suicide plasmid (λ pir-dependent replicon, kanamycin^R, *sacB* gene conferring sucrose sensitivity) using the NEBuilder HiFi DNA Assembly kit (New England Biolabs, Inc). Recombinant plasmids were transformed into *E. coli* S17-1 λ pir competent cells and later introduced

into *Y. pseudotuberculosis* IP2666 via conjugation. The resulting Kan^R, irgansan^R (*Yersinia* selective antibiotic) integrants were grown in the absence of antibiotics and plated on sucrose-containing media to select for clones that had lost *sacB* (and by inference, the linked plasmid DNA). Kan^S, sucrose^R, congo red-positive colonies were screened by PCR and sequenced.

To generate lacZ promoter constructs of *ymoBA* primer pairs pFU99a_ymoA_F/pFU99a_ymoA_R were used to amplify ~500 bp upstream *ymoB* which included the first ten amino acids of *ymoB*. These promoters and first ten amino acids of YmoB and H-NS were cloned into a BamHI- and Sall-digested pFU99a using the NEBuilder HiFi DNA Assembly kit (New England Biolabs, Inc). These reporter plasmids were electroporated into wildtype *Yersinia pseudotuberculosis* to measure *ymoBA* promoter activity.

Type III secretion system assays

Visualization of T3SS cargo secreted in broth culture was performed as previously described (Kwuan et al., 2013). Briefly, *Y. pseudotuberculosis* in LB low calcium media (LB plus 20 mM sodium oxalate and 20 mM MgCl₂) was grown for 1.5 h at 26°C followed by growth at 37°C for 1.5 h. Cultures were normalized by OD₆₀₀ and pelleted at 13.2 krpm for 10 min at room temperature. Supernatants were removed and proteins precipitated by addition of trichloroacetic acid (TCA) at a final concentration of 10%. Samples

were incubated on ice for at least 1 hr and pelleted at 13,200 rpm for 15 min at 4°C. Resulting pellets were washed twice with ice-cold 100% Acetone and subsequently resuspended in final sample buffer (FSB) containing 20% dithiothreitol (DTT). Samples were boiled for 5 min prior to running on a 12.5% SDS PAGE gel. Gel bands were imaged using Bio-Rad Image Lab Software Quantity and Analysis tools. YopE bands were quantified using this software and normalized to the BSA loading control.

Western Blot Analysis

To visualize more accurate secretion phenotypes, supernatant samples were obtained and prepared in the same manner as described above. Cell pellet samples were also prepared by resuspension in FSB plus 20%DTT and were boiled for fifteen minutes. At the time of loading, samples were normalized to the same number of cells. After having run the samples on a 12.5% polyacrylamide gel, proteins were transferred onto a blotting membrane (Immobilon-P) with a wet mini trans-blot cell (Bio-Rad). Blots were blocked for an hour in Tris-buffered saline with Tween 20 and 5% skim milk, and probed with the rabbit anti-RpoA (gift from Melanie Marketon), rabbit anti-LcrF (Böhme et al., 2012), rabbit anti-His, rabbit anti-YmoA (gift from Gregory Plano), and horseradish peroxidase-conjugated secondary antibodies (Santa Cruz Biotech). Following visualization, quantification of the bands was performed with Image Lab software (Bio-Rad).

RT-qPCR Sample Preparation

Cultures from each condition were pelleted by centrifugation for 5 minutes at 4,000 rpm. The supernatant was removed, and pellets were resuspended in 500 μ L of media and treated with 1 mL Bacterial RNA Protect Reagent (Qiagen) according to the manufacturer's protocol. Total RNA was isolated using the RNeasy Mini Kit (Qiagen) per the manufacturer's protocol. After harvesting total RNA, genomic DNA was removed via the TURBO-DNA-free kit (Life Technologies/Thermo Fisher). cDNA was generated for each sample by using the M-MLV Reverse Transcriptase (Invitrogen) according to the manufacturer's instructions, as previously described (Schwiesow et al., 2018). Each 15 μ L qPCR assay contained 7.5 μ L of 1:10 diluted cDNA sample, 7.5 μ L of Power CYBR Green PCR master mix (Thermo Fisher Scientific), and primers (Table 2) with optimized concentrations. The expression levels of each target gene were normalized to that of 16S rRNA present in each sample and calculated by the $\Delta\Delta C_t$ method. Three independent biological replicates were analyzed for each condition.

Reporter Plasmid Beta Galactosidase Assay

β -Galactosidase assays were carried out following manufactures protocol by Galacto-Light Plus β -Galactosidase reporter gene assay system (Applied Biosystems). *Y. pseudotuberculosis* cultures from each condition were pelleted by centrifugation for 5 minutes at 4,000 rpm. Pellets were lysed by

Lysis Solution provided by kit. Lysed samples were then provided β -Galactosidase- luminescence substrate and incubated for 1hr at 37°C. After incubation, samples received Accelerator prior to reading of luminescence of 0.1-1 sec/well. β -Galactosidase activity was quantified using a standard curve and normalized to total protein content which was quantified by Pierce BCA Protein Assay kit (ThermoFisher Scientific).

Bioinformatic prediction of CpxR binding sites

A training set of known CpxR binding sites in *E. coli* K-12 substr. MG1655 was used from RegulonDB (Santos-Zavaleta et al., 2019). This training set was used to generate a CpxR binding motif using MEME from MEME-suite 5.1.1 tools (Bailey et al., 2009). FIMO was then used to scan for a CpxR binding site near the regulatory region of the *ymoBA* promoter.

Protein purification

To purify CpxR with a C-terminus 6xHis tag, primer pairs F_pET28bCpxRHis and R_pET28bCpxRHis were used to amplify the *Yersinia* CpxR cds omitting the stop codon. This amplified PCR product was digested with the restriction enzymes NcoI and XhoI and cloned into a pET28b vector with a in frame C-terminus 6xHis affinity tag. This vector was then transformed into *E. coli* BL21 (DE3) pLysS component cells. Expression and purification of CpxR with

a C-terminal His(6)-tag has been described previously (Carlsson et al., 2007b).

Protein purification and electrophoretic mobility shift assays (EMSAs)

The DNA fragment containing the predicted the *yscW-lcrF* promoter contained the -206 to +12 bp relative to the +1 transcription start site of *yscW* were amplified from *Y. pseudotuberculosis* genomic DNA using primers (Table 2). Amplified products were digested with XhoI and BamHI and subsequently ligated into the pPK7179 plasmid. DNA templates for EMSAs were isolated from plasmid DNA after restriction digest with XhoI and BamHI. These fragments and linearized plasmid (which served as competitor DNA in the EMSAs) were purified using Elutip-d columns (Schleicher and Schuell). CpxR was incubated with DNA fragments (~5–10 nM) for 30 min at 37°C in 40 mM Tris (pH 7.9), 30 mM KCl, 100 µg/mL bovine serum albumin (BSA), and 1 mM DTT. Samples were loaded onto a non-denaturing 6% polyacrylamide gel in 0.5x Tris-borate-EDTA (TBE) buffer and run at 100 V for 90 min. The gel was stained with SYBR Green EMSA nucleic acid gel stain (Molecular Probes) and visualized using a Typhoon FLA 900 imager (GE).

Acknowledgments

This study was supported by National Institutes of Health (www.NIH.gov) grant R01AI119082 (to VA and PJK). DAB and PA received support from the National Human Genome Research Institute of the National Institutes of Health under Award Number 4R25HG006836. The funders had no role in study design, data collection and analysis, decision to publish, or preparation of the manuscript.

References

- Auerbuch, V., Golenbock, D. T., and Isberg, R. R. (2009). Innate immune recognition of *Yersinia pseudotuberculosis* type III secretion. *PLoS Pathog.* doi:10.1371/journal.ppat.1000686.
- Bailey, T. L., Boden, M., Buske, F. A., Frith, M., Grant, C. E., Clementi, L., et al. (2009). MEME Suite: Tools for motif discovery and searching. *Nucleic Acids Res.* doi:10.1093/nar/gkp335.
- Bliska, J. B., Guan, K., Dixon, J. E., and Falkow, S. (1991). Tyrosine phosphate hydrolysis of host proteins by an essential *Yersinia* virulence determinant. *Proc. Natl. Acad. Sci. U. S. A.* doi:10.1073/pnas.88.4.1187.
- Boddicker, J. D., Knosp, B. M., and Jones, B. D. (2003). Transcription of the *Salmonella* invasion gene activator, *hilA*, requires HilD activation in the absence of negative regulators. *J. Bacteriol.* doi:10.1128/JB.185.2.525-533.2003.

- Böhme, K., Steinmann, R., Kortmann, J., Seekircher, S., Heroven, A. K., Berger, E., et al. (2012). Concerted actions of a thermo-labile regulator and a unique intergenic RNA thermosensor control *Yersinia* virulence. *PLoS Pathog.* doi:10.1371/journal.ppat.1002518.
- Burghout, P., Beckers, F., De Wit, E., Van Boxtel, R., Cornelis, G. R., Tommassen, J., et al. (2004). Role of the pilot protein YscW in the biogenesis of the YscC secretin in *Yersinia enterocolitica*. *J. Bacteriol.* doi:10.1128/JB.186.16.5366-5375.2004.
- Camilleri, M. (2009). Serotonin in the gastrointestinal tract. *Curr. Opin. Endocrinol. Diabetes Obes.* doi:10.1097/MED.0b013e32831e9c8e.
- Carlsson, K. E., Liu, J., Edqvist, P. J., and Francis, M. S. (2007a). Extracytoplasmic-stress-responsive pathways modulate type III secretion in *Yersinia pseudotuberculosis*. *Infect. Immun.* doi:10.1128/IAI.01346-06.
- Carlsson, K. E., Liu, J., Edqvist, P. J., and Francis, M. S. (2007b). Influence of the Cpx extracytoplasmic-stress-responsive pathway on *Yersinia* sp.-eukaryotic cell contact. *Infect. Immun.* doi:10.1128/IAI.01450-06.
- Cordeiro, T. N., García, J., Bernadó, P., Millet, O., and Pons, M. (2015). A three-protein charge zipper stabilizes a complex modulating bacterial gene silencing. *J. Biol. Chem.* doi:10.1074/jbc.M114.630400.
- Cornelis, G. R. (1993). Role of the Transcription Activator VirF and the Histone-like Protein YmoA in the Thermoregulation of Virulence Functions in *Yersiniae*. *Zentralblatt für Bakteriologie.* doi:10.1016/S0934-

8840(11)80833-9.

Cornelis, G. R., Boland, A., Boyd, A. P., Geuijen, C., Iriarte, M., Neyt, C., et al. (1998). The Virulence Plasmid of *Yersinia*, an Antihost Genome.

Microbiol. Mol. Biol. Rev. doi:10.1128/mmbr.62.4.1315-1352.1998.

Cornelis, G. R., Sluiters, C., Delor, I., Geib, D., Kaniga, K., de Rouvoit, C. L., et al. (1991). *ymoA*, a *Yersinia enterocolitica* chromosomal gene

modulating the expression of virulence functions. *Mol. Microbiol.*

doi:10.1111/j.1365-2958.1991.tb01875.x.

Davis, A. J., and Meccas, J. (2007). Mutations in the *Yersinia*

pseudotuberculosis type III secretion system needle protein, YscF, that specifically abrogate effector translocation into host cells. *J. Bacteriol.*

doi:10.1128/JB.01396-06.

Dbeibo, L., van Rensburg, J. J., Smith, S. N., Fortney, K. R., Gangaiah, D.,

Gao, H., et al. (2018). Evaluation of CpxRA as a therapeutic target for uropathogenic *Escherichia coli* infections. *Infect. Immun.*

doi:10.1128/IAI.00798-17.

De la Cruz, M. A., Morgan, J. K., Ares, M. A., Yáñez-Santos, J. A., Riordan, J.

T., and Girón, J. A. (2016). The two-component system CpxRA

negatively regulates the locus of enterocyte effacement of enterohemorrhagic *Escherichia coli* involving σ_{32} and Ion protease.

Front. Cell. Infect. Microbiol. doi:10.3389/fcimb.2016.00011.

De la Cruz, M. A., Pérez-Morales, D., Palacios, I. J., Fernández-Mora, M.,

- Calva, E., and Bustamante, V. H. (2015). The two-component system CpxR/A represses the expression of Salmonella virulence genes by affecting the stability of the transcriptional regulator HilD. *Front. Microbiol.* doi:10.3389/fmicb.2015.00807.
- De Wulf, P., McGuire, A. M., Liu, X., and Lin, E. C. C. (2002). Genome-wide profiling of promoter recognition by the two-component response regulator CpxR-P in Escherichia coli. *J. Biol. Chem.* doi:10.1074/jbc.M203487200.
- Delhaye, A., Collet, J. F., and Laloux, G. (2016). Fine-tuning of the Cpx envelope stress response is required for cell wall homeostasis in Escherichia coli. *MBio.* doi:10.1128/mBio.00047-16.
- Gal-Mor, O., and Segal, G. (2003). Identification of CpxR as a positive regulator of icm and dot virulence genes of Legionella pneumophila. *J. Bacteriol.* doi:10.1128/JB.185.16.4908-4919.2003.
- Gangaiah, D., Raterman, E. L., Wu, H., Fortney, K. R., Gao, H., Liu, Y., et al. (2017). Both MisR (CpxR) and MisS (CpxA) are required for Neisseria gonorrhoeae infection in a murine model of lower genital tract infection. *Infect. Immun.* doi:10.1128/IAI.00307-17.
- Groisman, E. A. (2016). Feedback Control of Two-Component Regulatory Systems. *Annu. Rev. Microbiol.* doi:10.1146/annurev-micro-102215-095331.
- Hews, C. L., Cho, T., Rowley, G., and Raivio, T. L. (2019). Maintaining

- Integrity Under Stress: Envelope Stress Response Regulation of Pathogenesis in Gram-Negative Bacteria. *Front. Cell. Infect. Microbiol.* doi:10.3389/fcimb.2019.00313.
- Kumar, A., Russell, R. M., Pifer, R., Menezes-Garcia, Z., Cuesta, S., Narayanan, S., et al. (2020). The Serotonin Neurotransmitter Modulates Virulence of Enteric Pathogens. *Cell Host Microbe.* doi:10.1016/j.chom.2020.05.004.
- Kwuan, L., Adams, W., and Auerbuch, V. (2013). Impact of host membrane pore formation by the *Yersinia pseudotuberculosis* type III secretion system on the macrophage innate immune response. *Infect. Immun.* doi:10.1128/IAI.01014-12.
- Liu, J., Thanikkal, E. J., Obi, I. R., and Francis, M. S. (2012). Elevated CpxR~P levels repress the Ysc-Yop type III secretion system of *Yersinia pseudotuberculosis*. *Res. Microbiol.* doi:10.1016/j.resmic.2012.07.010.
- Miyadai, H., Tanaka-Masuda, K., Matsuyama, S. I., and Tokuda, H. (2004). Effects of lipoprotein overproduction on the induction of DegP (HtrA) involved in quality control in the *Escherichia coli* periplasm. *J. Biol. Chem.* doi:10.1074/jbc.M406390200.
- Nakayama, S. I., Kushiro, A., Asahara, T., Tanaka, R. I., Hu, L., Kopecko, D. J., et al. (2003). Activation of hilA expression at low pH requires the signal sensor CpxA, but not the cognate response regulator CpxR, in *Salmonella enterica* serovar Typhimurium. *Microbiology.*

doi:10.1099/mic.0.26229-0.

- Nakayama, S. I., and Watanabe, H. (1998). Identification of cpxR as a positive regulator essential for expression of the *Shigella sonnei* virF gene. *J. Bacteriol.* doi:10.1128/jb.180.14.3522-3528.1998.
- Olekhovich, I. N., and Kadner, R. J. (2007). Role of nucleoid-associated proteins Hha and H-NS in expression of *Salmonella enterica* activators HilD, HilC, and RtsA required for cell invasion. *J. Bacteriol.* doi:10.1128/JB.00905-07.
- Price, N. L., and Raivio, T. L. (2009). Characterization of the Cpx regulon in *Escherichia coli* strain MC4100. *J. Bacteriol.* doi:10.1128/JB.00798-08.
- Raffa, R. G., and Raivio, T. L. (2002). A third envelope stress signal transduction pathway in *Escherichia coli*. *Mol. Microbiol.* doi:10.1046/j.1365-2958.2002.03112.x.
- Raivio, T. L. (2014). Everything old is new again: An update on current research on the Cpx envelope stress response. *Biochim. Biophys. Acta - Mol. Cell Res.* doi:10.1016/j.bbamcr.2013.10.018.
- Raivio, T. L., and Silhavy, T. J. (1997). Transduction of envelope stress in *Escherichia coli* by the Cpx two- component system. *J. Bacteriol.* doi:10.1128/jb.179.24.7724-7733.1997.
- Rowley, G., Spector, M., Kormanec, J., and Roberts, M. (2006). Pushing the envelope: Extracytoplasmic stress responses in bacterial pathogens. *Nat. Rev. Microbiol.* doi:10.1038/nrmicro1394.

- Santos-Zavaleta, A., Salgado, H., Gama-Castro, S., Sánchez-Pérez, M., Gómez-Romero, L., Ledezma-Tejeida, D., et al. (2019). RegulonDB v 10.5: Tackling challenges to unify classic and high throughput knowledge of gene regulation in *E. coli* K-12. *Nucleic Acids Res.* doi:10.1093/nar/gky1077.
- Schwiesow, L., Lam, H., Dersch, P., and Auerbuch, V. (2016). Yersinia type III secretion system master regulator LcrF. *J. Bacteriol.* doi:10.1128/JB.00686-15.
- Schwiesow, L., Mettert, E., Wei, Y., Miller, H. K., Herrera, N. G., Balderas, D., et al. (2018). Control of hmu heme uptake genes in Yersinia pseudotuberculosis in response to iron sources. *Front. Cell. Infect. Microbiol.* doi:http://dx.doi.org/10.3389/fcimb.2018.00047.
- Snyder, W. B., Davis, L. J. B., Danese, P. N., Cosma, C. L., and Silhavy, T. J. (1995). Overproduction of nlpE, a new outer membrane lipoprotein, suppresses the toxicity of periplasmic lacZ by activation of the Cpx signal transduction pathway. *J. Bacteriol.* doi:10.1128/jb.177.15.4216-4223.1995.
- Szewczyk, J., and Collet, J. F. (2016). "The Journey of Lipoproteins Through the Cell: One Birthplace, Multiple Destinations," in *Advances in Microbial Physiology* doi:10.1016/bs.ampbs.2016.07.003.
- Warrens, A. N., Jones, M. D., and Lechler, R. I. (1997). Splicing by over-lap extension by PCR using asymmetric amplification: An improved

technique for the generation of hybrid proteins of immunological interest.

Gene. doi:10.1016/S0378-1119(96)00674-9.

Yamamoto, K., and Ishihama, A. (2006). Characterization of copper-inducible promoters regulated by CpxA/CpxR in *Escherichia coli*. *Biosci. Biotechnol. Biochem.* doi:10.1271/bbb.60024.

Biotechnol. Biochem. doi:10.1271/bbb.60024.

Yang, Y., Merriam, J. J., Mueller, J. P., and Isberg, R. R. (1996). The *psa* locus is responsible for thermoinducible binding of *Yersinia pseudotuberculosis* to cultured cells. *Infect. Immun.*

doi:10.1128/iai.64.7.2483-2489.1996.

Table 1. Strains used in this study.

Strain	Relevant Genotype	Source or References
IP2666/(WT)	Naturally lacks full-length YopT	(Bliska et al., 1991)
IP2666/($\Delta ymoA$)	Full in frame deletion of <i>ymoA</i>	(Böhme et al., 2012)
IP2666/($\Delta cpxA$)	<i>cpxA</i> in frame deletion of codons 41 to 449	(Liu et al., 2012)
IP2666/($\Delta cpxR$)	Full in frame deletion of <i>cpxR</i>	This work
IP2666/($\Delta ymoA$ $\Delta cpxA$)	Double deletion mutant of <i>ymoA</i> and <i>cpxA</i>	(Davis and Mecsas, 2007)

Table 2. *Y. pseudotuberculosis* primers used in this study.

Name	Primer Sequence ^a	References
qPCR_16s_F	AGCCAGCGGACCACATAAAG	(Yang et al., 1996)
qPCR_16s_R	AGTTGCAGACTCCAATCCGG	(Yang et al., 1996)
qPCR_ymoA_F	CCTGATGCGTTTAAGAAAATG	This work
qPCR_ymoA_R	GATGGTCTGCAGCTGAGTAAA	This work
qPCR_cpxP_F	CGGTGACGGTAAGATGATGATG	This work
qPCR_cpxP_R	CGCATCAAGTCACGCATTTG	This work
F5'ΔymoA	cgaattcctgcagcccggggGATAGACAGCTGTATTTATATGA C	This work
R5'ΔymoA	gcgtaagcaGGTTTTTCTTCTCGATATACAAATTAATATT G	This work
F3'ΔymoA	aagaaaaaccTGCTTAGCGCTGGTTAAG	This work
R3'ΔymoA	aggaacaaaagctggagctCCTGTATTATCACTTTCCTGC	This work
F5'ΔcpxA	cgaattcctgcagcccggggAATGGAGGGTTTCAATGTTG	This work
R5'ΔcpxA	gcggtagccaGTCGAGTAAACAGTGAG	This work
F3'ΔcpxA	ttactcgacTGGCTACCGCTGCATCCG	This work
R3'ΔcpxA	aggaacaaaagctggagctTGCACAACGTCTCATGGCG	This work
F5'ΔcpxR	cgaattcctgcagcccggggCCATTTTATGATGAATAGCAG	This work
R5'ΔcpxR	ctgttatcaCATGGTTATTTCTCCTCTC	This work
F3'ΔcpxR	aataaccatgTGATAAACAGTTTAACGACG	This work
R3'ΔcpxR	aggaacaaaagctggagctGTGACTACCAGCGTTTTAC	This work
F_pET28bCpxRHis	ttttCCATGGCCATGCATAAAATCCTATTAGT	This work
R_pET28bCpxRHis	ttttCTCGAGTGTTTCTGATACCATCAAGTAG	This work

pFU99a_ymoA_F ccttctgtctcacctcgagTAATTGGTATATTTTCAATGCTTGTT This work
TGGATATCAATAC

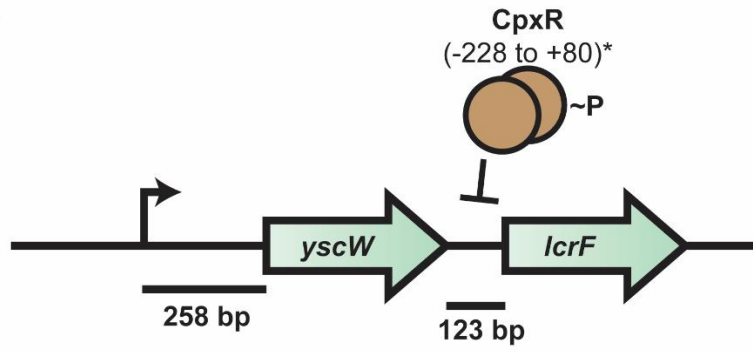
pFU99a_ymoA_R ttcattttaattcctcctgGTCATGCCGCTTAGGCGAG This work

^a Uppercase specifies primer that anneals to target for molecular cloning, lowercase is complementary sequence for NEB Gibson Assembly or extra nucleotides to facilitate efficient restriction digest

Table 3. Plasmids used in this study.

Name	Description	References
pPK7179- <i>yscW-lcrF</i>	DNA template for CpxR EMSA, Amp ^R	This work
pSR47S $\Delta ymoA$	Suicide vector for <i>ymoA</i> deletion, Kan ^R	This work
pSR47S $\Delta cpxA$	Suicide vector for <i>cpxA</i> deletion, Kan ^R	This work
pSR47S $\Delta cpxR$	Suicide vector for <i>cpxR</i> deletion, Kan ^R	This work
pET28b CpxR-His	pET28, CpxR-6xHis ⁺ , Kn ^R	This work
pFU99a <i>pymoBA::lacZ</i>	The promoter of <i>ymoBA</i> fused to <i>lacZ</i> , Cm ^R	This work

A.



B.

nM CpxR-His: 0 1500 1000 667 445



C.

nM CpxR-His: 0 1500 1000 667 445



Figure 1. CpxR does not bind to the *yscW-lcrF* promoter. (A) Schematic illustrating intergenic region purified CpxR was shown to bind. Genomic coordinates listed under CpxR are relative to the *lcrF* start codon. The transcriptional start site for the *yscW-lcrF* operon is 258 nucleotides upstream of *yscW* and is depicted by an arrow. Purified *Yersinia* CpxR was used for electrophoretic mobility shift assays (EMSAs) using DNA from the promoter regions of *yscW-lcrF* **(B)** and *cpxR* as the positive control **(C)**.

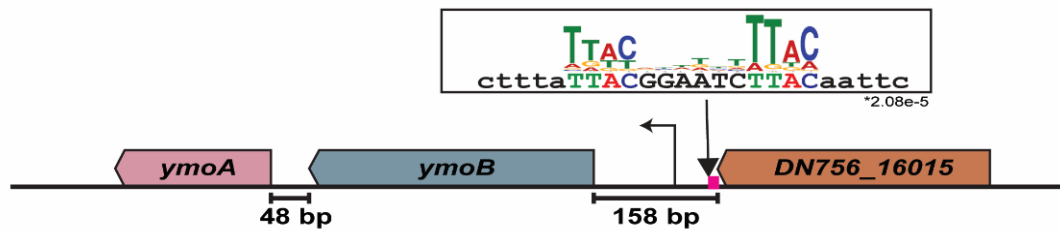


Figure 2. CpxR is predicted to bind upstream of the *ymoBA* promoter.

Schematic illustration of the predicted CpxR binding site upstream of the *ymoBA* operon. The transcriptional start site is indicated by an arrow. MEME-suite tools were used to predict a CpxR binding site. The FIMO e-value is noted below the box.

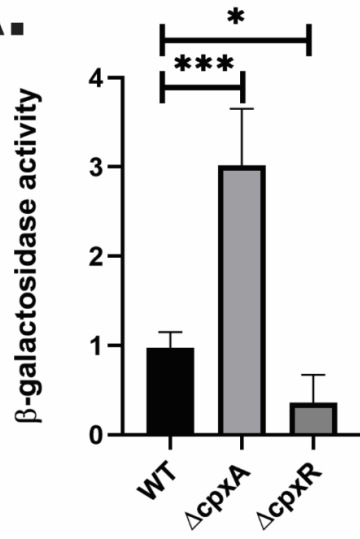
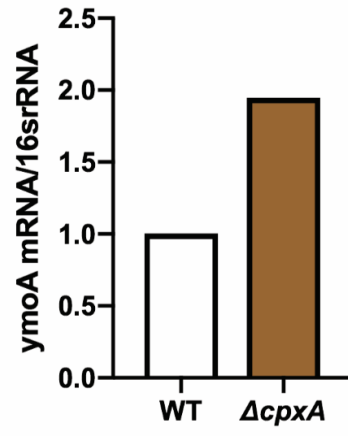
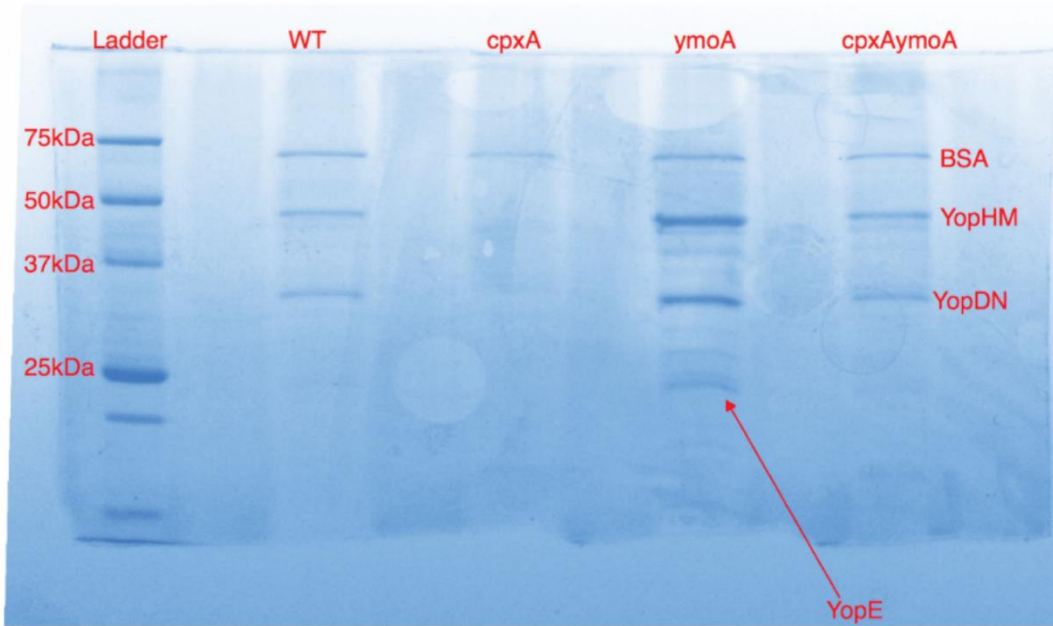
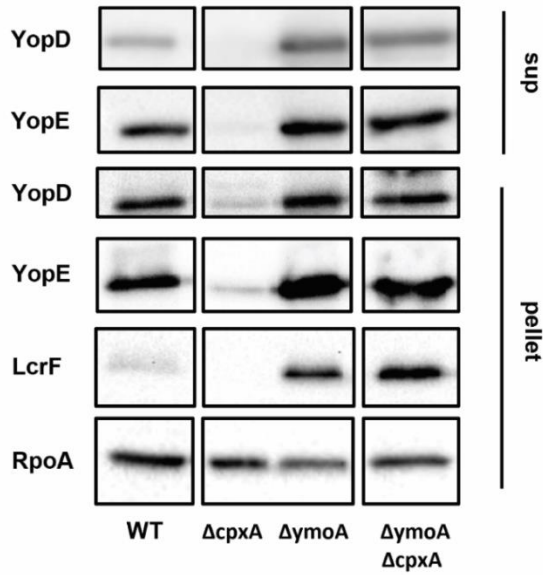
A.**B.**

Figure 3. CpxR promotes expression of YmoA. (A) *Yersinia* strains harboring either an empty pFU99a plasmid or a pFU99a plasmid with the *ymoBA* promoter region fused to *lacZ* were grown in low calcium LB for 1.5 hrs at 26°C and transferred to 37°C (T3SS inducing conditions) for 1.5 hrs. Promoter activity is depicted above as a function of β -galactosidase activity (ng β -galactosidase/ μ g of total protein). Strain backgrounds are noted on the x-axis. The average of three biological replicates are shown with standard deviation. Statistical analysis was performed using an unpaired Student's t-test (* $p < .05$, *** $p < .001$; ns, non-significant). **(B)** RNA was extracted from *Yersinia* strains grown under similar conditions as stated above and *ymoA* mRNA was evaluated by qPCR. mRNA levels were normalized to 16S rRNA levels. Strain background are noted on the x-axis. One biological replicate is shown above.

A.



B.



C.

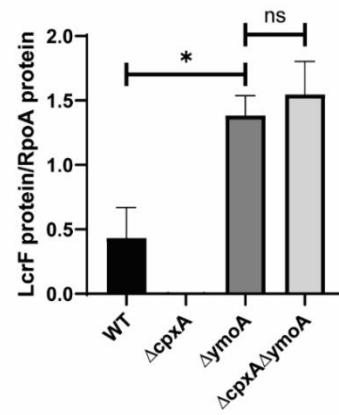


Figure 4. YmoA is crucial for CpxRA repression of LcrF and type III secretion activity. *Yersinia* strains were grown in low calcium LB for 1.5 hrs at 26°C and transferred to 37°C (T3SS inducing conditions) for 1.5 hrs. **(A)** The supernatant was harvested and separated on a 12.5% SDS polyacrylamide gel, and subsequently stained with Coomassie blue. Bovine serum albumin (BSA) was used as a protein precipitation control. One representative biological replicate is shown. **(B)** Whole cell extracts were separated on a 12.5% SDS polyacrylamide gel and transferred onto an Immobilon membrane. LcrF, YopD, and YopE -specific antibodies were detected by immunoblot and RpoA was used as a loading control. All samples were loaded on the same gel but cropped to remove samples not included in this study. One representative experiment out of three independent replicates is shown. **(C)** LcrF protein bands were quantified using Bio-Rad Image Lab Software Quantity and Analysis tools and normalized to RpoA. Shown is the average of three independent replicates and the standard error of the mean. Statistical analysis was performed using an unpaired Student's t-test (* $p < .05$ and n.s. non-significant).

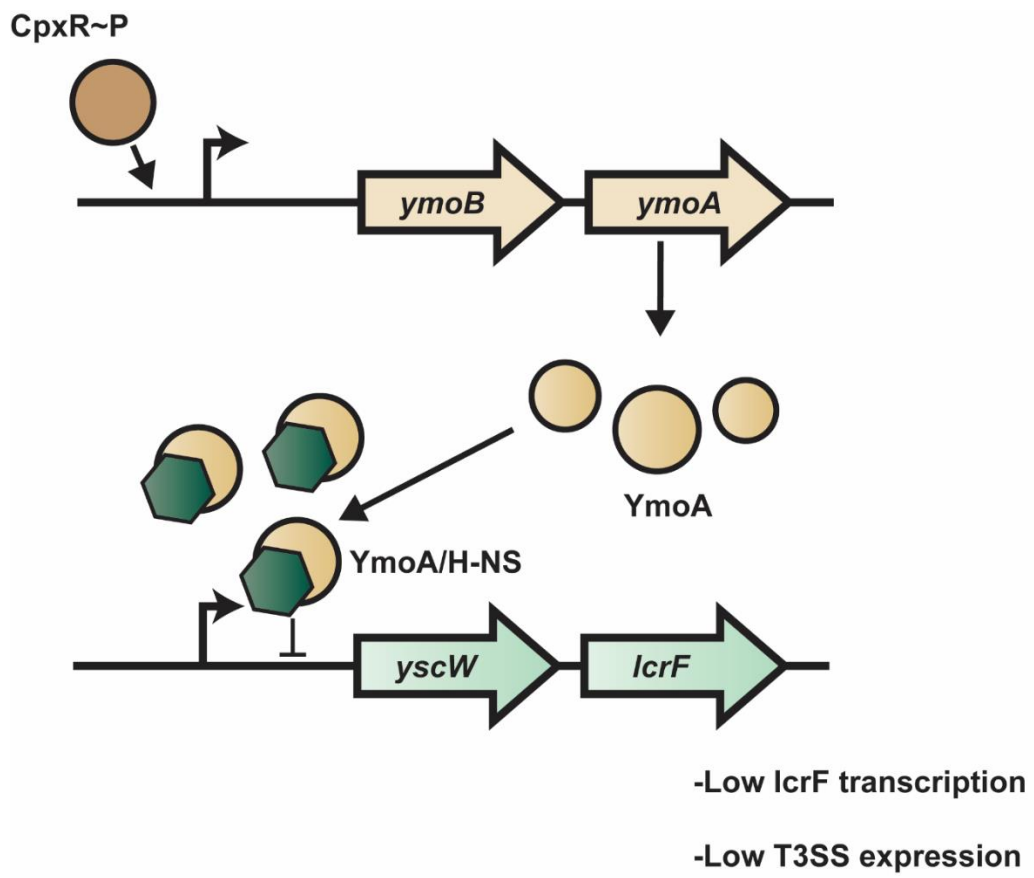


Figure 5. Putative model for how the CpxRA two-component regulatory system indirectly regulates the *Yersinia* T3SS. When CpxR is phosphorylated, activated CpxR promotes transcription of *ymoB-yoA*. YmoA is a known repressor of *yscW-IcrF*, which encodes the main transcriptional activator of genes encoding the T3SS.

Chapter 5

Defects in the Ysc type III secretion system modulate activity of the two-component regulatory system CpxRA

By David Balderas, Pablo Alvarez, & Victoria Auerbuch

Abstract

Dozens of Gram-negative bacterial pathogens, including *Salmonella sp.*, *Shigella flexneri*, *Pseudomonas aeruginosa*, enteropathogenic/enterohemorrhagic *Escherichia coli*, *Chlamydia sp.*, and *Yersinia sp.*, rely on a type III secretion system to cause disease and thrive in a specific niche of the host. The *Yersinia* secretion (Ysc) type III secretion system is assembled in a highly regulated step by step manner. Although we know the order of how the Ysc type III secretion system (T3SS) is constructed, it is not clear how assembly of the T3SS affects other cellular pathways. Interestingly, we found that growth of *Yersinia* with T3SS defects in low calcium media at 37°C (conditions that would normally induce type III secretion), induced expression of the two-component regulatory system, CpxRA. The two-component regulatory system CpxRA consists of a histidine kinase CpxA and a response regulator CpxR, a transcription factor that regulates multiple cellular processes. Furthermore, prevention of both early and middle T3SS substrates induced CpxRA activity. It has been shown that the CpxRA pathway regulates Ysc T3SS expression (see Chapter 4), suggesting a model wherein the CpxRA pathway and the T3SS participate in a feedback loop.

Importance

Transcriptional regulatory networks are responsible for how bacteria respond to their environment. However, it is not clear how the expression of virulence pathways affects global transcriptional regulatory networks. These data suggest that a key virulence pathway in pathogenic *Yersinia* influences the activity of a two-component regulatory system that regulates genes that contribute to mitigating extracytoplasmic stress.

Introduction

Human pathogenic *Yersinia* include *Yersinia pestis*, the causative agent of the plague, and two enteropathogens, *Yersinia enterocolitica* and *Yersinia pseudotuberculosis* (Putzker et al., 2001; Galindo et al., 2011). Although these species lead to different disease pathologies, they all require the *Yersinia* secretion (Ysc) type III secretion system (T3SS) to cause full virulence (Brubaker, 1991; Balada-Llasat and Mecsas, 2006). The Ysc T3SS is an injectosome apparatus that translocates effector proteins from the bacterial cytosol to the host cytosol (Plano and Schesser, 2013). These effector proteins help *Yersinia* evade phagocytic cells (i.e., neutrophils and macrophages) and remain extracellular. Evasion of phagocytosis allows for *Yersinia* to reside in lymphoid tissue and eventually disseminate and cause systemic infection (Pujol and Bliska, 2005).

The Ysc T3SS is encoded on a ~70 kb virulence plasmid called pYV/pCD1, which encodes over 20 proteins including structural proteins, effector proteins, chaperones, and regulators (Cornelis et al., 1998). The Ysc T3SS is assembled in a hierarchical manner to facilitate efficient translocation of effector proteins into host cells. First the basal body is formed by Sec-dependent secretion and assembly of both an outer membrane ring (YscC) and inner membrane rings (YscDJ) (Koster et al., 1997; Yip et al., 2005; Spreter et al., 2009; Diepold et al., 2010; Ross and Plano, 2011). Next the

export apparatus (YscRSTUV), ATPase complex (YscNKL), and cytoplasmic ring (YscQ) are assembled at the base of the complex (Dewoody et al., 2013). Together these protein complexes are referred to as the basal body, and now the assembled basal body can be utilized to translocate specific substrates to complete the injectisome and ultimately translocate effector proteins into host cells. These substrates are often referred to as early (the needle subunit), middle (pore forming complex) and late substrates (effector proteins).

The two-component regulatory system CpxRA is found in many Proteobacteria including *E. coli*. This two-component regulatory system encodes a histidine kinase, CpxA, and a response regulator, CpxR. Studies suggest that the CpxRA system responds to envelope stress, misfolded proteins, and mislocalized lipoproteins (Dorel et al., 2006; Bury-Moné et al., 2009). Once CpxA encounters this signal, autophosphorylation occurs and CpxA can then phosphorylate CpxR. Phosphorylation of CpxR allows CpxR to bind DNA and regulate transcription of a specific set of genes. The CpxR regulon is predicted to consist of over 30 operons, some of which mitigate envelope stress (*cpXP*, *degP*, *skp*, *ppiD*)(Choudhary et al., 2020). Interestingly, constitutive activation of the CpxRA system represses expression of the Ysc T3SS (Carlsson et al., 2007a; Liu et al., 2012; Fei et al.,

2020). This suggests CpxR negatively influences expression of the Ysc T3SS (see Chapter 4).

Our data presented here suggests that defects in the T3SS under T3SS inducing conditions leads to increased CpxRA activity. We further show that specifically prevention of middle substrates is responsible for the increase in CpxRA activity. Lastly, we show that overexpression of the T3SS chaperone LcrH/SycD modulates the CpxRA system. This suggests a feedback loop may exist where CpxRA repress the T3SS (see Chapter 4), and to prevent unnecessary repression, active type III secretion system antagonizes CpxRA activity. However, we failed to observe CpxRA activation in a *sycD* deletion strain suggesting the molecular mechanism inducing CpxRA activity may be more complicated.

Results

Loss of *iscR* affects CpxR activity.

Our previously published RNA-Seq data was performed to compare a *Y. pseudotuberculosis* mutant lacking the transcription factor *iscR* to the wildtype strain under T3SS inducing conditions (37°C in the absence of calcium) (Miller et al., 2014). These data suggested that deletion of *iscR* leads to upregulation of *cpxP*, *degP*, *skp*, *dsbA*, and *ompC* (Fig 1). All these genes have been shown to be activated by CpxR in *E. coli* K12 MG1655.

Furthermore, *cpxP*, *degP* and *skp* have only been shown to be activated by CpxR and no other regulator, which further suggests induction of CpxRA activity. We did not observe upregulation of *cpxR* or *cpxA* (Fig S1) suggesting loss of *iscR* leads to higher CpxRA activity not CpxRA expression levels. This result suggested that loss of *iscR* leads to increased CpxRA activity in *Yersinia*.

Loss of the virulence plasmid leads to increased CpxR activity.

From this data, set we know that over 50% of the genes downregulated in the *iscR* mutant are encoded on the virulence plasmid. The virulence plasmid encodes the genes responsible for expressing the T3SS. We wanted to explore if the increased CpxRA activity from the *iscR* mutant was due to a decrease in T3SS activity. To test this, we performed RT-qPCR with the following strains: wild-type, Δ *iscR*, pYV- (the wild-type strain lacking the virulence plasmid), and Δ *iscR*/pYV- (*iscR* mutant lacking the virulence plasmid). Interestingly the pYV- strain had a ~3-fold increase in *cpxP* mRNA compared to the wild-type strain suggesting that loss of the virulence plasmid alone increases CpxRA activity. Furthermore, loss of the virulence plasmid in the *iscR* mutant did not affect *cpxP* mRNA compared to the *iscR* mutant suggesting no synergism between *iscR* and the T3SS influencing CpxRA activity. Since the virulence plasmid encodes both the T3SS and the adhesin protein YadA, we wanted to test if deletion of *yadA* affects CpxRA activity. We

did not observe upregulation of *cpxP* mRNA in a *yadA* mutant suggesting deletion of *yadA* does not affect CpxRA activity (Fig S2). This result suggests that loss of T3SS activity leads to increased CpxRA activity.

Defective secretion of early and middle substrates influences Cpx activity.

Our previous result suggests that loss of T3SS activity during growth in T3SS inducing conditions leads to increased CpxRA activity. We wanted to better establish what part of T3SS assembly affects the CpxRA activity.

Interestingly, a $\Delta yscNU$ mutant, lacking one of the three major T3SS operons, also exhibited a ~4-fold induction of *cpxP* mRNA under T3SS inducing conditions (Fig 3). This mutant assembles the outer membrane (YscC) and inner membrane rings (YscDJ) but cannot assemble the export apparatus (YscRSTUV), ATPase complex (YscNKL), and cytoplasmic ring (YscQ). This prevents secretion of all three substrate classes: early (YscFOPIYX), middle (YopBDLcrV), and late (YopHOTJEM). Interestingly, a *yscF* mutant also exhibited a ~3-fold induction of *cpxP* mRNA expression. The gene *yscF* encodes for the T3SS needle filament, and deletion of this gene allows for assembly of the export apparatus (YscRSTUV), ATPase complex (YscNKL), and cytoplasmic ring (YscQ). This result suggests that assembly of the basal body does not affect CpxRA activity, rather prevention of T3SS substrates leads to activation of CpxRA. Substrates of the Ysc T3SS are categorized as

early substrates (YscFIYXOP), middle substrates (YopBDLcrV) and late substrates/effector proteins (YopHOTJEM). Deletion of *yscF* prevents secretion of early, middle, and late substrates (Cao et al., 2017). To determine if secretion of late substrates modulates Cpx activity, we performed the same experiment with a strain that lacks all late substrates ($\Delta yopHOTJEM$). This mutant had similar levels of *cpxP* compared to the wild-type strain suggesting late effectors do not affect CpxRA activity. These results suggest that blocking the T3SS prior to late substrate secretion is associated with Cpx activation.

Deletion of *lcrV* induces CpxRA activity.

We hypothesized that prevention of T3SS activity, specifically the obstruction of early and/or middle substrates results in increased CpxRA activity. To determine if prevention of middle substrates leads to an increase in CpxRA activity, we measured *cpxP* mRNA levels in an *lcrV* mutant. Middle substrates consist of LcrV (needle tip complex) and YopBD (translocation pore) (Dewoody et al., 2013). Previous data has shown that deletion of *lcrV* impairs secretion of middle substrates YopBD, but does not affect secretion of early or late substrates (Sarker et al., 1998). Deletion of *lcrV* led to increased *cpxP* mRNA levels and increased CpxRA activity when cultured under T3SS inducing conditions (Fig 4). It is important to note that deletion of *lcrV* affects expression levels of T3SS genes (unpublished). This suggests that

prevention of middle substrates induces CpxRA activity when *Yersinia* is grown under T3SS inducing conditions.

Overexpression of SycD modulates CpxRA activity.

The T3SS middle substrates in *Yersinia* have cognate chaperones: LcrH/SycD for YopB and YopD and LcrG for LcrV. It was shown in Enteropathogenic *E coli* (EPEC) that a T3SS effector chaperone (CesT) can bind CsrA, an RNA binding protein that reprograms bacterial gene expression (Katsowich et al., 2017). This chaperone can then modulate CsrA activity. We wanted to understand if a T3SS chaperone can modulate the CpxRA pathway in *Yersinia*. To test this, we overexpressed SycD in the absence of *cpxA*. The histidine kinase, CpxA, has both kinase and phosphatase ability and in the absence of *cpxA*, CpxR becomes hyper-phosphorylated. Thus, the *cpxA* mutant exhibits high *cpxP* mRNA levels or CpxRA activity (Fig 5). Interestingly, overexpression of SycD in the *cpxA* mutant led to downregulation of *cpxP* mRNA. As a control we overexpressed SycE, the chaperone for the effector protein YopE, and observed no effect on *cpxP* transcription. This result suggests overexpression of SycD, a T3SS middle substrate chaperone, can antagonize CpxRA activity.

Deletion of SycD does not lead to increased CpxRA activity.

Our previous data suggested that overexpression of SycD can modulate CpxRA activity. We would predict that deletion of *sycD* leads to higher CpxRA activity since our data suggests SycD represses CpxRA activity. Thus, we expected the *sycD* mutant to phenocopy a pYV- mutant (strain that lacks a functional type III secretion system) in terms of *cpxP* mRNA levels.

Surprisingly, the *sycD* deletion mutant did not exhibit increased levels of *cpxP*, but instead expressed *cpxP* to similar levels as the wild-type strain (Fig 6). This suggests that SycD either does not affect CpxRA activity during T3SS-inducing conditions or that SycD works with another protein to inhibit CpxRA activity.

Discussion

Our data supports the possible model that proper assembly of the *Yersinia* T3SS leads to downregulation of the CpxRA pathway. We go on to show that prevention of middle substrates (YopBDLcrV), by deleting the gene *IcrV*, causes an increase in CpxRA activity. Our data also shows that overexpression of SycD/LcrH leads to a decrease in CpxRA activity. All together these data suggest that activation of the T3SS leads to secretion of YopB and YopD and allows for their cognate chaperone, SycD, to modulate CpxRA activity. Surprisingly, deletion of *sycD* did not impact activity of the CpxRA pathway alluding to a more complicated pathway.

Interestingly, the CpxRA two-component regulatory pathway has been shown to regulate the T3SS in many pathogens including *Yersinia pseudotuberculosis*, *Citrobacter rodentium*, enterohemorrhagic *E. coli*, enteropathogenic *E. coli*, *Shigella sonnei*, and *Salmonella enterica* (Mitobe et al., 2005; Carlsson et al., 2007b; MacRitchie et al., 2008; Liu et al., 2012; De la Cruz et al., 2015; Shimizu et al., 2016; Vogt et al., 2019). In most pathogens, CpxR has been shown to serve a repressive role on T3SS expression. In many pathogens, such as *Yersinia*, CpxR must be overexpressed to repress T3SS activity in lab settings. On the other hand, overexpression of NlpE, a lipoprotein that has the ability to activate the CpxRA pathway due to misfolding in the periplasm, has been shown to affect T3SS activity in *Salmonella enterica* and enterohemorrhagic *E. coli* through a CpxR dependent mechanism (De la Cruz et al., 2015; Shimizu et al., 2016). It would be interesting to determine which environmental conditions/factors influence CpxRA's role on T3SS activity. This would provide more context on why the Ysc type III secretion system modulates CpxRA activity.

Although a great deal of research has been devoted to understanding how regulatory networks govern the production of virulence factors, it is not clear how the expression of virulence factors modulate transcriptional regulatory networks. The data we present here shows that defects in assembly of the Ysc T3SS represses activity of the two-component regulatory system CpxRA.

Previous experiments in enteropathogenic *E. coli* (EPEC) have shown that the T3SS modulates CsrA activity (Katsowich et al., 2017). These experiments demonstrated that an effector chaperone, CesT, of the T3SS directly interacts with and antagonizes CsrA, a global regulator of posttranscriptional gene expression (Vakulskas et al., 2015). CsrA is an RNA binding protein that binds to the 5' untranslated and/ or early coding regions of mRNAs to influence translation, mRNA stability, and/or transcript elongation. Studies in *E. coli* have found CsrA to copurify with over 700 transcripts, suggesting CsrA is a global regulator (Edwards et al., 2011). The CesT protein normally interacts with the effector protein Tir, however when Tir is translocated by the T3SS, CesT becomes free and interacts with CsrA which prevents CsrA from interacting with other mRNA targets. Interestingly, CsrA has been shown to affect T3SS activity in EPEC, suggesting a feedback loop may exist (Bhatt et al., 2009). We speculate that an analogous feedback loop exists in *Yersinia* in which T3SS activity blocks CpxRA activity, and CpxRA serves a repressive role in blocking *Yersinia* T3SS expression.

Although our data suggest SycD/LcrH antagonizes CpxRA, it is not clear how SycD/LcrH can modulate CpxRA. Our data suggests T3SS activity modulates CpxRA activity rather than CpxRA protein levels. SycD has been shown to bind to YopB and YopD and prevent premature translocation; however SycD and YopD also interact with the 30S ribosome in *Yersinia enterocolitica*

(Kopaskie et al., 2013). This suggests SycD has other molecular targets and one of those targets could directly affect CpxRA activity. Future experiments should be performed aimed at identifying protein partners of SycD.

In this paper we show that the defects in a major virulence factor, the *Yersinia* T3SS, represses activity of the two-component regulatory system CpxRA.

The CpxRA two-component regulatory system normally responds to extracytoplasmic stress or periplasmic misfolding. We were surprised to see that expression of the T3SS, which may lead to envelope perturbations, downregulates CpxRA activity. This may play a beneficial role in preventing repression of the T3SS, a role CpxRA has been shown to play in many T3SS positive bacteria including *Yersinia pseudotuberculosis*. Future experiments should be carried out to determine the molecular mechanism of how SycD, a chaperone of the T3SS, modulates CpxRA activity. This supports the model that the production of virulence factors modulates cellular stress response networks.

Materials and methods

Bacterial strains, plasmids, and growth conditions

All strains used in this study are listed in Table 1. *Y. pseudotuberculosis* strains were grown in M9 minimal media supplemented with casamino acids, referred to here as M9+3.6 μM FeSO_4 , at 26°C with shaking at 250 rpm,

unless otherwise indicated (Cheng et al., 1997). Conditions were achieved by subculturing an M9+3.6 μM FeSO_4 overnight culture to an optical density at 600 nm (OD_{600}) of 0.2 in fresh M9+3.6 μM FeSO_4 , and shaking for 3 hrs at 37°C.

Construction of *Yersinia* mutant strains

A 3xFLAG affinity tag was placed at the C-terminus of *sycD/lcrH* encoded at the native *sycD/lcrH* chromosomal locus to facilitate detection of SycD/LcrH with FLAG monoclonal antibody (Fig S2A). The 3xFLAG affinity tag was chromosomally added to the C-terminus of *sycD* through splicing by overlap extension (Warrens et al., 1997). Primer pair F*sycD_cds*/R*sycD_cds* (Table 2) was used to amplify ~500bp upstream of *sycD* plus the *sycD* coding region excluding the stop codon. Primer pair F3xFLAG/R3xFLAG was used to amplify the 3xFLAG tag. Primer pair F3'*sycD*/R3'*sycD* was used to amplify the ~500 bp downstream region of *iscR* including the stop codon. These amplified PCR fragments were cloned into a BamHI and SacI digested pSR47s suicide plasmid [λ pir-dependent replicon, kanamycin resistant (Kan^{R}), *sacB* gene conferring sucrose sensitivity] using the NEBuilder HiFi DNA Assembly kit (New England Biolabs, Inc). Recombinant plasmids were transformed into *E. coli* S17-1 λ pir competent cells and later introduced into *Y. pseudotuberculosis* IP2666 via conjugation. The resulting Kan^{R} , *irgansan*^R (*Yersinia* selective antibiotic) integrants were grown in the absence

of antibiotics and plated on sucrose-containing media to select for clones that had lost *sacB* (and by inference, the linked plasmid DNA). Kan^S, sucrose^R, congo red-positive colonies were screened by PCR and sequenced.

Generation of The Δ *sycD* mutants were generated via splicing by overlap extension (Warrens et al., 1997). Primer pairs F5/R5 Δ *sycD* (Table 2) were used to amplify ~1000 bp 5' of *sycD*. Primer pair F3/R3 Δ *sycD* were used to amplify ~1000 bp 3' of *sycD*. Amplified PCR fragments were cloned into a BamHI- and SacI-digested pSR47s suicide plasmid (λ pir-dependent replicon, kanamycin^R, *sacB* gene conferring sucrose sensitivity) using the NEBuilder HiFi DNA Assembly kit (New England Biolabs, Inc). Mutant strains were generated as described for the 3xFLAG-SycD strain above.

Quantitative PCR (qPCR) analysis.

A total of 5 mL of culture from each condition were pelleted by centrifugation for 5 minutes at 3,500 rpm. The supernatant was removed, and pellets were resuspended in 500 μ L of media and treated with 1 mL Bacterial RNA Protect Reagent (Qiagen) according to the manufacturer's protocol. Total RNA was isolated using the RNeasy Mini Kit (Qiagen) per the manufacturer's protocol. After harvesting total RNA, genomic DNA was removed via the TURBO-DNA-free kit (Life Technologies/Thermo Fisher). cDNA was generated for each sample by using the M-MLV Reverse Transcriptase (Invitrogen) according to

the manufacturer's instructions, as we previously described (Miller et al., 2014). Power SYBR Green PCR master mix (Thermo Fisher Scientific), and primers (Table 2) with optimized concentrations were used to measure target gene levels. The expression levels of each target gene were normalized to that of 16S rRNA present in each sample and calculated by the $\Delta\Delta C_t$ method. Three independent biological replicates were collected for each tested condition. For each target transcript, significant differential expression between different bacterial strains were defined by p-value <0.05 of two-way analysis of variance (one-way ANOVA with Tukey post-test).

Western blot analysis

Bacterial pellets were resuspended in final sample buffer plus 0.2 M dithiothreitol (FSBS+DTT) and boiled for 15 min. At the time of loading, samples were normalized to the same number of cells by OD₆₀₀. Protein samples were run on a 12.5% SDS-PAGE gel and transferred to a blotting membrane (Immobilon-P) with a wet mini trans-blot cell (Bio-Rad). Blots were blocked for an hour in Tris-buffered saline with Tween 20 and 5% skim milk, and probed with rabbit anti-IscR (Nesbit et al., 2009), rabbit anti-YopD (gift from Alison Davis and Joan Mecsas), goat anti-YopE (Santa Cruz Biotechnology), rabbit anti-RpoA (gift from Melanie Marketon), and horseradish peroxidase-conjugated secondary antibodies (Santa Cruz Biotech). Gels were imaged by Image Lab software (Bio-Rad).

Acknowledgments

This study was supported by National Institutes of Health (www.NIH.gov) grant R01AI119082 (to VA and PJK). DAB and PA received support from the National Human Genome Research Institute of the National Institutes of Health under Award Number 4R25HG006836. The funders had no role in study design, data collection and analysis, decision to publish, or preparation of the manuscript.

References

- Adams, W., Morgan, J., Kwuan, L., and Auerbuch, V. (2015). Yersinia pseudotuberculosis YopD mutants that genetically separate effector protein translocation from host membrane disruption. *Mol. Microbiol.* doi:10.1111/mmi.12970.
- Auerbuch, V., Golenbock, D. T., and Isberg, R. R. (2009). Innate immune recognition of Yersinia pseudotuberculosis type III secretion. *PLoS Pathog.* doi:10.1371/journal.ppat.1000686.
- Balada-Llasat, J. M., and Mecsas, J. (2006). Yersinia has a tropism for B and T cell zones of lymph nodes that is independent of the type III secretion system. *PLoS Pathog.* doi:10.1371/journal.ppat.0020086.
- Bhatt, S., Edwards, A. N., Nguyen, H. T. T., Merlin, D., Romeo, T., and Kalman, D. (2009). The RNA binding protein CsrA is a pleiotropic regulator of the locus of enterocyte effacement pathogenicity island of

- enteropathogenic *Escherichia coli*. *Infect. Immun.* doi:10.1128/IAI.00418-09.
- Bliska, J. B., Guan, K., Dixon, J. E., and Falkow, S. (1991). Tyrosine phosphate hydrolysis of host proteins by an essential *Yersinia* virulence determinant. *Proc. Natl. Acad. Sci. U. S. A.* doi:10.1073/pnas.88.4.1187.
- Brubaker, R. R. (1991). Factors promoting acute and chronic diseases caused by yersiniae. *Clin. Microbiol. Rev.* doi:10.1128/CMR.4.3.309.
- Bury-Moné, S., Nomane, Y., Reymond, N., Barbet, R., Jacquet, E., Imbeaud, S., et al. (2009). Global analysis of extracytoplasmic stress signaling in *Escherichia coli*. *PLoS Genet.* doi:10.1371/journal.pgen.1000651.
- Cao, S. Y., Liu, W. Bin, Tan, Y. F., Yang, H. Y., Zhang, T. T., Wang, T., et al. (2017). An interaction between the inner rod protein YscI and the needle protein YscF is required to assemble the needle structure of the *Yersinia* type three secretion system. *J. Biol. Chem.* doi:10.1074/jbc.M116.743591.
- Carlsson, K. E., Liu, J., Edqvist, P. J., and Francis, M. S. (2007a). Extracytoplasmic-stress-responsive pathways modulate type III secretion in *Yersinia pseudotuberculosis*. *Infect. Immun.* doi:10.1128/IAI.01346-06.
- Carlsson, K. E., Liu, J., Edqvist, P. J., and Francis, M. S. (2007b). Influence of the Cpx extracytoplasmic-stress-responsive pathway on *Yersinia* sp.-eukaryotic cell contact. *Infect. Immun.* doi:10.1128/IAI.01450-06.
- Cheng, L. W., Anderson, D. M., and Schneewind, O. (1997). Two

- independent type III secretion mechanisms for YopE in *Yersinia enterocolitica*. *Mol. Microbiol.* doi:10.1046/j.1365-2958.1997.3831750.x.
- Choudhary, K. S., Kleinmanns, J. A., Decker, K., Sastry, A. V., Gao, Y., Szubin, R., et al. (2020). Elucidation of Regulatory Modes for Five Two-Component Systems in *Escherichia coli* Reveals Novel Relationships. *mSystems*. doi:10.1128/msystems.00980-20.
- Cornelis, G. R., Boland, A., Boyd, A. P., Geuijen, C., Iriarte, M., Neyt, C., et al. (1998). The Virulence Plasmid of *Yersinia*, an Antihost Genome. *Microbiol. Mol. Biol. Rev.* doi:10.1128/mubr.62.4.1315-1352.1998.
- Davis, A. J., and Meccas, J. (2007). Mutations in the *Yersinia pseudotuberculosis* type III secretion system needle protein, YscF, that specifically abrogate effector translocation into host cells. *J. Bacteriol.* doi:10.1128/JB.01396-06.
- De la Cruz, M. A., Pérez-Morales, D., Palacios, I. J., Fernández-Mora, M., Calva, E., and Bustamante, V. H. (2015). The two-component system CpxR/A represses the expression of *Salmonella* virulence genes by affecting the stability of the transcriptional regulator HilD. *Front. Microbiol.* doi:10.3389/fmicb.2015.00807.
- Dewoody, R. S., Merritt, P. M., and Marketon, M. M. (2013). Regulation of the *Yersinia* type III secretion system: Traffic control. *Front. Cell. Infect. Microbiol.* doi:10.3389/fcimb.2013.00004.
- Diepold, A., Amstutz, M., Abel, S., Sorg, I., Jenal, U., and Cornelis, G. R.

- (2010). Deciphering the assembly of the Yersinia type III secretion injectisome. *EMBO J.* doi:10.1038/emboj.2010.84.
- Dorel, C., Lejeune, P., and Rodrigue, A. (2006). The Cpx system of *Escherichia coli*, a strategic signaling pathway for confronting adverse conditions and for settling biofilm communities? *Res. Microbiol.* doi:10.1016/j.resmic.2005.12.003.
- Edwards, A. N., Patterson-Fortin, L. M., Vakulskas, C. A., Mercante, J. W., Potrykus, K., Vinella, D., et al. (2011). Circuitry linking the Csr and stringent response global regulatory systems. *Mol. Microbiol.* doi:10.1111/j.1365-2958.2011.07663.x.
- Fei, K., Chao, H.-J., Hu, Y., Francis, M. S., and Chen, S. (2020). CpxR regulates the Rcs phosphorelay system in controlling the Ysc-Yop type III secretion system in *Yersinia pseudotuberculosis*. *Microbiology.* doi:10.1099/mic.0.000998.
- Galindo, C. L., Rosenzweig, J. A., Kirtley, M. L., and Chopra, A. K. (2011). Pathogenesis of *Y. enterocolitica* and *Y. pseudotuberculosis* in Human Yersiniosis. *J. Pathog.* doi:10.4061/2011/182051.
- Katsowich, N., Elbaz, N., Pal, R. R., Mills, E., Kobi, S., Kahan, T., et al. (2017). Host cell attachment elicits posttranscriptional regulation in infecting enteropathogenic bacteria. *Science (80-)*. doi:10.1126/science.aah4886.
- Kopaskie, K. S., Ligtenberg, K. G., and Schneewind, O. (2013). Translational

- regulation of yersinia enterocolitica mRNA encoding a type III secretion substrate. *J. Biol. Chem.* doi:10.1074/jbc.M113.504811.
- Koster, M., Bitter, W., De Cock, H., Allaoui, A., Cornelis, G. R., and Tommassen, J. (1997). The outer membrane component, YscC, of the Yop secretion machinery of *Yersinia enterocolitica* forms a ring-shaped multimeric complex. *Mol. Microbiol.* doi:10.1046/j.1365-2958.1997.6141981.x.
- Liu, J., Thanikkal, E. J., Obi, I. R., and Francis, M. S. (2012). Elevated CpxR~P levels repress the Ysc-Yop type III secretion system of *Yersinia pseudotuberculosis*. *Res. Microbiol.* doi:10.1016/j.resmic.2012.07.010.
- MacRitchie, D. M., Ward, J. D., Nevesinjac, A. Z., and Raivio, T. L. (2008). Activation of the Cpx envelope stress response down-regulates expression of several locus of enterocyte effacement-encoded genes in enteropathogenic *Escherichia coli*. *Infect. Immun.* doi:10.1128/IAI.01265-07.
- Miller, H. K., Kwuan, L., Schwiesow, L., Bernick, D. L., Mettert, E., Ramirez, H. A., et al. (2014). IscR Is Essential for *Yersinia pseudotuberculosis* Type III Secretion and Virulence. *PLoS Pathog.* doi:10.1371/journal.ppat.1004194.
- Mitobe, J., Arakawa, E., and Watanabe, H. (2005). A sensor of the two-component system CpxA affects expression of the type III secretion system through posttranscriptional processing of InvE. *J. Bacteriol.*

doi:10.1128/JB.187.1.107-113.2005.

Nesbit, A. D., Giel, J. L., Rose, J. C., and Kiley, P. J. (2009). Sequence-Specific Binding to a Subset of IscR-Regulated Promoters Does Not Require IscR Fe-S Cluster Ligation. *J. Mol. Biol.*

doi:10.1016/j.jmb.2009.01.055.

Plano, G. V., and Schesser, K. (2013). The *Yersinia pestis* type III secretion system: Expression, assembly and role in the evasion of host defenses. *Immunol. Res.* doi:10.1007/s12026-013-8454-3.

Pujol, C., and Bliska, J. B. (2005). Turning *Yersinia* pathogenesis outside in: Subversion of macrophage function by intracellular yersiniae. *Clin. Immunol.* doi:10.1016/j.clim.2004.07.013.

Putzker, M., Sauer, H., and Sobe, D. (2001). Plague and other human infections caused by *Yersinia* species. *Clin. Lab.*

Ross, J. A., and Plano, G. V. (2011). A C-terminal region of *Yersinia pestis* YscD binds the outer membrane secretin YscC. *J. Bacteriol.* doi:10.1128/JB.01137-10.

Sarker, M. R., Neyt, C., Stainier, I., and Cornelis, G. R. (1998). The *Yersinia* Yop virulon: Lcr V is required to extrusion of the translocators YopB and YopD. *J. Bacteriol.* doi:10.1128/jb.180.5.1207-1214.1998.

Schwiesow, L., Mettert, E., Wei, Y., Miller, H. K., Herrera, N. G., Balderas, D., et al. (2018). Control of hmu heme uptake genes in *Yersinia* pseudotuberculosis in response to iron sources. *Front. Cell. Infect.*

Microbiol. doi:<http://dx.doi.org/10.3389/fcimb.2018.00047>.

Shimizu, T., Ichimura, K., and Noda, M. (2016). The surface sensor NlpE of enterohemorrhagic *Escherichia coli* contributes to regulation of the type III secretion system and flagella by the Cpx response to adhesion. *Infect. Immun.* doi:10.1128/IAI.00881-15.

Spreter, T., Yip, C. K., Sanowar, S., André, I., Kimbrough, T. G., Vuckovic, M., et al. (2009). A conserved structural motif mediates formation of the periplasmic rings in the type III secretion system. *Nat. Struct. Mol. Biol.* doi:10.1038/nsmb.1603.

Vakulskas, C. A., Potts, A. H., Babitzke, P., Ahmer, B. M. M., and Romeo, T. (2015). Regulation of Bacterial Virulence by Csr (Rsm) Systems. *Microbiol. Mol. Biol. Rev.* doi:10.1128/mnbr.00052-14.

Vogt, S. L., Scholz, R., Peng, Y., Guest, R. L., Scott, N. E., Woodward, S. E., et al. (2019). Characterization of the *Citrobacter rodentium* Cpx regulon and its role in host infection. *Mol. Microbiol.* doi:10.1111/mmi.14182.

Warrens, A. N., Jones, M. D., and Lechler, R. I. (1997). Splicing by over-lap extension by PCR using asymmetric amplification: An improved technique for the generation of hybrid proteins of immunological interest. *Gene.* doi:10.1016/S0378-1119(96)00674-9.

Yip, C. K., Kimbrough, T. G., Felise, H. B., Vuckovic, M., Thomas, N. A., Pfuetzner, R. A., et al. (2005). Structural characterization of the molecular platform for type III secretion system assembly. *Nature.*

doi:10.1038/nature03554.

Table 1. Strains used in this study.

Strain	Relevant Genotype	Source or References
IP2666/(WT)	Naturally lacks full-length YopT	(Bliska et al., 1991)
IP2666/(Δ <i>iscR</i>)	<i>iscR</i> in frame deletion of codons 2 to 156	(Miller et al., 2014)
IP2666/(Δ <i>cpxA</i>)	<i>cpxA</i> in frame deletion of codons 41 to 449	(Liu et al., 2012)
IP2666/(Δ <i>yscF</i>)	<i>yscF</i> in frame deletion of codons 2 to 86	(Davis and Mecsas, 2007)
IP2666/(Δ <i>lcrV</i>)	<i>lcrV</i> in frame deletion of codons 19 to 346	(Davis and Mecsas, 2007)
IP2666/(Δ <i>yopD</i>)	<i>yopD</i> in frame deletion of codons	
IP2666/(Δ <i>yopB</i>)	<i>yopB</i> in frame deletion of codons 19 to 346	(Adams et al., 2015)
IP2666/(Δ <i>yadA</i>)	<i>yadA</i> in frame deletion of codons	
IP2666/(Δ <i>sycD</i>)	<i>sycD</i> in frame deletion of codons 3 to 156	This work
IP2666/(Δ <i>yscNLU</i>)	In frame deletion of <i>yscNOPQRSTU</i>	(Balada-Llasat and Mecsas, 2006)
IP2666/(pYV-)	Δ <i>yscBL</i> pYV cured	(Auerbuch et al., 2009)
IP2666/(Δ <i>iscR</i> pYV- Plasmid cured the IP2666/(Δ <i>iscR</i>) strain		(Schwiesow

) et al., 2018)
(Auerbuch et
IP2666($\Delta yop6$) Deletion of *yopHOJEM* al., 2009)

Table 2. *Y. pseudotuberculosis* primers used in this study.

Name	Primer Sequence^a	References
qPCR_cpxP_F	CGGTGACGGTAAGATGATGATG	This work
qPCR_cpxP_R	CGCATCAAGTCACGCATTTG	This work
F_pTRC99a_sycD	atttcacacaggaacagacATGCAACAAGAGACGACAG	This work
R_pTRC99a_sycD	cctgcaggtcgactctagagTCATGGGTTATCAACGCAC	This work
F_pTRC99a_sycE	atttcacacaggaacagacATGTATTCATTTGAACAAGC	This work
R_pTRC99a_sycE	cctgcaggtcgactctagagTCAACTAAATGACCGTGG	This work
qPCR_16s_F	AGCCAGCGGACACATAAAG	(32)
qPCR_16s_R	AGTTGCAGACTCCAATCCGG	(32)

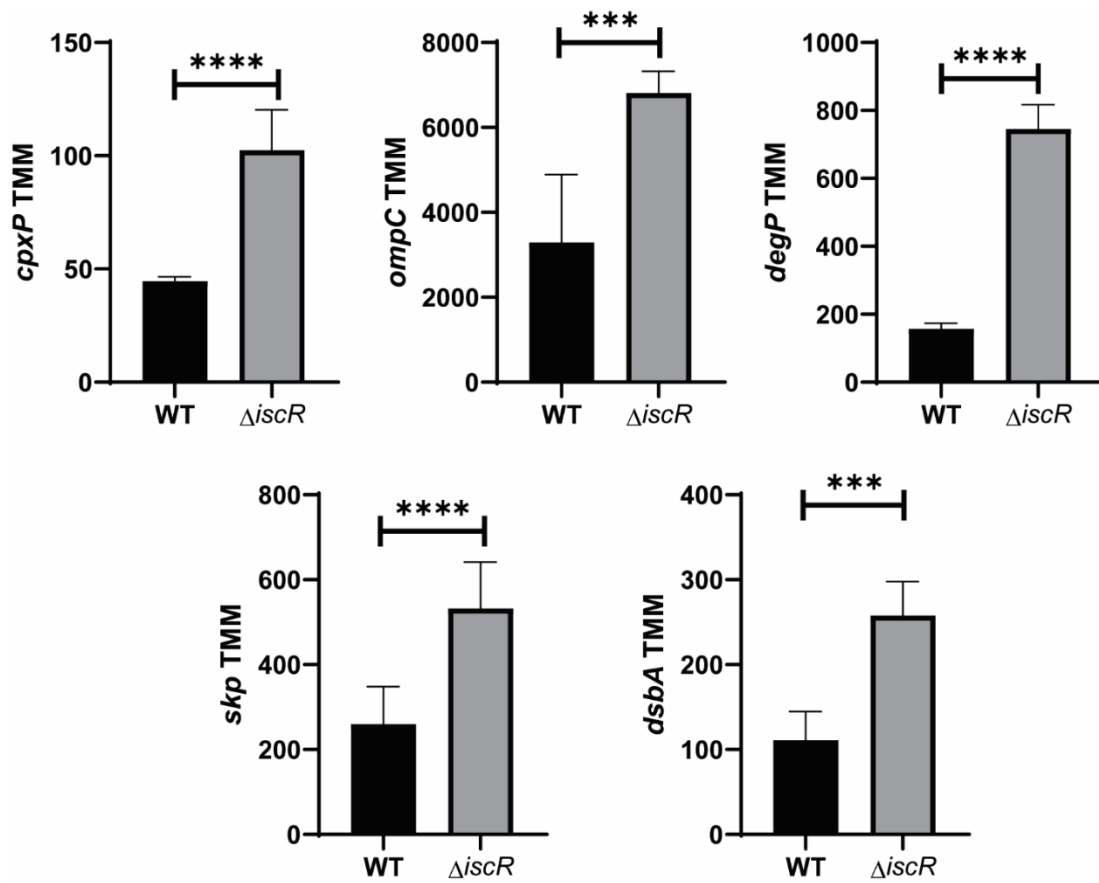


Figure 1. Deletion of *iscR* under T3SS-inducing conditions leads to upregulation of CpxR activated genes. Expression of *cpxP*, *degP*, *skp*, *dsbA*, and *ompC* in *Y. pseudotuberculosis* cultured in M9 minimal media for 3hr at 37°C (type III secretion system inducing conditions), as measured by RNA-Seq. Reads are represented by Trimmed Mean of M-values (TMM) of WT (black) and the *iscR* mutant (grey). ****p<0.0001; (EdgeR with a corrected FDR post-hoc test).

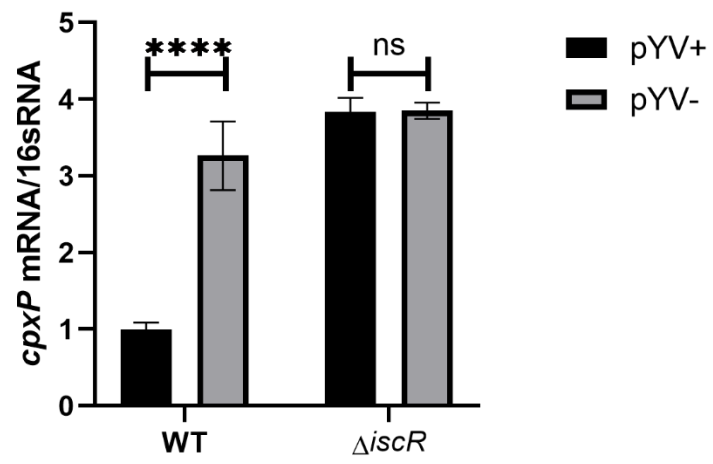


Figure 2. Deletion of T3SS genes leads to upregulation of *cpxP*.

Expression of *cpxP* mRNA relative to 16s rRNA, as measured by qRT-PCR.

Black bars represent strains with the virulence plasmid (pYV+) while grey bars indicate strains that no longer possess the virulence plasmid (pYV-).

**** $p < 0.0001$; ns non-significant (one way ANOVA with Dunnett's post-hoc test).

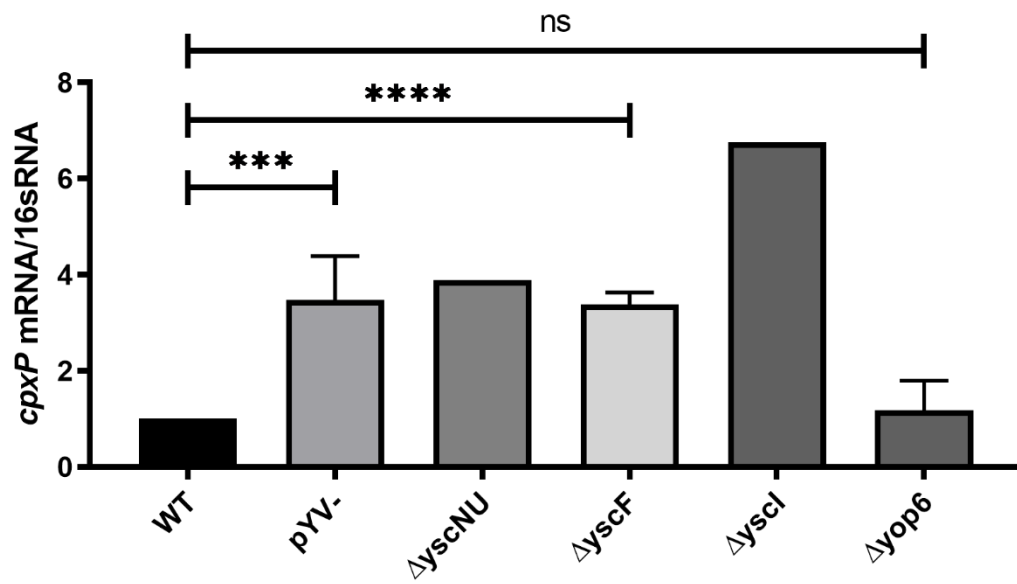


Figure 3. Impediment of early and middle substrates leads to activation of CpxRA. Expression of *cpxP* mRNA relative to 16s rRNA, as measured by qRT-PCR. Strain background are indicated under X-axis. Only performed one biological replicate for *yscNU* and *yscI* mutants thus no statistical analysis was performed on these strains. Statistical analysis was performed using an unpaired Student's t-test. Statistical values indicated are (**** $p < .0001$, *** $p < .001$, and ns non-significant).

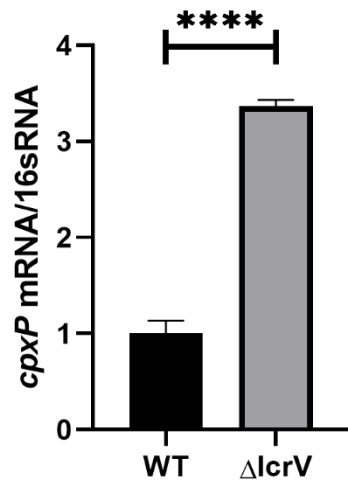


Figure 4. Impediment of middle substrates leads to activation of CpxRA.

Expression of *cpxP* mRNA relative to 16s rRNA, as measured by qRT-PCR.

Strain background are indicated under X-axis. Statistical analysis was

performed using an unpaired Student's t-test. Statistical values indicated are

(**** $p < .0001$).

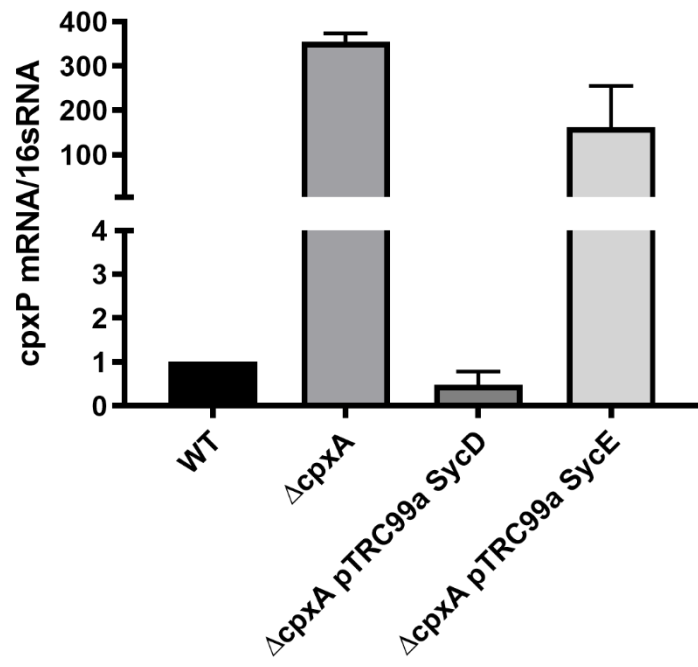


Figure 5. Overexpression of SycD leads to inhibition of CpxRA activity.

Expression of *cpxP* mRNA relative to 16s rRNA, as measured by qRT-PCR.

Strain background are indicated under X-axis. The proteins SycD and SycE

were overexpressed by the addition of 0.2mM IPTG. This experiment was

only performed with two biological replicates and no statistical analysis was

performed.

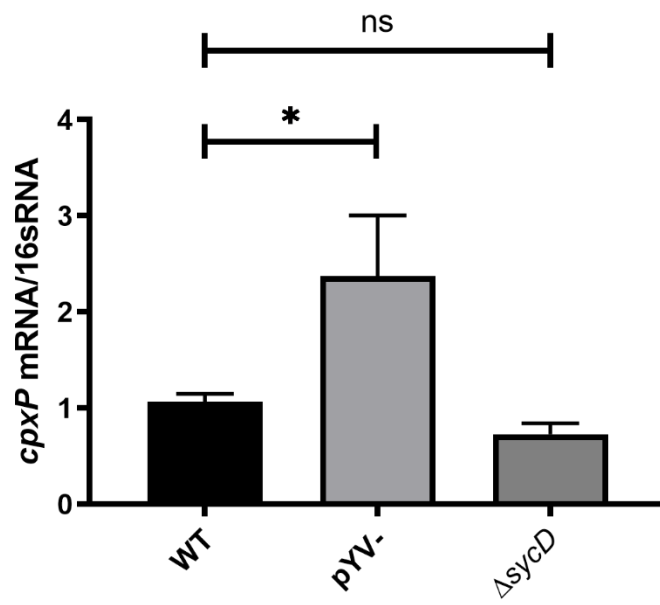


Figure 6. Deletion of *syncD* does not affect CpxRA activity. Expression of *cpxP* mRNA relative to 16s rRNA, as measured by qRT-PCR. Strain background are indicated under X-axis. Statistical analysis was performed using an unpaired Student's t-test. Statistical values indicated are (*p<.05 and ns non-significant).

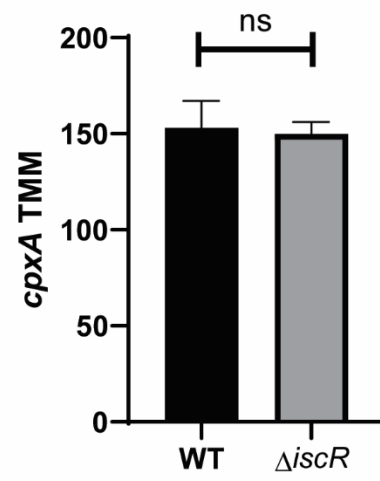
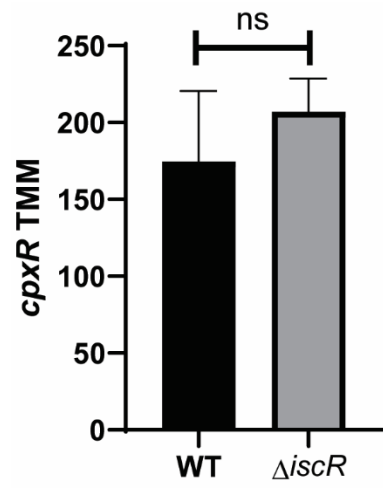


Figure S1. Deletion of *iscR* does not affect *cpxR* or *cpxA* mRNA levels.

Expression of *cpxR* and *cpxA* in *Y. pseudotuberculosis* cultured in M9 minimal media for 3hr at 37°C (type III secretion system inducing conditions), as measured by RNA-Seq. Reads are represented by Trimmed Mean of M-values (TMM) of WT (black) and the *iscR* mutant (grey). ns non-significant (EdgeR with a corrected FDR post-hoc test).

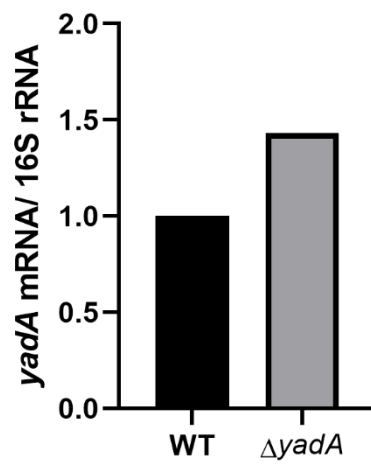


Figure S2. Deletion of *yadA* does not increase *cpxP* levels. Expression of *cpxP* mRNA relative to 16s rRNA, as measured by qRT-PCR. Strain background are indicated under X-axis. (Need to perform two more biological replicates)